arXiv:0809.4960v1 [hep-ph] 29 Sep 2008

UNIVERSITÉ PARIS-SUD XI

THÈSE

Spécialité: **PHYSIQUE THÉORIQUE**

Présentée
pour obtenir le grade de

Docteur de l'Université Paris XI

par

François-Xavier Josse-Michaux

Sujet:

Recent developments in thermal leptogenesis: the role of flavours in various seesaw realisations.

Soutenue le mercredi 25 juin 2008 devant la commission d'examen:

MM.	Asmaa Abada,	directrice de thèse,
	Sacha Davidson,	
	Ulrich Ellwanger,	Président du jury,
	Belen Gavela,	rapporteur,
	Thomas Hambye,	
	Michael Plümacher	rapporteur.

UNIVERSITÉ PARIS-SUD XI

THÈSE

Spécialité: **PHYSIQUE THÉORIQUE**

Présentée
pour obtenir le grade de

Docteur de l'Université Paris XI

par

François-Xavier Josse-Michaux

Sujet:

Recent developments in thermal leptogenesis: the role of flavours in various seesaw realisations.

Soutenue le mercredi 25 juin 2008 devant la commission d'examen:

MM.	Asmaa Abada,	directrice de thèse,
	Sacha Davidson,	
	Ulrich Ellwanger,	Président du jury,
	Belen Gavela,	rapporteur,
	Thomas Hambye,	
	Michael Plümacher	rapporteur.

Remerciements

Ce petit manuscrit pour clore ces trois années de thèse, ce petit chapitre pour remercier ceux grâce à qui ce travail à pu aboutir.
Avant d'arriver sur Paris, je ne savais pas encore ce que je voulais faire, si même je voulais devenir physicien. Alors merci à mes prof. de Paris 7, en particulier à Jean-Pierre Gazeau, pour ces cours de maths vivifiants du lundi matin, ainsi que pour le stage de License; merci à Jim Bartlett, à Pascal David et à Luc Valentin. Ces personnes m'ont donné envie de faire de la Physique, d'enseigner la Physique.
Si un jour cette possibilité m'est offerte, je le dois à ma directrice de thèse, Asmaa Abada. Merci Asmaa pour tes conseils et ton soutien, pour ta compréhension, merci pour ta gentillesse. Merci de m'avoir poussé à m'affirmer un peu plus. Merci de m'avoir enrôlé dans tes fructueux-savoureux projets, et de m'avoir permis de rencontrer de talentueux physiciens.
Merci donc à mes collaborateurs, en particulier à Sacha Davidson pour nos nombreux échanges, et qui de plus a accepté de faire partie de mon jury de thèse. Merci à Alessandro Ibarra, Marta Losada et à Antonio Riotto, en particulier de m'avoir accueilli au CERN pendant quelques jours. Merci à Stéphane Lavignac et à Pierre Hosteins-gageons que ce papier sorte un jour![1]
Je tiens à remercier Ulrich Ellwanger pour avoir accepté de présider mon jury de thèse, ainsi que les rapporteurs Belen Gavela -notamment pour ses remarques concernant ce manuscrit- et Michael Plümacher pour avoir accepté cette tache. Merci enfin à Thomas Hambye d'avoir accepté de faire partie de mon jury de thèse. J'ai hâte ou j'espère pouvoir travailler un jour avec vous.
Merci à Ana Margarida Teixeira, pour ses très nombreux coups de main, et en particulier, merci infiniment pour le travail titanesque que tu as accomplis en corrigeant ce manuscrit, qui te doit beaucoup.
Salutations enfin aux camarades-collègues/amis, la jeunesse du labo. Vu la croissance du nombre de thésards au LPT, bientôt le block entier n'y suffira pas: ce sera tant mieux! Salut donc aux troisième années alexeï, benoît, yacine[2], notamment pour les discussion politiques, salut aux deuxième année chloé, mathieu, pour les rires partagés.
Salut à mes collègue de promo 2008 du LPT: mathieu, razvan[1] et dérogation à l'ordre alphabétique pour nicolas : salut mon ami, et merci, tu étais là quand j'en avais besoin.

---

[1] Le papier est sorti! Il pèse 950 Ko et mesure 32 pages. Souhaitons-lui un bel avenir!

[2] Salutations spéciales aux collègues fumeurs.

Salut aux "jeunes" maintenant, même si on devrait pas, car c'est bien connu les jeunes y respectent rien : salut aux "-1", benjamin-ph[1] et à benjamin-th[1], salut à florian, et bien joué pour avoir lancé le sinje, dont il faut dire je suis pas peu fier du nom (devrais-je?), et salut à jean.
Salut aux "-2": andreas[1], charles, charles-christophe, mounir, s-florian.
Salutations également aux postdocs que j'ai cotoyé: paramita, ritesh, irene, nils.
C'est sympa de causer avec vous.
Salutations aussi à mes anciens camarades du magistère, devenus amis: justine, marine, julien, fabio & steph, xav & marie, miguel et marie-anne, maria et à ceux qu'on voit plus aussi: salut pascale et lihua! C'est vrai que ces années de magistère étaient chouettes, c'était bien de trouver des gens sympas avec qui causer et faire la fête. Maintenant qu'on va tous bouger à droite à gauche, j'espère qu'on continuera à ce voir!
Salut à mes potes de Rennes pierre, romain, malo, françois (grolo), erwann, tugdual...En particulier salut à mon colloc pierre, avec qui j'aurai vécu pendant la majeure partie de cette thèse, qui a du supporter mes tasses de cafés moisies, les mégots de cigarettes et la vaisselle s'empilant dans l'évier, sans trop broncher. Pierre, romain, merci les mecs de m'avoir soutenu dans les coups durs, et d'avoir été là quand il le fallait - ne serait-ce que pour faire la fête.
Si ces trois années ont été riches de joies, elles n'auront pas été avares de peines ni de douleurs. Aussi grandes furent-elles, tu as toujours été près de moi : merci, Constance, mon petit bout de femme. Sans toi, je ne sais pas si j'en serais là.

“ Ayez une connaissance exacte
et de détail de tout ce qui vous environne;
sachez où il y a une fôret, un petit bois,
une rivière, un ruisseau,
un terrain aride et pierreux
un lieu marécageux et malsain,
une montagne, une colline,
une petite élévation,
un vallon, un précipice,
un défilé, un champ ouvert,
enfin tout ce qui peut servir ou nuire
aux troupe que vous commandez.
S'il arrive que vous soyez hors d'état
de pouvoir être instruit par vous-meme
de l'avantage ou du desavantage du terrain,
ayez des guides locaux sur lesquels
vous puissiez compter sûrement."

Sun-Tzu, *l'Art de la guerre*, art. 7.

à mon frère et à mes soeurs,
pierre, julie et charlotte.

Contents

Remerciements **5**

Introduction **15**

1 Baryon Asymmetry of the Universe **17**

1.1 Evidence for a baryon asymmetry 17

1.1.1 Big-Bang Nucleosynthesis 17

1.1.2 Cosmic Microwave Background 20

1.2 Generating the Baryon number of the Universe 22

1.3 Models of Baryogenesis 24

1.3.1 GUT baryogenesis 24

1.3.2 Electroweak baryogenesis 25

1.3.3 Affleck-Dine baryogenesis 26

1.3.4 Baryogenesis via leptogenesis 26

2 Massive neutrinos **27**

2.1 Evidence for neutrino oscillations 27

2.2 Neutrino mixing in the 3 flavour scheme. 29

2.3 Non-oscillation experiments 31

2.4 Neutrino mass models 33

2.5 Seesaw models 35

2.5.1 Fermion singlet: type I seesaw 35

2.5.2 Scalar triplets: type II seesaw 37

2.5.3 Fermion triplets: type III seesaw 38

3 The single flavour approximation **39**

3.1 Basics of leptogenesis 39

3.2 CP violation 41

3.3 Leptogenesis in the single flavour approximation 45

3.4 Evaluation of the lepton asymmetry 49

3.5 Dependence on the initial conditions 52

3.6 Other processes 52

3.7 Upper-bound on the light neutrino mass scale . . . 56

4 Importance of lepton flavours 59

4.1 A toy model for flavoured Boltzmann equations . . . 59
4.2 Flavoured Boltzmann Equations . . . 62
4.3 Flavour structure . . . 64
  4.3.1 One flavour scheme . . . 64
  4.3.2 Two flavour scheme . . . 65
  4.3.3 Three flavour scheme . . . 67
4.4 $B-L$ conversion and the Baryon asymmetry . . . 67
4.5 A remark on the full flavour regime . . . 68

5 Flavours in type I leptogenesis 71

5.1 Flavoured leptogenesis . . . 72
5.2 Effect of lepton flavours in the type I seesaw . . . 74
  5.2.1 CP asymmetry . . . 74
  5.2.2 Washout factors . . . 77
  5.2.3 Qualitative picture . . . 77
5.3 Evaluation of the baryon asymmetry . . . 78
  5.3.1 Thermal initial population . . . 82
  5.3.2 Influence of the off-diagonal terms of the A matrix . . . 84
5.4 Constraints from a successful leptogenesis . . . 86
  5.4.1 Lower bound on heavy neutrino mass . . . 87
  5.4.2 Upper bound on light neutrino mass . . . 90
  5.4.3 Constraints on mixing angles and CP violating phases . . . 92
5.5 Summary . . . 92

6 Leptogenesis in the type II seesaw 95

6.1 Framework . . . 96
6.2 Inferring the unknown parameters . . . 98
  6.2.1 Inverting the seesaw . . . 98
  6.2.2 Right-handed neutrino spectrum . . . 104
6.3 Leptogenesis . . . 107
  6.3.1 Right-handed neutrinos as part of an $SU(2)_R$ doublet . . . 107
  6.3.2 Scalar triplets in leptogenesis . . . 109
  6.3.3 Supersymmetric leptogenesis . . . 110
  6.3.4 Reheating temperature and the gravitino problem . . . 111
  6.3.5 Boltzmann equations . . . 114
6.4 Results for the four typical solutions . . . 116
  6.4.1 Influence of flavours . . . 116
  6.4.2 Influence of mass corrections . . . 121

6.4.3 Dependence on the reheating temperature . . . 124
6.5 Dependence on the low energy parameters . . . 125
6.5.1 Dependence on the light-neutrino mass . . . 125
6.5.2 Dependence on low-energy mixing angles and phases. . . . 126
6.6 Summary . . . 128

Conclusions **131**

A A few words on particle physics **135**
A.1 The Standard Model . . . 135
A.2 Sphalerons . . . 136

B Thermodynamics **139**
B.1 Equilibrium thermodynamics . . . 140
B.2 Relating B and L numbers . . . 143
B.3 Out-of-equilibrium thermodynamics: Boltzmann equations . . . 145
B.4 Boltzmann equations in leptogenesis . . . 147

Bibliography **149**

Introduction

The Standard Model of particle physics (SM) is a renormalisable quantum field theory, based on the $SU(3) \times SU(2) \times U(1)$ gauge group. This model is very successful, since it can explain *almost* all observations. However, a few points are unexplained. For example, among many other questions, we do not understand why there are three (and only three) generations of fermions, why the fermions exhibit such a mass pattern, why there is such a flavour structure among quarks or leptons. We do not know why the electrical charge is quantified, what is the origin of CP violation and the anomally cancellation in the SM looks rather miraculous. If the Higgs mechanism indeed provides masses to the fermions, the stability of the Higgs mass under radiative corrections is a problem. There are also a few observations that possibly provide evidence for physics beyond the SM. Among the latter, is the origin of neutrino masses. About 3/4 of our Universe is constituted of Dark Energy, the exact nature of it we do not grasp. Only 1/4 of our Universe is made of matter, but only 15% of this matter is known, the remaining part, the Dark Matter, being yet unknown. Moreover, we do not know why is there matter at all, if the Universe was initially matter-antimatter symmetric.

In this thesis, we focus on two of these observations, namely the matter-antimatter asymmetry of the Universe and the fact that neutrinos are massive.

The dominance of matter over antimatter is an obvious and happy constatation that we do every day. Observations tell us however that matter dominates, but the domination is really small. This tiny number, the baryon asymmetry of the Universe, is unexplained in the SM. In chapter 1 we will discuss the most important observations, and present some of the possible explanations.

The other failure of the SM we are interested in stems from the observation of a deficit in solar and atmospheric neutrino fluxes. As we will explain in chapter 2, these deficits imply that neutrinos are massive particles, and this really constitutes a first experimental evidence of physics beyond the SM.

Among the different mechanisms advocated to explain neutrino masses, we consider in more detail the class of seesaw models, where some heavy fields which couple to light neutrinos are added to the SM particle content.

The seesaw model constitutes so far the preferred solution to the non-zero neutrino masses, mainly for two reasons. First, these heavy fields naturally emerge in larger gauge groups which attempt to unify the SM interactions. The second reason is that these fields provide an explanation for the observed matter-antimatter asymmetry, through the leptogenesis mechanism.

Chapters 3, 4, 5 and 6 are devoted to the study of leptogenesis, in which the heavy fields introduced can generate during their decay an excess of leptons over anti-leptons. The lepton asymmetry is then partly reprocessed into a baryon asymmetry. Chapter 3 can be viewed as an introduction to the work I have achieved during my thesis, which is discussed in chapters 4, 5 and 6.

In chapter 3, we discuss in detail leptogenesis, in particular the constraints under which does this mechanism accounts for the observed baryon asymmetry. Chapter 3 relies on the old wisdom based on the one-flavour approximation. This picture, even if yielding good estimates of the lepton asymmetry, is nevertheless incorrect.

Indeed, as explained in chapter 4, since the interactions involving charged leptons are usually in-equilibrium for the temperatures relevant in leptogenesis, lepton flavours have to be considered. We show in this chapter under which conditions the flavours must be included, and we show what are the good objects to study in this framework.

In chapter 5, we study the effects of lepton flavours in leptogenesis in the type I seesaw, where fermion singlets are added to the SM particle content. We show in this chapter how flavours affect leptogenesis. This chapter constitutes the main results obtained during my thesis, which are important results in all leptogenesis models, since the inclusion of flavours profoundly modifies the constraints derived in the one-flavour approximation.

Finally, in chapter 6 we investigate the effects of flavours in the type II seesaw, in which scalar triplets are added to the SM. The framework of this study is a supersymmetric grand-unified (SUSY-GUT) model, in which scalar triplets as well as fermion singlets naturally appear. In this chapter we study the influence of lepton flavours, as well as the effect of including second lightest fermion singlet in leptogenesis. We further correct the GUT relation between charged lepton and down-type quark masses. These inclusions and corrections are found to be fruitfull, since they render this model of SUSY-GUT leptogenesis a viable mechanism to account for the observed baryon asymmetry.

Chapter 1

Baryon Asymmetry of the Universe

It is an every-day observation that matter dominates over anti-matter. On Earth, matter is present everywhere around us, whereas antimatter is only significantly produced in accelerators. The Solar system or our galaxie as well, are clearly matter-antimatter asymmetric. One could think that the Universe contains as much matter as anti-matter, each kind living apart in distinct regions. However, if it was so, one would expect annihilations $X + \bar{X} \rightarrow 2\gamma$ to occur on matter-antimatter borders, and therefore high-energy photons would be produced with a clear signature. As we have not observed such annihilation, we must conclude that our Universe is globally matter-antimatter asymmetric.

More precisely, two distinct cosmological observations, based on two very different physics, give us similar probes: in a volume which contains 10^{10} photons, the number of particles exceeds that of antiparticles by 6:

$$\eta_B = \frac{n_b - n_{\bar{b}}}{n_\gamma} \simeq 6 \times 10^{-10} \; . \tag{1.1}$$

This quantity η_B is defined as the Baryon Asymmetry of the Universe (BAU)

1.1 Evidence for a baryon asymmetry

Let us briefly discuss the experimental evidences of the BAU.

1.1.1 Big-Bang Nucleosynthesis

Big-Bang Nucleosynthesis (BBN) [1, 2] is a remarkably trustful window on the early Universe, since it is based on well-known Standard Model physics. It predicts the abundance of light elements $D, {}^3He, {}^4He, {}^7He$ as a function of a small set of parameters, among which the matter-antimatter asymmetry η_B.

In the early Universe, at $T \simeq 20\,\mathrm{MeV}$, baryon-antibaryon pairs annihilate, leaving any baryon excess frozen-out and constant in a comoving volume. This amount of baryons consists of protons and neutrons, which are in thermal equilibrium together with $e^\pm$ and neutrinos. For $T \gtrsim 1\,\mathrm{MeV}$, these species undergo weak interactions:

$$n + \nu_e \leftrightarrow p + e^- \,, \quad p + \overline{\nu_e} \leftrightarrow n + e^+ \,, \quad n \leftrightarrow p + e^- + \overline{\nu_e},$$

which maintain the neutron-to-proton ratio at its equilibrium value:

$$\frac{n_n^{eq}}{n_p^{eq}} \simeq e^{-\frac{m_n - m_p}{T}} \simeq e^{-\frac{1.293\,\mathrm{MeV}}{T}} \,. \tag{1.2}$$

At high temperatures, protons and neutrons are most likely free particles, as light nuclei are disfavoured, due to the high energetic gamma rays of the thermal bath.
Since the rate of weak interactions, $\Gamma_{n\leftrightarrow p} \simeq G_F^2 T^5$, decreases faster than the Hubble expansion rate, $H(T) \simeq 1.66\sqrt{g_* G_N}\, T^2$, the electroweak interactions will freeze as the temperature of the Universe cools down. This occurs at $T_{fr} \simeq 0.8\,\mathrm{MeV}$ and at this temperature, according to eq.(1.2), the neutron-to-proton ratio is about $n_n/n_p \simeq 1/6$.
During the cooling process, light nuclei become energetically favoured, as the temperature drops below their different binding energies. ^4He, the more stable of them, is likely to be formed. However, direct production, $2p+2n \to {}^4He+\gamma$, is highly inefficient due to the small cross-section of the electroweak processes, and also due to the relative low density of species. Therefore ^4He is more likely produced through a series of chain reactions, which are depicted in fig.(1.1):

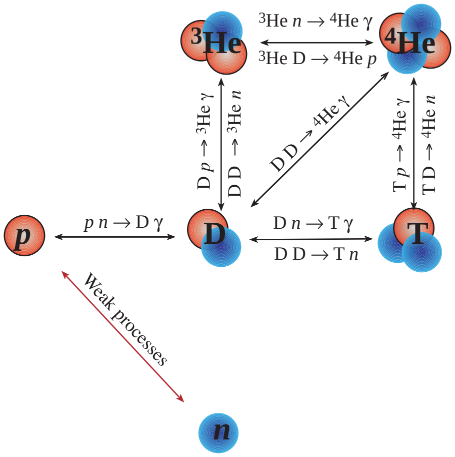

Figure (1.1): Schematic representation of the nucleosynthesis chain reaction. Picture taken from [3].

The deuterium production is a prior to the chain reaction, through the process

$$p + n \quad \to \quad D + \gamma \,.$$

However, given its small binding energy, $E_B \simeq 2.2\,\mathrm{MeV}$, as long as the gamma rays of the thermal bath are energetic enough to photo-dissociate D via $\gamma + D \to p + n$, no nuclei can be efficiently produced. This is the so-called "deuterium bottleneck".
The chain reaction begins when the deuterium to baryon ratio is ~ 1:

$$\frac{n_D}{n_b} \simeq \eta_B \left(\frac{T_{nuc}}{m_p}\right)^{3/2} e^{\frac{E_B}{T_{nuc}}} \simeq 1 \,.$$

This happens for $T \simeq 0.06\,\mathrm{MeV}$. Once deuterium production starts, the chain reaction rapidly occurs, until ^4He is synthethised. All neutrons are to be converted in ^4He, which mass fraction is then roughly found to be:

$$Y_p = \frac{2n_n}{n_n + n_p} \simeq 1/4.$$

Precise computations of this mass fraction show a tiny dependance on the baryon asymmetry [4]. A fit of Y_p, accurate over the value $\eta_B \simeq 6 \times 10^{-10}$, gives [5]:

$$Y_p \simeq 0.2485 \pm 0.0006 + 0.0016(\eta_{10} - 6)\,, \tag{1.3}$$

where $\eta_{10} = 10^{10}\eta_B$, is the normalised baryon-to-photon ratio.

In fact, the ^4He mass fraction is not a good indicator of the baryon-to-photon ratio. Rather, it strongly depends on the expansion rate, and so it is a good indicator of the time at which nucleosynthesis occured. Indeed, since in a first approximation all neutrons are captured in this nuclei, the later this capture happens, the longer time neutrons have to decay, and hence a lower mass fraction is obtained.

The prefered "baryometer" turns out to be deuterium, since its abundance directly results from the competition between production and destruction processes. The primordial D to H ratio is accurately fitted around its central value by [5]:

$$y_D = 2.64\,(1 \pm 0.03)\left(\frac{6}{\eta_{10}}\right)^{1.6}\,, \tag{1.4}$$

where $y_D = 10^5(D/H)$. This ratio clearly denotes a stronger dependence on the baryon asymmetry.

Moreover, the post-BBN evolution of the deuterium is easy to track, the latter being only destroyed in stars. Therefore, observations of D in "old" regions of the Universe yield the value of its primordial abundance:

$$y_D = 2.68^{+0.27}_{-0.25}\,. \tag{1.5}$$

Using this observation, the baryon-to-photon ratio is found to be

$$\eta_{10} = 6.0 \pm 0.4\,, \tag{1.6}$$

which is in excellent agreement with the value predicted by the cosmic microwave background observation, as we will see in the next section.

Comparatively, the ^4He primordial mass fraction is inferred to be

$$Y_P = 0.240 \pm 0.006\,, \tag{1.7}$$

which, together with the D abundance, provides the value

$$\eta_{10} = 5.7 \pm 0.4\,. \tag{1.8}$$

Similarly to deuterium and defining the number abundance of various nuclei relative to the Hydrogen abundance, $y_3 = 10^5({}^3He/H)$ and $y_{Li} = 10^{10}({}^7Li/H)$, the mass fraction of ${}^3He$ and ${}^7Li$ are found to be [4]:

$$\begin{aligned} y_3 &\simeq 3.1(1 \pm 0.01)\,\eta_{10}^{-0.6}, \\ y_{Li} &\simeq \frac{\eta_{10}^2}{8.5}\,. \end{aligned}$$

From these fits, and the corresponding primordial abundances inferred by observation, η_{10} can be deduced. However, the determinations of the primordial abundance for ${}^3He$ and ${}^7Li$ are more complex and model dependent, hence the inferred η_{10} should be regarded with less confidence. Fig.(1.2) shows how the analytical fits for the various mass fractions, together with the primordial abundances inferred from observation, can result in a determination of the baryon asymmetry.

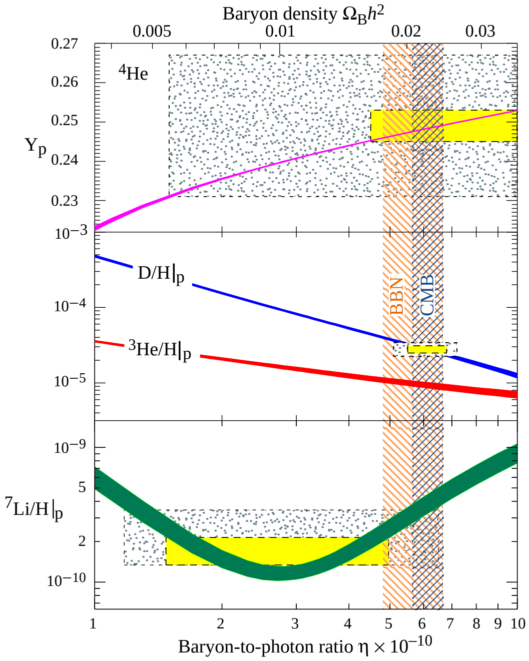

Figure (1.2): Abundance of light elements. Figure taken from [6].

In conclusion, BBN tells us that the baryon-to-photon ratio is non-zero, but small:

$$\eta_B = 5.7 \pm 0.4 \times 10^{-10}\,. \tag{1.9}$$

1.1.2 Cosmic Microwave Background

The observation of the CMB from the WMAP satellite [7] gives a very precise determination of the baryon-to-photon ratio, which is consistent with the BBN value given above. However, while BBN started around $T \simeq 0.08\,\text{MeV}$, $t \simeq 3$ min and was almost complete at $t \simeq 20$ min, the CMB photons come from matter-radiation decoupling, which occured at recombination, $T \sim 1\,\text{eV}$ or equivalently $t \simeq 4\,\times 10^5$ years [8].

As the temperature drops below $T \simeq 13.6\,\mathrm{eV}$, photons are no longer energetic enough to photo-dissociate Hydrogen, hence the reaction

$$e^- + p \leftrightarrow H + \gamma \tag{1.10}$$

deviates from equilibrium, resulting in the absorption of free electrons by protons and ionized atoms. The photons, which were in equilibrium with electrons, via scatterings and annihilations processes:

$$e- + e^+ \leftrightarrow \gamma + \gamma\,, \quad e^- + \gamma \leftrightarrow e^- + \gamma\,, \tag{1.11}$$

then decouple and become free streaming particles. The observation of these photons provides us a snapshot of the Universe at that time.

Before decoupling, the photons and the baryons are strongly coupled, and form a fluid which is liable to interactions with opposite effects. On the one hand, in a gravitational well, gravity pushes this fluid down the well, whereas on the other hand the radiation pressure tends to push it out. The fluid thus goes through accoustic oscillations, which last until the baryons and the photons decouple.

After their last scattering, photons freely propagate, and the surface of this last scattering appears to us as a sphere of homogeneous temperature $T_0 \simeq 2.273K$ corresponding to a decoupling temperature $T_{decoupling} \simeq 0.26\,\mathrm{eV}$. However, the temperature distribution is not fully homogeneous, and the study of the anisotropies provides an accurate determination of a set of cosmological parameters. More specifically, the angular distributions of rescaled anisotropies

$$\frac{\Delta T(\theta,\phi)}{T_{mean}} = \frac{T(\theta,\phi) - T_{mean}}{T_{mean}} \tag{1.12}$$

are decomposed on spherical harmonics

$$\frac{\Delta T(\theta,\phi)}{T_{mean}} = \sum_{\ell=1}^{\infty} \sum_{m=-\ell}^{\ell} a_{\ell\,m}\, Y^{\ell}_{m}(\theta,\phi)\,, \tag{1.13}$$

so that the study of the anisotropies is translated into the study of the angular power spectrum $C_\ell = \left\langle |a_{\ell,m}|^2 \right\rangle$. The cosmological parameters are extracted after a fit of the power spectrum, over a set of *priors*, which are theoretical assumptions [9]. By modifying the values of the differents parameters, the relative height and space between the different peaks vary. For example, fig.(1.3) show the different power spectra obtained by varying η_B around its central value, increasing or lowering the baryon asymmetry up to 50%.

We clearly see how the first accoustic peak, located at $\ell \simeq 200$, is influenced by the value of η_B. This first peak is precisely the one which provides the constraint on the baryon asymmetry.

Using WMAP 5 years only, the baryon asymmetry is found to be [9]

$$\eta_B = 6.225 \pm 0.17 \times 10^{-10}\,. \tag{1.14}$$

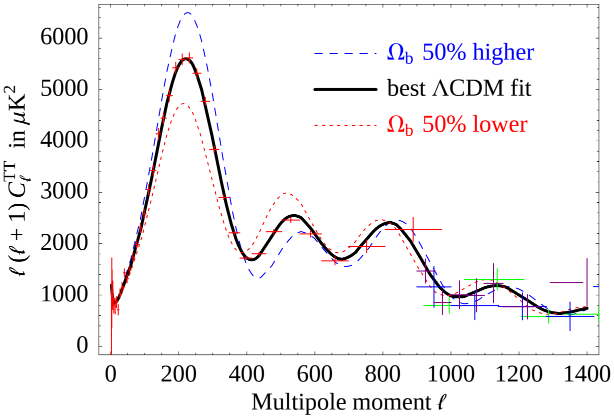

Figure (1.3): Temperature angular power spectrum. Figure taken from [3].

The combination of different observations leads [5] to the value

$$\eta_B = 6.11^{+0.26}_{-0.27} \times 10^{-10}\,, \tag{1.15}$$

at 95% confidence level. This is the value we will use throughout this thesis.

1.2 Generating the Baryon number of the Universe

The observed baryon asymmetry calls for explanation. One could argue that this asymmetry was an initial condition of the Universe, or that is has been produced in the very early stages of its evolution. Assuming that initially the Universe was asymmetric goes against a naturalness principle, and is not satisfactory. Furthermore, an inflationary period is believed to have occurred in the Standard Model of Cosmology, (see, *e.g.* [10]), during which the scale factor $a(t)$ of the Universe is increased by a factor $\sim 10^{30}$. Consequently, any asymmetry existing prior to inflation would have been extremely diluted, by a factor $\sim 10^{-30}$. Therefore, one has to suppose that the Universe was initially matter-symmetric, and find a way to produce $\eta_B \neq 0$ after the inflation period. We know that the annihilation of baryons and antibaryons is not fully efficient, and so one can wonder whether such an asymmetry could be produced at the freezing of annihilations. Following Appendix B [1], we have that for $1\,\mathrm{MeV} \lesssim T \lesssim 1\,\mathrm{GeV}$, baryons and antibaryons are in thermal equilibrium, with

$$\frac{n_b^{eq}}{n_\gamma} \simeq \frac{n_{\bar{b}}^{eq}}{n_\gamma} \simeq \left(\frac{m_p}{T}\right)^2 K_2(\frac{m_p}{T}) \simeq \left(\frac{m_p}{T}\right)^{3/2} e^{-m_p/T}. \tag{1.16}$$

Baryons and anti-baryons annihilate and their density decreases until the reactions freeze-out. Since the annihilation rate is $\Gamma_a \simeq n_b^{eq}\,\langle\sigma|v|\rangle$, with a thermally averages rate $\langle\sigma|v|\rangle \sim 1/m_\pi^2$, the decoupling occurs when $\Gamma_{annihilation} \simeq H(T)$, at a temperature $T_D \simeq 20\,\mathrm{MeV}$. At this temperature, the baryon-to-photon ratio is

---

[1] Cf. also chapter 5 and 6 of [1].

$$\frac{n_b^{eq}}{n_\gamma} \simeq \frac{n_{\bar{b}}^{eq}}{n_\gamma} \simeq 10^{-18} \ll 10^{-10}\,, \tag{1.17}$$

which is far below the observed matter-antimatter number density: the Standard Model of Cosmology cannot explain the baryon asymmetry. Therefore, a model is needed, in which this number is generated after inflation and before the freeze-out of baryon-antibaryon annihilations.

Sakharov's conditions

It has been shown that three conditions, known as Sakharov's conditions [11], are necessary to produce a baryon asymmetry in the Universe, starting from a symmetric initial state:

- baryon number must be violated,
- C (Charge conjugation) and CP (charge×parity) must not be conserved,
- the system needs to undergo an out-of-equilibrium period.

The first condition is somewhat obvious, if starting from $B = 0$ one aims at generating $B \neq 0$. The second condition requires both C and CP to be violated. Indeed, for a given process $X \leftrightarrow i$ in which the particle i bears a non-zero baryon number $N_{b,i}$ and X is any particle, if C were conserved, one would have $\mathcal{M}(X \to i) = \mathcal{M}(\bar{X} \to \bar{i})$ and therefore the global baryon number variation ΔB would be approximately given by the difference between baryon number creation Δb and antibaryon number creation $\Delta\bar{b}$:

$$\Delta B = \Delta b - \Delta\bar{b} \propto N_{b,i} \sum_X |\mathcal{M}(X \to i)|^2 + N_{b,\bar{i}} \sum_X |\mathcal{M}(\bar{X} \to \bar{i})|^2, \tag{1.18}$$

As $N_{b,i} = -N_{b,\bar{i}}$, one trivially observes that no baryon number can be generated.
If CP is conserved, then $\mathcal{M}(X \to i) = \mathcal{M}(i \to X) = \mathcal{M}(\bar{X} \to \bar{i})$, the last equality coming from CPT invariance. Again, it turns out that no excess of baryons over antibaryons can be generated.
Finally, a departure from thermal equilibrium is needed. Indeed, looking at the Boltzmann equation for the number densities, neglecting the expansion term, one has

$$\frac{dn_i}{dt} = \sum_X \int d\Pi_X d\Pi_i \left(n_X(1 \pm n_i)\,\Gamma(X \to i) - n_i\,(1 \pm n_X)\,\Gamma(i \to b)\right), \tag{1.19}$$

where $(1 \pm n)$ are Pauli blocking or stimulating factors, for fermions $(+)$ or bosons $(-)$. If the different species i and X were in thermal equilibrium all along their evolution, we would have

$$n_X(1 \pm n_i) = n_i\,(1 \pm n_X), \tag{1.20}$$

which, combined with the unitary condition:

$$\sum_X |\mathcal{M}(X \to a)| = \sum_X |\mathcal{M}(a \to X)| \tag{1.21}$$

would ensure that $dn_i/dt = 0$.

Another way to see how these three conditions arise is to consider how the baryon number behaves under C, P and T transformations. Being odd under C, we have

$$\langle B \rangle = \langle C\, C^{-1} B \rangle = \langle C^{-1} B C \rangle = - \langle B \rangle \, , \tag{1.22}$$

and so C conservation implies $\langle B \rangle = 0$.

Similarly, B is odd under CP so that the same argument holds.

Finally, in thermal equilibrium the system is described by a density matrix $\rho(t) = e^{-\beta H}$, so that one has

$$\langle B(t) \rangle = tr(e^{-\beta H} B(t)) = tr(e^{-\beta H}\, e^{-iHt} B(0)\, e^{iHt}) = \langle B(0) \rangle \, . \tag{1.23}$$

Given that initially $B(0) = 0$, no baryon asymmetry can be generated if the system is in thermal equilibrium.

These three conditions are the basic requirements that a model should fulfil in order to produce a non-vanishing baryon asymmetry.

1.3 Models of Baryogenesis

Sakharov's conditions can be satisfied in many different ways.

The first attempts to explain the BAU were based on Grand-Unified Theories (GUT) [12]. Indeed, C and CP violation are easily fulfilled, at least qualitatively if the Yukawa couplings are complex and the departure from thermal equilibrium is found to be naturally satisfied during the freeze-out of a heavy particle. Moreover, B violation, which was not known to occur in the SM, is a common by-product of any GUT theory.

1.3.1 GUT baryogenesis

The early realisations of GUT baryogenesis were based on the $SU(5)$ gauge group, in which a superheavy field, whose mass is related to the various breaking scales (usually 10^{12} GeV $\lesssim M_X \lesssim M_{GUT} \simeq 10^{16}$ GeV), decays when the temperature drops below its mass. This implies a Boltzmann suppression of inverse-reactions, and thus out-of-equilibrium decays. Under the condition that the X couplings to its decay-products are complex, these decays can produce a non-zero Baryon number, which was supposed to remain constant during the subsequent cooling of the Universe.

However, as already stated by Dimopoulos and Suskind in [12], "a quantum mechanical source of baryon-number violation (...) is possible (...) to seriously alter the results of this [paper]".

Indeed, in 1976, 't Hooft [13] showed that non-perturbative effects, which he called instantons, and which emerge from the SM gauge structure, are a possible source of B violation. This violation occurs due to the tunneling over an energy-barrier of the instantons. However, this instanton-effect was calculated in zero-temperature field theory, and the probability for such a

B violation to occur was shown to be exponentially suppressed.

Taking temperature into account, Kuzmin, Rubakov and Shapovnikov showed in 1985 [14] that while the tunnelling through the energy barrier was exponentially suppressed, a non-static gauge field configuration, lying on the top of the energy barrier, allows B violating processes to quantitatively occur. More precisely, they showed that this field configurations, called sphalerons, are in equilibrium for $10^2\,\text{GeV} \lesssim T \lesssim 10^{12}\,\text{GeV}$. These processes violate $B+L$, the excess of which they rapidly wash-out, whilst conserving the orthogonal $B-L$. We refer the reader to appendix A, where sphalerons are discussed in more detail.

The GUT early attempts were $B-L$ conserving, and given that any $B+L$ number created before sphalerons come into equilibrium is completely erased, such GUT-baryogenesis were ruled-out. It is customary now to effectively add another condition to Sakharov's three, which could be formulated as "Prevent B number creation from being erased by sphalerons". There are many ways to do so. For example, GUT models in which a $B-L$ number is created are not affected by sphalerons erasure, as we will see in chapter 6.

1.3.2 Electroweak baryogenesis

Another class of models consists in the electroweak-baryogenesis mechanism [16]. While GUT-baryogenesis was based on the out-of-equilibrium decays of a superheavy field, electroweak-baryogenesis relies on the possibility of having a strong departure from thermal equilibrium during the electroweak (EW) phase transition, when the Higgs field(s) acquires a non-zero vaccum expectation value (vev). The mechanism can be roughly described as follows. Assuming the electroweak phase-transition to be of first order, then, during the transition, two degenerate vacua will coexist, one corresponding to the broken phase, with $\langle\phi\rangle \neq 0$, while the other corresponds to the symmetric phase $\langle\phi\rangle = 0$. As the temperature drops down, the regions of broken phase grow until they fill all the space, a phenomena called "bubble nucleation".

In the SM, the only source of CP violation resides in the δ_{KM} phase of the CKM^2 mixing matrix for quarks, *i.e.* originates from the non-degeneracy of up and down quark type masses. As fermion mass generation is closely related to the Higgs mechanism, it is natural to think that CP will be violated during the EW phase-transition, when going from the unbroken phase $T \geq T_{EW}$ into a bubble of true vacuum $T \leq T_{EW}$.

Since sphalerons are in equilibrium for $T \geq T_{EW}$, but highly suppressed for lower temperatures, the creation of a net B number in the unbroken phase, close to the bubble frontier, can result in a non-zero B number in the broken phase if the phase transition is fast enough compared to the characteristic time of the sphaleron erasure.

Actually, it has been shown that electroweak-baryogenesis does not work in the SM.

The first reason lies in not having enough sources of CP violation to account for the observed baryon asymmetry [17]. The second reason comes from the fact that the strong first-order phase-transition needed for this mechanism to occur requires the Higgs mass to be small, $m_H \lesssim 40\,\text{GeV}$

---

[2] Cabibbo-Kobayashi-Maskawa.

in the SM. Given the LEP result, $m_H^{SM} \gtrsim 114\,\mathrm{GeV}$ [18], the electroweak-scale SM baryogenesis is clearly ruled out.

Supersymmetric extensions of the SM could solve this problem [19], by increasing the number of CP violating sources, and providing a sufficiently first-order phase-transition. For the minimal supersymmetric (MSSM) extensions to work, some fine-tuning is required [20]. Electroweak-baryogenesis in singlet extensions of the MSSM is found to be viable [21].

We do not consider this class of mechanism in this thesis.

1.3.3 Affleck-Dine baryogenesis

This class of models relies on flat directions of the supersymmetric scalar potentials [22]. During inflation, fermion condensates can form along flat directions of the superpotential and can develop large vevs. After inflation these condensates coherently oscillate around their minima, and baryon as well as lepton number can be stored in these oscillations.

Albeit being an interesting possibility, we will also not study Affleck-Dine baryogenesis here.

1.3.4 Baryogenesis via leptogenesis

There is another class of models for baryogenesis, which has received an increasing amount of attention since the original paper of Fukugita and Yanagida [23]: the leptogenesis mechanism. $SU(2)$ sphalerons violate $B+L$ via the effective interaction term (cf. appendix A)

$$\mathcal{O} = \prod_i q_L^i\, q_L^i\, q_L^i\, \ell_L^i\,. \tag{1.24}$$

On the other hand, the $B-L$ direction is conserved by these sphalerons. Hence the proposal of leptogenesis [24],[25]: a lepton number could be generated from the out-of-equilibrium decays of a heavy field which couples to leptons. Then this lepton number is converted, at least partly, into a baryon number.

This mechanism has the interesting feature of relating the observed baryon asymmetry of the Universe to the yet unexplained fact that the neutrinos are massive particles.

Indeed, in seesaw models, as we will see in the following chapter, the smallness of the light neutrino masses is usually explained through the addition of a heavy field, whose mass scale is typically of order of 10^{10} GeV. This field, which is assumed to be a Majorana spinor, can decay into leptons and anti-leptons, and can furthermore distinguish between them, granted that their couplings are complex.

If the seesaw indeed provides mass to the light neutrinos, leptogenesis occurs, at least qualitatively.

We will see in the next chapters that under a few assumptions this mechanism can naturally accommodate the observed baryon asymmetry.

Chapter 2

Massive neutrinos

Neutrinos have a very long history. Their existance was first postulated in 1930 by Pauli [26] to rescue the principle of energy-momentum conservation in β decays. Thus, neutrinos are even *older* than the Standard Model. In 1962, muon neutrinos were observed [27]. Finaly, tau neutrinos were observed in 2000 by the experiment DONUT at Fermilab [28], and so the tau neutrino became the last observed particle of the SM. Despite this long history, very little is known about neutrinos when compared to other species: neutrinos are elusive particles.

Only left-handed neutrinos have been observed. This is because if a right-handed ν_R would exist, it would be a singlet under the SM gauge group.Furthermore, given the experimental possibilities in the 70's, when the SM was being built, (almost) no evidence of neutrino masses were observed.

Therefore in the SM only the left-handed neutrino component was included. However, this construction faced, from 60's onward, two major problems: the solar and atmospheric neutrino anomalies.

2.1 Evidence for neutrino oscillations

The measurements of neutrino fluxes coming from different sources revealed a discrepency between the expected and the observed signals. This anomaly was observed both in the solar sector [29] and in the flux of muon neutrinos coming from Earth's atmosphere [30], and constitutes one of the first evidences of physics beyond the Standard Model. Here we just briefly discuss this question. We refer the reader to the review of Strumia and Vissani [31] for a quasi-exhaustive presentation of physics where neutrinos are involved.

Solar neutrinos

Historically, this was the first neutrino anomaly. Electron neutrinos are produced in the core of the Sun, according to the fusion reaction

$$4\,p + 2\,e^- \to {}^4He + 2\,\nu_e\,, \tag{2.1}$$

and given the small neutrino cross section, they escape from the core. A flux of ν_e is then measured on Earth. The first evidence came from the Homestake experiment [29], which uses Chlorine through the reaction in a water tank

$$\nu_e + {}^{37}Cl \rightarrow {}^{35}Ar + e^- \ . \tag{2.2}$$

Counting the number of ${}^{35}Ar$, it was possible to determine the flux of solar ν_e. This flux was measured to be only 1/3 of the expected one, hence the solar neutrino anomaly. At that time, it was not clear whether new physics was needed, or if solar models had to be revised. Later on, the SNO experiment [29] was built being sensitive to all neutrino flavours, and also able to discriminate ν_e from $\nu_{\mu,\tau}$. The total neutrino flux was measured to be in agreement with solar model predictions, while the deficit in ν_e was confirmed: whereas only ν_e are expected, all neutrinos flavours were observed. Being confident on the fact that only the electron flavour is created in the Sun, the disappearance of ν_e and the appearance of muon and tau flavours remained to be explained.

Atmospheric neutrinos

Another evidence comes from the detection of neutrinos produced in the upper atmosphere. High energetic cosmic rays enter the atmosphere, and interact with nuclei, thus producing pions. These pions decay into muons, according to

$$\begin{aligned} \pi^+ &\rightarrow \mu^+ + \nu_\mu \,, \\ \pi^- &\rightarrow \mu^- + \bar{\nu_\mu} \ . \end{aligned}$$

The high energetic muons subsequently decay

$$\begin{aligned} \mu^- &\rightarrow e^- + \nu_\mu + \bar{\nu_e} \,, \\ \mu^+ &\rightarrow e^+ + \bar{\nu_\mu} + \nu_e \ , \end{aligned}$$

leading to about a rate for ν_μ which is roughly twice that of ν_e. Atmospheric neutrino experiments measure the value

$$R = \frac{N(\nu_\mu)^{obs}/N(\nu_e)^{obs}}{N(\nu_\mu)^{MC}/N(\nu_e)^{MC}} \,, \tag{2.3}$$

which compares the observed ratio to the expected one. While $R = 1$ is expected, $R \simeq 0.65$ is observed [30]. This points towards an appearance of ν_e and/or a disappearance of ν_μ. The SuperKamiokande experiment [30] settled this question: the deficit from athmospheric neutrinos results from ν_μ disappearance.

Interpretation

Different solutions were advocated to explain these flavour conversions, such as neutrino oscillations [32], neutrino decays (cf ref. 56 of [31]), or decoherence of propagating ν (ref. 44 of [31]): the SK experiment showed that no-oscillation solutions were ruled-out at 4σ [33].

The oscillatory solution has as immediate consequence that neutrinos are massive particles.

2.2 Neutrino mixing in the 3 flavour scheme.

A neutrino involved in EW interaction is not a mass eigenstate. Labelling the mass basis eigenstates by ν_i, $i = 1, 2, 3$ and the flavour basis eigenstate by ν_α, $\alpha = e, \mu, \tau$, they are related through a unitary transformation:

$$|\nu_\alpha\rangle = \sum_{i=1}^{3} U^*_{\alpha i} |\nu_i\rangle \ , \tag{2.4}$$

The matrix U, called the PMNS[1] [34] mixing matrix, is a 3×3 unitary matrix which depends on 3 real mixing angles and on 6 CP-odd phases. Some of these phases can be rotated away by a redefinition of the fields. After this, for a general $n \times n$ unitary matrix, if neutrinos are pure Dirac spinors $n(n-1)/2$ mixing angles and $n(n-1)/2 - (n-1)$ phases remain, while $n(n-1)/2$ mixing angles and $n(n-1)/2$ phases if neutrinos are Majorana spinors. It is customary to express U as a product of three rotation matrices:

$$U = \begin{pmatrix} 1 & 0 & 0 \\ 0 & c_{23} & s_{23} \\ 0 & -s_{23} & c_{23} \end{pmatrix} \cdot \begin{pmatrix} c_{13} & 0 & s_{13}\, e^{-i\delta} \\ 0 & 1 & 0 \\ -s_{13}\, e^{i\delta} & 0 & c_{13} \end{pmatrix} \cdot \begin{pmatrix} c_{12} & s_{12} & 0 \\ -s_{12} & c_{12} & 0 \\ 0 & 0 & 1 \end{pmatrix} .\mathrm{diag}\left(e^{i\phi_1}, e^{i\phi_2}, 1\right) \ , \tag{2.5}$$

with $c_{ij} = \cos(\theta_{ij})$ and $s_{ij} = \sin(\theta_{ij})$. θ_{ij} are real mixing angles and δ the "Dirac" CP phase. If neutrinos are Majorana fields, there are two supplementary phases ϕ_1, ϕ_2, the "Majorana" CP phases, which are absent if neutrinos are Dirac fields.

Given this, the probability for a neutrino that propagates with a mean energy E to oscillate from a flavour α to a flavour β, after having travelled a distance L, is given by

$$\begin{aligned} P(\nu_\alpha \to \nu_\beta) &= \Big| \sum_j U^*_{\alpha\, j} U_{\beta\, j}\, e^{-i \frac{m_j^2 L}{2E_j}} \Big|^2 \\ = \delta_{\alpha\beta} &- 4 \sum_{i>j} \mathrm{Re}\left(U^*_{\alpha\, i}\, U_{\alpha\, j}\, U_{\beta\, i}\, U^*_{\beta\, j}\right) \times \sin^2\left(\frac{\Delta m^2_{i\, j}\, L}{4\, E}\right) \\ &+ 2 \sum_{i>j} \mathrm{Im}\left(U^*_{\alpha\, i}\, U_{\alpha\, j}\, U_{\beta\, i}\, U^*_{\beta\, j}\right) \times \sin\left(\frac{\Delta m^2_{i\, j}\, L}{4\, E}\right) , \end{aligned} \tag{2.6}$$

where $\Delta m^2_{i\, j} = m_j^2 - m_i^2$.

The determination of the mixing parameters results from the measurement of neutrino fluxes coming from different sources and at different distances from the emission source. Together with the natural sources, man-made sources such as reactors [35] or neutrino beams [36], are complementary in determining U.

In the atmospheric sector, the disappearance of ν_μ is explained by an oscillation $\nu_\mu \leftrightarrow \nu_\tau$, whose detection allows to constrain θ_{23} and Δm^2_{23}, therefore called atmospheric mixing angle and (difference of squared) mass(es). In the solar sector, the disappearance of ν_e is explained by $\nu_e \leftrightarrow \nu_\mu$

---

[1] Pontecorvo, Maki, Nakagawa and Sakata.

oscillations, the observation of the latter constraining the solar sector, θ_{12} and Δm^2_{12}. Finally the last sector, the so-called Chooz mixing angle θ_{13} and squared mass difference Δm^2_{13}, intervenes both in solar and atmospheric oscillations and is very constrained by the CHOOZ reactor experiment [35].

We display in fig.(2.1) the status of neutrino mixing in the relevant $(\Delta m^2_{ij} - \theta_{ij})$ plane for the different sectors. It shows the complementarity of natural and man-made sources of neutrinos, leading to the determination of the several parameters.

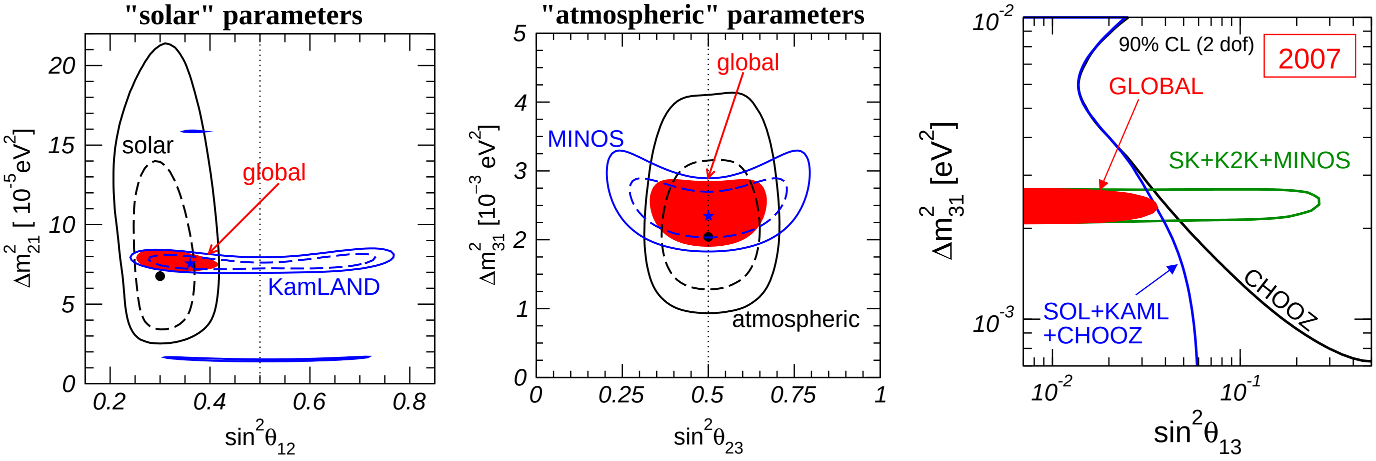

Figure (2.1): Values of squared masses differences and mixings angles determine by global fit of neutrino oscillation data. Figures taken from [37].

The global fit to these oscillation parameters, taken from [37], is given in the following table:

Parameter	Best fit	3σ
$\Delta m^2_{12}/10^{-5}\,\mathrm{eV}$	7.6	7.1–8.3
$\lvert\Delta m^2_{13}\rvert/10^{-3}\,\mathrm{eV}$	2.4	2.0–2.8
$\sin^2\theta_{12}$	0.32	0.26–0.40
$\sin^2\theta_{23}$	0.50	0.34–0.67
$\sin^2\theta_{13}$	0.007	≤ 0.050

The atmospheric mixing angle is observed to be maximal, while the solar angle is large but non-maximal, at a very high level of confidence. The last mixing angle θ_{13} is still only upper-constrained. The precise value of this mixing angle is very important, since it is necessary for it to have a non-zero value if CP violation coming from the Dirac CP phase is to be experimentally observed. The observation of a non-zero value for θ_{13} could also allow to determine the neutrino mass ordering. As of today the sign of $\Delta m^2_{13} \simeq \Delta m^2_{23}$ remains unknown, leaving two possibilities for the neutrino spectrum: either the mass ordering is normal hierarchic, with $m_1 \leq m_2 \leq m_3$, or it can be inverse hierarchic with $m_3 \leq m_1 \leq m_2$. Considering the oscillation probability, we see that only the third term

$$\propto 2\sum_{i>j} \mathrm{Im}\left(U^*_{\alpha\, i}\, U_{\alpha\, j}\, U_{\beta\, i}\, U^*_{\beta\, j}\right) \times \sin\left(\frac{\Delta m^2_{ij}\, L}{4\, E}\right) \tag{2.7}$$

can lift this degeneracy. Since the Jarlskog invariant [38],

$$|U^*_{\alpha\, i}\, U_{\alpha\, j}\, U_{\beta\, i}\, U^*_{\beta\, j}| \equiv J = s_{12}\, c_{23}\, s_{23}\, c^3_{13}\, s_{13}\, \sin(\delta)\,, \tag{2.8}$$

depends on sin(θ_{13})sin(δ), we see that a non-zero value of θ_{13} is crucial.
The oscillation experiments provided the first proof that neutrinos are massive. Nevertheless, these oscillations neither depend on the neutrino mass scale nor on the nature of neutrinos, that is, on having Dirac or Majorana neutrinos. In the last case, two additionnal CP violating phases $\phi_{1,2}$ exist, which do not enter in the oscillation probability.
Hence, non-oscillation experiments are required in order to complete the picture.

2.3 Non-oscillation experiments

Cosmology

It may not be straightforward how cosmological observations could constrain neutrino parameters. Nevertheless, robust constraints are derived, when different observations are combined [39]. Were neutrinos massive enough, they would have contribute to distort the photon power spectrum during recombination. Observations of the CMB alone [40] give an upper-bound on m_ν:

$$\Sigma m_\nu \lesssim 1.3\,\mathrm{eV}\,(95\%\mathrm{C.L.})\,. \tag{2.9}$$

The effect of neutrinos is not seen on the CMB, but rather on large scale structure formation. Being massive, neutrinos carry a fraction of the total mass density, Ω_m, which has been precisely measured by WMAP, for instance. However this mass fraction is small. Furthermore, neutrinos have an important free-streaming length ℓ_F, since they are only charged under $SU(2)$. Therefore, on scales that are smaller than ℓ_F, neutrinos are unable to cluster, that is, to participate in the formation of large-scale structures, the clustering on these scales being somewhat delayed. As the temperature of the Universe lowers, neutrinos become non-relativistic and their free-streaming length is reduced. Hence neutrinos begin to cluster, as ordinary matter. Therefore, the heavier the neutrinos are, the earlier do they cluster, allowing large-scale structure formation at higher temperature (earlier times).
The constraint on neutrino mass from WMAP 5 year analysis, including many different observations, reads [40]

$$\Sigma m_\nu \lesssim 0.61\,\mathrm{eV} \quad (95\%\mathrm{C.L.})\,. \tag{2.10}$$

Beta decay

The beta decay experiment constitutes the best direct test of neutrino masses. The effect of neutrino masses is to distort the end-point of the beta-decay energy spectrum of the beta decay. Indeed, in the decay

$$d \to u + e^- + \overline{\nu_e}\,, \tag{2.11}$$

the energy of the electron is $E_e = Q - E_\nu$, which is maximal for $E_e = Q - m_\nu$. Here Q stands for the energy released in the β decay, *e.g.* for tritium beta decay, ${}^3H \to {}^3He + e + \overline{\nu_e}$, $Q = m_{^3H} - m_{^3He} \simeq 18.6$ keV.
Around the end-point, the energy spectrum of the electron is $\propto \sqrt{(Q-E_e)^2 - m_{\nu_e}^2}$, and so $m_{\nu_e} \neq 0$ will imply a deviation from the line $Q - E_e$. So far, the best constraint comes from MAINZ [41] and TROITSK [42] experiments:

$$m_{\nu_e} \lesssim 2.2\,\mathrm{eV}\,. \tag{2.12}$$

The future beta decay experiment, Katrin [43], which is schedules to begin data taking on 2010, is expected to reach a sensivity of 0.2 eV to neutrino masses.

Neutrinoless double-beta decay

The experiments of neutrinoless double-beta decay [44] are very important for neutrino physics, since the observation of such a process would imply that neutrinos are Majorana particles. As can be seen in fig.2.3, $0\nu\,\beta\beta$ consists in the reaction

$$(A, Z) \to (A, Z+2) + 2\,e^-\,, \tag{2.13}$$

which violates lepton number by two units.

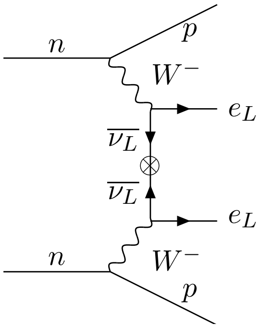

Figure (2.2): Feynman diagram for neutrinoless double-beta decay.

The decay rate for this process,

$$\Gamma_{0_\nu\,\beta\beta} \propto |\mathcal{M}|^2\, |m_{ee}|^2\,, \tag{2.14}$$

depends on m_{ee} which is the ee entry of the neutrino mass matrix

$$\begin{aligned} m_{ee} &= \sum_i U_{ei}^2\, m_i \\ &= \cos^2(\theta_{13}) \left(m_1\, e^{2\mathrm{i}\,\phi_1} \cos^2(\theta_{12}) + m_2\, e^{2\mathrm{i}\,\phi_2} \sin^2(\theta_{12}) \right) + m_3 \sin^2(\theta_{13})\,. \end{aligned} \tag{2.15}$$

We see that these processes also depends on the Majorana CP violating phases $\phi_{1,2}$. However, there is an uncertainty of order $\mathcal{O}(3)$ on the nuclear matrix elements, which further depend on the nuclei used [31].

The status of $0\nu\,\beta\beta$ is controversial, since the observation of a positive signal has been claimed by members of the Heidelberg-Moscow experiment [45], corresponding to $|m_{ee}| \lesssim 0.1 - 0.9\,\mathrm{eV}$, but this signal has not been confirmed by, for example NEMO or CUORICINO [44], which obtained the bounds $|m_{ee}| \lesssim 0.7 - 1.2\,\mathrm{eV}$ and $|m_{ee}| \lesssim 0.2 - 0.9\,\mathrm{eV}$, respectively. Hence the importance of future $0\nu\,\beta\beta$ experiments.

2.4 Neutrino mass models

The observation of neutrino oscillations lead us to the conclusion that neutrinos are massive particles, which necessarily implies to somehow extend the Standard Model. In fact, these observations provided the first evidence of physics beyond the SM.

It has been noticed by Weinberg [46] that, given the quantum numbers of lepton and Higgs fields, the Lagrangian can contain the following non-renormalisable dimension 5 operator

$$\mathcal{L}^{d=5} = \frac{1}{2}\, f_{\alpha\,\beta} \left(\overline{\ell^c_{L\,\alpha}}\, \tilde{\phi}^* \right) \left(\tilde{\phi}^\dagger\, \ell_{L\,\beta} \right) , \tag{2.16}$$

which violates lepton number by two units. Actually, this operator is the only dimension 5 operator built out of SM fields, and invariant under the SM gauge group.

After the Higgs develops a vev, this term gives a Majorana mass to the light neutrinos $m_\nu \simeq f_{\alpha\beta}\, v^2$, the smallness of m_ν coming from the smallness of f. In Weinberg's paper, the coefficient $f_{\alpha\beta}$ was expected to be $\propto M^{-1} \lesssim 10^{-12}/m_W$, hence producing a neutrino mass $m_\nu \simeq 10^{-5} - 10^{-1}\,\mathrm{eV}$.

This operator may result from an underlying theory, where light neutrinos couple to some field, stabilised at some high scale M, the integration of which would give rise to the Weinberg operator eq.(2.16). Thus, the appealing feature that light neutrino masses could be a window to (very) high energy physics.

There is other possibilities to generate neutrino mass. For example, a natural solution is to introduce right-handed neutrinos, which couple to the left ones via an additional Yukawa coupling λ, the smallness of m_ν being explained by the smallness of λ. This coupling should then be $\lesssim 10^{-12}$.

Many other possibilities and models can account for neutrino masses. Given the SM field content, let us see what are the possible extensions.

For that purpose we consider the following fields, whose quantum numbers under $SU(3) \times SU(2)_L \times U(1)_Y$ are given below:

field	label	G_{321}
lepton doublet	ℓ_L	$(\mathbf{1},\mathbf{2},\mathbf{-1/2})$
charged lepton singlet	e_R	$(\mathbf{1},\mathbf{1},\mathbf{-1})$
neutral lepton singlet	ν_R	$(\mathbf{1},\mathbf{1},0)$
Higgs doublet	ϕ_d	$(\mathbf{1},\mathbf{2},-1/2)$
Higgs doublet*	ϕ_u	$(\mathbf{1},\mathbf{2},1/2)$

In the above notation, we label the SM Higgs field ϕ_d, while $\phi_u \equiv \tilde{\phi_d} = \mathrm{i}\,\sigma_2\,\phi_d^*$, σ_2 being the Pauli matrix.

Given the fields considered, it is straightforward to determine the possible extensions of the SM which would give masses to the neutrinos either at tree level or due to radiative corrections:

Extension of the Higgs sector			
Product	G_{321}	field	mass term
$\ell_L \otimes \ell_L$	$(\mathbf{1},\mathbf{1},-1)$	singlet scalar η^+	Majorana (LH) mass
$\ell_L \otimes \ell_L$	$(\mathbf{1},\mathbf{3},-1)$	triplet scalar Δ	Majorana (LH) mass
$e_R \otimes e_R$	$(\mathbf{1},\mathbf{1},-2)$	singlet scalar k^{++}	Majorana (RH) mass
Extension of the fermionic sector			
$\ell_L \otimes \phi_u$	$(\mathbf{1},\mathbf{1},\mathbf{0})$	singlet ν_R	neutrino Dirac type mass
$\ell_L \otimes \phi_u$	$(\mathbf{1},\mathbf{3},\mathbf{0})$	triplet Σ	Majorana (LH) neutrino mass

In the above table, RH and LH denote right and left handedness, respectively. In addition to the mass terms above, the right-handed neutrinos can also have a Majorana mass term $\overline{\nu_R}_i\,\nu_{Rj}M_{ij}$, appearing as a bare mass term in the SM potential. As stated above, the minimal extension of the SM consists in including right-handed neutrinos (RHn) which couple to left-handed ones via $\lambda_{ij}\,\ell_L\,\phi_u\,\overline{\nu_R} + h.c.$. When ϕ acquires a vev, this term provides a conventional Dirac type mass for neutrinos $m_\nu\,(\nu_L\,\overline{\nu_R} + \overline{\nu_L}\,\nu_R)$. For neutrino masses of $m_\nu \lesssim 0.5\,\mathrm{eV}$, the neutrino Yukawa coupling should be $\lambda \lesssim 10^{-12} \sim 10^{-6}h_e$, where h_e is the Yukawa coupling of the electron. Such a model is perfectly viable; after all $h_e \sim 10^{-6}\,h_t$. This model, called νMSM, has been studied for example in [47], and has several cosmological implications.

Nevertheless, one could argue (even if this cannot be seen has a proof on itself) that since the inclusion of right-handed neutrinos induces a violation of the lepton number, it is quite natural to link it to some high energy scale at which $B-L$ is broken. Another argument is that such small couplings, even if possible, are non-natural. We adopt this point of view and do not consider this scenario.

In the Zee [48] or Zee-Babu [49] models, which are based on the inclusion of the fields η^+ and k^{++}, neutrino masses emerge from radiative effects at either one or two loops, and the suppression of neutrino masses comes from these loop factors. We do not consider here these models, but examine the class of seesaw models explained hereafter, in which neutrino masses are generated at tree level and which up to now provides the preferred explanation for neutrino masses.

2.5 Seesaw models

Common to all these models, is having a suppression of the neutrino mass which indirectly originates from the introduction of a new mass scale, typically far higher than the electroweak scale.

2.5.1 Fermion singlet: type I seesaw

This mechanism was originally the first of the seesaw class [50], and originates from grand unification theory. Indeed, in $S0(10)$ models, the minimal representation which is complex and anomaly free, is a **16** spinorial representation. This representation contains all SM fermions fields of one generation plus one extra field, singlet under the SM gauge group, which can be identified as a right-handed neutrino.

In these GUT models, typically the RHn is not a gauge singlet. It couples to some Higgs representation, which acquires its vev at a high scale, of order $10^{12} - 10^{16}\,\mathrm{GeV}$. Integrating out this heavy field at the electroweak scale gives the effective term eq.(2.16).

Such a GUT embedding is nevertheless not necessary at all, since the Majorana mass term can be put by hand as a bare mass term in the Lagrangian, the right-handed neutrino being singlet under G_{321}. In such a case, the neutrino Yukawa sector reads

$$\mathcal{L}_\nu = -\lambda^\dagger_{\alpha\, i}\, \nu_R^i\, \overline{\ell}_\alpha\, \phi_u^* - \frac{1}{2}\, M_{ij} \overline{\nu_R^c}^i \nu_R^j + h.c.\,, \tag{2.17}$$

where $\psi^c = C\,\overline{\psi}^T$ is the charge conjugated of ψ.

After the SM Higgs acquires its vev,$\langle \phi_u \rangle = v \simeq 174\,\mathrm{GeV}$, the first term provides a Dirac mass for the neutrinos

$$\mathcal{L}_\nu \supset -m_D^{\alpha\, i}\, \overline{\nu_L}^i\, \nu_R^j\,, \tag{2.18}$$

with

$$m_D = \lambda\, v/\sqrt{2}\,. \tag{2.19}$$

Using the identity

$$\overline{\nu_L}\, \nu_R = \frac{1}{2}\left(\overline{\nu_L}\, \nu_R + \overline{\nu_R^c}\, \nu_L^c\right)$$

the above mass term can be written

$$\mathcal{L}_\nu = -\frac{1}{2}\, \left(\overline{\nu_L}, \overline{\nu_R^c}\right) \begin{pmatrix} 0 & m_D \\ m_D^T & M \end{pmatrix} \begin{pmatrix} \nu_L^c \\ \nu_R \end{pmatrix}.$$

Assuming $M \gg m_D$, the diagonalisation of the matrix above gives us two eigenstates per generation, which are Majorana spinors. At leading order, one state is given by

$$N = \nu_R + \nu_R^c$$

with mass M. For now we will call this state *the* right-handed neutrino. The other state is at leading order

$$\nu = \nu_L + \nu_L^c ,$$

mostly composed of the left-handed neutrino, as implied from low energy observations. The mass of this light neutrino is given by the seesaw relation [50]:

$$m_\nu^{ij} = v^2 \lambda_{ik} \, M_k^{-1} \, \lambda_{jk} , \tag{2.20}$$

in the basis where M is diagonal.
The light neutrino mass matrix is diagonalised by the PMNS matrix U introduced earlier:

$$D_m = U^T \, m_\nu \, U , \tag{2.21}$$

where $D_m = \mathrm{diag}(m_1, m_2, m_3)$.
In addition to the nine low-energy parameters, enlarging the fermionic sector by three right-handed neutrinos provides nine extra parameters: three masses + three mixing angles + three CP violating phases. There are different ways of parametrising these unknown parameters, namely the bottom-up approach, where one fixes the low-energy sector to reconstruct the high-energy one, or the converse top-down approach in which one fixes the high-energy sector. These two parametrisations are useful depending on whether one considers either an effective or a full theory, respectively. In this thesis we use the intermediate Casas-Ibarra [51] parametrisation, where one fixes both low and high energy parameters to infer the neutrino Yukawa coupling λ. This useful parametrisation derives from the fact that since $\lambda.\lambda^\dagger$ is an hermitian matrix, it can be diagonalised by an orthogonal matrix R, satisfying $R.R^T = 1$. The matrix R is parametrised in terms of three complex angles. Here we use the following parametrisation

$$R = \begin{bmatrix} c_3 c_2 & c_3 s_2 & s_3 \\ -c_1 s_2 - s_1 s_3 c_2 & c_1 c_2 - s_1 s_3 s_2 & s_1 c_3 \\ s_1 s_2 - c_1 s_3 c_2 & -s_1 c_2 - c_1 s_3 s_2 & c_1 c_3 \end{bmatrix} , \tag{2.22}$$

where, as for the PMNS matrix, $c(s)_{ij} = \cos(\sin)(z_{ij})$, the z_{ij}s being complex angles. One can therefore reconstruct λ, according to

$$\lambda_{1\alpha} = \left(\sqrt{M}.R.\sqrt{m}.U^\dagger\right)_{1\alpha} , \tag{2.23}$$

where $M = \mathrm{diag}(M_1, M_2, M_3)$ is the heavy neutrino mass matrix. Hence, in this parametrisation, among the 18 parameters, 15 are free: in the low energy sector, once the solar and atmospheric Δm^2 and mixing angles are fixed, the neutrino mass scale -min(m_i)- and the mass ordering -sign(Δm_{13}^2)- remain free, as well as the mixing angle θ_{13} and the three CP phases $\delta - \phi_{1,2}$. In the high energy sector, the R matrix and the 3 right-handed neutrinos masses are unconstrained, hence there are 9 free parameters [2]. As stated above, among these parameters, min(m_i), θ_{13},

---

[2] Actually there are 3 more degrees of freedom which are the CP parities of the RHns, and one should use $R' = R.\mathrm{diag}(\pm 1, \pm 1, \pm 1)$, with R given by eq.(2.22). Here we consider the case $R' = R$.

sign(Δm^2_{23}) and δ are expected to be determined in a near future, whereas the 11 remaining parameters will probably not. This is clearly a problem if one wants to make some predictions, hence the will to reduce this number. There are different ways to do so.
In the above discussion, we assumed that 3 right-handed neutrinos are added to the SM particle content. Actually, the minimal extension of the SM requires only 2 RHns to generate the 2 oscillation frequencies. In this model [52], the lightest LH neutrino is massless $\min(m_i) = 0$, hence the 6 yet free low-energy parameters are reduced to 4, since additionnaly the Majorana CP violating phase associated to $\min(m_i)$, ϕ_1, can be rotated away. Furthermore, the high-energy sector reduces to 4 unknowns, although there is little experimental or theoretical support for this hypothesis.

2.5.2 Scalar triplets: type II seesaw

This model consists in the addition of a scalar triplet Δ charged as $(\mathbf{1},\mathbf{3},\mathbf{1})$ under $SU(3) \times SU(2)_L \times U(1)_Y$ [53]. This field is a real scalar triplet under $SU(2)$, which lies in the adjoint representation. Δ can couple to a product of two left-handed fields. Writing

$$\Delta = \begin{pmatrix} \Delta^+ & \sqrt{2}\,\Delta^{++} \\ \sqrt{2}\,\Delta^0 & -\Delta^+ \end{pmatrix}, \tag{2.24}$$

and assuming that Δ takes a non-zero vev along its $U(1)_{em}$ singlet direction, $\langle \Delta^0 \rangle = v_L \neq 0$, a Majorana mass term for light neutrinos can be generated. Indeed, since $Q_Y(\Delta) = -2\,Q_Y(\ell_L)$, we have in the Lagrangian the additional term

$$\mathcal{L} \supset -\frac{1}{2}\, f_{ij}\, \ell^T_{L\,i}\, \Delta\, (\mathrm{i}\sigma_2)\, C\, \ell_{L\,j} \overset{\langle \Delta^0 \rangle = v_L}{\longrightarrow} -\frac{1}{2}\left(m^{II}_\nu\right)_{ij}\, \nu^T_{L\,i}\, C\, \nu_{L\,j}\,. \tag{2.25}$$

In this so-called type II seesaw, the light-neutrino mass is given by $m_\nu = f\, v_L$ and its suppression originates from the small vev of Δ^0 $v_L \ll v$. This smallness can be understood from the other couplings of the triplet that are allowed in the Lagrangian, in particular its coupling with the SM Higgs doublet ϕ_d:

$$\mathcal{L}_\Delta \supset -\mu_\Delta\, \phi^T_d\, (\mathrm{i}\sigma_2)\, \Delta\, \phi_d - M^2_\Delta\, \mathrm{Tr}(\Delta^\dagger\, \Delta) + ... \tag{2.26}$$

where the dots represent higher order couplings. When ϕ and Δ develop their vev, assuming $M_\Delta \gg v$, one obtains a seesaw like relation between v_L and v:

$$v_L = -\frac{\mu_\Delta\, v^2}{M^2_\Delta} \ll v\,. \tag{2.27}$$

This ensures the smallness of m^{II}_ν. This mechanism naturally occurs in GUT models, where scalar triplets are contained in the higher dimensional represention of Higgses used to break the GUT group down to the SM. In such a GUT framework, it is frequent that both type I and type II seesaw mechanisms occur.

2.5.3 Fermion triplets: type III seesaw

Finally, a third type of seesaw mechanism can occur, where fermion triplets Σ are added to the SM particle content [54]. These fermion triplets couple to leptons via additional couplings $\propto \lambda_\Sigma \, \overline{\ell} \, \phi_u \, \Sigma + h.c.$. Since these triplets reside in the adjoint representation of $SU(2)_L$, a Majorana mass term for Σ is allowed $\propto M_\Sigma \, \overline{\Sigma} \, \Sigma^c$. In these scenarios, masses for the light neutrinos are generated according to:

$$m_\nu^{III} = -\frac{v^2}{2} \, \lambda_\Sigma^T \, M_\Sigma^{-1} \, \lambda_\Sigma \,, \tag{2.28}$$

which is similar to the type I seesaw formula.

Probing the seesaw ?

All these mechanisms are built to account for a suppressed light neutrino mass. However, the scale at which $B - L$ is violated depends on the model and on its input parameters, naturally implying very different low-energy signatures [55]. It would be very interesting to determine which scenario is the most likely to occur, since this knowledge has important implications, notably in the building of a high energy model consistent with low-energy data.

Seesaw and leptogenesis

The seesaw models share the interesting feature that the light neutrino mass is suppressed owing to the introduction of a intermediate scale -M, M_Δ or M_Σ- between the SM one and the GUT one, the seesaw scale, at which the lepton number is violated. This is a welcome by-product of seesaw, which is used in leptogenesis models. In chapters 3, 4 and 5, we will investigate leptogenesis in type I seesaw, while leptogenesis in type I+II seesaw is studied in chapter 6. We do not consider leptogenesis in the type III seesaw. In [56], it has been found that the role played by Σ in leptogenesis is similar to the one played by fermion singlets.

Chapter 3

Leptogenesis in the single flavour approximation

In the previous chapter we have seen that the seesaw mechanism, in addition to explaining neutrinos masses and mixings, implies the violation of lepton number. This L violation is a welcome by-product of these models, and is the building-block of the Fukugita and Yanagida seminal paper [23], where the foundations of leptogenesis were first laid.

In this chapter, we introduce leptogenesis in the so-called one-flavour approximation [57, 58, 59], which in most cases provides good estimates of the baryon asymmetry. Here we focus our discussion on the type I seesaw, the type II being latter addressed in chapter 6.

3.1 Basics of leptogenesis

In the type I seesaw model, the added right-handed neutrinos are very heavy particles, and only interact with leptons and the Higgs boson, via their Yukawa couplings. Being heavy, the right-handed neutrinos decouple early from the thermal bath. When they decouple, their decay will create leptons and antileptons, and if CP is violated during these decays, an excess of leptons over antileptons can be obtained. Once right-handed neutrinos are completely frozen out, the lepton-antilepton asymmetry will evolve without being affected, as all other processes are CP conserving. Then the fast $B + L$ violating processes that are in-equilibrium partly convert this lepton asymmetry into a baryon asymmetry. This very rough picture highlights the three main features of leptogenesis:

- A lepton-antilepton asymmetry is created due to CP-odd couplings/processes.
- At the same time, leptons and antileptons are liable to inverse reactions that potentially wash-out the asymmetry.
- Sphalerons partly convert the lepton asymmetry into a baryon asymmetry.

We will discuss the different points in detail hereafter, but let us first give a qualitative picture of thermal leptogenesis.

The right-handed neutrinos are assumed to be Majorana spinors, and so can decay into both lepton and antilepton, due to the Yukawa coupling

$$\mathcal{L} \supset \lambda_{\alpha i}\overline{N}_i \, \ell_\alpha \, \phi + \lambda^\dagger_{\alpha i} \, N_i \, \overline{\ell}_\alpha \, \phi^* \, , \tag{3.1}$$

ℓ_α being the lepton doublet of flavour α, while ϕ is the SM Higgs doublet.

As we saw in the previous chapter, this coupling λ is in all generality a 3×3 complex matrix, which, if complex, implies that N_i's interactions distinguish between leptons and antileptons: a CP asymmetry can be created in the decays of RHns. This CP asymmetry is defined by the difference between the decay rate into leptons and antileptons

$$\varepsilon_{CP} \equiv \frac{\Gamma(N \to \ell\phi) - \Gamma(N \to \overline{\ell\phi})}{\Gamma(N \to \ell\phi) + \Gamma(N \to \overline{\ell\phi})} \, . \tag{3.2}$$

In the thermal scenario of leptogenesis, a population of right-handed neutrino is first created from the thermal bath via inverse decays $\ell\phi \to N$, $\overline{\ell\phi} \to N$ and scatterings. From these inverse decays and scatterings a lepton asymmetry is produced, defined as:

$$Y_L \equiv \frac{n_L - n_{\overline{L}}}{s} \, , \tag{3.3}$$

where $Y_x = n_x/s$ is the comoving number density, the number density to entropy density ratio. During the thermalisation of RHns, Y_L is proportionnal to $-\varepsilon_{CP} Y_N$.

Then, as the temperature of the Universe decreases, RHns begin to decouple and decay, creating an asymmetry $\propto \varepsilon_{CP} Y_N$, that potentially cancels out with the former one. However, during and after thermalisation of RHns, the lepton asymmetry undergoes washout processes and so is partly depleted. An exact cancellation is therefore avoided. The surviving asymmetry is then $\propto \varepsilon_{CP} \, Y_N \, (1 - 1/C_{wo}) \simeq \varepsilon_{CP} \, \eta \neq 0$, where $C_{wo} \gtrsim 1$ reflects the washout of the asymmetry. η is called the efficiency factor; it reflects the competition between production and depletion of the asymmetry, as well as the ability of those process to thermalise the N's. In thermal leptogenesis, $\eta \simeq \mathcal{O}(0.1)$. The overall factor is the equilibrium density of RHn at the beginning of the leptogenesis epoch, and is roughly 10^{-3}. A baryon asymmetry is then generated owing to sphaleron processes that partly convert the L asymmetry into a B asymmetry, with a conversion factor that depends on the model and on the temperature, but is roughly $-1/2$.

The amount of baryon asymmetry produced by leptogenesis is then approximately

$$Y_B \simeq - \times 10^{-3} \, \eta \, \varepsilon_{CP} \, , \tag{3.4}$$

a value to be compared with the observed baryon asymmetry (cf appendix B for relating Y_X to n_X):

$$Y_B^{obs.} = \frac{n_b - n_{\overline{b}}}{s} = \frac{\eta_B}{7.04} \simeq 8.7 \times 10^{-11} \, . \tag{3.5}$$

It implies that the CP asymmetry generated in RHn decays is required to be

$$\varepsilon_{CP} \gtrsim \text{few } \times 10^{-7} \ , \tag{3.6}$$

which constrains the parameters of the model. Let us now discuss the different points in more detail.

3.2 CP violation

We have defined ε_{CP} as the difference between the decay rate into leptons and antileptons. This CP asymmetry emerges from the interference between the tree level decay rate and the 1-loop corrected one. Indeed, at tree level, for the decay of a right handed neutrino, and given that $\Gamma(N_i \to \ell_\alpha \phi) \propto |\lambda_{\alpha i}|^2$ and $\Gamma(N_i \to \overline{\ell_\alpha \phi}) \propto |\lambda^\star_{\alpha i}|^2$, trivially no CP asymmetry is possible.
If we define the tree level decay amplitude by $\mathcal{A}_{tree} = \alpha$, the CP conjugate process is $\overline{\mathcal{A}}_{tree} = \alpha^\star$, and their respective one-loop corrections are $\mathcal{A}_{1-loop} = \alpha\beta\mathcal{F}$ and $\overline{\mathcal{A}}_{1-loop} = \alpha^\star\beta^\star\mathcal{F}$, where $\mathcal{F}$ is related to the loop function, and β is some dimensionless coupling, then the CP asymmetry is given by

$$\begin{aligned} \varepsilon_{CP} &= \frac{\int [\mathcal{D}] \left(|\alpha \, (1+\beta\mathcal{F}) \, |^2 - |\alpha^* \, (1+\beta^*\mathcal{F}) \, |^2 \right)}{\int [\mathcal{D}] \left(|\alpha \, (1+\beta\mathcal{F}) \, |^2 + |\alpha^* (1+\beta^*\mathcal{F}) \, |^2 \right)} \ , \\ &\simeq -2 \, \mathrm{Im}\, \{\beta\} \ \mathrm{Im} \left\{ \int [\mathcal{D}]\mathcal{F} \right\} \ , \end{aligned} \tag{3.7}$$

where $\int [\mathcal{D}]$ stands for phase-space integration.
We see that a non-vanishing ε_{CP} requires both β and $\mathcal{F}$ to be complex, *i.e.* the 1-loop corrections have to develop an absorptive part, that is, on-shell particles must be running in the loop. Moreover, the tree level and the loop corrections have to differ by a relative phase which comes from β.

Evaluation of ε_{CP}

In this model, the CP asymmetry arises from the interference between the tree level decay diagram and the one-loop corrections, whose Feynman diagrams are depicted in fig.(3.1).

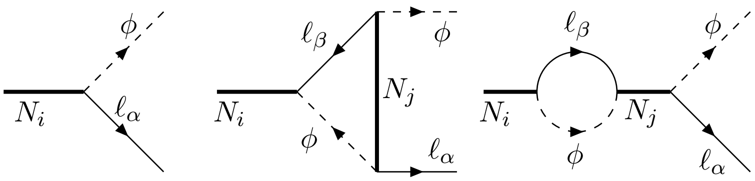

Figure (3.1): One-loop diagrams contributing to the asymmetry from the N_i decay.

There are two types of corrections to the tree level diagram (a): one from the vertex correction (b) and another one from the self-energy correction (c) [60]- [61], with

$$\varepsilon_{CP} = \varepsilon_{CP}^{vertex} + \varepsilon_{CP}^{self} \,.$$

Since the decaying right-handed neutrinos are unstable particles, one cannot handle them in terms of asymptotic *in*- and *out*- states. One should rather deduce their properties from their on-shell contribution to lepton-lepton scatterings [62]. The latter being stable, the usual formalism applies. Then, from the $S-$matrix elements of such scatterings, the CP violating properties of RHn decays are inferred.

Nevertheless, it appears that in the case where the differences between RHn masses are large compared to their width differences, that is if $|M_{N_i} - M_{N_j}| \gg |\Gamma_i - \Gamma_j|$, the naïve calculation and the careful one give the same results. We first assume such non-degeneracy of RHn masses, and evaluate ε^{vertex} and ε^{self} in the naïve prescription. We then discuss the resonant regime, and how it affects the self-energy contribution.

Evaluation of $\varepsilon_{CP}^{vertex}$

For the process $N_i \to \ell_\alpha H$, the tree level amplitude reads

$$\mathrm{i}\,\mathcal{M}_{i,\alpha}^{0} = \mathrm{i}\,\lambda_{\alpha i}^{*}\,\overline{u}_{\ell_\alpha}(p_\ell)\,\mathrm{P_R}\,u_{N_i}(p_N)\ , \tag{3.8}$$

where $\mathrm{P_{R(L)}}$ is the right(left) chirality projector $\mathrm{P_{R(L)}} = (1+(-)\gamma_5)/2$.

The vertex correction reads

$$\mathrm{i}\,\mathcal{M}_{i,\alpha}^{vertex} \;=\; \sum_{j=1,2,3}\sum_{\beta}(\mathrm{i})^6\,\lambda_{j\alpha}^{*}\lambda_{j\beta}^{*}\,\lambda_{i\beta}\,\overline{u}_{\ell_\alpha}(p_\ell)\,\mathcal{F}\,u_{N_i}(p_N)\,, \tag{3.9}$$

where

$$\mathcal{F} = \mathrm{P_R}\left(\int[\mathcal{D}]\,\frac{1}{\not{k}-M_j}\,\mathrm{P_R}\,\frac{1}{\not{q}-m_\beta+\mathrm{i}\varepsilon}\,\mathrm{P_L}\,\frac{1}{q_H^2-m_H^2+\mathrm{i}\varepsilon}\right)\,. \tag{3.10}$$

The absorptive part of the loop-function comes from the fact that internal leptons (ℓ_β) and Higgses are on-shell. Moreover, we can neglect their masses, as $m_\ell, m_H \ll M_j$[1].

In the loop function, k, q and q_H are internal momenta, with $p_N = q + q_H$ and $k = q_H + p_\ell$. After a straightforward calculation, one obtains for the loop function:

$$\mathcal{F} = \frac{-\mathrm{i}}{16\,\pi^2}\frac{1}{M_i}\left(f_1\left(\frac{M_j^2}{M_i^2}\right)\not{p}_N + f_2\left(\frac{M_j^2}{M_i^2}\right)\not{p}_\ell\right)\,. \tag{3.11}$$

As lepton masses are neglected, the part $\propto \not{p}_\ell$ will not contribute and we neglect it in the following. In the expression above we introduce the function $f_1(x)$:

$$f_1(x) = \sqrt{x}\left(1-(1+x)\log{(1+\frac{1}{x})}\right)(\mathrm{i}\pi-(1+\log x)) - (1+x)L_2\left(-\frac{1}{x}\right)\ , \tag{3.12}$$

---

[1] This assumptions holds at $T=0$. When taking temperature into account, particles acquire effective masses due to screening of the thermal plasma. While lepton masses can still be neglected, $m_H(T) \simeq 0.4T$, and so at high temperatures m_H can in fact be heavier than M_{N_i}.

where $L_2(x)$ is the dilogarithm function.
The CP conjugated process $N_i \rightarrow \overline{\ell_\alpha} + H^*$ reads at tree level:

$$\mathrm{i}\,\overline{\mathcal{M}}^{0}_{i,\alpha} = \mathrm{i}\,\lambda_{\alpha i}\, v_{N_i}(p_N)\,\mathrm{P_L}\,\overline{v}_{\ell_\alpha}\ , \tag{3.13}$$

whereas the corresponding vertex correction reads:

$$\mathrm{i}\,\overline{\mathcal{M}}^{vertex}_{i,\alpha} = \sum_{j=1,2,3}\sum_{\beta}(\mathrm{i})^6\,\lambda_{j\alpha}\,\lambda_{j\beta}\,\lambda^*_{i\beta}\,\frac{-\mathrm{i}}{16\pi^2}\frac{1}{M_i}f_1\left(\frac{M_j^2}{M_i^2}\right)\,v_{N_i}(p_N)\,\mathrm{P_L}\,\not{p}_N\,\overline{v}_{\ell_\alpha}(p_\ell). \tag{3.14}$$

Then the evaluation of $\varepsilon_{CP}^{vertex}$ is straightforward. The numerator simply reads

$$\mathrm{num}(\varepsilon_{i,\alpha}^{vertex}) = \frac{1}{16\,\pi^2}\frac{1}{M_i}\,4\left(\sum_{j=1,2,3}\mathrm{Im}\left\{f_1\left(M_j^2/M_i^2\right)\right\}\mathrm{Im}\left\{\lambda^*_{\alpha i}\lambda_{\alpha j}\left(\lambda^\dagger\lambda\right)_{ij}\right\}\right)\frac{1}{2}M_i^3\ , \tag{3.15}$$

where we have detailed the different contributions, and used global four-momentum conservation $p_N = p_\ell + p_H$. The numerator is $\propto \lambda^4$. In this expression we write $\left(\lambda^\dagger\lambda\right)_{ij} = \sum_\beta \lambda^\dagger_{i\beta}\,\lambda_{\beta j}$.
For the denominator one considers only the leading term:

$$\mathrm{den}(\varepsilon_{i,\alpha}^{vertex}) = M_i^2\,\left(\lambda^\dagger\lambda\right)_{ii}\ . \tag{3.16}$$

Thus we find the well known result concerning CP violation coming from the vertex correction [61]:

$$\varepsilon_{i,\alpha}^{vertex} = \frac{1}{8\pi}\sum_{j=2,3}\frac{\mathrm{Im}\left\{\lambda^*_{\alpha i}\lambda_{\alpha j}\left(\lambda^\dagger\lambda\right)_{ij}\right\}}{(\lambda^\dagger\lambda)_{ii}}\,f\left(\frac{M_j^2}{M_i^2}\right)\ . \tag{3.17}$$

Notice that the sum is made over $j \neq i$, since the contribution from N_i running into the loop is the same for both CP conjugated processes. In the expression above, the loop function $f(x)$ is the imaginary part of $f_1(x)$:

$$f(x) = \sqrt{x}\left(1-(1+x)\log\left(1+\frac{1}{x}\right)\right). \tag{3.18}$$

Evaluation of ε_{CP}^{self}

Let us now turn to the evaluation of the the self-energy contribution to the CP asymmetry, still in the case of non-degenerate masses.
While the tree level contribution is given by eq.(3.8), the one loop correction reads

$$\begin{aligned}\mathrm{i}\,\mathcal{M}^{self}_{i,\alpha} &= -2\sum_{j=1,2,3}\lambda^*_{\alpha j}\,\lambda^*_{\beta j}\,\lambda_{\beta i}\\ &\times\ \overline{u}_{\ell_\alpha}(p_\ell)\,\mathrm{P_R}\,\frac{1}{\not{p}_j - M_j}\,\mathrm{P_R}\int[\mathcal{D}]\,\frac{1}{\not{q}-m_\beta+\mathrm{i}\varepsilon}\,\frac{1}{q_H^2-m_H^2+\mathrm{i}\varepsilon}\,\mathrm{P_L}\,u_{N_i}(p_N)\ ,\end{aligned} \tag{3.19}$$

with obviously $p_j = p_N$, and $q_H = q - p_N$. The overall factor 2 comes from the fact that both components of the $SU(2)$ doublet can run into the loop. Analogous to the vertex correction, the contribution from $j = i$ cancels out with the CP conjugated process.

Neglecting Higgs and lepton masses, the loop function is

$$\mathcal{F} = \int \frac{d^4q}{(2\pi)^4} \frac{\not{q}}{q^2 + \mathrm{i}\varepsilon} \frac{1}{(p_N - q)^2 + \mathrm{i}\varepsilon} , \tag{3.20}$$

and is clearly divergent. Using dimensional regularisation, and going on-shell $p_N^2 = M_i^2$, one obtains

$$\mathcal{F} = \frac{\not{p}_N}{(4\pi^2)} \left(\frac{1}{2} \left(\frac{2}{\varepsilon} - \gamma + \ln(4\pi) - \mathrm{i}\pi \right) + 1 \right) + \mathcal{O}(\varepsilon) , \tag{3.21}$$

where $\varepsilon = 4 - d$ and γ is the Euler constant.

The evaluation of the self-energy correction then follows the same lines than the vertex correction. The CP conjugate process $N_i \to \overline{\ell_\alpha}\phi^*$ presents the same divergence as above, but the CP asymmetry resulting in the difference of the two partial decay rates is finite:

$$\varepsilon_{i,\alpha}^{self} = \frac{1}{8\pi} \sum_{j \neq i} \frac{\mathrm{Im}\left\{ \lambda_{\alpha i}^* \lambda_{\alpha j} \left(\lambda^\dagger \lambda \right)_{ij} \right\}}{\left(\lambda^\dagger \lambda \right)_{ii}} g\left(\frac{M_j^2}{M_i^2} \right) , \tag{3.22}$$

with

$$g(x) = \frac{\sqrt{x}}{1 - x} . \tag{3.23}$$

Had we included lepton number conserving self-energy diagrams, we would have obtained an additional contribution

$$\varepsilon_{i,\alpha}^{self'} = \frac{1}{8\pi} \sum_{j \neq i} \frac{\mathrm{Im}\left\{ \lambda_{\alpha i}^* \lambda_{\alpha j} \left(\lambda^\dagger \lambda \right)_{ji} \right\}}{\left(\lambda^\dagger \lambda \right)_{ii}} g_c\left(\frac{M_j^2}{M_i^2} \right) , \tag{3.24}$$

with $g_c(x) = x^{-1/2}\, g(x)$, which in the hierarchical limit is suppressed when compared to the lepton number violating one eq.(3.22).

Adding the two contributions, and assuming that right-handed neutrinos are non-degenerate, the CP asymmetry in the lepton flavour α produced by the decay of a right-handed neutrino N_i is finally given by [61]:

$$\varepsilon_{i,\alpha} = \frac{1}{8\pi} \sum_{j \neq 1} \frac{\mathrm{Im}\left\{ \lambda_{\alpha i}^* \lambda_{\alpha j} \left(\lambda^\dagger \lambda \right)_{ij} \right\}}{\left(\lambda^\dagger \lambda \right)_{ii}} \left(f(x_j) + g(x_j) \right) . \tag{3.25}$$

A remark on the calculation of ε_{CP}^{self}

We see that while the vertex-correction is well defined, the self-energy correction is divergent for both CP conjugated processes, although the difference is finite for non-degenerate RHn.

One expects the self-energy CP asymmetry to vanish when the right-handed neutrinos are exactly degenerate, since then the CP violating phases of the mixing matrix can be rotated away. We see that in the naïve estimation above, the function $g(x)$ diverges when $x \to 1$, a clear proof that this treatment is incorrect. Actually, this comes from the fact that in the degenerate case, the widths of the RHns cannot be neglected, as will be shown below.

One way to deduce the CP violating properties of N decays is to look at Higgs-lepton two-body scatterings mediated by on-shell N_i [62]-[63]. The unstable nature of right-handed neutrinos is taken into account by summing self-energy corrections in the propagator, which near the pole has a Breit-Wigner form:

$$S(q^2) \propto \frac{1}{q^2 - M_i^2 + \mathrm{i}\, M_i\, \Gamma_i} \ , \tag{3.26}$$

where Γ_i is the width of N_i, given by

$$\Gamma_i = \frac{\left(\lambda^\dagger \lambda\right)_{ii} M_i}{8\,\pi} \ . \tag{3.27}$$

It has been found in [63] that the self-energy correction reads (in the simplified 2 RHn scheme):

$$g^{cor}(x) = -\frac{\sqrt{x}(x-1)}{(x-1)^2 + (x\, a_j - a_i)^2} \ , \tag{3.28}$$

with $a_k = \Gamma_k / M_i$.

Then, in the non-degenerate case, for $|M_{N_i} - M_{N_j}| \gg |\Gamma_i - \Gamma_j|$, one recovers the function $g(x)$ of eq.(3.23). When RHns are exactly degenerate, no divergence appears as $g^{cor}(1) = 0$, as expected.

Having evaluated the CP asymmetry produced by N_i decays, let us now consider the mechanism that produces a lepton asymmetry.

3.3 Leptogenesis in the single flavour approximation

In the single flavour approximation, one assumes that only the processes involving the lightest RHn contribute to the production of a lepton asymmetry. In the case of a hierarchical spectrum, $M_1 \ll M_{2,3}$, any asymmetry produced during $N_2(N_3)$ leptogenesis, at $T \sim M_2(M_3)$ is supposed be completely wiped out during the N_1 leptogenesis era, at $T \sim M_1$.

Another approximation concerns the decay products: in this simplified picture only the total lepton asymmetry is considered, without taking account the flavour content of the leptons produced. Hence N_1 decays into L in a CP violating way and the CP asymmetry is obtained by summing over lepton flavours:

$$\varepsilon_1 = \sum_\alpha \varepsilon_{1,\alpha} = \frac{1}{8\pi} \sum_{j \neq 1} \frac{\mathrm{Im}\left\{ \left(\lambda^\dagger \lambda\right)^2_{1j} \right\}}{\left(\lambda^\dagger \lambda\right)_{11}} \left(f(x_j) + g(x_j) \right) \ . \tag{3.29}$$

Assuming $M_1 \ll M_{2,3}$, and given the asymptotic behaviour of the loop function

$$f(x) + g(x) \overset{x \gg 1}{\longrightarrow} -\frac{3}{2\sqrt{x}} \, , \tag{3.30}$$

and further using the seesaw formula for the light neutrino mass

$$m_\nu^{\alpha\beta} = \lambda_{\alpha k} M_k^{-1} \lambda^T_{k\beta} \ , \tag{3.31}$$

the CP asymmetry can be re-expressed as

$$\varepsilon_1 = \frac{3\,M_1}{16\,\pi}\,\frac{\mathrm{Im}\left\{(\lambda^T.m_\nu^*.\lambda)_{11}\right\}}{v^2\,(\lambda^\dagger\lambda)_{11}}\;. \tag{3.32}$$

Davidson and Ibarra have shown [64] that the CP asymmetry can be bounded from above by a function that only depends on right-handed and light neutrino masses. This bound reads

$$|\varepsilon_1| \lesssim \varepsilon^{DI} = \frac{3}{16\pi}\frac{M_1(m_\nu^{\max} - m_\nu^{\min})}{v^2}\,, \tag{3.33}$$

where $m_\nu^{\max}(m_\nu^{\min})$ is the largest (smallest) light neutrino mass. This bound was improved in [65]:

$$|\varepsilon_1| \lesssim \varepsilon^{DI}\beta(m_\nu^{\min}, \tilde{m}_1)\,, \tag{3.34}$$

where the function β is roughly given by:

$$\beta(m_\nu^{\min}, \tilde{m}_1) \simeq \begin{cases} 1 - m_\nu^{\min}/\tilde{m}_1 & \text{if } m_\nu^{\min} \ll m_\nu^{\max} \\ \sqrt{1 - m_\nu^{\min\,2}/\tilde{m}_1^2} & \text{if } m_\nu^{\min} \simeq m_\nu^{\max} \end{cases}\;. \tag{3.35}$$

In the above equation, the smallest light neutrino mass is compared to the rescaled decay rate,

$$\tilde{m}_1 = 8\,\pi\,\frac{v^2}{M_1}\Gamma_{N_1} = \left(\lambda^\dagger\lambda\right)_{11}\frac{v^2}{M_1}. \tag{3.36}$$

The Davidson-Ibarra bound of eq.(3.33) has important consequences for leptogenesis, since it fixes the mass scale of right-handed neutrinos. Indeed, given that the baryon asymmetry produced by leptogenesis should at least match the observed one

$$Y_B \simeq 1.38 \times 10^{-3}\,\eta\,\varepsilon_1 \gtrsim Y_B^{obs} \simeq 8.7 \times 10^{-11}\;, \tag{3.37}$$

M_1 is lower bounded by:

$$\begin{aligned} M_1 &\gtrsim 6.5 \times 10^8\,\mathrm{GeV}\left(\frac{1}{\eta}\right) \times \left(\frac{Y_B}{Y_B^{obs}}\right)\left(\frac{m_{\mathrm{atm}}}{m_\nu^{\max} - m_\nu^{\min}}\frac{1}{\beta(m_\nu^{\min}, \tilde{m}_1)}\right), \\ &\simeq 6.5 \times 10^8\,\mathrm{GeV}\left(\frac{1}{\eta}\right)\;. \end{aligned} \tag{3.38}$$

We will evaluate the efficiency factor η later; for the moment it is enough to say that $\eta \lesssim 1$. We thus see that the RHn mass scale has to be far beyond the electroweak scale, and this has many important implications.

One of them is that the seesaw mechanism is hardly testable (if even possible), since such a high mass scale will (presumably) never be reached in laboratory experiments, and furthermore since the low-energy effects of RHns are highly suppressed.

Another caveat emerges when leptogenesis is embedded in a supersymmetric (SUSY) framework, and stems from the tension with gravitino over-production. We will discuss this issue in chapter 6, when studying leptogenesis in a SUSY-GUT framework.

Basic framework of leptogenesis

After having discussed its different building-blocks, let us see how leptogenesis works in the single flavour approximation [2].

For the sake of illustration, we first consider a very simplified scheme, where we only include the leading terms at order $\mathcal{O}(\lambda^4)$ that are decays and inverse-decays, and the on-shell contribution of $\Delta L = 2$ scatterings [58], included for consistency. We then evaluate the efficiency of leptogenesis in different washout regimes, and finally list the various processes which should be included in leptogenesis.

The study of the evolution of the number densities $n_x(t)$ is found to be more tractable in terms of comoving number densities, $Y_x = n_x/s$, since both the number density n_x and the entropy density s scale as T^3.

The final lepton asymmetry is evaluated by solving the set of Boltzmann equations (BEs) for Y_L and Y_N, which drive their evolution:

$$\begin{aligned}\frac{dY_N(z)}{dz} &= -D(z)\,K_1\,(Y_N(z) - Y_N^{eq}(z))\,,\\ \frac{dY_L(z)}{dz} &= \varepsilon_1\,D(z)\,K_1\,(Y_N(z) - Y_N^{eq}(z)) - W_{id}(z)\,K_1\,Y_L(z)\,,\end{aligned} \tag{3.39}$$

and compare the comoving number densities to their equilibrium value Y_X^{eq}. In these equations, the evolution parameter is $z = M_1/T$ and the decays $D(z)$ and inverse decays $W_{id}(z)$ reads:

$$\begin{aligned}D(z) &= z\,\frac{\mathcal{K}_1(z)}{\mathcal{K}_2(z)}\,,\\ W_{id}(z) &= \frac{1}{2}\frac{Y_N^{eq}}{Y_\ell^{eq}}\,D(z) = \frac{1}{4}\,z^3\,\mathcal{K}_1(z)\,,\end{aligned} \tag{3.40}$$

where $\mathcal{K}_i(z)$ are the modified Bessel function of the second kind. The lepton asymmetry production term is $\varepsilon_1\,K_1\,D(z)$, where ε_1 is defined in eq.(3.29), and the parameter K_1 reflects how fast are decays compared to the Hubble expansion rate:

$$K_1 = \frac{\Gamma(N_1)}{H(M_1)} = \frac{\tilde{m}_1}{m^*}\,, \tag{3.41}$$

alternatively defined in terms of the ratio of the effective neutrino mass $\tilde{m}_1$, defined in eq.(3.36) over the equilibrium neutrino mass m^*,

$$m^* = \frac{v^2}{M_{Pl}}\sqrt{\frac{256\,\pi^5\,g_*}{45}} \simeq 1.08\,\times 10^{-3}\,\mathrm{eV}\ , \tag{3.42}$$

where $v \sim 174\,\mathrm{GeV}$ is the SM Higgs vev, $M_{Pl} \sim 1.22\,\times 10^{19}\,\mathrm{GeV}$ is the Planck mass, and $g_* = 106.75$ is the SM effective number of degrees of freedom at $T \gg T_{EW}$. For $K_1 \gg 1$ or alternatively $\tilde{m} \gg m^*$, decays are in-equilibrium and lepton asymmetries are strongly washed out, while for $K_1 \ll 1$ or $\tilde{m} \ll m^*$, the asymmetries are weakly washed out, as decays are out of equilibrium.

---

[2] We use the labelling convention of [59] ($D(z), K_1, ...$), upon which this section is inspired.

As for the equilibrium densities, even if a Maxwell-Boltzmann distribution is used for the evaluation of the interaction rates, we correct them with a factor $3\zeta(3)/4 \simeq 0.9$, ζ being the Riemann Zeta function, to match the latter with the high energy behaviour of a Fermi-Dirac distribution [66], so that Y_N^{eq} reads:

$$Y_N^{eq}(z) = \frac{45}{2\,\pi^4\, g_*}\frac{3\zeta(3)}{4}\, z^2\, \mathcal{K}_2(z) \overset{z \lll 1}{\simeq} 3.9 \times 10^{-3}\ . \tag{3.43}$$

We see how the Sakharov's conditions are fulfilled in this leptogenesis scenario:

- Baryon number violation: in this case, if L was not violated during decays, we see that starting from a vanishing Y_L no asymmetry could be generated.
- CP violation: $\varepsilon_1 \neq 0$ is mandatory.
- Departure from thermal equilibrium: it is clearly seen above that, if right-handed neutrinos are in-equilibrium all along their evolution, the production term is null. Notice that this last point is only satisfied if the contribution of on-shell RHns to $\Delta L = 2$ scatterings has been included.

Typical solutions of the set of eqs.(3.39) are depicted in fig.(3.2), for various values of K_1, while the CP asymmetry is arbitrarily set to $\varepsilon_1 = 10^{-6}$.

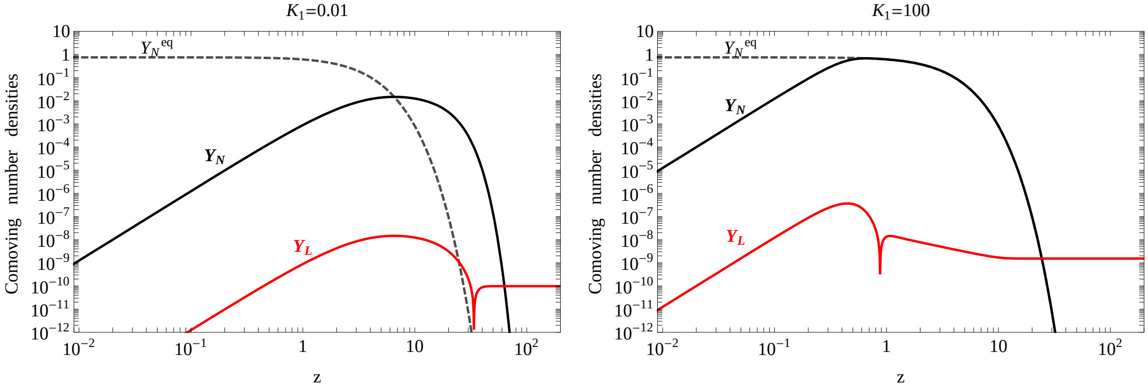

Figure (3.2): Evolution of comoving number densities, solutions of eqs.(3.39), as functions of $z = M_1/T$. The grey dashed line represents $Y_{N_1}^{eq}$, the number density of N_1 in thermal equilibrium, whereas the black line stands for Y_N, the solution of the Boltzmann equation. In red (light grey) is depicted the lepton asymmetry Y_L. For all these plots the CP asymmetry is taken equal to $\varepsilon_1 = 10^{-6}$, while the washout parameter is $K_1 = 0.01(100)$ on the left (right).

These solutions exhibit a very different behaviour.

3.4 Evaluation of the lepton asymmetry

This evaluation proceeds mainly in two parts, which correspond to the different contributions to the final asymmetry.
We work in the thermal scenario of leptogenesis, hence before decaying, right-handed neutrinos have to be produced. This thermalisation occurs due to scatterings/inverse decays of leptons present in the thermal bath. During this first stage, an (anti-)asymmetry is created.
If $K_1 \gg 1$, since decays and inverse decays are far in-equilibrium, the thermalisation of RHns is fast and the latter reach thermal equilibrium at high temperatures. Conversely, if $K_1 \ll 1$, thermal equilibrium occurs late, as can be seen in fig.(3.2). In both cases, during this first stage a lepton asymmetry is produced, which is $\propto \varepsilon_1 Y_N$.
Once thermal equilibrium is reached, the subsequent evolution of RHns and of the lepton asymmetry also depends on K_1. In the strong washout regime, $K_1 \gg 1$, the fast decays maintain Y_N close to its equilibrium value, whereas in the opposite weak washout regime $K_1 \ll 1$, these decays occur late, when RHns are far out of equilibrium. During this second stage, a lepton asymmetry is produced, which may cancel out with the former one. This can be seen in fig.(3.2), where the compensation between first and second stage asymmetry production is visible in the peak occuring at $z \sim 30(1)$ for $K_1 = 0.01(100)$.
Finally, as the temperature decreases, as RHns become too diluted, together with the fact that the different processes are freezing, the lepton asymmetry reaches its final value.
Let us evaluate this value in the two characteristic washout regimes.

Strong washout regime: $K_1 \gg 1$
In the strong washout regime, the main contribution to the production of a lepton asymmetry comes from the second stage, after RHns are thermalised, because thermalisation is fast when inverse decays are far in-equilibrium. Thus, defining $\Delta N = Y_N - Y_N^{eq}$, the fact that the fast processes keep N close to its equilibrium abundance implies that:

$$\Delta N'(z) = -K_1\, D(z)\, \Delta N(z) - {Y_N^{eq}}'(z) \simeq 0\,. \tag{3.44}$$

The formal solution of eq.(3.39) for the lepton asymmetry then reads:

$$\begin{aligned} Y_L(z) &= \varepsilon_1 \int_0^z dx\, K_1\, D(x)\, \Delta N(x)\, e^{-K_1 \int_x^z W_{id}(y)\, dy}\,, && (3.45)\\ &= -\varepsilon_1 \int_0^z dx\, {Y_N^{eq}}'(x)\, e^{-K_1 \int_x^z W_{id}(y)\, dy}\,. && (3.46)\end{aligned}$$

We can rewrite the integrand of eq.(3.45) as $\int e^{-f}$, with

$$f(x) = K_1 \int_x^z dy\, W_{id}(y) - \ln({Y_N^{eq}}'(x))\,.$$

This integral is evaluated using a saddle point approximation, and gets its maximum for

$$\frac{K_1}{4}\sqrt{\frac{\pi}{2}}\,\overline{x}^{5/2}\, e^{-\overline{x}} \simeq 1\,,$$

that is, for

$$\overline{x} \simeq -\frac{5}{2}\,\mathrm{ProductLog}\left[\frac{-4\,K_1^{-2/5}}{5\,\pi^{1/5}}\right],$$

where ProductLog(z) is the Lambert $W(z)$ function[3]. For $K_1 \gtrsim 1$, we find that the main contribution is for $z \gtrsim 1$, as $\overline{x} \propto \ln(K_1)$. The lepton asymmetry in this strong washout regime is then accurately given by

$$Y_L \simeq \varepsilon_1 \left(\frac{0.4}{K_1^{1.16}}\right) Y_N^{eq}(z_{in})\,, \tag{3.47}$$

and the efficiency factor is therefore

$$\eta_s = 0.4/K_1^{1.16}\,. \tag{3.48}$$

Weak washout regime: $K_1 \ll 1$

The regime of weak washout is depicted in the left panel of fig.(3.2). In this regime, since inverse decays are slow compared to the Hubble expansion rate, the right-handed neutrinos reach thermal equilibrium at $z_{eq} \gg 1$. Once thermalised, RHns do not stay in thermal equilibrium, but rather decay late.

These decays produce a lepton asymmetry that cancels out the one produced during thermalisation. However, since leptons have more time to participate in inverse reactions, this cancellation is only partial, preventing $Y_L = 0$.

Let us evaluate the different contributions.

Before the Ns reach their thermal equilibrium abundance, Y_N^{eq} dominates over Y_N and so

$$\begin{aligned} Y_N'(z) &\simeq K_1\,D(z)\,Y_N^{eq}(z)\,, \\ Y_L'(z) &\simeq -\varepsilon_1\,K_1\,D(z)\,Y_N^{eq}(z) - W_{id}(z)\,K_1\,Y_L(z)\,. \end{aligned} \tag{3.49}$$

The lepton asymmetry is then given by

$$Y_L^{<}(z) \simeq -\varepsilon_1\,K_1 \int_0^z dx\,D(x)\,Y_N^{eq}(x)\,e^{-K_1\int_x^z dy\,W_{id}(y)}\,. \tag{3.50}$$

Defining for convenience $n_0 = 135\zeta(3)/8\pi^4 g_*$, such that $D(x)\,Y_N^{eq}(x) = 4\,n_0\,W_{id}(x)$, the lepton asymmetry produced at $z \lesssim z_{eq}$ is

$$Y_L^{<}(z) \simeq -\varepsilon_1\,4\,n_0\left(1 - e^{\frac{-3\pi}{8}K_1}\right)\,. \tag{3.51}$$

For temperatures below T_{eq}, Y_N dominates over Y_N^{eq}, in such a way that

$$Y_N'(z) = -K_1\,D(z)\,Y_N(z) \rightarrow Y_N^{>}(z) = Y_N^{eq}(z_{eq})\,e^{-\frac{K_1}{2}(z^2-z_{eq}^2)}\,. \tag{3.52}$$

---

[3] The Lambert function has an accurate asymptotic expansion for $z \gtrsim 3$: $W(z) = \ln(z) - \ln(\ln(z)) + \ldots$ [67].

The equilibrium temperature is defined by $Y_N(z_{eq}) = Y_N^{eq}(z_{eq})$. Given that

$$Y_N^{<}(z_{eq}) \simeq K_1 \int_0^{z_{eq}} dx\, D(x)\, Y_N^{eq}(x) \simeq n_0\, K_1 \frac{\alpha\, z_{eq}^3}{3\,\alpha + z_{eq}^3}\,, \tag{3.53}$$

where $\alpha = \frac{3\pi}{2}$, and as $Y_N^{eq}(z_{eq}) = n_0\, z_{eq}^2\, K_2(z_{eq})$ one immediately obtains z_{eq}:

$$z_{eq} = -\frac{3}{2}\mathrm{ProductLog}\left[-2^{2/3}\,\left(\frac{\pi}{3}\right)^{1/3}\, K_1^{-2/3}\right] \propto \ln(1/K_1)\,.$$

The equilibrium is reached when $Y_N = Y_N^{eq}$, at $z_{eq} \sim 10$ in fig.(3.2).
We are now able to determine the final lepton asymmetry:

$$\begin{aligned} Y_L(z) &= \varepsilon_1 \int_0^{z} dx\, D(x)\, \left(Y_N(x) - Y_N^{eq}(x)\right)\, e^{-K_1 \int_x^z dy\, W_{id}(y)}\,, \\ &= \varepsilon_1 \left[-\int_0^{z_{eq}} dx\, D(x)\, Y_N^{eq}(x) e^{-K_1 \int_x^z dy\, W_{id}(y)} + \int_{z_{eq}}^{z} dx\, Y_N'(x)\right]\,, \\ &= \varepsilon_1 \left[-4\, n_0\, \left(1 - e^{-\frac{\alpha}{4} K_1}\right) - n_0\, \alpha\, K_1\right] \\ Y_L &\simeq \varepsilon_1 \times 1.3\, K_1^2\, Y_N^{eq}(z_{in})\,. \end{aligned} \tag{3.54}$$

As expected, we find that the lepton asymmetry is non-zero due to the washout of the lepton asymmetry produced during thermalisation. The efficiency factor in the weak washout regime is then

$$\eta_w = 1.3\, K_1^2\,. \tag{3.55}$$

Global parametrisation

Finally, we can give a value of η for all washouts from a simple interpolation [58]:

$$\eta \simeq \left(\eta_w^{-1} + \eta_s^{-1}\right)^{-1} \simeq \left(0.8 K_1^{-2} + 2.5\, K_1^{-1.16}\right)^{-1}\,. \tag{3.56}$$

Resulting baryon asymmetry

As the Universe cools down, at $T \gtrsim M_1/100$, all processes are frozen and the lepton asymmetry remains constant, until being partly converted by sphalerons into a baryon asymmetry. In the single flavour approximation, one has [68]:

$$Y_B = -\frac{8\, n_g + 4\, n_H}{14\, n_g + 9\, n_H}\, Y_L\,, \tag{3.57}$$

where $n_g = 3$ is the number of fermion generations, and n_H is the number of Higgs doublets in the considered model ($n_H = 1$ in the SM). Hence,

$$Y_B = -28/51\, Y_L \simeq -1.38\, \times 10^{-3}\, \varepsilon_1\, \eta\,. \tag{3.58}$$

This has to be compared with the observed value $Y_B^{obs} \simeq 8.7\, \times 10^{-11}$: assuming for example $\varepsilon_1 = 10^{-6}$, K_1 should lie between ~ 0.15 and ~ 15.

3.5 Dependence on the initial conditions

In the thermal scenario, since right-handed neutrinos have to be produced by inverse decays, it is clear that a minimal amount of washout is required.

Actually, had we assumed that initially RHn were already thermalised, or even that their abundance was the dominant one, washout processes would not be required at all. These scenarios, which we may call equilibrium [59] or dominant [58], assume that before leptogenesis occurs, for $T \gg T_{lepto}$, some mechanism produces RHns. On the one hand these scenarios are model-dependent, but on the other hand the constraints derived for the thermal scenario are weakened. To illustrate this, we plot in fig. (3.3) the efficiency factor as a function of K_1, for the different scenarios, with $Y_N(z_{in}) = 0$ in the thermal case, $Y_N(z_{in}) = Y_N^{eq}(z_{in})$ in the equilibrium one and $Y_N(z_{in}) = 10\, Y_N^{eq}(z_{in})$ in the dominant scenario.

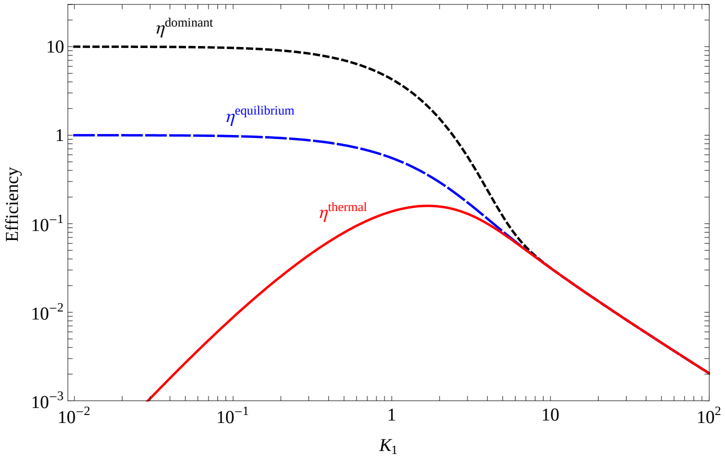

Figure (3.3): Efficiency factor of leptogenesis assuming different initial conditions. In red (solid line) the thermal scenario is plotted, while in long-dashed blue and short-dashed black, the equilibrium and dominant scenarios are respectively represented.

We observe that in the two latter cases, the efficiency is maximal for a vanishing washout, with maximum values $\eta^{eq} \simeq 1$ and $\eta^{dom} \simeq 10$, while in the thermal scenario a maximal efficiency is reached for $K_1 \simeq 2$, for which $\eta^{th} \simeq 0.16$.

We further notice that for $K_1 \gtrsim 10$, all scenarios yield the same efficiency: in a sense, the strong washout regime is more robust since it does not depend on the thermal history of the right-handed neutrinos [69].

3.6 Other processes

In the discussion above we only have included decays and inverse decays. But there are many other processes to take into account, that strongly modify the previous results. Let us discuss these terms.

$\mathcal{O}(\lambda^2)$ and $\mathcal{O}(\lambda^4)$ processes

Decays and inverse decays are $\mathcal{O}(\lambda^2)$, but no CP violation is possible at this order, and one needs to include $\mathcal{O}(\lambda^4)$ as discussed in the beginning of the chapter. At this order, in addition to decays and inverse decays, $2-to-2$ scatterings mediated by N exchange should be included.

- $s-$channel N exchange: $\Delta L = 0$ processes $\ell_\alpha \phi \leftrightarrow \ell_\beta \phi$ and $\Delta L = 2$ processes $\ell_\alpha \phi \leftrightarrow \overline{\ell_\beta \phi}$.
- $t-$ and $u-$channel N exchange: $\Delta L = 0$ processes $\overline{\phi}\phi \leftrightarrow \ell_\alpha \overline{\ell_\beta}$ and $\Delta L = 2$ processes $\overline{\phi\phi} \leftrightarrow \ell_\alpha \ell_\beta$.

We represent in fig.(3.4) the diagrams for the lepton number violating processes.

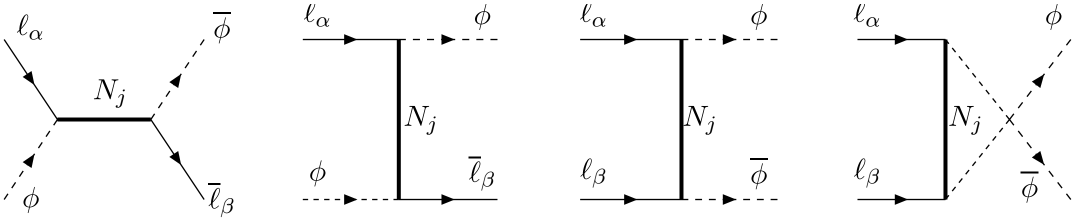

Figure (3.4): Feynman diagrams of $\Delta L = 2$ scatterings mediated by $N_j, j = 1, 2, 3$.

The $s-$channel receives contributions from on-shell RHns, with a corresponding rate $\gamma_N^{os} \propto \gamma_D(\lambda)^4$. As the production term of the lepton asymmetry is $\varepsilon_1 K_1 D(x) \propto \gamma_D (\lambda)^4$, the resonant $s-$channel contribution has to be included for consistency at lowest order, as we did before. Then, when including $\Delta L = 2$ scatterings, this should be carefully done in order to avoid double counting, and the on-shell part has to be subtracted from the total $\Delta L = 2$ interaction rates [58, 59].

When off-shell $\Delta L = 2$ processes are in-equilibrium, their late scatterings can spoil a successful leptogenesis by dramatically washing out the lepton asymmetry. The term that potentially washes out the lepton asymmetry is given at low temperature by [70]:

$$W_{\Delta L=2}(z) \simeq \frac{0.186}{z^2} \left(\frac{M_1}{10^{10}\,\mathrm{GeV}} \right) \left(\frac{\overline{m}}{1\,\mathrm{eV}} \right)^2 , \tag{3.59}$$

where $\overline{m}^2 = m_1^2 + m_2^2 + m_3^3$. However, for $z \gtrsim 15$ this term is small compared to inverse decays $K_1 W_{id}$, and can safely be neglected. Since at low temperature inverse decays read

$$K_1 W_{id}(z \gg 1) \simeq \frac{K_1}{4} \sqrt{\frac{\pi}{2}}\, z^{3/2}\, e^{-z} , \tag{3.60}$$

this condition somehow constrains M_1 and K_1 [71]:

$$\frac{M_1}{10^{14}\,\mathrm{GeV}} \lesssim 0.1 \times K_1 . \tag{3.61}$$

If the relation above holds, we can neglect $\Delta L = 2$ scatterings; on the other hand, if this constraint is not satisfied, to prevent the lepton asymmetry from being washed out by these processes implies to upper-constraint the light neutrino mass scale, as we will see at the end of the chapter.

$\Delta L = 1$ **processes** $\mathcal{O}(\lambda^2 h_t^2)$ **and** $\mathcal{O}(\lambda^4 h_t^2)$

Given the size of the top Yukawa coupling, processes involving $h_t Q_3 H_u t_R^c$ should be included. At $\mathcal{O}(\lambda^2 h_t^2)$, these processes consist in $2 \leftrightarrow 2$ Higgs mediated scatterings, both in $s-$channel $\ell N \leftrightarrow \bar{t} Q_3$ and $t-, u-$ channels $\ell \overline{Q}_3 \leftrightarrow N \bar{t}$ and $\ell t \leftrightarrow N Q_3$. These processes are represented in fig.(3.5).

At this order in the couplings, three body decays and inverse decays $N \leftrightarrow \ell \overline{Q}_3 t$ should also be included. Actually, these processes are phase-space suppressed, and are not quantitatively relevant [72], hence we will neglect them. The scattering processes violate lepton number by one unit, and act as source term for heavy neutrino production and as damping term for the lepton asymmetry.

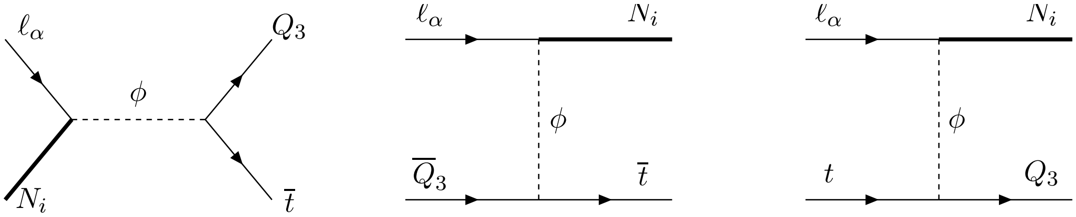

Figure (3.5): Feynman diagrams of neutrino-top quark scatterings.

The interesting feature of these scatterings is that at high temperature, contrary to decays and inverse decays that, scaling as z^2, are suppressed, the scatterings involving top quarks become constant at high temperature. Thus, for $z \ll 1$, thermalisation of RHns is significantly faster.

When evaluating the lepton asymmetry in the regime $K_1 \ll 1$, we noted that $Y_L \neq 0$ only owing to the partial washout due to inverse decays, and this dependence was illustrated in the fact that $Y_L \propto K^2$. Including $\Delta L = 1$ scatterings strongly modifies the situation, and the lepton asymmetry now scales as $Y_L \propto K$.

However, going to order $\mathcal{O}(\lambda^4 h_t^2)$, CP is violated in $\Delta L = 1$ scatterings, which then also act as source terms for the lepton asymmetry. One then recovers the dependence of $Y_L \propto K^2$ in the weak washout regime, as source and damping terms now similarly act and cancel each other at order K.

It has been shown in [71, 73] that the CP asymmetry in scatterings is the same as in decays and inverse decays. For consistency, $2 \leftrightarrow 3$ scatterings should be included, but as for the three body decays they are phase-space suppressed and do not quantitatively contribute in leptogenesis.

We illustrate the effect of top-quark scatterings in fig.(3.6), where we compare the lepton asymmetry computed with and without the $\Delta L = 1$ processes (included both in washout and in source terms), in the regimes of weak and strong washout. When $\Delta L = 1$ top scatterings are included, the Boltzmann equations for the comoving number densities are:

$$\begin{aligned}
\frac{dY_N(z)}{dz} &= -P(z)\,K_1\,(Y_N(z) - Y_N^{eq}(z))\,, \\
\frac{dY_L(z)}{dz} &= \varepsilon_1\,P(z)\,K_1\,(Y_N(z) - Y_N^{eq}(z)) - K_1\,W(z)\,Y_L(z)\,,
\end{aligned} \tag{3.62}$$

where the production and washout terms are defined by [59]:

$$\begin{aligned}
P(z) &= D(z) + 2\,S_s(z) + 4\,S_t(z)\,, \\
W(z) &= W_{id}(z)\left(1 + \frac{1}{D(z)}\left(2\,S_s(z)\frac{Y_N(z)}{Y_N^{eq}(z)} + 4\,S_t(z)\right)\right)\,,
\end{aligned} \tag{3.63}$$

where S_s and S_t represent the Higgs-mediated scatterings in the $s-$ and $t-$ channels. We refer the reader to appendix B where these scatterings are discussed in more detail.

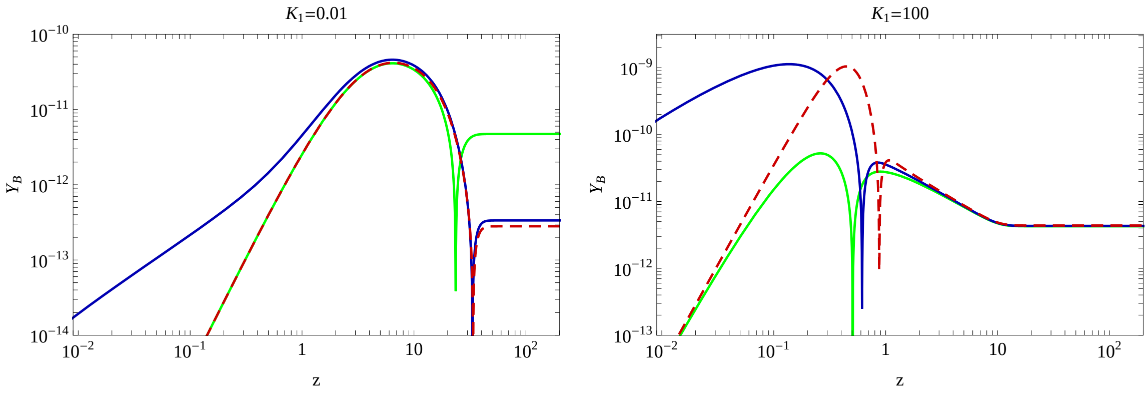

Figure (3.6): Influence of neutrino-top quark scatterings on the baryon asymmetry. The dashed-red line depicts the case in which scatterings are neglected, the green (light grey) line the case where scatterings are included only as damping term, while the blue (dark grey) curve represents the case where scatterings are added both as source and damping terms.

We clearly see the influence of scatterings in the plots: when one considers only the contribution of scatterings to the washout, they prevent the cancellation of the lepton asymmetry produced during thermalisation with the one generated in decays of the RHn, so that the final Y_L is $\propto K_1$ instead of being $\propto K_1^2$. When the CP asymmetry in scatterings is included, we see that Y_L gets suppressed as K_1^2.

Among $\Delta L = 1$ scatterings, one should take into account scatterings involving Higgs bosons-$U(1)$ or $SU(2)$ gauge bosons couplings [58, 73]. These scatterings behave similarly to the top-quark scatterings, accelerating the thermalisation of right-handed neutrinos, and acting as a source and damping terms for the lepton asymmetry. We neglect these terms in this thesis, even if they are of the same order -or even larger than the top-quark scatterings-, as their inclusion does not drastically modify the picture here drawn.

3.7 Upper-bound on the light neutrino mass scale

The requirement that leptogenesis should explain the observed baryon asymmetry of the Universe has led to a constraint on the light neutrino mass scale. Indeed, we have in the single flavour approximation the (improved) Davidson-Ibarra bound on the CP asymmetry eqs.(3.33)-(3.34):

$$|\varepsilon_1| \lesssim \frac{3}{16\pi}\frac{M_1(m_\nu^{\max} - m_\nu^{\min})}{v^2} \times \beta(m_\nu^{\min}, \tilde{m}_1)\,, \tag{3.64}$$

which decreases as the light neutrinos become degenerate in mass. Indeed, for $m_1 \sim m_2 \sim m_3 \sim m$, and assuming $M_1 \ll M_2, M_3$, one has:

$$|\varepsilon_1| \lesssim \frac{3}{32\pi}\frac{M_1\,\Delta m^2_{atm}}{m\,v^2} \times \beta(m_\nu^{\min}, \tilde{m}_1)\,. \tag{3.65}$$

In this quasi-degenerate case, $m \gtrsim m_{atm} \gg m_*$, and as $m_1 \lesssim \tilde{m}_1 \lesssim m_3$, we are in the strong washout regime. Thus we can apply eq.(5.28) which tells us that $Y_B \propto 1/K$, hence

$$Y_B \;\simeq\; -1.38 \times 10^{-3}\,\varepsilon_1\,\eta(\tilde{m}_1) \propto \frac{M_1}{m^2}\;. \tag{3.66}$$

In order to keep Y_B large enough, increasing the light neutrino mass scale could be compensated by increasing RHn mass. On the other hand, one cannot increase M_1 harmlessly.
There is a strong constraint coming from the requirement that off-shell $\Delta L = 2$ scatterings do not wash-out the lepton asymmetry. These scatterings are potentially dangerous at low temperature, when other processes relevant in leptogenesis are already frozen. Their contribution is given in this case by [70]

$$W_{\Delta L=2}(z) \simeq \frac{3\times 0.186}{z^2}\left(\frac{M_1}{10^{10}\,\mathrm{GeV}}\right)\left(\frac{m}{1\,\mathrm{eV}}\right)^2. \tag{3.67}$$

This term implies a washout of the baryon (lepton) asymmetry, which then can be expressed as

$$Y_B = Y_B^{<}\,e^{-\frac{3\times 0.186}{z_B}\left(\frac{M_1}{10^{10}\,\mathrm{GeV}}\right)\left(\frac{m}{1\,\mathrm{eV}}\right)^2}\;, \tag{3.68}$$

where $Y_B^{<}$ is the would-be baryon asymmetry without $\Delta L = 2$ scatterings of eq.(3.66). Maximising Y_B with respect to M_1 and to the effective neutrino mass $\tilde{m}$, and then requiring that the baryon asymmetry at least matches the observed value, the authors of [74, 59, 65] have derived an upper-bound on the neutrino masses $m_i, i = 1, 2, 3$:

$$m_i \lesssim 0.12\,\mathrm{eV}\,. \tag{3.69}$$

This bound on the light neutrino mass is certainly one of the most important phenomenological implication of successful leptogenesis in the one flavour approximation.
However, we will see in chapter 5 that this bound will no longer hold when lepton flavours are included.
Finally, let us remark that this strong bound only applies in the case the heavy neutrinos are hierarchical. Indeed, as shown in [65], the DI bound, which is roughly

$$\varepsilon^{DI} \sim \frac{M_1\Gamma_j}{M_j^2} \times \frac{m_3 - m_1}{\tilde{m}_j}\,, \tag{3.70}$$

gets suppressed for two reasons. On the one hand, the second factor comes from the orthogonality of the R matrix and explains the strong suppression of the CP asymmetry in the limit of degenerate light neutrinos. On the other hand, the first term of eq.(3.70) implies a suppression of the CP asymmetry when heavy neutrinos are very hierarchical. However, since we are interested in the regime of degenerate light neutrinos, it might be more natural to suppose that the heavy neutrinos are degenerate too, unless postulating accidental compensation between right-handed neutrino masses and neutrino Yukawa couplings. When the RHns are close to the resonance, both suppressions do not occur. The first one gets enhanced by a resonance factor, while the second suppression does not occur due to the absence of an orthogonality relation. The author of [65] have thus shown that in the single flavour approximation, the constraint eq.(3.69) can be avoided. Nevertheless, we will show in chapter 5 that assuming hierarchical RHns (even a very weak hierarchy), the inclusion of flavours relaxes the constraint eq.(3.69).

Chapter 4

On the importance of lepton flavours in leptogenesis

In the previous chapter we have studied leptogenesis in the one-flavour approximation, where one deals with the total lepton asymmetry, which is the sum over lepton flavours $L = \sum_\alpha L_\alpha$. Right-handed neutrinos decay into leptons and antileptons, and in this approximation one considers that the lepton asymmetry produced evolves coherently, until being converted into a baryon asymmetry through the $B + L$ violating sphalerons.
However, lepton doublets interact also via the Yukawa term $\mathcal{L} \supset -h_\alpha \, \bar{\ell}_\alpha \, \phi \, e_R^\alpha$, which gives mass to charged leptons after electroweak symmetry breaking. This interaction, if efficient, will decohere the lepton doublet, by projecting it onto a flavour basis, in which case the electron, muon and tau flavours can possibly be differentiated [78]- [75, 76].
If flavours are distinguishable, we should consider the asymmetry produced in each lepton flavour direction, instead of the collective asymmetry, for which accidental cancellations are always possible.
In this chapter, which is mostly based on the appendix of [75], we do not investigate the effects of lepton flavours in leptogenesis. This study will be led in chapter 5 and 6, in the framework of type I and type II seesaws, respectively. Here, we discuss how to handle flavoured lepton asymmetries: how should the Boltzmann equations be modified, what are the good quantities to consider, and especially under which conditions are flavours relevant in leptogenesis.

4.1 A toy model for flavoured Boltzmann equations

We want to derive the set of Boltzmann equations for lepton flavours. We could infer, given the BE for the lepton asymmetry, the structure of these equations. However, in this approach, the flavour structure, and more importantly, the relevance of flavour, may appear rather ambiguous. We thus derive the BEs, looking at the evolution of the flavoured leptonic number density operator

$$f_{\Delta\ell}^{\alpha\beta} = f_\ell^{\alpha\beta} - f_{\bar{\ell}}^{\alpha\beta} = a^\dagger_{\ell_\alpha} a_{\ell_\beta} - a^\dagger_{\bar{\ell}_\beta} a_{\bar{\ell}_\alpha} \ , \tag{4.1}$$

where $a^\dagger_{\ell_\alpha}(a_{\ell_\alpha})$ and $a^\dagger_{\bar{\ell}_\alpha}(a_{\bar{\ell}_\beta})$ are the particle and antiparticle number creation (annihilation) operators, respectively. Actually, this number density operator is not truly the leptonic one, but rather the leptonic doublet one, since lepton number is stored both in $SU(2)$ doublets and singlets. Moreover, as seen from eq.(4.1), $f^{\alpha\beta}_{\Delta\ell}$ is a matrix in flavour space [77, 78].

A complete derivation of the BEs would require to also consider the Lorentz structure of the different fields. Here, we just give an heuristic derivation based on simple quantum mechanics, and reintroduce by hand at a later stage the Lorentzian structure. Nevertheless, such a treatment enables us to determine the flavour structure of the BE, and furthermore to determine explicitely which objects should be studied in flavoured leptogenesis.

The operators we introduce obey the same statistic that the fields they represent, namely anti-commutation relations for the fermionic fields ℓ:

$$\left\{a_{\ell^\alpha}, a^\dagger_{\ell^\beta}\right\} = \delta_{\alpha\beta} \ , \{a_{\ell^\alpha}, a_{\ell^\beta}\} = 0 \ , \left\{a^\dagger_{\ell^\alpha}, a^\dagger_{\ell^\beta}\right\} = 0 \ , \tag{4.2}$$

and similarly for the e^c_R and N_1. The Higgs field obeys bosonic commutation relations:

$$\left[a_\phi, a^\dagger_\phi\right] = \delta_{\alpha\beta} \ , [a_\phi, a_\phi] = 0 \ , \left[a^\dagger_\phi, a^\dagger_\phi\right] = 0 \ . \tag{4.3}$$

We first discuss the $N_1 - \ell$ interaction. We only consider the interaction with the lightest right-handed neutrino N_1, droping the indice in N_1. The interaction Hamiltonian can be written as

$$H^N = \lambda_{\rho 1} a^\dagger_N a_\phi a_{\ell_\rho} + \lambda^*_{\rho 1} a_N a^\dagger_\phi a^\dagger_{\ell_\rho} \ . \tag{4.4}$$

The evolution of the leptonic doublet number density is given by the perturbative expansion of the Heisenberg equations of motion (we use here the expectation value instead of the operator):

$$\begin{aligned} \frac{\partial f^{\alpha\beta}_\ell}{\partial t} &= -\left[H^N\left[H^N, f^{\alpha\beta}_\ell\right]\right] \ , \\ &= \lambda_{\alpha 1}\lambda^\dagger_{1\rho}\left(f_N(1+f_\phi)(\delta_{\rho\beta} - f^{\rho\beta}_\ell) - (1-f_N)f_\phi f^{\rho\beta}_\ell\right) \\ &+ \ \left(f_N(1+f_\phi)(\delta_{\alpha\rho} - f^{\alpha\rho}_\ell) - (1-f_N)f_\phi f^{\alpha\rho}_\ell\right)\lambda_{\rho 1}\lambda^\dagger_{1\beta} \, . \end{aligned} \tag{4.5}$$

In this expression, we define the RHn and Higgs distribution function as $f_N = a^\dagger_N a_N$ and $f_\phi = a^\dagger_\phi a_\phi$.

The first and third terms of this expression represent decays of right-handed neutrinos whereas the second and fourth terms stand for the inverse decays. If we neglect Pauli blocking and Bose enhancement factors $(1 \pm f)$, we can rewrite this expression as

$$\frac{\partial f^{\alpha\beta}_\ell}{\partial t} = 2 f_N \left(\lambda\lambda^\dagger\right)_{\alpha\beta} - f_\phi \left\{f_\ell, \left(\lambda\lambda^\dagger\right)\right\}_{\alpha\beta} \ . \tag{4.6}$$

The evolution of the antileptonic number density is directly deduced from the previous one:

$$\frac{\partial f^{\alpha\beta}_{\bar{\ell}}}{\partial t} = 2 f_N \left(\lambda\lambda^\dagger\right)^\dagger_{\alpha\beta} - f_\phi \left\{f_{\bar{\ell}}, \left(\lambda\lambda^\dagger\right)^\dagger\right\}_{\alpha\beta} \ , \tag{4.7}$$

with $\left(\lambda\lambda^\dagger\right)^{\alpha\beta} = \left(\lambda_{\alpha 1}\lambda^\dagger_{1\beta}\right)$. For simplicity, we have taken the Higgs field to be real[1]. We therefore obtain the evolution of the leptonic doublet asymmetry

$$\begin{aligned} \frac{\partial f^{\alpha\beta}_{\Delta\ell}}{\partial t} &= 2 f_N \left((\lambda\lambda^\dagger) - (\lambda\lambda^\dagger)^\dagger \right)_{\alpha\beta} \\ &- f_\phi \left[\left\{ f_{\Delta\ell}, \frac{(\lambda\lambda^\dagger) + (\lambda\lambda^\dagger)^\dagger}{2} \right\}^{\alpha\beta} + 2 \left\{ f^{eq}_\ell, \frac{(\lambda\lambda^\dagger) - (\lambda\lambda^\dagger)^\dagger}{2} \right\}^{\alpha\beta} \right] , \end{aligned} \tag{4.8}$$

where we define the "equilibrium" leptonic number density

$$f^{\alpha\beta}_\ell + f^{\alpha\beta}_{\bar{\ell}} = 2 f^{eq\,\alpha\beta}_\ell \, . \tag{4.9}$$

The first and third terms of eq.4.8 are nul at this order of expansion in the couplings. Forgetting about it for a while, eq.4.8 can be further simplified if we assume that the Higgs fields are in thermal equilibrium $f_\phi = f^{eq}_\phi$, and use the equilibrium condition for decays $f^{eq}_N = f^{eq}_\phi f_\ell$, that, once symmetrised, reads

$$f^{eq}_N A_{\alpha\beta} = f^{eq}_\phi \left\{ f^{eq}_\ell, \frac{A}{2} \right\}^{\alpha\beta} . \tag{4.10}$$

We thus obtain

$$\frac{\partial f^{\alpha\beta}_{\Delta\ell}}{\partial t} = 2 \left(f_N - f^{eq}_N \right) \left((\lambda\lambda^\dagger) - (\lambda\lambda^\dagger)^\dagger \right)_{\alpha\beta} - f^{eq}_\phi \left\{ f_{\Delta\ell}, \frac{(\lambda\lambda^\dagger) + (\lambda\lambda^\dagger)^\dagger}{2} \right\}^{\alpha\beta} . \tag{4.11}$$

The first term represents the production of a lepton asymmetry in the decays of N. Having only made the expansion to second-order, no CP asymmetry can emerge, and the production term is nul. However, if we introduce in the interaction Hamiltonian an effective coupling mimicking the one obtained when calculating ε_{CP}, cf. eq.(3.29), that is

$$H^{N,eff} \sim \sum_{j,\beta} \lambda^*_{j\alpha}\lambda^*_{j\beta}\lambda_{1\beta} \times g(x_j) a_N a^\dagger_\phi a^\dagger_{\ell_\alpha} + \sum_{j,\beta} \lambda_{j\alpha}\lambda_{j\beta}\lambda^*_{1\beta} \times g(x_j) a^\dagger_N a_\phi a_{\ell_\alpha} \, , \tag{4.12}$$

we can obtain non-zero CP violation. Assuming this to be the case, and defining the washout factor $K_1 = \sum_\alpha |\lambda_{\alpha 1}|^2$ and the flavoured washout factors $\kappa_{\alpha\beta} = (\lambda\lambda^\dagger)^{\alpha\beta}$, we rewrite the evolution equation as:

$$\frac{\partial f^{\alpha\beta}_{\Delta\ell}}{\partial t} = 2 \left(f_N - f^{eq}_N \right) K_1 \varepsilon_{\alpha\beta} - f^{eq}_\phi \left\{ f_{\Delta\ell}, \kappa \right\}^{\alpha\beta} . \tag{4.13}$$

For the moment, we have only considered the neutrino Yukawa couplings, but we also have to include the charged lepton Yukawa couplings, among which we will only consider the interaction involving the tau Yukawa. Assuming that the process $\phi \leftrightarrow \ell_\tau \tau^c_R$ is in-equilibrium, it contributes to the interaction Hamiltonian as

$$H^\tau = h_{\rho\tau} a^\dagger_\phi a_{\tau^c} a_{\ell_\rho} + h^*_{\rho\tau} a_\phi a^\dagger_{\tau^c} a^\dagger_{\ell_\rho} \, . \tag{4.14}$$

---

[1] Had we considered the Higgs to be a complex scalar field, we would have obtained an asymmetry stored in the Higgs degrees of freedom, which could be expressed in terms of the $B/3 - L_\alpha$ one, via a conversion matrix, C_ϕ in [79, 76].

In the basis where the charged Yukawa couplings are diagonal, $h_{\rho\tau} = h_\tau \delta_{\rho\tau}$, their contribution to the lepton doublet asymmetry evolution can be written as:

$$\begin{aligned}\frac{\partial f_{\Delta\ell}^{\alpha\beta}}{\partial t} &= 2\left(f_N - f_N^{eq}\right) K_1 \varepsilon_{\alpha\beta} - f_\phi^{eq}\left\{f_{\Delta\ell}, \kappa\right\}^{\alpha\beta} \\ &- |h_\tau|^2 \left(f_{\Delta\tau^c} f_\ell^{eq} + f_{\tau^c}^{eq} f_{\Delta\ell}\right)^{\alpha\beta} \left(\delta_{\alpha\tau} + \delta_{\beta\tau}\right) \ , \end{aligned} \tag{4.15}$$

with $f_{\Delta\tau^c} = f_{\tau^c} - f_{\bar\tau^c}$ and $f_{\tau^c}^{eq} = (f_{\tau^c} + f_{\bar\tau^c})/2$.

Before moving further on, it is instructive to look at the equation for the equilibrium density defined eq.(4.9). Neglecting the contribution from the interaction Hamiltonian H^N, we find

$$\frac{\partial f_\ell^{eq\,\alpha\beta}}{\partial t} = 2|h_\tau|^2\,\delta_{\alpha\tau}\delta_{\beta\tau}\,f_\phi^{eq} - |h_\tau|^2 f_{\tau^c}^{eq}\left(\delta_{\alpha\tau}\,f_\ell^{eq\,\tau\beta} + f_\ell^{eq\,\alpha\tau}\,\delta_{\tau\beta}\right) \ . \tag{4.16}$$

Here we took two flavours into account, which are labelled τ and μ for simplicity. We see that neither the $\mu\mu$ component, nor the $\tau\tau$ one are affected by the charged Yukawa interactions, owing to the equilibrium condition of the interaction rate, which is similar to eq.(4.10). On the other hand, for the non-diagonal entries, we have

$$\frac{\partial f_\ell^{eq\,\mu\tau}}{\partial t} = -|h_\tau|^2 f_{\tau^c}^{eq}\, f_\ell^{eq\,\mu\tau} \ , \tag{4.17}$$

and similarly for $f_\ell^{eq\,\tau\mu}$.

We see that when the charged Yukawas are in-equilibrium, "equilibrium" densities of quantum-correlations are exponentially damped [75], and do not affect the flavour-eigenstate "equilibrium" densities. Therefore, we now write $f_\ell^{eq\,\alpha\beta} = f_\ell^{eq}\,\delta_{\alpha\beta}$.

4.2 Flavoured Boltzmann Equations

Eq.(4.15) above clearly shows the flavour structure that the Boltzmann equations should have. Before discussing this, we make a few transformations in order to extrapolate this equation to the comoving number density asymmetry, through the following "rough" procedure [2]:

- we factorise the equilibrium distribution function, using for the last two terms the equilibrium conditions $f_\phi^{eq} f_\ell^{eq} = f_N^{eq}$ and $f_{\tau^c}^{eq} f_{\ell^\tau}^{eq} = f_\phi^{eq}$,
- we "sort of" integrate over the phase-space to work with number densities,
- we reintroduce the expansion of the Universe through

$$\frac{\partial}{\partial t} \rightarrow \frac{d}{dt} - 3H(T) \ ,$$

---

[2] Had we kept the spinorial structure, all the steps indicated would have been rigorous. Since we are confident on this point, we use a simple matching procedure for our equations. Following the different steps indicated does allow us to identify the different terms without ambiguity.

and change time to $z = M_1/T$ and number densities to comoving number densities. At this point we get,

$$\begin{aligned}\frac{dY^{\alpha\beta}_{\Delta\ell}}{dz} &= \frac{1}{z\,s\,H(T)}\left(\varepsilon_{\alpha\beta}K_1\left[\frac{n_N^{eq}}{Y_N^{eq}}\right](Y_N - Y_N^{eq}) - \left[\frac{n_N^{eq}}{Y_N^{eq}}\frac{Y_N^{eq}}{Y_\ell^{eq}}\right]\frac{1}{2}\left\{Y_{\Delta\ell},\kappa\right\}^{\alpha\beta}\right)\\ &- \frac{1}{z\,s\,H(T)}\left(\left[\frac{n_\phi^{eq}}{Y_\ell^{eq}}\right]|h_\tau|^2\left(Y_{\Delta\tau^c}\,\delta_{\alpha\beta} + \frac{Y_{\tau^c}^{eq}}{Y_\ell^{eq}}\,Y^{\alpha\beta}_{\Delta\ell}\right)(\delta_{\alpha\tau}+\delta_{\beta\tau})\right)\ .\end{aligned}$$

The last step consists in "sort of" redefining the couplings in order to reintroduce the usual interaction rates. In an accurate calculation, the interaction rates naturally appear when integrating over the phase-space.

Further using the fact that $Y_{\tau^c}^{eq} = Y_\ell^{eq}/2$, we obtain the flavoured Boltzmann equations for the comoving number densities:

$$\begin{aligned}\frac{dY^{\alpha\beta}_{\Delta\ell}}{dz} &= \varepsilon_{\alpha\beta}K_1 D(z)(Y_N - Y_N^{eq}) - W_{id}(z)\frac{1}{2}\left\{Y_{\Delta\ell},\kappa\right\}^{\alpha\beta}\\ &- \frac{z}{sH(M_1)}\frac{\gamma_\tau}{Y_\ell^{eq}}\left(2\,Y_{\Delta\tau^c}\,\delta_{\alpha\beta} + Y^{\alpha\beta}_{\Delta\ell}\right)\left(\frac{\delta_{\alpha\tau}+\delta_{\beta\tau}}{2}\right)\ ,\end{aligned} \tag{4.18}$$

The last term represents the depletion of the lepton $SU(2)$ doublet asymmetries by the charged Yukawa interaction, with [25],[80]:

$$\frac{\gamma_\alpha}{n_\ell^{eq}} \simeq 10^{-2}|h_\alpha|^2 T\ . \tag{4.19}$$

When extrapolating from eq.(4.15) to the BE for comoving number densities, the matching with the τ^c interaction term may seem arbitrary. However, we can derive the evolution equation for the τ^c asymmetry [80], by looking at the evolution of the operator

$$f_{\Delta\tau^c} = a^\dagger_{\tau^c}a_{\tau^c} - a^\dagger_{\bar{\tau}^c}a_{\bar{\tau}^c}\ . \tag{4.20}$$

Doing so, and using the same matching procedure as before, we find

$$\begin{aligned}\frac{dY_{\Delta\tau^c}}{dz} &= -\frac{z}{sH(M_1)}2|h_\rho|^2\left(2\,Y_{\Delta\tau^c} + Y^{\tau\tau}_{\Delta\ell}\right)\\ &= -\frac{z}{sH(M_1)}\frac{\gamma_\tau}{Y_\ell^{eq}}\left(2\,Y_{\Delta\tau^c} + Y^{\tau\tau}_{\Delta\ell}\right)\ ,\end{aligned} \tag{4.21}$$

hence justifying the quoted rate eq.(4.19).

Given the expression above we can now deduce the temperature regime for which lepton flavours are relevant in leptogenesis.

We see that the interaction projecting lepton doublets onto the flavour space is in-equilibrium if [75, 76]

$$z\,\gamma_\alpha \gtrsim H(M_1)\,, \tag{4.22}$$

which provides a bound on the decaying right-handed neutrino mass. Evaluating the equilibrium condition at the temperature for which the asymmetry will be mostly produced, $T \sim M_1$, this bound reads:

$$M_1 \lesssim 7 \times 10^{15} h_\alpha^2 \,\mathrm{GeV}\,, \tag{4.23}$$

Therefore:

- τ-Yukawas are in-equilibrium if $M_1 \lesssim 10^{12}$ GeV,
- muon-Yukawas are in-equilibrium for $M_1 \lesssim 3 \times 10^9$ GeV,
- electron-Yukawas are in-equilibrium for $M_1 \lesssim 6 \times 10^4$ GeV.

However, thermal equilibrium does not guarantee that the lepton doublet is to be projected onto flavour space [81]. Indeed, we see that the terms involving $N - \ell$ couplings in eq.(4.18) are independent of the choice of the flavour basis, which is obviously not the case for the charged Yukawa interactions. The condition for the flavour basis to be relevant is actually more stringent than the equilibrium condition eq.(4.23). The processes decohering the lepton doublets have to be faster than the processes which recohere lepton doublets at the time the asymmetry is produced, that is [81, 82]

$$\frac{z\gamma_\alpha}{H(M_1)} \gtrsim W_1(z)\,. \tag{4.24}$$

Considering only inverse decays, and evaluating them at their maxima, $z \simeq 2$, one finds

$$M_1 \;\; \lesssim \;\; 5 \times 10^{15}\,\mathrm{GeV}\frac{h_\alpha^2}{\kappa_{\alpha\alpha}}\;, \tag{4.25}$$

where $\kappa_{\alpha\alpha}$ parametrises the individual washout of the flavour α. For the flavour τ, this constraint reads:

$$M_1 \lesssim \frac{10^{12}\,\mathrm{GeV}}{\kappa_{\tau\tau}}\,. \tag{4.26}$$

Under this constraint, flavours are fully relevant in leptogenesis. The situation where charged Yukawas are in-equilibrium but not faster than recohering processes is more involved, and we postpone its discussion until the end of the chapter.

4.3 Flavour structure

4.3.1 One flavour scheme

This case is encountered if $M_1 \gtrsim 10^{12}$ GeV, and in this case none of the charged Yukawas are in-equilibrium. It has been shown in [82] that by a rotation of lepton doublet states, one can recover the BE of the one flavour case studied in the previous chapter, that is

$$\begin{aligned}\frac{dY_N(z)}{dz} &= -D(z)K_1\left(Y_{N_1}(z) - Y^{eq}_{N_1}(z)\right)\;,\\ \frac{dY_L(z)}{dz} &= \varepsilon_1 D(z)K_1\left(Y_{N_1}(z) - Y^{eq}_{N_1}(z)\right) - W_{id}(z)K_1Y_L\;,\end{aligned} \tag{4.27}$$

with $\varepsilon_1 = Tr[\varepsilon]$. For $M_1 \gtrsim 10^{12}$ GeV, the results of the previous chapter hold.

4.3.2 Two flavour scheme

Let us now consider the case where only the tau Yukawas are in equilibrium, that is $3\times 10^9\,\text{GeV} \lesssim M_1 \lesssim 10^{12}\,\text{GeV}$.

In this case, the tau flavour is distinguishable, but neither the muon nor the electron flavours are. Hence, the lepton produced in N_1 decays will be projected onto the tau direction, as well as onto an orthogonal direction to that of the tau. This second direction is composed of the muon and electron flavour directions that coherently mix, and which we will label $L_\perp = L_e + L_\mu$. We have a two flavour regime $(L_\tau, L_\perp)$ and in this case eq.(4.18) holds, with $\alpha = \tau$ and $\beta = \perp$:

$$\begin{aligned}
\frac{dY_N(z)}{dz} &= -D(z)K_1\left(Y_{N_1}(z) - Y^{eq}_{N_1}(z)\right) \ , \\
\frac{dY^{\perp\perp}_{\Delta\ell}(z)}{dz} &= \varepsilon_{\perp\perp}K_1 D(z)(Y_N(z) - Y^{eq}_N(z)) - W_{id}(z)\kappa_{\perp\perp}Y^{\perp\perp}_{\Delta\ell}(z) \\
&- W_{id}(z)\frac{1}{2}\left(\kappa_{\perp\tau}Y^{\tau\perp}_{\Delta\ell}(z) + Y^{\perp\tau}_{\Delta\ell}(z)\kappa_{\tau\perp}\right) \ , \\
\frac{dY^{\perp\tau}_{\Delta\ell}(z)}{dz} &= \varepsilon_{\perp\tau}K_1 D(z)\,(Y_N(z) - Y^{eq}_N(z)) - W_{id}(z)\,Y^{\perp\tau}_{\Delta\ell}(z)\left(\frac{\kappa_{\perp\perp} + \kappa_{\tau\tau}}{2}\right) \\
&- \kappa_{\perp\tau}\left(\frac{Y^{\perp\perp}_{\Delta\ell}(z) + Y^{\tau\tau}_{\Delta\ell}(z)}{2}\right) - \frac{D_\tau}{2}Y^{\perp\tau}_{\Delta\ell}(z) \ , \\
\frac{dY^{\tau\perp}_{\Delta\ell}(z)}{dz} &= \frac{dY^{\perp\tau}_{\Delta\ell}(z)}{dz}(\perp\leftrightarrow\tau) \ , \\
\frac{dY^{\tau\tau}_{\Delta\ell}(z)}{dz} &= \frac{dY^{\perp\perp}_{\Delta\ell}(z)}{dz}(\perp\leftrightarrow\tau) - D_\tau\left(2Y_{\Delta\tau^c}(z) + Y^{\tau\tau}_{\Delta\ell}(z)\right) \ .
\end{aligned} \tag{4.28}$$

In these equations, the CP asymmetries $\varepsilon_{\perp\perp}$ and $\varepsilon_{\perp\tau}$ are defined by

$$\begin{aligned}
\varepsilon_{\perp\perp} &\equiv \varepsilon_{ee} + \varepsilon_{\mu\mu} \ , \\
\varepsilon_{\perp\tau} &\equiv \varepsilon_{e\tau} + \varepsilon_{\mu\tau} \ ,
\end{aligned}$$

and similar relations hold for the washout parameters κ. We also define for convenience

$$D_\tau = \frac{z}{H(M_1)}\frac{\gamma_\tau}{Y^{eq}_\ell} \simeq \frac{7\times 10^{15}\,\text{GeV}}{M_1} \times h^2_\tau \simeq \frac{7\times 10^{11}\,\text{GeV}}{M_1}. \tag{4.29}$$

Notice that, according to eq.(4.21), the Boltzmann equations for the τ diagonal entry can be written:

$$\frac{dY^{\tau\tau}_{\Delta\ell}(z)}{dz} = \frac{dY^{\perp\perp}_{\Delta\ell}(z)}{dz}(\perp\leftrightarrow\tau) + \frac{dY_{\Delta\tau^c}}{dz} \ . \tag{4.30}$$

Since the leptonic τ doublet $\ell^{\tau\tau}$ interacts with right-handed neutrinos, its evolution equation receives contributions from the interaction Hamiltonian H^N, corresponding to an asymmetry production and depletion. However, since $\ell^{\tau\tau}$ also interacts with the right-handed singlet τ^c, it receives a further contribution from H^τ.

This is quite satisfactory, since we do not want to study the asymmetry stored in lepton doublets, but the lepton asymmetry

$$L_\alpha = L_{\ell^\alpha} + L_{e^\alpha_R} = L_{\ell^\alpha} - L_{e^{\alpha\,c}_R} \ , \tag{4.31}$$

which is stored in lepton doublets as well as in singlets [80].

The muon-Yukawas being out of equilibrium, the leptonic asymmetry $Y_{\ell\perp}$ is not influenced by any effect of this type: muon (or electron) isosinglet density is too far from thermal equilibrium to disrupt the $\ell_\perp$ propagation.

The off-diagonal terms are however sensitive to the τ^c population, which acts as a damping term. Furthermore, the term $\propto D_\tau Y_{\Delta\ell}^{\alpha\beta}$ exponentially drives the quantum-correlations to zero: when the interactions involving charged Yukawa couplings of a given flavour are in-equilibrium, the quantum correlations between this flavour and the orthogonal one(s) are exponentially damped, and the flavours, being distinguishable, evolve separately. Notice that since we did not include the free Hamiltonian $H^0 \propto \omega_\tau\, a^\dagger_{\ell_\tau} a_{\ell_\tau} + w_\perp\, a^\dagger_{\ell_\perp} a_{\ell_\perp}$, the number densities are not liable to flavour oscillations [75], which have been studied in detail in [82]. Actually these oscillations only affect the quantum correlations by inducing a faster damping [82].

We illustrate this damping in fig.(4.1), were we depict the evolution of the different asymmetries according to the set of Boltzmann equations in eqs.(4.21-4.28).

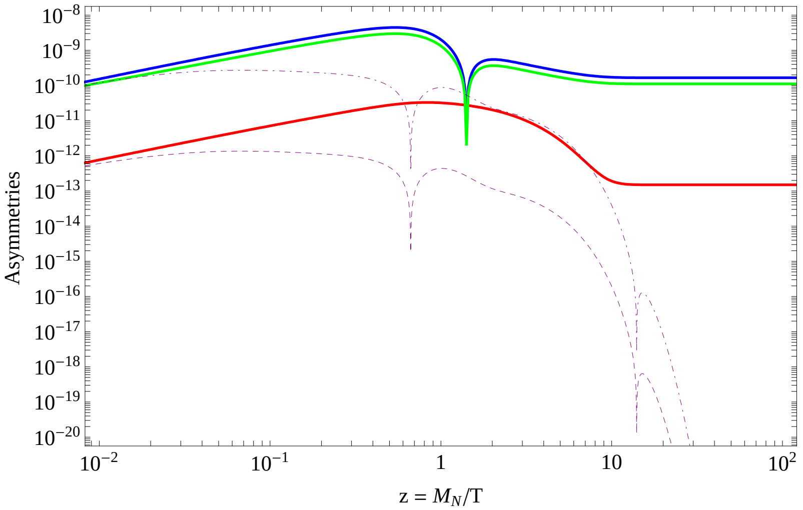

Figure (4.1): Evolution of comoving number densities. The thick lines represent diagonal terms of the flavoured Boltzmann equation, with $Y_L^{\tau\tau}$ in blue (upper curve), $Y_{\Delta\ell}^{\tau\tau}$ in green (light grey) and $Y_{\Delta\ell}^{\perp\perp}$ in red (lower curve), respectively. The thin purple lines represent the quantum-correlations, *i.e.* the off-diagonal terms when the charged Yukawas are in-equilibrium. The dashed line stands for $Y_{\Delta\ell}^{\perp\tau}$ whereas the dot-dashed one for $Y_{\Delta\ell}^{\tau\perp}$. The input parameters have been chosen, so that the components are distinguishable, with $\kappa_{\perp,\perp} = \kappa_{\perp,\tau} = 0.1$, $\kappa_{\tau,\perp} = \kappa_{\tau,\tau} = 20$ for the washout parameters and $\varepsilon_{\perp,\perp} = \varepsilon_{\perp,\tau} = 0.1 \times 10^{-6}$, $\varepsilon_{\tau,\perp} = \varepsilon_{\tau,\tau} = 20 \times 10^{-6}$ for the CP asymmetries.

In these equations, we have chosen the washout parameters and CP asymmetries in order to distinguish the different components. The effect of charged Yukawa interactions in damping the quantum correlations is clear, hence in the temperature regime where these interactions are in-equilibrium the off-diagonal terms can be safely neglected.

Furthermore, we plotted in this graph the leptonic doublet asymmetry $Y_{\Delta\ell}^{\tau\tau}$ (green-light grey) and the lepton asymmetry $Y^{\tau\tau}_{\Delta L} = Y^{\tau\tau}_{\Delta\ell} - Y_{\Delta\tau^c}$ (blue-upper curve). We see that the singlet contribution to the leptonic asymmetry accounts only for $\mathcal{O}(1)$, and thus, for now, we will neglect it on the evolution of the asymmetries.

4.3.3 Three flavour scheme

If $M_1 \lesssim 3 \times 10^9\,\mathrm{GeV}$, then both muon and tau Yukawas are in equilibrium. These interactions decohere the lepton doublet by projecting it onto a three flavour basis (L_τ, L_μ, L_e). The muon and electron flavours being now distinguishable, muonic and electronic quantum-correlations are exponentially damped, and one is left with the set of Boltzmann equations for the lepton number densities:

$$\frac{dY_L^{\alpha\alpha}(z)}{dz} = \varepsilon_{\alpha\alpha}\, K_1\, D(z)\, \big(Y_N(z) - Y_N^{eq}(z)\big) - W_{id}(z)\, \kappa_{\alpha\alpha}\, Y_L^{\alpha\,\alpha}(z)\ , \tag{4.32}$$

with $\alpha = e, \mu, \tau$.

4.4 $B - L$ conversion and the Baryon asymmetry

In the previous section we have derived the Boltzmann equations for the lepton asymmetries. However, as explained in appendix A, sphalerons conserve $B/3 - L_\alpha$ asymmetries [68], but not the leptonic ones. Therefore, it is preferable to work with

$$Y_{\Delta\alpha} \equiv \frac{1}{3} Y_{\Delta B} - Y_{\Delta L^\alpha}\ , \tag{4.33}$$

computed from the leptonic doublet asymmetries by

$$Y_{\Delta\alpha} = \sum_\beta A_{\alpha\beta} Y_{\Delta\ell^\beta}\ , \tag{4.34}$$

where the sum is made over all flavours that were distinguishable during leptogenesis. Details about the derivation of the entries of the conversion matrix $A_{\alpha\beta}$ are given in the appendix B. This relation is obtained by expressing the chemical potentials of the $B/3 - L_\alpha$ asymmetries in terms of the leptonic doublet ones, and it depends on the different processes that are in-equilibrium at the temperature leptogenesis occurs [83, 84].

Since we do not consider B violating processes, the Boltzmann equations for Y_N and for the $B/3 - L_\alpha$ asymmetries are finally given by (dropping the redundant double indices):

$$\begin{aligned} \frac{dY_N(z)}{dz} &= -D(z) K_1 \left(Y_{N_1}(z) - Y_{N_1}^{eq}(z)\right)\ , \\ \frac{dY_{\Delta\alpha}(z)}{dz} &= -\varepsilon_\alpha\, K_1\, D(z)\, \big(Y_N(z) - Y_N^{eq}(z)\big) - W(z)\, \kappa_\alpha \sum_\beta A_{\alpha\beta}\, Y_{\Delta\beta}(z)\ . \end{aligned} \tag{4.35}$$

This set of equations is written here in all generality, and the expressions of the production term $D(z)$ and of the washout one $W(z)$ depend on the model, as well as the parameters which govern these equations, κ_α, K_1 and ε_α.

Finally, $B/3-L_\alpha$ asymmetries are conserved, until they are converted by sphalerons. The baryon asymmetry is then related to the individual asymmetries by:

$$Y_B = a_{sph} \times \sum_\alpha Y_{\Delta\alpha} \ , \tag{4.36}$$

the sum being over the flavour that were distinguishable when leptogenesis occurs. The conversion factor is $a_{sph} \sim 1/3$, and its value also depends on the model, and on whether the sphalerons freeze before or after the electroweak-phase transition [83, 84].

4.5 A remark on the full flavour regime

In section 4.3, when we discussed the flavour structure of the BEs, the criterion used for the relevance of a given flavour in leptogenesis was presented eq.(4.23) and translates into having the interactions involving charged lepton Yukawa couplings in-equilibrium, $\Gamma_\alpha \gtrsim H(M_N)$.
However, as explained around eqs.(4.24)-(4.26), thermal equilibrium does not guarantee that the lepton doublets will be projected onto the flavour basis. A more accurate constraint comes from the requirement that the decohering rates γ_α are faster than any recohering interaction, either the production term $D(z)$ or the washout one $W(z)$ [81]. Considering only inverse decays as depletion reactions, and requiring that at least the interaction involving the charged tau Yukawa couplings are in-equilibrium, a bound on M_1 can be derived:

$$M_1 \lesssim \frac{10^{12}\,\mathrm{GeV}}{\kappa_\alpha} \left(\frac{h_\alpha}{h_\tau}\right)^2 . \tag{4.37}$$

If this constraint is satisfied, then the flavours are fully relevant in leptogenesis.
Given the equilibrium condition for sphalerons, $M_1 \lesssim 10^{12}$ GeV, which is roughly the same than the equilibrium condition for tau-Yukawas, we see that only in the strong washout regime is the constraint of eq.(4.37) more stringent than the equilibrium condition eq.(4.23).
Let us consider a lepton doublet (asymmetry) produced in decays of N_1 at a temperature $T \sim M_1$, in the case where the tau-Yukawas are in-equilibrium. If during the caracteristic time for two $\ell - H - \tau^c$ interactions to happen, inverse decays have time to occur, the lepton doublet will not be projected onto the flavour basis, and the faster the decays/inverse decays, the more coherently the lepton doublet will evolve.
In such case, the lepton asymmetry should be computed by solving the set of BEs including off-diagonal terms. As already stated, ref. [82] shows that by an appropriate redefinition of the lepton doublets, corresponding to a rotation in flavour space (allowed since the N-interactions are the ℓ-labelling ones), one recovers the single flavour picture.
However, through this redefinition, couplings are also modified, and so the differences between including or neglecting quantum correlations are less transparent. In order to study the validity of the full flavour regime, we solve the sets of eqs.(4.28) with and without quantum correlations.
We depict in fig. (4.2) the effect of these correlations by showing a contour plot of the ratio of the lepton doublet asymmetry for a given flavour computed with and without these terms,

$Y^{with}_{\Delta\ell^{\alpha\alpha}}/Y^{without}_{\Delta\ell^{\alpha\alpha}}$, allowing M_1 to vary around the central value $M_1 = 10^{12}\,\text{GeV}$ and the washout parameter around $K_1 = 1$. For simplicity, we have taken the CP asymmetries and the washout parameters of the different flavours to be equal. One expects that if the condition of eq.(4.37) is not satisfied, the damping of the quantum correlations will be inefficient and these off-diagonal terms will significantly contribute to the lepton asymmetry (in fact, given our choice of parameters, in an equal amount). On the other hand, if eq.(4.37) holds, the quantum correlations will be damped and the ratio is expected to approach unity.

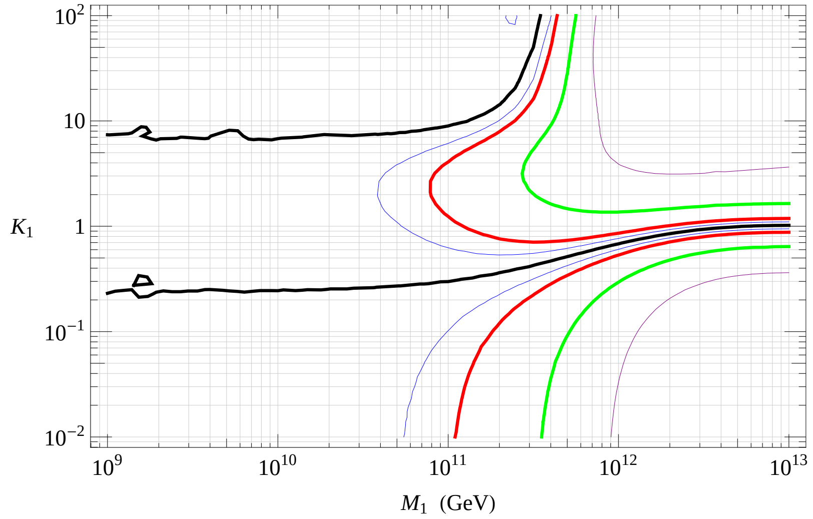

Figure (4.2): Contour plot of the ratio between the lepton doublet asymmetries computed with and without quantum correlations. The black line stands for $Y^{with}_{\Delta\ell^{\alpha\alpha}}/Y^{without}_{\Delta\ell^{\alpha\alpha}} = 1$, whereas the blue, red, green and purple lines represents deviation (from left to right) of 5%, 10%, 30% and 60%, respectively.

We see in fig.(4.2) that for $M_1 \lesssim 5 \times 10^{11}\,\text{GeV}$, the inclusion of quantum correlations modifies the results up to 30%, while for $M_1 \lesssim 10^{11}\,\text{GeV}$, the approximate eq.(4.35) gives very accurate results, and so in that case quantum correlations can be safely neglected.

To conclude on the validity of eqs.(4.35) regarding a precise determination of the lepton asymmetry, we can say that for $M_1 \lesssim 10^{11}\,\text{GeV}$, the quantum correlations are effectively damped and one can use eqs.(4.35). For $5 \times 10^{11}\,\text{GeV} \gtrsim M_1 \gtrsim 10^{11}\,\text{GeV}$, the results are valid only up to $10\% - 30\%$, while for $M_1 \gtrsim 5 \times 10^{11}\,\text{GeV}$, a precise computation does indeed require the inclusion of quantum correlations. For heavier M_1, the one flavour approximation is valid.

However, we stress that the results here presented have been derived in the Standard Model (plus RHns). Had we considered a supersymmetric extension, the discussion would have been dramatically different. Indeed, in SUSY extensions, the charged Yukawa couplings is now corrected by the ratio of Higgs vevs, $h_\tau^2 \times (1 + \tan^2(\beta))$, where $\tan(\beta) = v_u/v_d$ is the ratio of the SUSY Higgs vevs. Hence for $\tan^2(\beta)) \gtrsim 3(10)$, the results are valid up to 10% for $M_1 \lesssim 10^{12(14)}\,\text{GeV}$, so that for $M_1 \lesssim 10^{12}\,\text{GeV}$, as required for sphalerons to be in-equilibrium, flavours are always fully relevant in supersymmetric leptogenesis.

In the following, we will neglect quantum correlations.

Chapter 5

On the role of lepton flavours in type I leptogenesis

In this chapter we are going to study leptogenesis in the type I seesaw mechanism, were three right-handed neutrinos are added to the SM model particle content in order to explain neutrino masses. The Lagrangian contains the extra terms

$$\mathcal{L} \supset -\lambda_{\alpha i}\overline{N}_i\,\ell_\alpha\,\phi - \frac{1}{2}\overline{N}_i M_i N_i^c + h.c.\,, \tag{5.1}$$

which provide masses to neutrinos from the seesaw mechanism. These masses are not yet measured, but rather the differences of squared masses are deduced from the oscillations of neutrinos. However, should we believe that leptogenesis is indeed the mechanism responsible for the observed BAU, an upper bound on the light neutrino mass can be derived [74, 59, 65], $m_i \lesssim 0.12\,\mathrm{eV}$, a bound that may be soon tested.

On the other hand, the right-handed sector is experimentally unconstrained. This is one of the gaps of leptogenesis that may be never filled in. Nevertheless, the Davidson-Ibarra bound [64] constrains the right-handed neutrino mass scale to be above $M_1 \gtrsim 10^9\,\mathrm{GeV}$. Moreover, CP violation in the leptonic sector -related to the CP phases of U and R- should be quantitatively large enough so that CP asymmetry is larger than $\varepsilon_{CP} \gtrsim 10^{-7}$.

All these constraints have been derived in the single flavour picture, where one considers that the lepton involved in the decays of the RHn evolves coherently after being produced. Nonetheless, we saw in the previous chapter that for $M_1 \lesssim 10^{11-12}\,\mathrm{GeV}$, not only are the interactions involving charged lepton Yukawa couplings in-equilibrium, but their rate can also be faster than recohering processes, the decays and inverse decays, in which case the flavours are relevant and should be included for a precise computation of the baryon asymmetry obtained by leptogenesis.

This chapter, which is mostly based on [71] and [90], is organised as follows: firstly, we set up the framework of flavoured leptogenesis and we qualitatively discuss how lepton flavours affect the key-parameters of leptogenesis, namely the CP asymmetries and the washout factors. Secondly, we evaluate the resulting baryon asymmetry produced by leptogenesis, and show how it differs from the one-flavour picture provided in chapter 3. Finally, we consider the constraints derived for the low and high-energy parameters.

5.1 Flavoured leptogenesis

We first recall the various definitions and the framework of Boltzmann equations. We consider a hierarchical spectrum for the right-handed neutrinos $M_1 \ll M_2, M_3$, and thus neglect contributions from the heavier neutrinos in the lepton asymmetry production. Indeed, since in this case the leptons produced by $N_{2,3}$ leptogenesis participate via inverse decays in the thermalisation of N_1, one can consider that the lepton asymmetry produced during $N_{2,3}$ leptogenesis epoch will be washed out. However, this assumption, if valid in the single approximation [85], is not strictly justified when flavours are taken into account [86], as the lepton flavour content may differ for the lepton involved in $N_{2,3}$ leptogenesis and the one involved in N_1 leptogenesis. This point will be discussed in the following chapter; presently, we only consider the processes that involve N_1. The BEs for right-handed neutrinos $N \equiv N_1$ and $\Delta_\alpha \equiv B/3 - L_\alpha$ asymmetry comoving number densities are [71]:

$$\begin{aligned} \frac{dY_N^{eq}(z)}{dz} &= -K_1\, P(z)\, \left(Y_N(z) - Y_N^{eq}(z)\right)\ , \\ \frac{dY_{\Delta\alpha}(z)}{dz} &= -\varepsilon_\alpha\, K_1\, P(z)\, \left(Y_N(z) - Y_N^{eq}(z)\right) + W(z)\, \kappa_\alpha \sum_\beta A_{\alpha\beta}\, Y_{\Delta\beta}(z)\,, \end{aligned} \tag{5.2}$$

In these equations, individual washout parameters are given by

$$\kappa_\alpha = \frac{\Gamma(N \to \ell\phi)}{H(M_1)} = |\lambda_{1\alpha}|^2 \frac{v^2}{M_1\, m^*} = \frac{\tilde{m}_\alpha}{m^*}\ , \tag{5.3}$$

with the effective neutrino mass $\tilde{m}_\alpha$ being given by

$$\tilde{m}_\alpha = |\lambda_{1\alpha}|^2 \frac{v^2}{M_1}\,, \tag{5.4}$$

and $K_1 = \sum_\alpha \kappa_\alpha$. The other quantities have been defined in chapter 3, section 3.3. We nevertherless recall the BE for the lepton asymmetry in the single flavour picture:

$$\frac{dY_L(z)}{dz} = \varepsilon_1\, K_1\, P(z)\, \left(Y_N(z) - Y_N^{eq}(z)\right) - W(z)\, K_1\, Y_L(z)\,. \tag{5.5}$$

The individual CP asymmetries ε_α are given by eq.(3.25):

$$\varepsilon_\alpha = \frac{1}{8\pi} \sum_{j \neq 1} \frac{\mathrm{Im}\left\{\lambda^*_{\alpha i}\lambda_{\alpha j}\left(\lambda^\dagger\lambda\right)_{ij}\right\}}{(\lambda^\dagger\lambda)_{ii}}\, \left(f(x_j) + g(x_j)\right), \tag{5.6}$$

where

$$f(x) + g(x) = \sqrt{x}\left(\frac{2-x}{1-x} - (1+x)\log\left(1 + \frac{1}{x}\right)\right). \tag{5.7}$$

The total CP asymmetry is the sum of the individual ones $\varepsilon_1 = \sum_\alpha \varepsilon_\alpha$.

The set of equations (5.2) governs the $B - L_\alpha$ asymmetry evolutions. As explained in the

previous chapter, these $B-L_\alpha$ asymmetries are deduced from the leptonic doublet asymmetries, by relating the chemical potentials of the $B-L_\alpha$ asymmetry to the ones of ℓ_α according to the different processes that are in-equilibrium at the temperature at which leptogenesis occurs.
We saw that if $M_1 \lesssim 10^9\,\text{GeV}$, interactions involving muon and tau charged lepton Yukawa couplings are in-equilibrium, and are potentially faster than decays and inverse decays, thus projecting the lepton asymmetry onto a three flavour basis (L_e, L_μ, L_τ). Given that for $T \lesssim 10^9\,\text{GeV}$, interactions involving charm, bottom and top quark Yukawa couplings are also in-equilibrium, the conversion matrix A reads [71]:

$$A = \begin{pmatrix} -151/179 & 20/179 & 20/179 \\ 25/358 & -344/537 & 14/537 \\ 25/358 & 14/537 & -344/537 \end{pmatrix} . \tag{5.8}$$

One then has to solve the coupled BEs for those three distinguishable flavours. The BEs are governed by individual CP asymmetries ε_α, $\alpha = e, \mu, \tau$ and individual washouts κ_α, $\alpha = e, \mu, \tau$.
If the decaying RHn is heavier, with $10^9\,\text{GeV} \lesssim M_1 \lesssim 10^{12}\,\text{GeV}$, then only tau Yukawas are in-equilibrium (together with b, c, t quarks), so that the lepton asymmetry is projected onto the tau direction $(L_\tau, \varepsilon_\tau, \kappa_\tau)$ and onto an orthogonal direction in flavour space, which coherently mixes electron and muon flavours $(L_o, \varepsilon_o, \kappa_o) = (L_e + L_\mu, \varepsilon_e + \varepsilon_\mu, \kappa_e + \kappa_\mu)$.
In this two flavours scheme the A-matrix reads:

$$A = \begin{pmatrix} -417/589 & 120/589 \\ 30/589 & -390/589 \end{pmatrix} . \tag{5.9}$$

For $M_1 \gtrsim 10^{12}\,\text{GeV}$, none of the charged lepton Yukawas are in-equilibrium, thus the one flavour approximation holds and one solves the BE for $(Y_{B-L}, \varepsilon_1, K_1)$.
Finally, the baryon asymmetry produced by sphalerons conversion is [68]:

$$Y_B = \frac{12}{37} \sum_\alpha Y_{\Delta\alpha} \, , \tag{5.10}$$

where the factor 12/37 is obtained in the SM, and the sum is made over the flavours which were distinguishable when the asymmetries were produced.

In this chapter, similarly to chapter 3, we consider $\Delta L = 1$ two-body decays and inverse decays which act as source and damping terms, and whose expressions are given by eq.(3.40). We further include $\Delta L = 1$ 2-to-2 scatterings involving the third generation of quark doublets and top quark singlets, whose contribution to the washout term is given by [59]

$$W_{scat}(z) = 2\, S_s(z) \left(\frac{Y_N(z)}{Y_N^{eq}(z)} \right) + 4\, S_t(z) \ , \tag{5.11}$$

where the precise expression of these scatterings is given in appendix B. Finally the total washout reads:

$$W(z) = W_{id}(z) + W_{scat}(z). \tag{5.12}$$

Neutrino-top scatterings also contribute to the production of the lepton asymmetry, the CP asymmetry in scatterings being equal to CP asymmetry in decays [73, 75]. The production term is thus:

$$P(z) = D(z) + 2\gamma_s(z) + 4\gamma_t(z)\ . \tag{5.13}$$

Furthermore, as we want to study the impact of lepton flavours in leptogenesis, M_1 should not be too heavy, $M_1 \leq 10^{12}\,\mathrm{GeV}$. Therefore, as explained in chapter 3, for values of K_1 between 0.01 and 100, we can safely neglect off-shell $\Delta L = 2$ while the on-shell contribution is included.

5.2 Effect of lepton flavours in the type I seesaw

The key parameters for leptogenesis, which are the couplings of light neutrinos to the heavy states λ and the mass of the right-handed neutrinos, are all we need to know to evaluate Y_B. Going in the basis where charged leptons and RHns mass matrices are diagonal, we use the Casas-Ibarra parametrisation [51] for the Yukawa couplings:

$$\lambda_{i\alpha} = \left(\sqrt{M}.R.\sqrt{m}.U^\dagger\right)_{i\alpha}\ , \tag{5.14}$$

where the PMNS matrix U and the matrix R are defined in chapter 2, section 2.5.1. We recall that the type I seesaw yet contains 15 independent degrees of freedom to fit a single observable: the baryon asymmetry. Even though we cannot hope to determine the would-be high-energy masses and mixings, we can nevertheless try to shed some light on the optimal regions of the parameter space. Such a work has been done in the context of flavoured leptogenesis in [87], and we do not carry here such a detailled analysis.

Using the above parametrisation, let us see how the inclusion of lepton flavours influence CP asymmetries and washout factors.

5.2.1 CP asymmetry

Assuming a strong hierarchy in the heavy neutrino sector, and using the parametrisation of eq.(5.14), eq.(5.6) can be recast into

$$\varepsilon_\alpha = -\frac{3}{16\pi}\frac{M_1}{v^2}\frac{\mathrm{Im}\left\{\sum_{\beta,\rho} m_\beta^{1/2}\, m_\rho^{3/2} U^*_{\alpha\beta}\, U_{\alpha\rho}\, R_{1\beta}R_{1\rho}\right\}}{\sum_\beta m_\beta |R_{1\beta}|^2}\ . \tag{5.15}$$

Summing over the lepton flavours, the total CP asymmetry in decays is found to be

$$\varepsilon_1 = -\frac{3}{16\pi}\frac{M_1}{v^2}\frac{\mathrm{Im}\left\{\sum_\beta m_\beta^2\, R_{1\beta}^2\right\}}{\sum_\beta m_\beta |R_{1\beta}|^2}\ , \tag{5.16}$$

no longer dependent on the low-energy phases of the PMNS matrix.However, these phases appear with a factor $\propto m_{1,2}^{1/2}$ or $m_{1,2}^{3/2}$, and so are suppressed compared to the dominant term $\propto m_3^2$. Thus we expect them to play a subdominant role in the general case of a complex R matrix, or if light neutrinos are very hierarchical. On the contrary, if CP is violated only in the low-energy sector, *i.e.* if R is real, we see that whereas ε_1 vanishes, individual CP asymmetries do not [71]. However it has been found that relying only on low-energy phases, a viable leptogenesis requires a sizable amount of fine-tuning [88].

In general, the CP asymmetries will receive contribution from both high and low-energy sectors[1]. An important point to notice is the modification of the Davidson-Ibarra bound on the CP asymmetry. Indeed, in the one flavour approximation, when summing over lepton flavours and assuming a strong hierarchy between right-handed neutrinos, the CP asymmetry is bounded by

$$\varepsilon_1^{max} = \frac{3}{16\pi}\frac{M_1(m_3 - m_1)}{v^2} \times \beta(m_1, \tilde{m}_1)\,. \tag{5.17}$$

Hence, for degenerate neutrinos, $m_1 \simeq m_3$, and thus the CP asymmetry scales as m_1^{-1}.

When lepton flavours are included, the bound on individual CP asymmetries is modified. Indeed, in the limit of hierarchical RHns, eq.(5.6) reads

$$\varepsilon_\alpha \simeq \frac{3\,M_1}{16\,\pi\,v^2}\sum_\beta \frac{\mathrm{Im}\left\{\lambda_{\alpha\,1}\lambda_{\beta\,1}\left(m^\dagger\right)_{\alpha\,\beta}\right\}}{(\lambda^\dagger\,\lambda)_{11}}\,. \tag{5.18}$$

Then, writting $\lambda_{\alpha\,1} = \Phi_\alpha\,\tilde{\lambda}_\alpha$, where $\tilde{\lambda} = |\lambda|$ and Φ stands for the phase of λ, the above expression reads

$$\varepsilon_\alpha \simeq \frac{3\,M_1}{16\,\pi\,v^2}\frac{1}{\sum_\rho \tilde{\lambda}_\rho^2}\sum_\beta \mathrm{Im}\left\{\Phi_\alpha\Phi_\beta\left(m^\dagger\right)_{\alpha\,\beta}\right\}\tilde{\lambda}_\alpha\,\tilde{\lambda}_\beta\,, \tag{5.19}$$

The washout factors are given by

$$K_1 = \sum_\alpha \kappa_\alpha = \sum_\alpha \frac{\tilde{\lambda}_\alpha^2\,v^2}{M_1}\,. \tag{5.20}$$

Using $m_{\alpha\beta} = \left(U^* d_m U^\dagger\right)_{\alpha\beta}$, and since

$$\sum_{k,\beta} m_k\,\tilde{\lambda}_\beta\,\mathrm{Im}\left\{\Phi_\alpha\Phi_\beta U_{\alpha\,k}U_{\beta\,k}\right\} \lesssim \max(m)\sqrt{\sum_\beta \tilde{\lambda}_\beta^2}\,, \tag{5.21}$$

we obtain that the individual CP asymmetries are bounded by [75]:

$$\varepsilon_\alpha \lesssim \frac{3}{16\,\pi}\frac{M_1\,m_3}{v^2} \times \sqrt{\frac{\kappa_\alpha}{K_1}}\,. \tag{5.22}$$

This is an important result, since in the limit of degenerate light neutrinos, instead of scaling as m^{-1} like the total CP asymmetry, individual CP asymmetries scale as m hence are not suppressed. We study in fig.(5.1) the validity of the bound of eq.(5.70) by plotting $\varepsilon_\alpha/\varepsilon_\alpha^{\max}$ as a function of m_1. As this bound is derived assuming a strong hierarchy for the right-handed neutrino masses, we plot $\varepsilon_\alpha/\varepsilon_\alpha^{\max}$ for different ratios $M_i/M_j = r = 5, 50$. We see that even for $r = 5$, the bound on ε_α can be safely used.

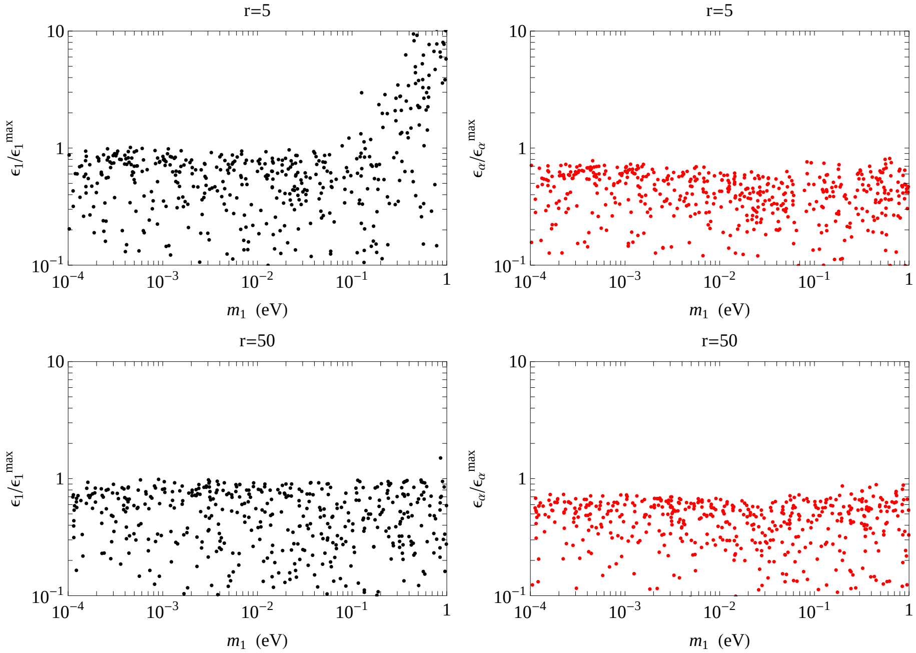

Figure (5.1): Scatter plot of $\varepsilon_\alpha/\varepsilon_\alpha^{max}$ as a function of m_1, for different ratios of heavy neutrino masses. These plots have been obtained by a random scan of the parameter space, imposing the perturbativity constraint $\lambda_{ij} < \sqrt{4\pi}$. M_1 ranges from 10^9 GeV to 10^{11} GeV, and m_1 from 10^{-4} eV to 1 eV, even if the upper limit is already above the cosmological bound.

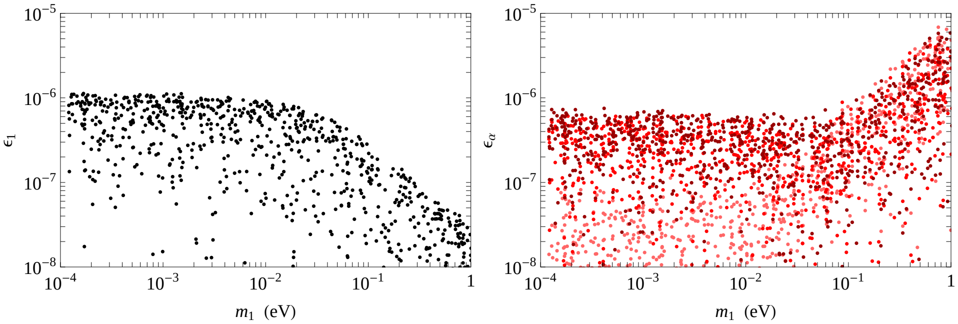

Figure (5.2): Scatter plot of ε_1 (left panel) and ε_α (right panel) as a function of the m_1. M_1 is set at 10^{10} GeV, and we take $r = 100$.

The different behaviour in the degenerate regime between the flavoured case and the single flavour approach can be seen in fig.(5.2), where we display ε_1 and ε_α as a function of m_1.
In the degenerate regime when $m_1 \gtrsim m_{atm} \simeq 5 \times 10^{-2}$ eV, we clearly see that while the total CP asymmetry is suppressed and scales as m_1^{-1}, such a suppression does not occur for individual CP asymmetries. On the contrary, since in the degenerate regime $\varepsilon_\alpha \propto m_3 \simeq m_1$, the flavoured asymmetries indeed increase with m_1.

---

[1] cf. *e.g.* [89].

5.2.2 Washout factors

Using the Casas-Ibarra parametrisation, we can rewrite the washout factors as

$$\begin{aligned} K_1 &= \sum_\beta \frac{m_\beta}{m_*} |R_{1\beta}|^2 \,, \\ \kappa_\alpha &= \sum_\beta \frac{m_\beta}{m_*} |R_{1\beta}\, U^*_{\alpha\beta}|^2 \,. \end{aligned} \tag{5.23}$$

Then, while the total washout parameter reads

$$K_1 = k_1|c_3c_2|^2 + k_2|c_3s_2|^2 + k_3|s_3|^2 \,,\; k_i = m_i/m_* \,. \tag{5.24}$$

The dependence of K_1 on m_3 being $k_3|s_3|^2$, the dependence of, for instance, the electron-flavour washout κ_e on m_3 is given by $k_3\, s_{13}^2|s_3e^{i\delta}|^2$ and is very suppressed given the bound $\theta_{13} \lesssim 0.05$. Then, besides the fact that the individual washouts are smaller than their sum K_1, one has in general an interesting non-democracy of washout strengths. Indeed, it is possible that one flavour is only weakly washed out while still having $K_1 \gg 1$. Furthermore, due to the orthogonality of the matrix R, we see that $\tilde{m}_1$ is bounded from below by m_1. In general such bounds on $\tilde{m}_\alpha$ do not exist. Then one can have $\tilde{m}_\alpha \lesssim m_1$, which is particularly interesting in the strong washout/degenerate regime.

In this sense, one somehow evades the constraint of the one-flavour picture, where the total washout is upper bounded by $K_1 \lesssim 20 \times (\varepsilon_1/5\ \times 10^{-6})^{0.86}$.

5.2.3 Qualitative picture

The rough picture of flavoured leptogenesis follows the same lines as the single flavour approximation. First, a thermalisation period during which a lepton asymmetry is produced in hollow. Then, after RHns reach thermal equilibrium, decay processes wash-out the lepton asymmetry. When the Universe has cooled down to about $M_1/100$, the different processes are frozen, and the lepton asymmetry remains constant until being converted by sphalerons.

The difference with respect to the single flavour approximation concerns how the different lepton flavours are coupled to the decaying RHn, that is the rate at which they are produced or washed out. We illustrate this difference in fig.(5.3), by plotting contours of the baryon asymmetry obtained by solving the set of BEs in eqs.(5.2), normalised to the observed value $Y_B^{obs} = 8.7\times10^{-11}$, in the case where flavours are included (left panel) or not (right panel). Leading to this plot we did not use the seesaw formula for the Yukawa couplings, since then we do not control the different washout parameters. Instead we uses the κ_αs as input parameters, setting the CP asymmetries to their maximal values. We further choose $M_1 = 10^{10}\,\text{GeV}$, so that we work in a two flavour scheme, and set for convenience $m_1 = 10^{-5}\,\text{eV}^2$.

In this figure we clearly see the influence of having included flavours. While in the single flavour

---

[2] Recall that $\tilde{m}_1 \geq m_1$, hence for $K_1 = 10^{-2}$, m_1 has to be lighter than the quoted value.

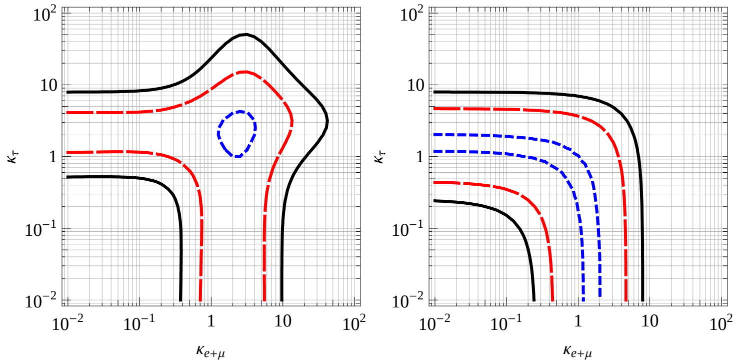

Figure (5.3): Contour plot of Y_B^{num}/Y_B^{obs}, for $\kappa_{e+\mu}$ and κ_τ varying from 10^{-2} to 10^2. The left (right) panel represents the case with (without) flavours. The different contours stand for a ratio of $1, 2$ and 4 and are respectively depicted in black, long-dashed red and dashed blue.

case the total washout is required to be $0.1 \lesssim K_1 \lesssim 10$, in the flavoured case we see that a total washout $K_1 = \kappa_{e+\mu} + \kappa_\tau$ as large as $10 - 50$ is still possible, if one of the individual washouts is close to its optimal value $\kappa_\alpha \simeq 3$.

5.3 Evaluation of the baryon asymmetry

To begin with, we neglect the effects of the flavour conversion due to sphalerons [90], typically $\mathcal{O}(0.1)$, which thus have a subdominant effect. These terms will be studied later on. The BEs for the number density then reads:

$$\begin{aligned} \frac{dY_N(z)}{dz} &= -K_1\, P(z)\, \Delta N(z)\ , \\ \frac{dY_{\Delta\alpha}(z)}{dz} &= -\varepsilon_\alpha\, K_1\, P(z)\, \Delta N(z) - W(z)\, \tilde{\kappa}_\alpha\, Y_{\Delta\alpha}(z)\,, \end{aligned} \tag{5.25}$$

where $\Delta N(x) = Y_N(x) - Y_N^{eq}(x)$ and we introduce $\tilde{\kappa}_\alpha = -A_{\alpha\alpha}\,\kappa_\alpha$ (recall that diagonal entries of the conversion matrix A are negatives). The formal solution of this equation for the $\Delta\alpha$ asymmetry is

$$Y_{\Delta\alpha}(z) = -\varepsilon_\alpha K_1 \int_{z_{in}}^{z} dx\, P(x)\, \Delta N(x)\, e^{-\tilde{\kappa}_\alpha \int_x^z dy\, W(y)}\,. \tag{5.26}$$

As in the single flavour case, the $\Delta\alpha$ asymmetry evolves differently according to the specific washout regime.

All flavours in the strong washout regime

In the case where $\kappa_\alpha \gg 1$, $Y_N(z) \simeq Y_N^{eq}(z)$, so that $\Delta N(x) = -{Y_N^{eq}}'/K_1\, P(x)$ and

$$Y_{\Delta\alpha} \simeq \varepsilon_\alpha \int_{z_{in}}^{z} dx\, {Y_N^{eq}}'(x)\, e^{-\tilde{\kappa}_\alpha \int_x^z dy\, W(y)}\,. \tag{5.27}$$

In this integral, since the main contribution to the asymmetry production comes from $z \gtrsim 1$, the scattering term in the washout can be neglected, and therefore we recover the result of the one-flavour approximation, namely

$$Y_{\Delta\alpha} \simeq -\varepsilon_\alpha \times \left(\frac{0.4}{\tilde{\kappa}_\alpha^{1.16}}\right) Y_N^{eq}(z_{in}), \tag{5.28}$$

with $Y_N^{eq}(z_{in}) \simeq 3.9 \times 10^{-3}$. The efficiency factor for the flavour α in the strong washout regime is thus given by:

$$\eta_\alpha^s \simeq \frac{0.4}{\tilde{\kappa}_\alpha^{1.16}}\,. \tag{5.29}$$

By summing over the flavours, the baryon asymmetry is found to be

$$Y_B = -\frac{12}{37}\sum_\alpha \varepsilon_\alpha \left(\frac{0.4}{\tilde{\kappa}_\alpha^{1.16}}\right)\; Y_N^{eq}(z_{in})\,. \tag{5.30}$$

This shows the difference with respect to the one-flavour approximation, for which the baryon asymmetry in the strong washout regime is

$$Y_B^{1f} \propto \frac{\sum_\alpha \varepsilon_\alpha}{\left(\sum_\alpha \kappa_\alpha\right)^{1.16}}\;. \tag{5.31}$$

If, for example, $\kappa_1 = 3$ and $\kappa_2 = 7$ ($K_1 = 10$), then assuming equal CP asymmetries, the baryon asymmetry in the flavoured case is ~ 2.5 times the unflavoured one; for instance if $\kappa_1 = 1$ and $\kappa_2 = 14$ ($K_1 = 15$), then the enhancement is of one order of magnitude.

All flavours in the weak washout regime

In the case where $\kappa_\alpha \ll 1$ for all distinguishable flavours, when $\Delta L = 1$ scatterings are included in both source and damping terms, one expects the $B - L$ asymmetry to scale as $K_1\,\kappa_\alpha$. Indeed, during the first stage of RHn thermalisation, an (anti-)asymmetry is produced, which is proportional to $\varepsilon_\alpha K_1$, and is latter washed out by decays of the RHn. However, since this asymmetry undergoes washout processes that are $\propto \kappa_\alpha$, the surviving part is $\propto K_1\kappa_\alpha$.

The evaluation of $Y_{\Delta\alpha}$ follows the same lines as in the single flavour case, where one distinguishes anti-asymmetry production for $z \lesssim z_{eq}$ during thermalisation of the N, and the asymmetry production at $z \gtrsim z_{eq}$ that cancels out with the former one:

$$\begin{aligned} Y_{\Delta\alpha}(z) &= -\varepsilon_\alpha \int_0^z dx\, K_1\, P(x)\, \Delta N(x) e^{-\tilde{\kappa}_\alpha \int_x^z dy W(y)} \\ &\simeq \varepsilon_\alpha \left(K_1 \int_0^{z_{eq}} dx\, P(x) Y_N^{eq}(x) e^{-\tilde{\kappa}_\alpha \int_x^z dy W(y)} + \int_{z_{eq}}^z dx\, Y_N'(x) e^{-\tilde{\kappa}_\alpha \int_x^z dy W(y)} \right) \end{aligned} \tag{5.32}$$

The first term represents the asymmetry produced in hollow during N thermalisation. Its evaluation is simplified using the approximate expression for the source term [59]:

$$P(z) \simeq \frac{K_s}{K_1} + z\,, \quad K_s = \frac{9 m_t^2}{8\pi^2\, v^2} K_1 \tag{5.33}$$

where $K_s \simeq 0.1 K_1$ parametrises the strength of the $\Delta L = 1$ scatterings. In this weak washout case, at high temperatures RHn are far below their thermal equilibrium, $Y_N(z \lesssim z_{eq}) \ll Y_N^{eq}(z \lesssim z_{eq})$, and so a similar expression can be found for the damping term

$$W(z) = W_{id}(z)\left(1 + \frac{\beta}{z}\right), \beta \simeq \frac{2\,K_s}{3\,K_1} + 2\ . \tag{5.34}$$

The first term can be written as

$$Y_{\Delta\alpha} \simeq \varepsilon_\alpha \frac{K_1}{\tilde{\kappa}_\alpha} 4\,n_0 \int_0^{z_{eq}} dx\,(\tilde{\kappa}_\alpha W_{id}(x))\left(\frac{K_s}{K_1} + x\right) e^{-\tilde{\kappa}_\alpha \int_x^{z_{eq}} W_{id}(y)\left(1+\frac{\beta}{y}\right)dy}\ , \tag{5.35}$$

where we note that

$$n_0 = \frac{1}{2}\,Y_N^{eq}(z \ll 1) = \frac{135\zeta(3)}{8\pi^4\,g_*}\ . \tag{5.36}$$

The expression in eq.(5.35) can be further simplified since the leading contribution comes from $z \sim 1$, such that the source term in this weak washout regime reads $D(z) + S(z) \simeq K_s/K_1$. Given that

$$\int_x^\infty dy\,y^2 K_1(y) = x^2 K_2(x) \tag{5.37}$$

with $x^2 K_2(x) \simeq 2$ for $x \lesssim 1$, and using the fact that

$$\int_0^\infty dy\,y^3 K_1(y) = \frac{3\pi}{2} \equiv \tilde{\alpha}\ , \tag{5.38}$$

one obtains the antisymmetry production during thermalisation:

$$Y_{\Delta\alpha}^{<} \simeq \varepsilon_\alpha \frac{K_1}{\tilde{\kappa}_\alpha} 4n_0\,\frac{K_s}{K_1}\left(1 - e^{-\frac{\tilde{\kappa}_\alpha}{4}\tilde{\alpha}}\right) e^{-\frac{\tilde{\kappa}_\alpha}{4}\,2\beta}\ . \tag{5.39}$$

For $z \gtrsim z_{eq}$, when RHns dominate over their equilibrium abundance, and since the washout terms can be neglected, the asymmetry produced in the decay can be writen as:

$$\begin{aligned} Y_{\Delta\alpha}^{>} &= -\varepsilon_\alpha \int_{z_{eq}}^{z} K_1\,P(x)\,Y_N(x) \\ &\simeq \varepsilon_\alpha \int_{z_{eq}}^{z} Y_N'(x) \simeq -\varepsilon_\alpha\,n_0\,\frac{K_s}{K_1}\tilde{\alpha}\ . \end{aligned} \tag{5.40}$$

Adding the two contributions, the $B - L$ asymmetry is given in the weak washout regime by

$$\begin{aligned} Y_{\Delta\alpha} &= Y_{\Delta\alpha}^{<} + Y_{\Delta\alpha}^{>} \\ &\simeq -\varepsilon_\alpha \times (3.7 K_1\,\tilde{\kappa}_\alpha)\,Y_N^{eq}(z_{in})\,. \end{aligned} \tag{5.41}$$

In this weak washout regime, the efficiency factor is therefore found to be:

$$\eta_\alpha^w \simeq 3.7 K_1\,\tilde{\kappa}_\alpha\,. \tag{5.42}$$

Finally, the baryon asymmetry in this case is

$$Y_B = -\frac{12}{37}\sum_\alpha \varepsilon_\alpha \times (3.7 K_1\, \tilde{\kappa}_\alpha)\, Y_N^{eq}(z_{in}) \,, \tag{5.43}$$

clearly differing from the baryon asymmetry evaluated in the one flavour case:

$$Y_B^{1f} \propto -\left(\sum_\alpha \varepsilon_\alpha\right) \times K_1 \left(\sum_\alpha \kappa_\alpha\right) Y_N^{eq}(z_{in}) \,. \tag{5.44}$$

In the regime of weak washout, the inclusion of lepton flavours is found to lower the baryon asymmetry when compared to the unflavoured case.

Mixed regime: some flavours weakly washed out, but $K_1 \gg 1$

This case does not correspond to any of the cases encountered in the single flavour picture.
We assume that one flavour, labelled β, is only weakly washed out with $\kappa_\beta \ll 1$, while the total washout is strong since all other $\kappa_\alpha \gg 1, \alpha \neq \beta$.
This case has the interesting feature of combining the fast RHn thermalisation, owing to strong inverse decays or scatterings, and which typically ensure a copious asymmetry production, with the fact that the flavour β, being only weakly washed out, is somewhat protected from the strong washouts of the fast RHn decays. Let us see this in detail.
During the first stage of thermalisation, one has

$$Y_{\Delta\beta}^{<\prime}(z) \simeq \varepsilon_\beta\, Y_N'(z) - \tilde{\kappa}_\beta\, W(z)\, Y_{\Delta\beta}(z) \,. \tag{5.45}$$

This gives a contribution

$$Y_{\Delta\beta}^{<} \simeq \varepsilon_\beta \int_0^{z_{eq}} dx\, Y_N'(x)\, e^{-\tilde{\kappa}_\beta \int_x^{z_{eq}} dy\, W(y)} \,. \tag{5.46}$$

As $\tilde{\kappa}_\beta \ll 1$ and the RHns reach thermal equilibrium at high temperatures, in this integral we can approximate $e^{-\tilde{\kappa}_\beta \int W} \simeq 1 - \tilde{\kappa}_\beta \int W$, such that

$$Y_{\Delta\beta}^{<} \simeq \varepsilon_\beta Y_N(z_w) - \varepsilon_\beta\, \tilde{\kappa}_\beta \left(\int_0^{z_w} dx\, Y_N(x) \int_x^{z_w} dy\, W(y)\right) , \tag{5.47}$$

where z_w reflects the temperature below which the washout cannot be neglected with $z_w \gtrsim 1$. Therefore, in a second stage, for $z \gtrsim z_w$, one has

$$Y_{\Delta\beta}'(z) \simeq \varepsilon_\beta\, Y_N'(z) \to Y_{\Delta\beta}^{>} \simeq -\varepsilon_\beta\, Y_N(z_w) \,. \tag{5.48}$$

Adding the two contributions gives:

$$Y_{\Delta\beta} = Y_{\Delta\beta}^{<} + Y_{\Delta\beta}^{>} \simeq -\varepsilon_\beta\, \tilde{\kappa}_\beta \left(\int_0^{z_w} dx\, Y_N(x) \int_x^{z_w} dy\, W(y)\right) . \tag{5.49}$$

The washouts freeze after they reach their maxima, which is evaluated to occur at $z_w \simeq 2.4$, and for which the above integrand is $\simeq 0.4 Y_N^{eq}(z_{in})$. Therefore, the $B-L$ asymmetry in the flavour β is given by

$$Y_{\Delta\beta} \simeq -\varepsilon_\beta\, 0.4\, \tilde{\kappa}_\beta\, Y_N^{eq}(z_{in}) \,, \tag{5.50}$$

hence $\eta_\beta^m \simeq 0.4\,\tilde{\kappa}_\beta$. For the flavour(s) α which is (are) strongly washed out, the result eq.(5.28) still holds.

Global parametrisation

Similarly to the global parametrisation in the single flavour picture, by means of a simple interpolation we can infer the efficiency factor for all washout regimes

$$\eta \simeq \left(\eta_w^{-1} + \eta_s^{-1}\right)^{-1} \,, \tag{5.51}$$

which provides a good idea of the result, even if some fine-tuning is still required in order to best fit the numerical results. As an illustrative example, we consider a two-flavour case, $Y_{\Delta\alpha} - Y_{\Delta\beta}$. We plot in fig.(5.4) the efficiency factor for flavour β, whose washout parameter varies from 10^{-4} to 10^2, while fixing $\kappa_\alpha = 100$. Hence, the total washout is strong, and eqs.(5.28,5.50) apply.

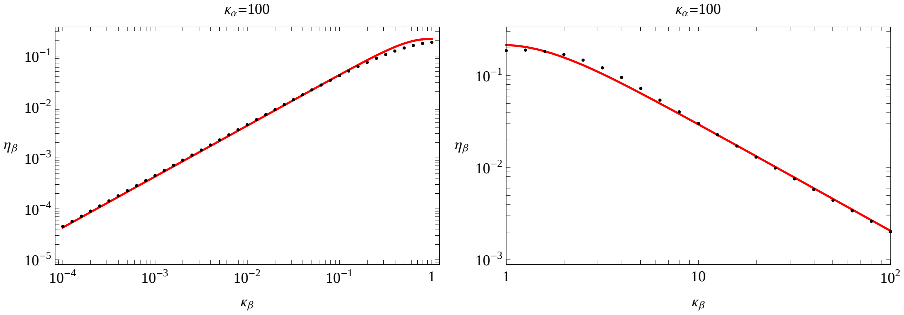

Figure (5.4): Individual efficiency factor η_β as a function of the corresponding washout κ_β. We impose that the other flavour is strongly washed-out, with $\kappa_\alpha = 100$. The black points represent the numerical results, while the red line stands for the approximate formulae given in eqs.(5.28,5.50).

We observe a good agreement between the formulae derived and the numerical results. However if we allow the washout of flavour α to vary, setting for example $\kappa_\alpha = \kappa_\beta$, we see in fig.(5.5) that the formula of eq.(5.41), which is depicted in blue, is accurate only for $\kappa \lesssim 0.05$. For $\kappa \gtrsim 0.01$, some fine-tuning of eq.(5.41) is preferable to best fit the result. In the plot of fig.(5.5), we represent in a red dashed line the formula

$$\eta_\beta \simeq \frac{1}{\left((1.3\,K_1\,\kappa_\beta^{0.7})^{-0.4} + (0.4\,\kappa_\beta^{-1.16})^{-0.4}\right)^{1/0.4}} \,, \tag{5.52}$$

which gives an accurate result for $\kappa_\beta \gtrsim 0.01$. However, this is an important fine-tuning of the parameters, and can be thus disregarded.

5.3.1 Thermal initial population

The evaluation of the efficiency factor in the equilibrium scenario is very similar to the one flavour case [69]. Indeed, we saw in chapter 3 that in this scenario, washout is not necessary to

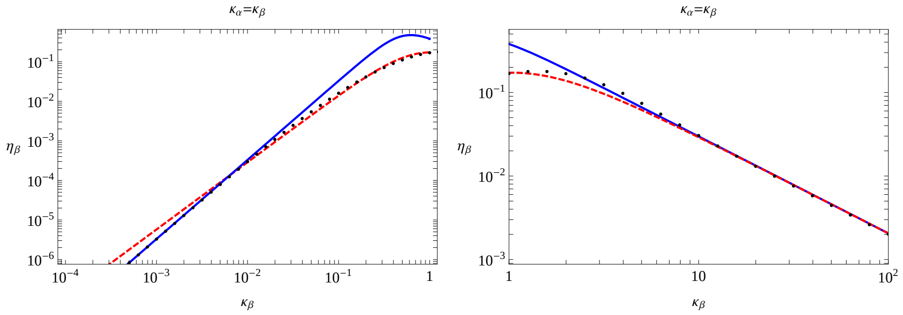

Figure (5.5): Individual efficiency factor η_β as a function of the corresponding washout κ_β, in the case where the washout of the other flavours also varies, with $\kappa_\alpha = \kappa_\beta$. The black points represent the numerical results, while the blue line stands for the approximate formulae given in eqs.(5.28,5.41). The dashed red line represents the fit of eq.(5.52).

produce a population of RHns. Nevertheless, for the sake of illustration, we represent in fig.(5.6) the eficiency factor for a given flavour, in the thermal case (dashed-blue) and in the case where the Ns are initially in thermal equilibrium.

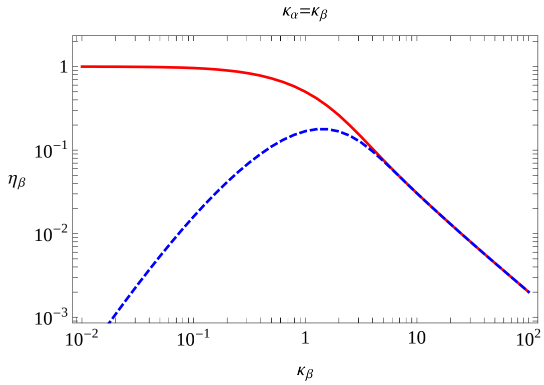

Figure (5.6): Efficiency factor of a given flavour β, in the thermal case (dashed blue) and in the case where the N are initially in thermal equilibrium (red).

In the case where all flavours are weakly washed out,

$$Y_{\Delta\alpha}(z) = \varepsilon_\alpha \int_{z_{in}}^{z} dx\, Y_N'(x) e^{-\tilde{\kappa}_\alpha \int_x^z dy\, W(y)}\,, \tag{5.53}$$

the exponential term can be neglected, and given that $Y_N(z_{in}) = Y_N^{eq}(z_{in})$ one simply has

$$Y_{\Delta\alpha} \simeq -\varepsilon_\alpha\, Y_N^{eq}(z_{in})\ , \tag{5.54}$$

resulting in a maximal efficiency factor $\eta = 1$.

On the other hand, when all flavours are strongly washed-out, decays maintain RHns in thermal equilibrium. Therefore, similarly to the thermal case, one can neglect high temperature contribution, and so

$$\begin{aligned} Y_{\Delta\alpha}(z) &= \varepsilon_\alpha \int_{z_{in}}^{z} dx\, Y'_N(x)\, e^{-\tilde{\kappa}_\alpha \int_x^z dy\, W(y)} \\ &\simeq \varepsilon_\alpha \int_{z_{in}}^{z} dx\, Y_N^{eq\prime}(x\,) e^{-\tilde{\kappa}_\alpha \int_x^z dy\, W(y)} \\ &\simeq \varepsilon_\alpha \frac{n_0\, 4}{\tilde{\kappa}_\alpha} \int_{z_{in}}^{z} dx\, \tilde{\kappa}_\alpha\, W(x)\, e^{-\tilde{\kappa}_\alpha \int_x^z dy\, W(y)}\ . \end{aligned} \tag{5.55}$$

The $B - L$ asymmetry is equal to the one derived for the thermal case:

$$Y_{\Delta\alpha} \simeq -\varepsilon_\alpha \frac{0.4}{\tilde{\kappa}_\alpha^{1.16}} \times Y_N^{eq}(z_{in})\ . \tag{5.56}$$

We see that the strong washout regime provides a similar dependence on the washout factor, regardless of the thermal history of the RHns. This, together with the fact that the atmospheric and solar neutrino masses point towards the strong washout regime,

$$\begin{aligned} \tilde{m} &\simeq m_{sol} \rightarrow \kappa \simeq 8\,, \\ \tilde{m} &\simeq m_{atm} \rightarrow \kappa \simeq 45\,, \end{aligned} \tag{5.57}$$

indicates that the strong washout regime is a more robust and reliable regime.

5.3.2 Influence of the off-diagonal terms of the A matrix

So far we have only included the dominant terms which are the diagonal entries of the matrix A, since the off-diagonal terms are $\mathcal{O}(0.1)$. Nonetheless, it is worth studying them.

When considering the dominant order, we saw that each flavour could be washed out very differently. As the off-diagonal terms couple flavours among themselves, it is likely that a flavour, being suppressed by either a very weak or a very strong washout, may nontheless provide a non-negligible contribution to the final baryon asymmetry, having been pushed up by another flavour.

The evaluation of this off-diagonal term has been done in [90], where we showed that while preventing a complete washout of flavours in particular cases, the effect of the diagonal terms on the baryon asymmetry is less than 20%. Here we illustrate these results.

The off-diagonal term contributes to the $B - L$ asymmetry as:

$$Y_{\Delta\alpha}^{od}(z) = \kappa_\alpha \sum_{\beta\neq\alpha} A_{\alpha\beta} \int_{z_{in}}^{z} dx\, W(x)\, Y_{\Delta\beta}(x)\, e^{-\tilde{\kappa}_\alpha \int_x^z dy\, W(y)}\ , \tag{5.58}$$

and so does not depend on the initial condition of the right-handed neutrinos. The evaluation of the above integral is made difficult by the fact that it implies knowing the dynamic of the individual flavours.

We thus make a few approximations. First, we neglect the off-diagonal terms entering in the BE for the flavour β. This is quite justified, since its effect on the flavour α is $A_{\alpha\beta}^2 \ll 1$. Then we assume that $Y_{\Delta\beta}(z) \simeq Y_{\Delta\beta}(\infty)$ so that $Y_{\Delta\beta}$ is factorised out of the integral. We then obtain, dropping out the sum on β:

$$\begin{aligned} Y^{od}_{\Delta\alpha} &\simeq \kappa_\alpha A_{\alpha\beta}\, Y_{\Delta\beta} \int_{z_{in}}^{\infty} dx\, W(x)\, e^{-\tilde{\kappa}_\alpha \int_x^\infty dy\, W(y)} \\ &\simeq \frac{A_{\alpha\beta}}{A_{\alpha\alpha}}\, Y_{\Delta\beta}\left(1 - e^{\tilde{\kappa}_\alpha \overline{\alpha}}\right) \end{aligned} \tag{5.59}$$

where

$$\overline{\alpha} = \int_{z_{in}}^{\infty} dx\, W(x) \simeq 1.3\ . \tag{5.60}$$

Had we only included inverse decays, we would have obtained $\overline{\alpha} = 3\pi/8$.

The relative factors $A_{\alpha\beta}/A_{\alpha\alpha}$ strongly differ from one flavour to the other. For example, in a two-flavour scheme, the relative factors are

$$\begin{aligned} Y^{nd}_{\Delta e\mu} &\simeq -0.3 Y_{\Delta\tau}\left(1 - e^{-\tilde{\kappa}_{e\mu}\overline{\alpha}}\right) \\ Y^{nd}_{\Delta\tau} &\simeq -0.08 Y_{\Delta e\mu}\left(1 - e^{-\tilde{\kappa}_{\tau}\overline{\alpha}}\right)\ . \end{aligned} \tag{5.61}$$

If $\kappa_\alpha \gg 1$, the off-diagonal term is about $\sim (A_{\alpha\beta}/A_{\alpha\alpha})\, Y_{\Delta\beta}$, while if $\kappa_\alpha \ll 1$, this term is roughly $\sim (A_{\alpha\beta}/A_{\alpha\alpha})\, Y_{\Delta\beta} \times \tilde{\kappa}_\alpha \overline{\alpha}$.

The $B - L$ flavour conversion is expected to have a significant impact in the case where one flavour is very strongly or very weakly washed-out. Indeed, flavour conversion acts as a source term for the asymmetry. Therefore in the former case, it partly compensates the washout from RHns decays, and so we expect a small increase in the asymmetry. In the weak washout case, this extra source term further cancels with the asymmetry produced during thermalisation. So, in the weak washout case, one expects a depletion of the asymmetry.

We illustrate in fig.(5.7) the effect of including the off-diagonal terms on the efficiency factor. We consider a two-flavour regime, with washout varying from 10^{-2} to 10^{2}[3]. On the left hand side, the CP asymmetries of the different flavours are chosen equal and arbitrary, while on the right hand side the CP asymmetries are set to their maximum values, cf. eq.(5.70).

Looking only at washout effects (left panels), we see that, as expected, the flavour conversion affects $\Delta\alpha$ asymmetries mostly when $\kappa_\alpha \gg 1$ or $\ll 1$. The fact that the flavour $\Delta e\mu$ is (much) more affected comes from the relative size of the matrix elements of A: $A_{e+\mu,\tau} \simeq 0.2 = 4\, A_{\tau,e+\mu}$.

When realistic values are used for the CP asymmetries (right panels), we see that the global behaviour remains unchanged, albeit this further restricts the influence of the off-diagonal terms to the case where $\sqrt{\kappa_\alpha/K_1}$ is not strongly suppressed.

What about the baryon asymmetry?

Individual asymmetries are affected by ±50%, and given that $Y_B = 12/37 \sum_\alpha Y_{\Delta\alpha}$, the baryon asymmetry is affected up to 20%, Y_B being enhanced in the strong washout regime, and depleted in the weak washout regime. This can be seen in fig.(5.8).

We see that the flavour conversion does not significantly modify the baryon asymmetry. However

---

[3] For simplicity, we set $\kappa_e = 0$ so that the washout of $Y_{\Delta e+\mu}$ is $\kappa_{e+\mu} = \kappa_\mu$.

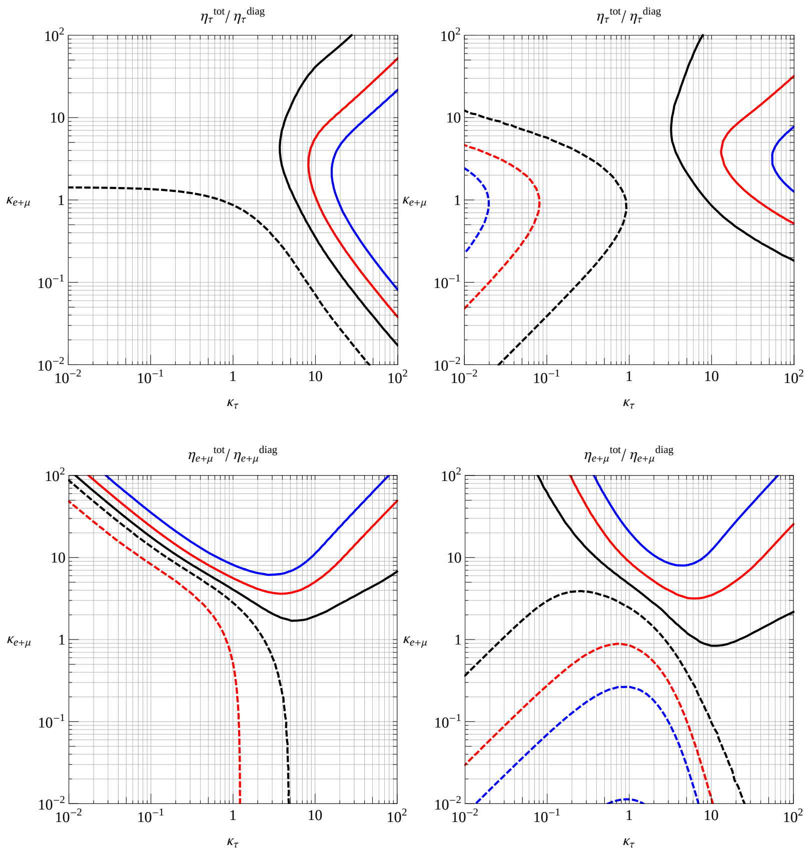

Figure (5.7): Influence of the flavour conversion on the asymmetry in lepton flavours. The influence on the flavour τ $(e+\mu)$ is displayed in the up (down) panel. The contours represent different ratios of $\eta_\alpha^{total}/\eta_\alpha^{diag}$, with either equal CP asymmetries $\varepsilon_\tau = \varepsilon_{e\mu}$ (left panel) or else CP asymmetries set to their maxima $\varepsilon_\alpha = \varepsilon_\alpha^{max}$ (right panel) . An increase in the efficiency is represented by solid lines, whereas the dashed lines represent a reduction of η, with a colour code: black (±5%), red (±20%) and blue (±50%).

we notice that for some specific configurations, it prevents Y_B from vanishing: in the case where $\varepsilon_{e\mu}+\varepsilon_\tau = 0$, and $\tilde{\kappa}_{e\mu} = \tilde{\kappa}_\tau$, without flavour conversion the baryon asymmetry is zero, while with flavour conversion one has

$$\begin{aligned} Y_B &\simeq \frac{12}{37}\,(Y_{\Delta e\mu} + Y_{\Delta\tau}) \\ &\simeq 7\times 10^{-2}\,Y^d_{\Delta\tau}\ , \end{aligned} \tag{5.62}$$

which is non zero, even if compatibility with the observed baryon asymmetry may be hardly obtained.

5.4 Constraints from a successful leptogenesis

We saw in chapter 3 that requiring a successful leptogenesis in the single flavour picture somewhat constrains light and heavy neutrinos. It is mandatory that the decaying RHn is heavy enough,

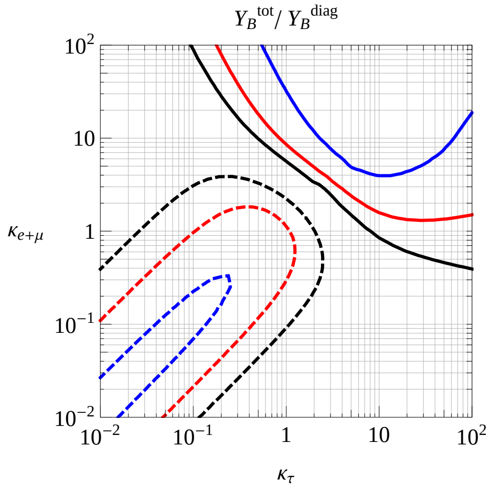

Figure (5.8): Influence of the flavour conversion on the baryon asymmetry. The contours represent different values of the ratio Y_B^{total}/Y_B^{diag}, the enhancement being depicted by solid lines and the reduction by dashed lines, with the colour code: black (±5%), red (±10%), blue (±20%).

$M_1 \gtrsim 2 \times 10^9\,\mathrm{GeV}$, and that light neutrino masses are lighter than $\sim 0.12\,\mathrm{eV}$. Concerning the different mixing angles and CP violating phases, the only generic constraint derived is the necessity that the matrix R contains CP-odd phases, otherwise no CP asymmetry can be generated.

Given the importance of this constraint, and the fact that the inclusion of lepton flavours strongly modifies the key parameters of leptogenesis, it is interesting to investigate the possible influence of lepton flavours on the above constraints.

5.4.1 Lower bound on heavy neutrino mass

Concerning the lower bound on RHn masses, the inclusion of lepton flavours is a mixed blessing. On the one hand, when light neutrinos are (very) hierarchical, since the upper bound on the CP asymmetry is roughly the same, we do not expect any important modifications to the lower bound on M_1. Actually, since individual CP asymmetries are roughly 1/3 of the total one, we even expect in general a slight increase of M_1^{min}. On the other hand, assuming hierarchical RHns, when light neutrinos are (quasi) degenerate, we see that while ε_1 becomes suppressed, the CP asymmetries in each lepton flavour are in fact enhanced. In this degenerate limit, we expect the lower bound on M_1 to decrease. Let us see this in detail, for both the thermal and the equilibrium RHn abundance scenarios.

From the bound on each individual CP asymmetry [75],

$$\varepsilon_\alpha \lesssim \frac{3M_1 m_{\max}}{16\pi v^2}\sqrt{\frac{\kappa_\alpha}{K_1}}\ , \tag{5.63}$$

one has

$$\begin{aligned} |Y_{\mathcal{B}}| &\simeq 1.26\times 10^{-3}\sum_\alpha \varepsilon_\alpha\,\eta_\alpha \\ &\lesssim 1.26\times 10^{-3}\,\frac{3\,M_{N_1}\,m_{\rm max}}{16\pi v^2}\sum_\alpha\sqrt{\frac{\kappa_\alpha}{\kappa}}\,\eta_\alpha\,, \end{aligned} \tag{5.64}$$

from which a lower bound on M_{N_1} is derived,

$$M_{N_1} \gtrsim 7.1\times 10^{8}\,{\rm GeV}\left(\frac{m_{\rm atm}}{m_{\rm max}}\right)\left|\frac{Y_{\mathcal{B}}}{Y_{\mathcal{B}}^{obs}}\right|\frac{1}{\sum_\alpha\sqrt{\frac{\kappa_\alpha}{\kappa}}\,\eta_\alpha}\,. \tag{5.65}$$

Since the lower bound on M_1 is inversely proportional to the efficiency η_α, it will therefore depend on the thermal history of the decaying right-handed neutrino. In the case where N_1 are produced by scatterings, the efficiency is maximised for a washout $\kappa_\alpha \simeq 1$, where $\eta_\alpha \simeq 0.2$. In the case where N_1 are non-thermally produced, the efficiency reaches its mamximal value of 1 for a very weak washout $\kappa_\alpha \ll 1$. The lower bound also depends on the alignment of flavours, and in the case of democratic washouts one has [90]:

$$M_{N_1} \gtrsim \begin{cases} 4.1\times 10^{8}\,{\rm GeV} & \text{in the thermal case} \\ 2.5\times 10^{9}\,{\rm GeV} & \text{in the dynamical case}\,. \end{cases} \tag{5.66}$$

This bound is close to the one derived in the one-flavour approximation, where $M_{N_1} \gtrsim 4.2\times 10^{8}$ GeV in the thermal case and $M_{N_1} \gtrsim 2.1\times 10^{9}$ GeV in the dynamical one [58].

The parameter space $M_1 - \tilde{m}_1$ compatible with successful leptogenesis is shown in fig.(5.9), where we represent the thermal scenario (up panels) and the case where the Ns are in thermal equilibrium at high temperature (down panels), both in the flavoured case (right panels) and in the single flavour approximation (left panels).

These scatter plots have been obtained by numerically solving the set of BEs, using the Casas-Ibarra parametrisation for the neutrino Yukawa couplings. We choose a normal mass ordering for both low and high energy sectors, setting the solar and atmospheric mass differences, together with the corresponding mixing angles, to their best fit values, while $\theta_{13} \lesssim 13°$. For the light neutrino mass, we impose the constraint $m_1 \lesssim 1\,{\rm eV}$. We use as perturbative limit $\lambda \lesssim 1$, hence the upper-bound on M_1. The hierarchy for heavy neutrinos is imposed $M_3 = rM_2 = r^3 M_1$, with $r = 10$. The low-energy CP violating phases, as well as those of R, are not constrained.

We scan over 33000 random sets, and select the solutions satisfying $8.7\times 10^{-11} \lesssim Y_B \lesssim 2\times 8.7\times 10^{-11}$. When scanning over the different parameters, we tried to target the lower part of the curve, with unequal success, hence the lower bound numerically differs from analytical estimates, by a factor $2-3$.

We clearly see in these plots the different behaviour regarding the washout.

In both scenarios, the transition between strong and weak washout rapidly occurs in the one flavour case at $\tilde{m}_1 \simeq m_*$, while this transition occurs at slightly higher $\tilde{m}_1$ in the flavoured case, due to the $A < 1$ matrix elements. Furthermore, we clearly see that washouts are necessary in the thermal scenario, with $\tilde{m} \gtrsim 10^{-4}\,{\rm eV}$ or equivalently $K_1 \gtrsim 0.1$, while this is not the case in

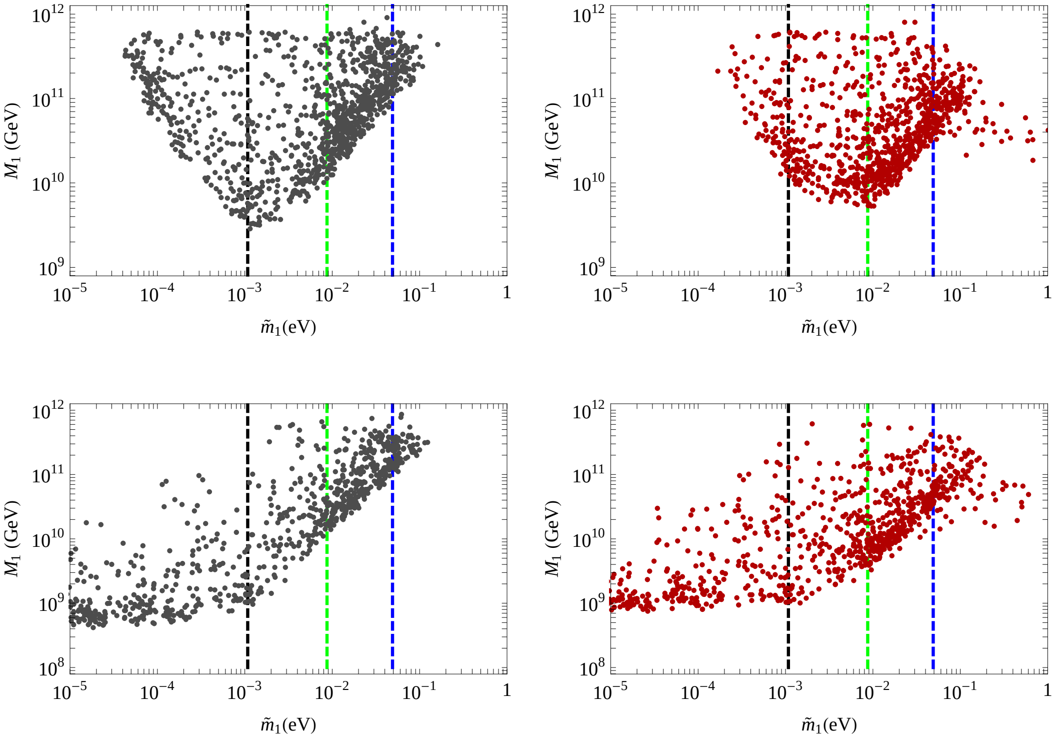

Figure (5.9): $M_1 - \tilde{m}_1$ parameter-space compatible with successful leptogenesis: bound on M_1, in the case of a zero (thermal) initial N_1 abundance for the up (down) panels. The right (left) panels show the allowed (M_1-$\tilde{m}_1$) parameter space in the case the lepton flavours are included (neglected). The vertical lines represent the equilibrium mass $m_* \simeq 1.08 \times 10^{-3}\,\text{eV}$ (dashed-black), the solar mass $\sqrt{\Delta m^2_{\text{sol}}} \simeq \sqrt{7.6 \times 10^{-5}}\,\text{eV}$ (in green) and the atmospheric mass $\sqrt{\Delta m^2_{\text{atm}}} \simeq \sqrt{2.4 \times 10^{-3}}\,\text{eV}$ (in blue).

the equilibrium scenario.

Moreover, we see the important impact of lepton flavours in the limit of degenerate light neutrinos, with a re-opening of the parameter space. Accordingly, the lower bound on M_1 is turned down in this regime, with for example a diminution of one order of magnitude when $\tilde{m}_1 \simeq 0.1\,\text{eV}$.

Influence of $\Delta L = 2$ and the "full flavour regime"

An important point to notice is that the above plot have been obtained neglecting $\Delta L = 2$ scatterings, and assuming that the flavours were fully relevant in leptogenesis. These assumptions are justified as long as

$$M_1/10^{14}\,\text{GeV} \lesssim c_1\, 0.1\, \kappa_\alpha \tag{5.67}$$

$$M_1/10^{12}\,\text{GeV} \lesssim c_2\, \kappa_\alpha^{-1}\ , \tag{5.68}$$

respectively. Here $c_{1,2}$ are numerical factors that are $\mathcal{O}(1)$.

If satisfied, eq.(5.68) implies that lepton flavours are fully relevant in leptogenesis as explained in chapter 4, while eq.(5.67) tells us that $\Delta L = 2$ lepton violating scatterings can be safely neglected.

We wonder about the robustness of the above discussion regarding these two constraints. On the one hand, strengthening the constraint of eq.(5.67) reduces the $M_1 - \tilde{m}_1$ parameter-space by increasing the minimal allowed washout, whereas on the other hand strengthening eq.(5.68) lowers the upper bound on M_1.

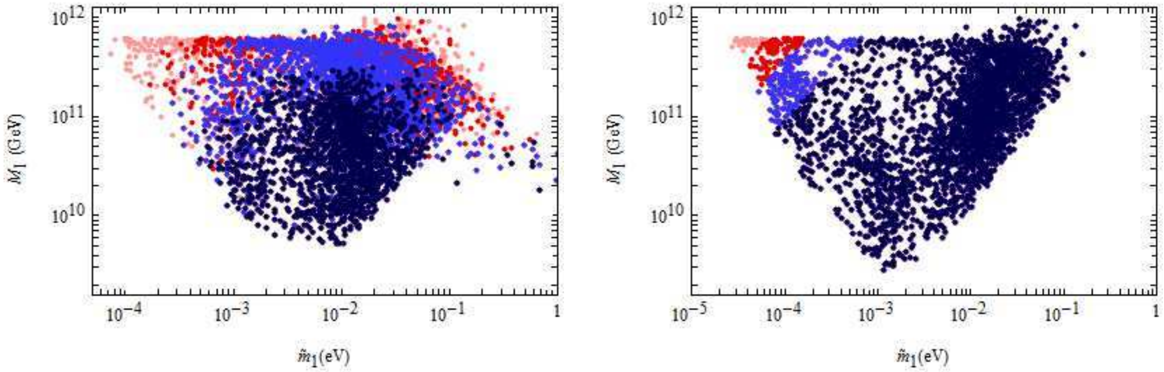

Figure (5.10): Influence of $\Delta L = 2$ and of recohering processes, in the flavoured case (left) and unflavoured case (right). In light red is depicted the case $c = 10$, whereas in dark red, light blue and dark blue are represented the case $c_1 = c_2 = c$, with $c = 1$, $c = 0.6$ and $c = 0.1$, respectively.

In order to quantify this point, we illustrate in fig.(5.10) the $M_1 - \tilde{m}_1$ parameter-space which is allowed by leptogenesis when the above constraints are included. These constraints are strengthened/weakened by modifying the factor $c_{1,2}$: we thus vary c_1 and c_2 for the flavoured case, and only c_1 in the single flavour case. For simplicity, we took $c_1 = c_2 = c$, with $c = 10$ depicted in light red, which would correspond to the case eqs.(5.67-5.68) are satisfied. In dark red is depicted the case $c = 1$, in light blue $c = 0.6$ and in dark blue $c = 0.1$. We see how the allowed parameter-space dramatically reduces when we strengthen the constraint.

Since the plots of figs.(5.9),(5.11) have been obtained assuming $c = 0.8$, we can say that the conclusion of the previous (and following) section applies.

5.4.2 Upper bound on light neutrino mass

The reason why the light neutrino mass is bounded from above in the single flavour approximation is twofold. First, in the one flavour approximation, when summing over lepton flavours and assuming a strong hierarchy for the right-handed neutrinos, the CP asymmetry is bounded by

$$\varepsilon_1^{max} = \frac{3}{16\pi} \frac{M_1(m_3 - m_1)}{v^2} \times \beta(m_1, \tilde{m}_1)\,. \tag{5.69}$$

Hence, for degenerate neutrinos, $m_1 \simeq m_3$ and the CP asymmetry scales as m_1^{-1} and is therefore suppressed. This suppression could be compensated by increasing the heavy neutrino mass scale. However, M_1 cannot be increased harmlessly: $\Delta L = 2$ washouts that are $\propto M_1$ must be out of equilibrium, which means that M_1 is upper-constrained and so is m_{min}.

When lepton flavours are included in leptogenesis, the situation is drastically different, since the flavoured CP asymmetries are no longer suppressed. Indeed, the upper-bound on the CP asymmetry in a lepton flavour α reads

$$\varepsilon_\alpha \lesssim \frac{3}{16\,\pi}\frac{M_1\,m_3}{v^2} \times \sqrt{\frac{\kappa_\alpha}{K_1}}\,, \tag{5.70}$$

no longer suppressed for degenerate light neutrinos. Therefore, the bound

$$m_1 \lesssim 0.12\,\mathrm{eV} \tag{5.71}$$

no longer holds. We can see this in the scatter plots of fig.(5.11), which have been obtained in a similar way as the plots of fig.(5.9). It is clear how the inclusion of lepton flavours re-opens the parameter space in the degenerate/strong-washout regime.

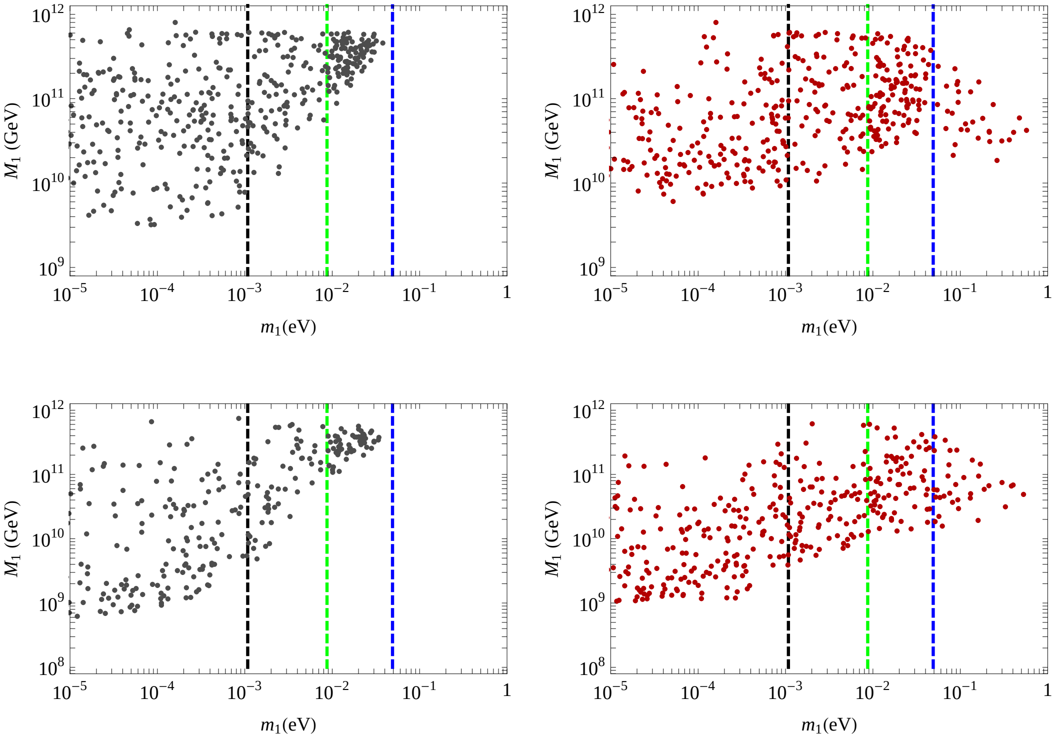

Figure (5.11): Successful leptogenesis: M_1-m_1 parameter-space, in the case of a vanishing (equilibrium) initial RHn abundance for the up (down) panels. The right (left) panels show the allowed (M_1-m_1) parameter space for the flavoured (unflavoured) case. The vertical lines represent the equilibrium mass $m_* \simeq 1.08\,\times 10^{-3}\,\mathrm{eV}$ (dashed-black), the solar mass $\sqrt{\Delta m^2_{\mathrm{sol}}} \simeq \sqrt{7.6\,\times 10^{-5}}\,\mathrm{eV}$ (in green) and the atmospheric mass $\sqrt{\Delta m^2_{\mathrm{atm}}} \simeq \sqrt{2.4\,\times 10^{-3}}\,\mathrm{eV}$ (in blue).

Working in the flavoured framework, the authors of [82] have derived an upper-bound on m_1, under the constraint that flavours are fully relevant in leptogenesis. However this bound roughly reads $\overline{m} \lesssim 2\,\mathrm{eV}$, which is already above the cosmological constraint on neutrino mass.

5.4.3 Constraints on mixing angles and CP violating phases

Constraining the seesaw parameters from leptogenesis is an ambitious task that requires a systematic analysis of the different high energy phases. Such work has been attempted, both in the the single flavour approximation *e.g.* in [91], as well as in flavoured picture [87, 88, 92]. Due to the degeneracy among the parameters, even if favourable configurations have been identified, it has not been possible to clearly constraint the parameters. Hence the necessity to tie the constraints coming from leptogenesis with other (non-)observations, such as lepton-flavour violating processes [93]. But even then, high energy parameters would remain unconstrained, and only most favourable parameter space regions could be determined.

5.5 Summary

In this chapter, we have studied the effects of lepton flavours in the type I seesaw model of leptogenesis. Actually, the conclusions to which we are led are not particular to the type I seesaw, but rather they are generic conclusions which may apply in all leptogenesis models, under the constraint that at the time the asymmetry is created, the interactions involving the charged lepton Yukawa couplings are in-equilibrium/faster than the coherent processes.

However, we made this study in the type I seesaw, and so let us summarise the results we derived in this case.

In the flavoured treatment of leptogenesis, the individual asymmetries $Y_{\Delta\alpha}$ are independently produced and washed out. For example, the washout factor $\propto \lambda^2$ depends only on the coupling of the lepton flavour to the right-handed neutrino. This coupling being in general different for the distinct flavours, the latter are differently washed out. This non-alignment of lepton flavours is particularly interesting in the strong washout regime $K_1 \gg 1$, since it is possible to have flavours which are only weakly washed out, allowing to somewhat escape the usual constraint that K_1 should not be larger than ~ 15. A similar effect is found for the CP asymmetries.

We showed that in the relevant temperature regime, the CP asymmetries in each lepton flavour have to be considered, instead of the total CP asymmetry (summed over the flavours). This has mainly two consequences. The first one comes from the fact that the ε_αs depend on the low-energy CP violating phases of the PMNS mixing matrix. Therefore, one could ask, relying only on this low-energy phases, whether or not leptogenesis could work. Such a study has been done in [88], where it was shown that while leptogenesis is indeed possible in that case, there is however no clear constraint on the seesaw parameters, owing to the unknown R-matrix elements. It has been further shown, in [94], that leptogenesis is actually insensitive to these low-energy phases, in the sense that for any values of the PMNS matrix, one can always find a configuration of the R-matrix for which leptogenesis works.

The other consequences, which have a direct implication for the low energy phenomenology, stem from the modification of the upper-bound on the ε_αs for hierarchical heavy neutrinos. Since the CP asymmetries in lepton flavours are no longer suppressed in the limit of (quasi) degenerate light-neutrinos, the upper-bound on this mass scale, which was derived in the single flavour picture, does not hold in the flavoured context.

We studied the lower-bound on the lightest right-handed neutrino mass, and showed that the bound derived in the single flavour case is only slightly modified, and still sets the scale of leptogenesis to be $M_1 \gtrsim (2-3)\times 10^9\,\mathrm{GeV}$.

Finally, we can say that while the inclusion of lepton flavours somewhat weakens the constraints derived in the single flavour picture, it only significantly affects leptogenesis in the strong wash-out regime. Furthermore, the inclusion of flavours does not provide any significant constraints on either the high-energy CP violating sector, or the low-energy one. This comes from our complete ignorance of the neutrino Yukawa couplings, which are not constrained in the SM type I seesaw. However, this is not always the case, as we will see in the next chapter, where we consider a grand-unified framework, where the latter couplings are theoretically predicted.

Chapter 6

Leptogenesis in the type II seesaw

We saw in the previous chapter that leptogenesis in the type I seesaw can explain the observed baryon asymmetry under the main constraint that the lightest right-handed neutrino is heavier than $\sim 4 \times 10^9$ GeV. However, we also observed that while the low-energy sector is somehow constrained by low-energy observations, we have failed to constrain the high-energy sector. This lack of predictivity originates from our ignorance of the neutrino Yukawa couplings λ and the masses and mixings of right-handed neutrinos. Indeed, in the SM, these masses are bare mass terms, which are thus unconstrained.

In $SO(10)$-based grand unified theories, the RHns are no longer gauge singlets, and thus the Majorana mass term can only arise from the dynamical breaking of an underlying symmetry. Moreover, due to the unifying picture, the neutrino Yukawa couplings are related to the Yukawa couplings of other field(s), and therefore one could think of a predictive GUT framework in which to embed the type I seesaw.

However in $SO(10)$-GUT scenarios, the typical mass of the lightest RHn predicted by a type I seesaw is $M_1 \lesssim 10^7$ GeV, and so hardly compatible with thermal leptogenesis [95].

Nevertheless, we saw in chapter 2 that different realisations of the seesaw mechanism are possible. In the (pure) type II seesaw [53], where one advocates the exchange of scalar $SU(2)_L$ triplets, a mass term

$$m_\nu \sim v_L f_L \tag{6.1}$$

is obtained, the smallness of m_ν being explained by the small vev of an $SU(2)_L$ triplet, $v_L \ll v$. Such a small vev could appear quite unnatural. On the contrary, for GUT models that are based on $SU(2)_L \times SU(2)_R$ [96, 97], such a suppression appears very naturally, due to a seesaw-like relation among the vevs of the different Higgs representations that the model contains.

In the type II seesaw[1], light neutrino mass emerges from the neutrino couplings with fermion singlets (the RHn) and $SU(2)_L$ triplets. Since these models contain two sources of lepton number violation, it is interesting to look at the feasibility of leptogenesis.

---

[1] Here we label pure type II seesaw the case where only scalar triplets are added, and type II seesaw the case where fermion singlets and scalar triplets are added.

In this chapter, we investigate the viability of leptogenesis in a supersymmetric GUT model, based on a Left-Right symmetric type II seesaw model. This study is based on [98], where we complete the previous study of [99] by the inclusion of lepton flavours and heavier neutrino effects. We first introduce the GUT framework in which this study is conducted, untill the type II seesaw relation is obtained. Inverting this relation will allow us in a second time to infer the high-energy parameters (right-handed neutrino masses and couplings...), using a reconstruction procedure developped in [99]. The knowledge of neutrino Yukawa couplings and RHn masses enables us to discuss the thermal scenario of leptogenesis in this SUSY-GUT framework. This scenario has *a priori* important differences with respect to the type I scenario discussed in the previous chapter, mainly coming from the gauging of $SU(2)_R$, the inclusion of a scalar triplet and the fact that we now work in a supersymmetric extension of the SM, with its inherent problems. We finally conduct a numerical study of leptogenesis in this framework, discussing in particular the influence of the key parameters of our model, and if the requirement of a viable leptogenesis yields constraints for the parameter-space.

6.1 Framework

This supersymmetric GUT model is based on $G_{3221} = SU(3) \times SU(2)_L \times SU(2)_R \times U(1)_{B-L}$. Our model consists of three **16** representation, which account for all SM fermions plus 3 right-handed neutrinos. This **16**, which is spinorial, is the smallest complex representation of $SO(10)$. Given the product decomposition under $SO(10)$,

$$\mathbf{16} \times \mathbf{16} = \mathbf{10_s} + \mathbf{120_a} + \mathbf{126_s} \,, \tag{6.2}$$

fermion bilinears can be formed by coupling this product to the appropriate Higgs representations, either the symmetric $\mathbf{10_s}$ and $\mathbf{126_s}$ or the antisymmetric $\mathbf{120_a}$. Another solution consists in using non-renormalisable operators, which couple fermion bilinears to products of Higgses, whose decompositions contain one of the representations above.

We consider here only symmetric representations, which consist in two fundamental **10**'s and a rank 5 (complex anti-self dual) $\overline{\mathbf{126}}$. The inclusion of a (self-dual) **126** is then necessary in order to prevent supersymmetry breaking at the GUT scale by a non-vanishing D-term. Therefore, the superpotential contains the following Yukawa couplings:

$$W_Y = Y^u_{ij}\,\mathbf{16}_i\,\mathbf{16}_j\,\mathbf{10}_u + Y^d_{ij}\,\mathbf{16}_i\,\mathbf{16}_j\,\mathbf{10}_d + f_{ij}\,\mathbf{16}_i\,\mathbf{16}_j\,\overline{\mathbf{126}} \,. \tag{6.3}$$

Due to the symmetry of the chosen Higgs representation, the couplings $Y^{a,b}$ and f are complex symmetric matrices. Assuming that only the $SU(2)_L$ doublets of the **10**s acquire a vev, the relation above tells us that at the GUT scale

$$m_u = m_D \,, \quad m_d = m_e \,. \tag{6.4}$$

The GUT framework therefore constrains the neutrino Dirac type mass m_D to be equal to the up quark type mass m_u. On the other hand, the relation $m_d = m_e$ among down-quark and charged

lepton masses is clearly not satisfactory [100], and we will correct it later on.
Under the Pati-Salam group $SU(4) \times SU(2)_L \times SU(2)_R$ [96], the $\overline{\mathbf{126}}$ decomposes as follows [2]:

$$\overline{\mathbf{126}} = (\mathbf{6},\mathbf{1},\mathbf{1}) + (\overline{\mathbf{10}},\mathbf{3},\mathbf{1}) + (\mathbf{10},\mathbf{1},\mathbf{3}) + (\mathbf{15},\mathbf{2},\mathbf{2})\,. \tag{6.5}$$

In the type II seesaw, we assume that the two scalar triplets of $\overline{\mathbf{126}}$, $\Delta_L = (\mathbf{1},\mathbf{3},\mathbf{1},\mathbf{1})$ and $\Delta_R = (\mathbf{1},\mathbf{1},\mathbf{3},-\mathbf{1})$ under G_{3221}, respectively couple to light and heavy neutrinos, according to:

$$\mathcal{L}_m = \frac{1}{2} f_L^{ij}\,\Delta_L\,L_i\,L_j + \frac{1}{2}\,f_R^{ij}\,\Delta_R N_i^c\,N_j^c + Y_{ij}^u L_i H_u\,N_j^c\,. \tag{6.6}$$

A non-zero vev of the $SU(2)_R$ triplet then implies a Majorana mass for right-handed neutrinos, whereas a vev for $SU(2)_L$ triplet implies a Majorana mass for the left-handed neutrinos.
We suppose here that the breaking of G_{3221} occurs due to Δ_R, whose vev v_R lies at an intermediate scale between the GUT and the electroweak scales. This breaking leads to a Majorana mass term of RHns, which violates $B-L$ by two units.
After electroweak symmetry breaking, the light neutrino masses receive two contributions, one coming from the type I seesaw [50]:

$$m^I_{\nu ij} = -v_u^2 \lambda_{ik} M_k^{-1} \lambda^T_{kj} = -\frac{v_u^2}{v_R}\,\lambda_{ik}\,f^{-1}_{R\,k}\,\lambda_{jk}\,, \tag{6.7}$$

where v_u is the vev of the up-type Higgs doublet, $v_u = v\sin(\beta)$, and one coming from the pure type II seesaw [53]:

$$m^{II}_{\nu\,ij} = v_L\,f_L^{ij}\,. \tag{6.8}$$

The smallness of the type I mass is obvious, since in this model the breaking of $B-L$ occurs far above the electroweak scale, $v_R \gg v_u$. Conversely, the smallness of pure type II contribution comes from the suppression of the $SU(2)_L$ triplet vev.
For instance, this seesaw-like relation for v_L can be obtained through the addition of a $\mathbf{54}$ dimensional Higgs that couples both to the $\mathbf{10}$s and to the $\overline{\mathbf{126}}$. The Higgs sector of the superpotential contains

$$W_H \supset \rho_1 \mathbf{54}\,\overline{\mathbf{126}}\,\overline{\mathbf{126}} + \rho_2 \mathbf{10}\,\mathbf{10}\,\mathbf{54} + M_{126}\overline{\mathbf{126}}\,\mathbf{126} + ..., \tag{6.9}$$

where $\rho_{1,2}$ are model-dependent couplings, the knowledge of which is beyond the scope of this chapter. Since under G_{3221}, the $\mathbf{54}$ contains a bi-triplet $\mathbf{54} \supset \Delta_{54} = (\mathbf{1},\mathbf{3},\mathbf{3},\mathbf{0})$, it can couple to the $SU(2)_{L,R}$ triplets of $\overline{\mathbf{126}}$ and to the the product of two) Higgs bidoublets $\mathbf{10} \supset \mathbf{\Phi} = (\mathbf{1},\mathbf{2},\mathbf{2},\mathbf{0})$, $\mathbf{10}\times\mathbf{10} \supset (\mathbf{1},\mathbf{3},\mathbf{3},\mathbf{0})$, according to

$$W_H \supset \rho_1\,\Delta_{54}\,\Delta_R\,\Delta_L + \rho_2 \Phi\,\Phi\,\Delta_{54}\; + M_\Delta \Delta_L \Delta_R. \tag{6.10}$$

Minimising the scalar potential with respect to v_L, one obtains the seesaw relation for the $SU(2)_L$ triplet vev:

$$v_L \simeq -\frac{\rho_1\rho_2 v^2 v_R}{M_\Delta^2} \ll v\,, \tag{6.11}$$

---

[2] For the different decomposition, see, for example, ref. [101].

which ensures that the (pure) type II contribution to light neutrino mass is indeed suppressed. In general, the superpotential contains many other terms (as indicated by the dots), which can contribute to the above relation. Therefore, in general v_L depends on many other couplings. Nevertheless, we always have

$$v_L = \frac{v_u^2}{M_{\Delta_L}} \,, \tag{6.12}$$

M_{Δ_L} being defined as a function of the relevant couplings.
Moreover, we assume here that G_{3221} is Left-Right (LR) symmetric [97], so that the Lagrangian invariant under G_{3221} is also invariant under the $SU(2)_L \leftrightarrow SU(2)_R$ exchange

$$\begin{pmatrix} \nu_L \\ e_L \end{pmatrix} \leftrightarrow \begin{pmatrix} N^c \\ e^c \end{pmatrix} \,, \quad \Phi \leftrightarrow \Phi^T \,, \quad \Delta_L \leftrightarrow \Delta_R \,. \tag{6.13}$$

This LR symmetry enforces $f_L = f_R \equiv f$, leading to two important consequences:

- Firstly, the seesaw relation now reads [53]

  $$m_\nu = \frac{v_u^2}{M_\Delta} f - \frac{v_L^2}{v_R} \lambda \, f^{-1} \, \lambda \ . \tag{6.14}$$

  Given the low-energy constraints on m_ν, and the GUT relation between the neutrino and the up-quark Yukawa couplings, we can extract f.

- Secondly, the right-handed neutrino masses simply read

  $$M = f \, v_R \,, \tag{6.15}$$

  and so the knowledge of f from the seesaw relation in turn predicts the RHn spectrum, a clear gain when compared to the non-GUT seesaw, where the RHn masses are put by hand.

6.2 Inferring the unknown parameters

6.2.1 Inverting the seesaw

Starting from the seesaw relation of eq.(6.14), the authors of [99, 102] have developed a procedure which allows to determine the properties of the complex symmetric matrix f, assuming the knowledge of m_ν and λ. Here we summarise their results, which are the building-blocks of our study [98]. Given the symmetry of λ, it is possible to find $\lambda^{1/2}$ such that $\lambda = \lambda^{1/2} . \lambda^{1/2\,T}$. Hence eq.(6.14) can be written

$$Y = \alpha \, X + \beta \, X^{-1} \tag{6.16}$$

where

$$Y = \lambda^{-1/2} . \, m_\nu . \, \left(\lambda^{-1/2}\right)^T \ , \ X = \lambda^{-1/2} . \, f . \, \left(\lambda^{-1/2}\right)^T \ , \tag{6.17}$$

and

$$\alpha = v_L = \frac{v_u^2}{M_\Delta}\ ,\ \beta = \frac{v_u^2}{v_R}\,. \tag{6.18}$$

The complex symmetric matrix Y is then diagonalised by an orthogonal matrix O_Y, which also diagonalises X:

$$\begin{aligned} \mathrm{diag}(y_1, y_2, y_3) &= O_Y^T.Y.O_Y \\ \mathrm{diag}(x_1, x_2, x_3) &= O_Y^T.X.O_Y\,. \end{aligned} \tag{6.19}$$

The equation (6.16) then leads to a second degree equation for the eigenvalues $y_i = \alpha x_i + \beta x_i^{-1}$, which is easily solved:

$$x_i^\pm = \frac{1}{2\alpha}\left(y_i \pm \mathrm{sign}(\mathrm{Re}(y_i))\sqrt{y_i^2 + 4\,\alpha\,\beta}\right)\,. \tag{6.20}$$

The couplings f are then given by:

$$f = \lambda^{1/2}.X.\left(\lambda^{-1/2}\right)^T = \lambda^{1/2}.O_Y.\mathrm{diag}(x_1, x_2, x_3).O_M^T.\left(\lambda^{-1/2}\right)^T\,. \tag{6.21}$$

Finally, the masses of the RHns are obtained after the diagonalisation of f, through an unitary matrix U_f

$$M_i = f_i\, v_R\ ,\ f_i = \left(U_f^\dagger.f.U_f^*\right)_{ii}\ , \tag{6.22}$$

where the f_is are positive, and by convention $f_1 \leq f_2 \leq f_3$. The unitary matrix U_f relates the basis where the right-handed neutrino mass matrix is diagonal to the basis where the coupling λ is symmetric. We place ourselves in the former basis, which implies a redefinition of $\lambda^{new} = U_F^\dagger \lambda^{old}$. Since there are two possible choices for each eigenvalue x_i, there are 8 different solutions for the matrix f, that is for the right-handed neutrino spectrum. These 8 solutions (2^n for n generations) constitute the "eight-fold" ambiguity [99] of the LR symmetric seesaw mechanism: for one low-energy spectrum, we have eight possible solutions, which can be distinguished through their high-energy effects.

Behaviour of the different solutions

In the above relations, the contributions from the different seesaws are clear: β stands for the type I contribution whereas α denotes the pure type II seesaw.
It is instructive to consider the asymptotic value $4\alpha\,\beta \ll |y_i|^2$, since in this case the ± solutions exhibit the different seesaw contributions:

$$x_i^+ \simeq \frac{y_i}{\alpha}\ ,\ x_i^- \simeq -\frac{\beta}{y_i}\,. \tag{6.23}$$

The " $+$ " solution corresponds to the dominance of the pure type II while " $-$ " solutions correspond to a dominance of the type I.

The different solutions for f are labelled according to the constitutive $x_i^\pm$: for example $(+,+,-)$ refers to the solution built from (x_1^+, x_2^+, x_3^-). For the f_is, in general one cannot clearly assess which seesaw is the dominant one, apart from the $f^{(+,+,+)}$ which clearly tends, in the $4\alpha\,\beta \ll |y_i|^2$ limit, towards a pure type II solution. Similarly, in this limit the $f^{(-,-,-)}$ solution approaches the type I case.

However, we notice that from the asymptotic behaviour of the x_is we can infer the evolution of right-handed neutrino masses as a function of the $B-L$ breaking scale v_R.

Indeed, for the " $+$ " solution, as $x_i^+ \simeq y_i/\alpha \propto v_R$, one expects at high v_R that the RHn mass will continuously increase with v_R. For the " $-$ " solutions, since $x_i^- \simeq -\beta/y_i \propto 1/v_R$, $v_R\, f_i \sim$ constant, and one expects that at high $B-L$ breaking scale the " $-$ " RHn masses will also become constant. The value of this constant is of major importance for leptogenesis.

In the opposite asymptotic limit, $4\alpha\,\beta \gg |y_i|^2$, we have

$$x_i^\pm \simeq \pm \text{sign}(\text{Re}(y_i))\sqrt{\beta/\alpha} \tag{6.24}$$

which shows that the type I and the pure type II somehow cancel each other in m_ν. Indeed, in this case, one roughly has $f \sim \lambda\,\sqrt{\beta/\alpha}$ and

$$m_\nu^{II} \simeq \sqrt{\alpha\beta}\lambda \sim m_\nu^I \; . \tag{6.25}$$

In the intermediate regime, type I and II contributions are of the same order.

We are interested in the dependency of the different parameters on the $B-L$ breaking scale. Therefore, in the following, we fix the ratio

$$\frac{\beta}{\alpha} = \frac{v_u^2}{v_R\, v_L} = \frac{M_\Delta}{v_R} \simeq 0.1 \; . \tag{6.26}$$

In fact, depending on the different couplings, $\beta/\alpha(M_\Delta)$ could be either larger or smaller than $1(v_R)$. Its value roughly sets the relative importance of the different seesaw contributions to the light neutrino masses. Modifying this value only accounts for a translation of the solution on the v_R axis. We choose $\beta/\alpha = 0.1$ due to numerical instabilities encountered with $\beta/\alpha = 1$ in the high v_R regime.

Fixing parameters

In the type I seesaw, we saw that there are 18 parameters among which only 4 are known. Let us see how many parameters we have in our type II framework.

We place ourselves in the basis where charged lepton (and down-type quark) and RHn masses (f) are diagonal. Then, using the GUT relation $m_D = m_u$, we have

$$\lambda = U_q^T.\text{diag}(y_u, y_c, y_t).U_q \tag{6.27}$$

$$m_\nu = U_\ell^*.\text{diag}(m_1, m_2, m_3).U_\ell^\dagger\,, \tag{6.28}$$

where y_q [3] is the Yukawa coupling for the q-quark, and m_i are light neutrino masses. The unitary matrices U_q and U_ℓ are related to the CKM [103] and PMNS [34] mixing matrices. They respectively read:

$$U_q = P_u.V_{CKM}.P_d\,, \tag{6.29}$$

$$U_\ell = P_e.U_{PMNS}.P_\nu\,. \tag{6.30}$$

At the GUT scale, since quarks and leptons belong to the same **16** representation, they cannot be independently rotated, hence the matrices P_k $(k = u, \nu, e, d)$.

However, at low energy $P_{e,d,u}$ can be rotated away, while the matrix P_ν contains the usual Majorana CP violating phases. All these matrices contain 3 phases, among which two global phases can be re-absorbed. We parametrise these matrices as follows:

$$P_k = \mathrm{diag}(e^{\mathrm{i}\phi_1^k}, e^{\mathrm{i}\phi_2^k}, e^{\mathrm{i}\phi_3^k})\,, k = u, \nu \tag{6.31}$$

$$P_l = \mathrm{diag}(e^{\mathrm{i}\phi_1^l}, e^{\mathrm{i}\phi_2^l}, 1)\,, k = e, d\,. \tag{6.32}$$

Hence, at the GUT scale, we have 7 additional CP violating phases when compared to the type I seesaw. This is a welcome feature regarding leptogenesis, even if these extra phases induce a loss of the predictivity for our model.

The input values for the quark masses and for the CKM matrix at M_Z have been taken from Refs. [104] and [105], respectively, and subsequently evolved to the GUT scale using the Mathematica package REAP [106] with an effective SUSY threshold $M_{SUSY} = 1$ TeV and $\tan\beta = 10$. The light neutrino mass spectrum has been assumed to be hierarchical, with $m_1 = 10^{-3}$ eV, and the oscillation parameters have been set to the best fit values of [107], while keeping θ_{13} only upper-constrained $\theta_{13} \lesssim 13°$. Renormalisation group effects induce a multiplicative factor for the different Yukawa couplings: for the first two generations of quarks, renormalisation induces a factor ~ 0.41, the top quark Yukawa factor being ~ 0.56, while the neutrino sector is multiplied by a factor ~ 1.08.

All in all, we are left with 17 "free" parameters: the light neutrino mass scale, the ordering of the neutrino spectrum and the mixing angle θ_{13}; we also have 10 free CP phases. The $B - L$ breaking scale can vary from $\sim 10^{12}$ GeV to 10^{16} GeV; however perturbativity of the couplings f restricts this range: for the value $\alpha/\beta = 0.1$ that we choose, from $\sim 10^{12}$ GeV to $\sim 5 \times 10^{14}$ GeV. Finally, there is another constraint coming from the reheating temperature, which we will discuss later and which gives us another parameter, T_{RH} which is allowed to lie between 10^9 GeV and 10^{11} GeV. Working in a supersymmetric framework, we have to fix the ratio of the low-energy Higgs doublet vev $v_u/v_d = \tan(\beta)$. As already said, we choose here $\tan(\beta) = 10$ as a representative value.

Considering the large number of parameters, and our limited computation ability, it is not feasible to scan over the full parameter range, but we instead fixed some of the parameters. We list in the following table the usual values for the inputs that we used, distinguishing the parameters which we usually vary from those whose value is fixed (NMO stands for neutrino mass ordering, which is chosen normal ordered).

---

[3] In general, the Yukawa couplings we use are linear combinations of those of eq.(6.3), and their precise relation is beyond the scope of this chapter.

v_R(GeV)	T_{RH}(GeV)	$m_{\nu 1}$(eV)	θ_{13}	$\phi_2^{u,\nu}$
$10^{12} - 5 \times 10^{14}$	$5 \times 10^9 - 10^{11}$ GeV	$10^{-5} - 10^{-1}$	$0 - 13°$	$0, \pi/4$

(6.33)

NMO	β/α	$\tan(\beta)$	$\phi_{1,3}^{u,\nu}$	$\phi_1^{e,d}$	$\phi_2^{e,d}$
NH	0.1	10	0	0	0

(6.34)

Correcting the GUT relation $m_e = m_d$

Since the only source for the Dirac mass term is the $SU(2)_L$ doublet of the two **10** Higgses, we have $m_u = m_D$ and $m_e = m_d$. The latter relation is, strictly speaking, not a problem since the Dirac-type mass of light neutrinos is unknown. However, the relation $m_e = m_d$ is clearly wrong, and must be improved.

A usual correction is to assume that the $SU(2)_L$ doublets of the $\overline{\mathbf{126}}$ also acquire a vev at the electroweak scale. Doing this, one thus obtains [100]:

$$\begin{aligned} m_d &= v_{10}^d \, \lambda^d + v_{126}^d \, f \, , \\ m_e &= v_{10}^d \, \lambda^d - 3 \, v_{126}^d \, f \, , \\ m_u &= v_{10}^u \, \lambda^u + v_{126}^u \, f \, , \\ m_\nu &= v_{10}^u \, \lambda^u - 3 \, v_{126}^u \, f \, , \end{aligned} \tag{6.35}$$

such that the GUT relations for the masses are

$$\begin{aligned} m_D &= m_u - 4 \, v_{126}^u \, f \, , \\ m_e &= m_d - 4 \, v_{126}^d \, f \, . \end{aligned} \tag{6.36}$$

Inserting the first relation in the seesaw formula, one could in principle invert it in the same way as previously explained. However, the fact that $m_e \propto f$ renders the extraction of f a really hard task.

We could assume that an anti-symmetric **120** does the job, but our model does not contain such a representation. The remaining possibility is to invoke adjoint **45** representations which couple to the **10** and create an effective **120**, as can be seen from the following decomposition:

$$\mathbf{10} \times \mathbf{45} = \mathbf{10} \times \mathbf{120} \times \mathbf{320} \, . \tag{6.37}$$

Neglecting the higher dimensional representation, we see that both the **10** and the **120** can contribute to the fermion masses. However, the **10** equally contributes to leptons and quarks, and so we neglect it (should it take a vev, a redefinition of λ^d would absorb it). Therefore, we need the **120** to acquire a vev. Among the different possibilities, the only products which leave G_{SM} invariant at the GUT scale after the **45** develops a vev are

$$\begin{aligned}\mathcal{L} \supset\ & \frac{Y_1}{\Lambda}\,(\mathbf{16}\times\mathbf{16})_{|(\mathbf{1},\mathbf{2},\mathbf{2})}\times[(\mathbf{1},\mathbf{2},\mathbf{2})_{10}\times(\mathbf{1},\mathbf{1},\mathbf{3})_{45}]\\ +\ & \frac{Y_2}{\Lambda}\,(\mathbf{16}\times\mathbf{16})_{|(\mathbf{15},\mathbf{2},\mathbf{2})}\times[(\mathbf{1},\mathbf{2},\mathbf{2})_{10}\times(\mathbf{15},\mathbf{1},\mathbf{1})_{45}]\ ,\end{aligned} \tag{6.38}$$

where we wrote the decomposition under the Pati-Salam group $SU(4)\times SU(2)_L\times SU(2)_R$. We see that the two terms contribute differently: the first one is $\propto(\mathbf{1},\mathbf{1},\mathbf{3})_{45}$, and so a vev in this direction does not distinguish quarks from leptons. On the contrary, the second term, which is $\propto(\mathbf{15},\mathbf{1},\mathbf{1})_{45}$, clearly does.

Considering that only the latter term acquires a vev, at the GUT scale the relation $m_e = m_d$ can be corrected as:

$$m_e = v_d\left(\lambda_d - \frac{3v_{\hat{15}}}{\Lambda}Y_2\right)\ , \tag{6.39}$$

$$m_d = v_d\left(\lambda_d + \frac{v_{\hat{15}}}{\Lambda}Y_2\right)\ , \tag{6.40}$$

where $v_{\hat{15}}\,v_d = \langle(\mathbf{15},\mathbf{1},\mathbf{1})_{45}\rangle$. Once corrected, the masses of charged leptons and down type quarks at the GUT scale are found to be:

$$\begin{array}{lll} m_d = 0.94\text{ MeV} & m_s = 17\text{ MeV} & m_b = 0.98\text{ GeV}\ ,\\ m_e = 0.346\text{ MeV} & m_\mu = 73.0\text{ MeV} & m_\tau = 1.25\text{ GeV}\ .\end{array} \tag{6.41}$$

However, for a consistent correction of the relation $m_e = m_d$, since we only include one **45**, we should obtain that $m_\tau^2 - m_b^2 \sim m_\mu^2$, which is not the case with the values above.

Nevertheless, supersymmetric threshold effects arising from the SUSY breaking sector (see, *e.g.* [108] and references therein) allow to solve this problem. Indeed, at the tree level, the down quarks couple only to one Higgs doublet, H_d, which is not the case for their scalar partner, given that $W \supset \mu\,H_u.H_d + Y_d\,Q.H_d\,D^c$. Once SUSY breaking terms are included, this will provide a correction to the down quark masses, according to [108]:

$$m_b \to m_b\,(1+\delta_{m_b}\tan(\beta))\ , \tag{6.42}$$

where

$$\delta_m \simeq \frac{2\alpha_s}{3\pi}\,\frac{\mu\,M_3}{m^2_{\tilde{b}_R}}\ , \tag{6.43}$$

which is evaluated to be $\delta_m \lesssim 2\%$. Once these corrections are added, the bottom quark mass is $m_b(M_{GUT}) \simeq 1.17\,\text{GeV}$, which is just enough to fit m_e and m_d with the procedure discussed before.

The two mass matrices differ $m_e \neq m_d$, and so we introduce a unitary matrix U_m, the matrix rotating from the basis where m_e is diagonal to the basis where m_d is diagonal:

$$m_e = \hat{m}_e \to m_d = U_m^T.\hat{m}_d.U_m\,. \tag{6.44}$$

The precise expression of U_m is found after fitting the charged lepton and down quark masses, and is given by

$$U_m = e^{i\phi_g^m} \begin{pmatrix} e^{i\phi_1^m} & 0 & 0 \\ 0 & e^{i\phi_2^m} & 0 \\ 0 & 0 & 1 \end{pmatrix} V(\theta_{12}^m, \theta_{13}^m, \theta_{23}^m, \delta^m) \begin{pmatrix} e^{i\phi_3^m} & 0 & 0 \\ 0 & e^{i\phi_4^m} & 0 \\ 0 & 0 & 1 \end{pmatrix} . \tag{6.45}$$

V is a CKM-like mixing matrix, with three real angles and one complex phase. The different values we will use for the phases of U_m are listed below, with the corresponding non-zero phases of the matrices P_k.

Sets	θ_{12}^m	θ_{13}^m	θ_{23}	δ^m	ϕ_g^m	ϕ_1^m	ϕ_2^m	ϕ_3^m	ϕ_4^m	$\pi/4$
1	1.07	0.22	0.21	5.80	3.21	4.37	5.86	0.87	6.16	ϕ_2^u
2	1.07	0.22	0.21	5.80	3.21	4.37	5.86	0.87	6.16	ϕ_2^ν
3	0.17	0.066	0.29	0.23	3.14	0.54	0.015	6.27	0.0032	ϕ_2^u
4	0.28	0.089	0.37	0.062	3.15	3.12	6.03	2.94	6.19	ϕ_2^u

Perturbativity of the couplings

Now that we have been able to reconstruct the couplings f, let us see how they depend on the $B-L$ breaking scale.

First of all, given the asymptotic behaviour of the x_is, we can say that among the different solutions, the case $(+,+,+)$ will reach the highest values of f, and so of M, while on the contrary the case $(-,-,-)$ will reach the lowest ones.

We thus plot in fig.(6.1) the evolution of the coupling f_i for these two solutions, as a function of the $B-L$ breaking scale, also considering different values of the smallest light neutrino mass. We assume here a normal mass ordering and put all phases ϕ_i^k and θ_{13} to zero; furthermore, we neglect U_m for the moment.

We observe that the coupling f becomes non-perturbative for $v_R \gtrsim 10^{15}\,\text{GeV}$. From now, we therefore restrict ourselves to $v_R \lesssim 10^{15}\,\text{GeV}$.

6.2.2 Right-handed neutrino spectrum

Let us study the right-handed neutrino spectra for the different solutions.

In fig.(6.2), we plot the masses $M_i, i = 1,2,3$ for the 8 solutions $(\pm,\pm,\pm)$ as a function of the $B-L$ breaking scale v_R. We choose $m_1 = 10^{-3}\,\text{eV}$, the other parameters being fixed as before. Qualitatively, we see that the different solutions behave as expected: $(+,+,+)$ masses continuously increase with v_R, whereas $(-,-,-)$ masses must reach a plateau.

Moreover, a " $-$ " solution for x_i entails that one of the masses reaches such a plateau. The precise relation between x_i^- and the mass M_j which stabilises can be found in the appendix B of [99].

Finally, we can classify the different solutions using the plateau argument, and group them in four pairs, $(\pm,+,+)$, $(\pm,-,+)$, $(\pm,+,-)$ and $(\pm,-,-)$ as displayed in fig.(6.2).

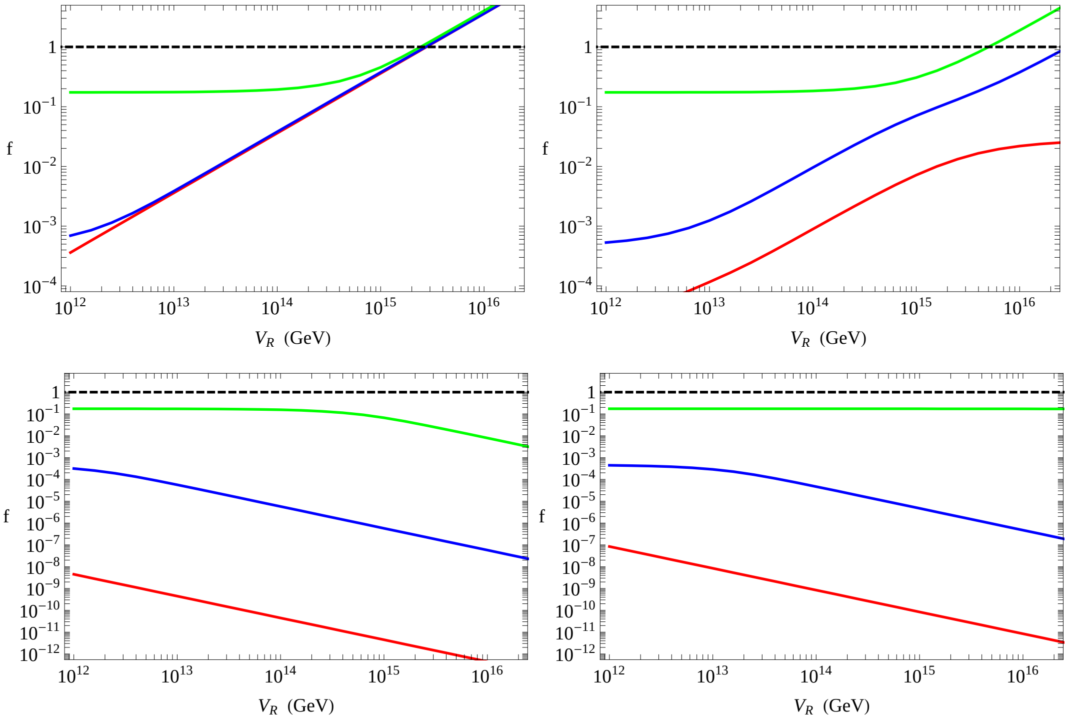

Figure (6.1): Evolution of the coupling f as a function of the $B-L$ breaking scale v_R for the case $(+,+,+)$ (up panels) and $(-,-,-)$ (down panels), for different light-neutrino masses m_1, with $m_1 = 0.1\,\text{eV}$, and $10^{-5}\,\text{eV}$ for the left and right panels, respectively. In green (upper-curves) we depict f_3, in blue f_2 and in red f_1.

- In the first pair $(\pm,+,+)$, right-handed neutrino masses keep growing with increasing v_R, at least until $f \sim 1$ is reached. For $v_R \lesssim 10^{14}\,\text{GeV}$, we have $M_1 \leq M_2 \ll M_3$. A priori, one could think of N_1 and N_2 as potential candidate for leptogenesis.

- In the second case $(\pm,-,+)$, the lowest RHn mass rapidly reaches a plateau, for $v_R \gtrsim 10^{13}\,\text{GeV}$. The constant value is $M_1 \simeq 10^9\,\text{GeV}$, closed to but still slightly below the type I leptogenesis bound $M_1 \lesssim M_1^{\text{min,I}} \sim (2-3) \times 10^9\,\text{GeV}$. We notice that $M_1 \sim M_2$ at low v_R. Here also, N_1 and N_2 are "leptogenesis-friendly", albeit M_1 seems too light.

- The third pair $(\pm,+,-)$ exhibits a very different mass pattern: above the $B-L$ breaking scale considered, $M_1 \simeq 10^5\,\text{GeV}$, while M_2 varies from $10^9\,\text{GeV}$ to $10^{11}\,\text{GeV}$ for $10^{12}\,\text{GeV} \lesssim v_R \lesssim 10^{14}\,\text{GeV}$. Thus N_1 cannot be of any help for leptogenesis, while N_2 clearly is.

- In the fourth type of solutions, $(\pm,-,-)$ cases, both M_1 and M_2 reach a plateau. M_1 stabilises around $10^5\,\text{GeV}$, and thus N_1 is too light for leptogenesis, while N_2, reaching a constant mass value $M_2 \simeq M_1^{\text{min,I}}$ provides an interesting possibility.

Therefore, in the following, we will focus only on four typical solutions: $(+,+,+)$ which corresponds to the pure type II in the high v_R limit; $(-,-,-)$ which conversely corresponds to

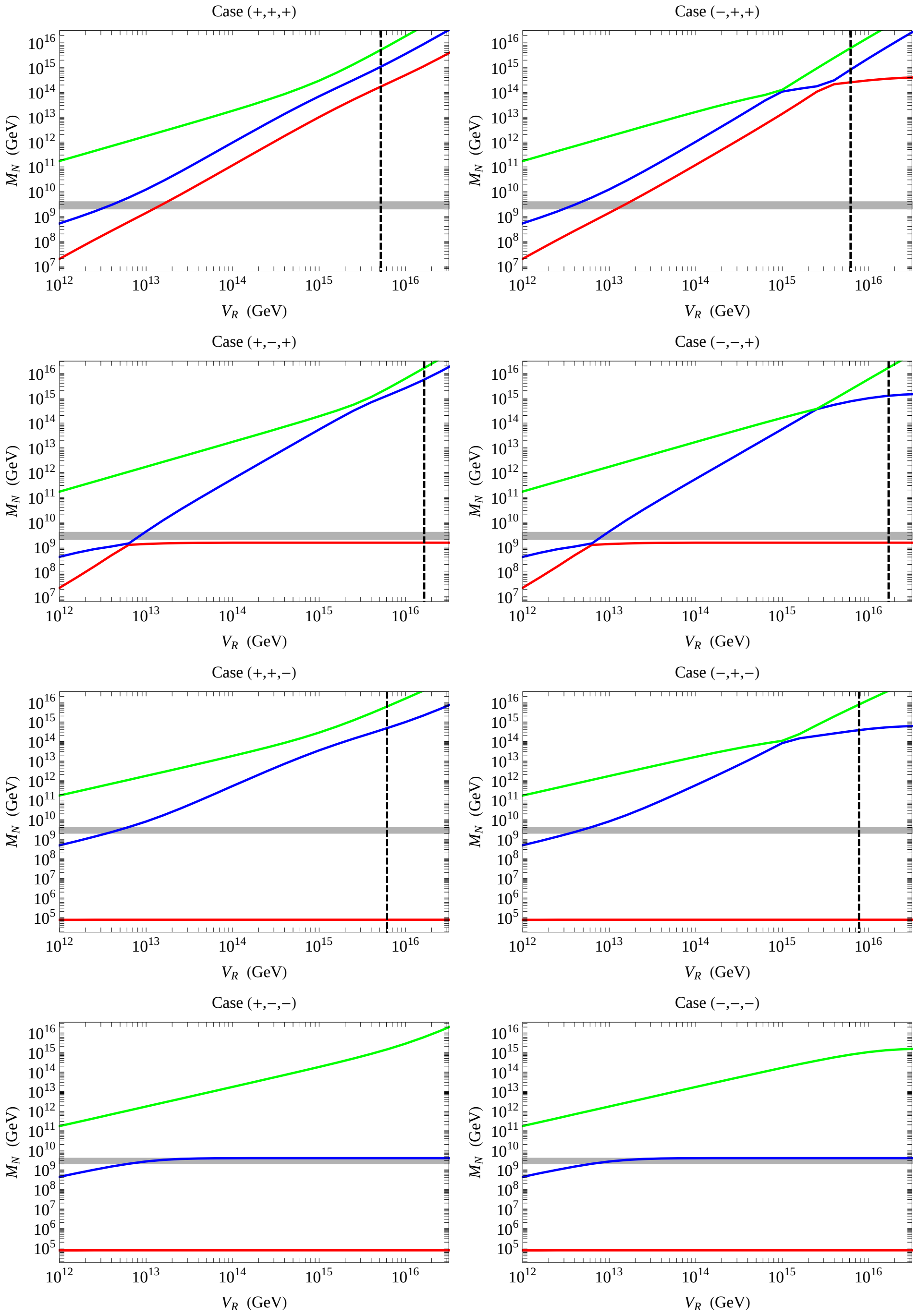

Case (+,+,+)

Case (−,+,+)

Case (+,−,+)

Case (−,−,+)

Case (+,+,−)

Case (−,+,−)

Case (+,−,−)

Case (−,−,−)

Figure (6.2): Spectra of right-handed neutrinos resulting from the different solutions for f, as a function of v_R. The colour code is similar to fig.(6.1). The vertical dashed line represents the perturbative limit for f, while the horizontal gray band denotes the lower bound on M, as derived in the type I seesaw (see previous chapter).

the type I solution in the high v_R limit; solutions $(+,+,-)$ and $(+,-,+)$, which are interesting mixed type I-pure type II solutions.

6.3 Leptogenesis

Now let us proceed to the analysis of leptogenesis in this scenario, which has already been widely studied in the single flavour approximation [99], [109]- [115].

The sources of lepton number violation consist in interactions involving right-handed neutrinos and scalar triplets. The former are found similar to the type I seesaw, except for the fact that the RHns are no longer singlets, since they belong to an $SU(2)_R$ doublet. Thus they interact with the additional gauge bosons, which may have consequences for leptogenesis.

Furthermore, the inclusion of $SU(2)_L$ Δ_L triplets induces additional CP asymmetries, as we will see below.

Before examining these points, a remark is in order, regarding the different right-handed neutrino spectra discussed above.

In leptogenesis, it is customary to assume that the contributions of the heavier neutrinos are negligible, since the asymmetries produced during $N_{2,3}$ decays will be erased by the inverse decays which produce N_1. In our case, since $M_3 \gg M_2, M_1$, it is true that the asymmetry produced during N_3 decays will be washed-out by $N_{1,2}$ processes. However, we see that in the $(\pm, \pm, -)$ cases, M_1 is too small for leptogenesis, while M_2 has potentially the good order of magnitude. Hence when evaluating the produced baryon asymmetry, we must consider both N_1 and N_2 processes, while N_3 ones can be disregarded.

6.3.1 Right-handed neutrinos as part of an $SU(2)_R$ doublet

Having gauged $SU(2)_R \times U(1)_{B-L}$, our model contains four extra gauge bosons $\sim B', W_R^0, W_R^{1,2}$, which acquire mass when the $SU(2)_R$ Higgs triplet Δ_R develops a vev. Right-handed neutrinos are charged under G_{3221}, $N^c = (1, 1/2, 1, 1)$, and so they interact with the extra gauge bosons through different processes [109, 112]:

- Decays of N into W_R, either with on-shell W_R via two-body decays when $M_1 \gtrsim M_{W_R}$, or into off-shell W_R via three-body decays, when $M_1 \lesssim M_{W_R}$.

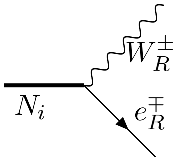

Figure (6.3): Two-body RHn decays.

- Gauge boson mediated scatterings: either (a) right-handed quark-lepton W_R mediated scatterings , through $s-$ channel $N\, e_R \leftrightarrow \overline{u_R}\, d_R$, and $t-$, $u-$ channels $N\, d_R \leftrightarrow e_R\, u_R$ and $N\, \overline{u_R} \leftrightarrow e_R\, \overline{d_R}$, or (b) lepton-lepton scatterings involving two Ns, via Z' mediated scatterings in the $s-$ channel $N\, N^c \leftrightarrow e_R\, \overline{e_R}$, and W_R $t-, u-$ channels $e_R\, \overline{e_R} \leftrightarrow N\, \overline{N}$ and $e_R\, N_i \leftrightarrow N_j\, e_R$.

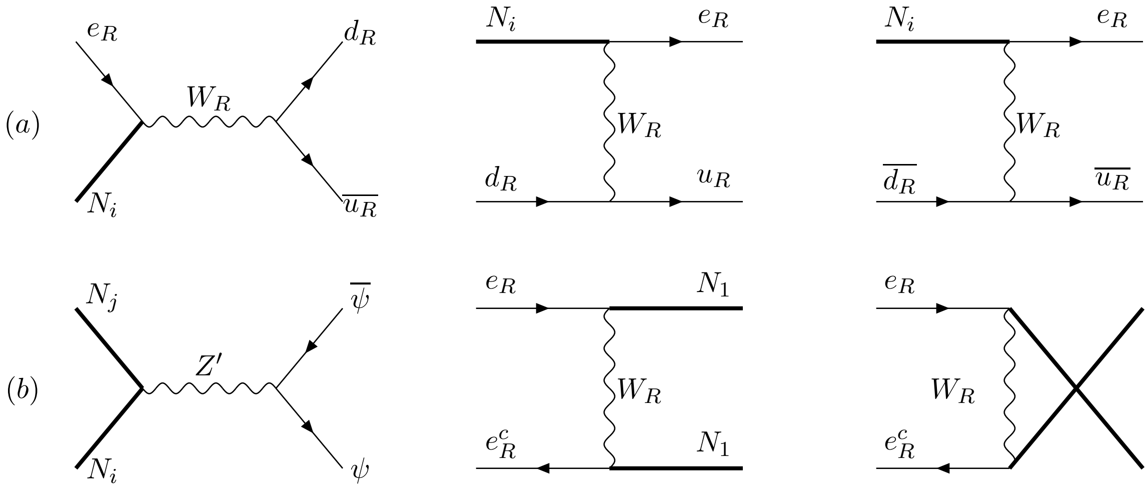

Figure (6.4): Gauge bosons scatterings.

The decay channel of N into W_R may affect leptogenesis by diluting the CP asymmetry generated in RHn decays into leptons [116]. However, as $M_\Delta \gg M_1$ we can neglect this dilution. The potential danger associated to these new interactions comes from scatterings, which tend to keep right-handed neutrinos in-equilibrium with the thermal bath. Two cases may happen: either $M_i \gtrsim M_{W_R}$ or $M_1 \lesssim M_{W_R}$. It has been shown in [109] that in the former case no lepton asymmetry can be generated, unless $M_i \gtrsim 10^{16}$ GeV when the scatterings $e_R\, W_R^+ \to N \to \overline{e_R}\, W_R^-$ become out of equilibrium. In the considered case, under the constraint $v_R \lesssim 10^{15}$ GeV, we do not reach such high values for the M_i. However, since $M_{W_R} \simeq g_R\, v_R/2 \simeq v_R/3$ and $M_i = f_i v_R$, this case may be only encountered in the $(+,+,+)$ solution for the heaviest right-handed neutrino, for $v_R \simeq 10^{15}$ GeV.

Thus the danger may only arise from the other case $M_i \lesssim M_{W_R}$, when scatterings mediated by the extra gauge bosons force the RHns to be in thermal equilibrium, and so prevent the third Sakharov condition from being satisfied. The condition for these scatterings to be out of equilibrium is [109]

$$M_i \lesssim 9\,\times 10^{12}\,\text{GeV} \times \left(v_R/10^{14}\,\text{GeV}\right)^{4/3}\ , \tag{6.46}$$

while the condition for the scatterings to be slower than $\Delta L = 1$ scatterings is

$$M_i \lesssim 2 \times 10^{13}\, K_i \times \left(\frac{v_R}{10^{14}\,\text{GeV}}\right)^2 \times \left(0.06\left(\frac{v_R}{M_i}\right)^2 + 1.15\right)\ , \tag{6.47}$$

where K_i is the washout factor of the RHn N_i (see below).

These two conditions are fulfilled for both N_1 and N_2, for the $B-L$ breaking scale we considered

$v_R \lesssim 5 \times 10^{14}$ GeV and for light neutrino masses $m_1 \lesssim 0.3$ eV. Actually, this constraint may only apply for heavy RHns, $M_i \gtrsim 10^{11}$ GeV, for which one encounters an even stronger constraint which stems from the gravitino problem, as we will see hereafter. For that reason, we can safely neglect the effect of the $SU(2)_R \times U(1)_{B-L}$ gauge bosons.

6.3.2 Scalar triplets in leptogenesis

Additional CP asymmetries

The first thing to notice is that Δ_L contributes to the leptonic CP asymmetry in two different ways [111]. Since Δ_L couples to leptons and to the Higgs doublet, a CP asymmetry can be generated during Δ_L decays through the interference between the tree level $\Delta_L \to L_i L_j$ and the vertex correction involving right-handed neutrinos, depicted in fig.(6.5).

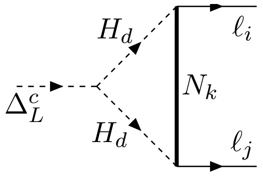

Figure (6.5): Vertex correction for Δ_L decays.

These decays violate lepton number by two units. However, since we have $M_{\Delta_L} \simeq v_R/3$, the triplet is much heavier than the lightest RHn, $M_{\Delta_L} \gg M_1$. Therefore the asymmetry produced during these decays will be washed out by the subsequent processes involving N_2 and N_1, and so we can neglect all processes with on-shell Δ_Ls.

The other possible contribution comes from the vertex correction of the right-handed neutrino decay diagram, with an off-shell Δ_L running in the loop:

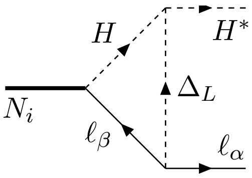

Figure (6.6): Additional CP asymmetry for the type II seesaw.

As the couplings of Δ_L to lepton and Higgses are both complex, they induce a new interference term with the tree level diagram $N \to \ell\phi$. The corresponding CP asymmetry in lepton flavours reads [113, 117]:

$$\varepsilon_{i\alpha}^{II} = \frac{3}{8\pi} \sum_{k=1,3} \frac{\mathrm{Im}\left\{\lambda_{ik}\,(m^*_{\nu^{II}})_{k\alpha}\,\lambda^*_{i\alpha}\right\}}{(\lambda\lambda^\dagger)_{ii}} \frac{M_i}{v_u} f^{II}\left(\left(\frac{M_\Delta}{M_i}\right)^2\right) , \tag{6.48}$$

where the loop function is given in the MSSM by [111, 113]:

$$f^{II}(y) \quad = \quad x \log\left(\frac{1+x}{x}\right) \overset{x \gg 1}{\longrightarrow} 1 \ . \tag{6.49}$$

6.3.3 Supersymmetric leptogenesis

The supersymmetric version of thermal leptogenesis is not very different from the SM one [118, 58]. Indeed, given the energy scale considered, $\sim M_i \gg 1\text{TeV}$, the soft SUSY breaking terms are negligible, and the masses of fermions and sfermions are equal $M_N = M_{\tilde{N}}$. Furthermore, from the Yukawa couplings in the superpotential

$$W \supset \lambda_{i\alpha} L_\alpha . H_u N_i^c \ , \tag{6.50}$$

$$\Gamma(N_i \to \ell_\alpha H_u) \ = \Gamma(N_i \to \bar{\ell}_\alpha H_u^*) \ = \Gamma(N_i \to \tilde{\ell}_\alpha \tilde{H}_u) \ = \Gamma(N_i \to \tilde{\ell}_\alpha^* \bar{\tilde{H}}_u) \ = \ \frac{M_i}{16\pi} \left|\lambda_{i\alpha}\right|^2 \ , \tag{6.51}$$

$$\Gamma(\widetilde{N_i^c} \to \bar{\ell}_\alpha \bar{\tilde{H}}_u) \ = \Gamma(\widetilde{N_i^c} \to \tilde{\ell}_\alpha H_u) \ = \ \frac{M_i}{8\pi} \left|\lambda_{i\alpha}\right|^2 \ . \tag{6.52}$$

Supersymmetry implies the equality of the total decay widths, $\Gamma_{N_i} \ = \Gamma_{\widetilde{N_i^c}} \ = M_i(\lambda\lambda^\dagger)_{ii}/4\pi$. Hence a lepton asymmetry is created through decays of right-handed neutrinos N and (RH) sneutrinos $\tilde{N}$ in an amount equal to that of the slepton asymmetry

$$\varepsilon_{N_i, L_\alpha} = \varepsilon_{\tilde{N^c}_i, L_\alpha} = \varepsilon_{N_i, \tilde{L}_\alpha} = \varepsilon_{\tilde{N^c}_i, \tilde{L}_\alpha} \ . \tag{6.53}$$

The CP asymmetry generated in N_i decays is [61]:

$$\varepsilon^I_{i\alpha} = \frac{1}{8\pi} \sum_{j \neq i} \frac{\text{Im}\left\{\lambda_{i\alpha} (\lambda\lambda^\dagger)_{ij} \lambda^*_{j\alpha}\right\}}{(\lambda\lambda^\dagger)_{ii}} f_I\left(\left(\frac{M_j}{M_i}\right)^2\right) \ . \tag{6.54}$$

Since we have an additional scalar trilinear coupling $\tilde{L} H_u \tilde{N}^c$, the vertex correction is modified when compared to the SM case, as well as the self-energy correction, since twice more particles are running in the loop. The type I correction thus reads in the MSSM [61]:

$$f_I(x) \quad = \quad \sqrt{x}\left(\frac{2}{1-x} - \log\left(\frac{1+x}{x}\right)\right) \overset{x \gg 1}{\longrightarrow} -\frac{3}{\sqrt{x}} \ . \tag{6.55}$$

As we saw in chapter 3, when RH neutrinos are almost degenerate, the self-energy correction should be treated with care. As we can see in fig.(6.2), for example in the $(+,-,+)$ at low v_R, we have such a (partial) degeneracy $M_1 \simeq M_2$. We therefore use for the CP asymmetry the following formula [73]:

$$\varepsilon^I_{i\alpha} = \frac{1}{8\pi} \frac{1}{(\lambda\lambda^\dagger)_{ii}} \sum_{j \neq i} \text{Im}\left\{\lambda_{i\alpha} \lambda^*_{j\alpha} \left[(\lambda\lambda^\dagger)_{ij} (C^{ij}_v + 2C^{ij}_{s,a}) + 2\,(\lambda\lambda^\dagger)_{ji}\, C^{ij}_{s,b}\right]\right\} \ , \tag{6.56}$$

where C^{ij}_v is the vertex correction

$$C^{ij}_v = -\sqrt{x} \log\left(\frac{1+x}{x}\right), \sqrt{x} = \frac{M_j}{M_i} \ , \tag{6.57}$$

the other term standing for the self-energy correction

$$C^{ij}_{s,a} = \sqrt{x}\, C^{ij}_{s,b} = \frac{\sqrt{x}(1-x)}{(1-x)^2 + x\,(\lambda\lambda^\dagger)^2_{ij}\,/16\pi^2}\ . \tag{6.58}$$

In the limit of hierarchical RHns, $x \gg 1$ and the terms $C_{s,b}$ can be neglected, so that we recover the non-resonant formula eq.(6.54).

Another difference in the supersymmetric version of leptogenesis, is the relation among chemical potentials, from which we deduce the conversion between the lepton doublet asymmetry and the $B - L_\alpha$ asymmetries,

$$Y_{L_\alpha}(z) = \sum_\beta A_{\alpha\beta} Y_{\Delta\beta}\ . \tag{6.59}$$

For $M_1 \lesssim 10^9\,\text{GeV} \times (1+\tan\beta^2)$, tau- and muon-Yukawa couplings are in equilibrium, thus the three flavoured asymmetries $Y_{\Delta e}$,$Y_{\Delta\mu}$,$Y_{\Delta\tau}$ are distinguishable. In the MSSM, the A matrix is given by [88]:

$$A = \begin{pmatrix} -93/110 & 6/55 & 6/55 \\ 3/40 & -19/30 & 1/30 \\ 3/40 & 1/30 & -19/30 \end{pmatrix}. \tag{6.60}$$

For M_1 between $10^9\,\text{GeV} \times (1+\tan\beta^2)$ and $10^{12}\,\text{GeV} \times (1+\tan\beta^2)$, only the tau-Yukawas are in equilibrium, thus the lepton asymmetry is projected onto a 2 flavour-space ($Y_{\Delta e+\mu} = Y_{\Delta e+\Delta\mu}, Y_{\Delta\tau}$). The conversion $L \leftrightarrow B-L$ now reads:

$$A = \begin{pmatrix} -541/761 & 152/761 \\ 46/761 & -494/761 \end{pmatrix}. \tag{6.61}$$

Finally, if M_i is above $10^{12} \times (1+\tan\beta^2)$ GeV, none of the interactions involving charged lepton Yukawa couplings are in equilibrium, and we recover the flavour-independent treatment of leptogenesis with $A = -\text{diag}(1,1,1)$.

Finally, with two light Higgs doublets, the baryon asymmetry resulting from the fast $B+L$ violating processes is [83]:

$$Y_B = \frac{10}{31}\sum_\alpha Y_{\Delta\alpha}\ . \tag{6.62}$$

With our choice of $\tan\beta = 10$, the 3 flavour regime will generally apply, since in most of the solutions $((-,-,-), (+,+,+)$, etc...) the RH neutrino masses are below 10^{11} GeV.

Let us turn to the discussion of the major problem a supersymmetric scenario of leptogenesis faces: the constraint on the reheating temperature of the Universe, T_{RH}.

6.3.4 Reheating temperature and the gravitino problem

The standard scenario of cosmology relies on the existence of an inflationary period [1, 10], which explains, among other issues, the observed homogeneity and isotropy of the Universe. The inflationary epoch lasts until the field responsible for driving inflation, the inflaton, reaches the minimum of its potential. At this time, the energy density of the Universe is dominated by the vacuum energy of the inflaton. As this field oscillates around its minimum, it reheats the Universe by a release of its potential energy. Then, when $T \simeq T_{RH}$, the inflaton field decays, creating degrees of freedom, and so the temperature drops down.

Therefore all species existing before the reheating of the Universe will be completely diluted by the entropy production. Similarly, any pre-existing lepton asymmetry will be washed-out, so that it is mandatory that leptogenesis takes place after reheating $T_{\rm lepto} \lesssim T_{RH}$. As $T_{\rm lepto} \sim M_1 \sim 10^9\,$GeV thermal leptogenesis requires $T_{RH} \gtrsim 10^9\,$GeV.

On the other hand, such high temperatures can be problematic when one comes to local supersymmetry [119]. Indeed, in such a case, the SUSY partner of the graviton field, the spin 3/2 gravitino, imposes stringent constraints on the reheating temperature [120]. The gravitino only interacts gravitationaly, thus very weakly. Essentially two situations can occur. The lifetime of the gravitinos can be larger than the age of the Universe, in which case they might either overclose the Universe or their relic density may give an overabundant dark matter density [121]. In the opposite case, gravitinos can be unstable, and their decays can either spoil the success of Big Bang Nucleosynthesis [122], or their decay products, if stable, can also provide an overabundant dark matter relic density.

The constraints on the reheating temperature come from the fact that the thermal production of gravitinos, which happens during or just after the reheating stage, is more efficient for high reheating temperatures. Indeed, the Boltzmann equation for the gravitino number density $n_{3/2}$, in a bath dominated by the inflaton field and radiation, reads [123, 124]:

$$\begin{aligned} \tfrac{d\rho_\phi}{dt} &+3H(T)\,\rho_\phi = -\Gamma_\phi\,\rho_\phi\,, \\ \tfrac{d\rho_R}{dt} &+4H(T)\,\rho_R = \Gamma_\phi\,\rho_\phi\,, \\ \tfrac{dn_{3/2}}{dt} &+3H(T)\,n_{3/2} = \gamma(T)\,, \end{aligned}$$

where $\rho_R = \pi^2 g_* T^4/30$ is the radiation energy density, and ρ_ϕ the energy density of the inflaton scalar field. The decay width of the inflaton field is related to the reheating temperature by:

$$\Gamma_\phi = \frac{T_{RH}}{M_{pl}}\sqrt{\frac{8\pi^3}{90}\,g_*}\ . \tag{6.63}$$

where in the MSSM the effective number of degrees of freedom is $g_* = 228.75$. The thermal production rate of gravitino is roughly [124] $\gamma(T) \simeq 10\,T^6/M_{pl}^2$.

Since gravitinos interact only gravitationnaly, one can consider that the density after reheating remains unchanged until gravitinos decay (if ever), such that one has

$$Y_{3/2} \simeq 6\times 10^{-12}\frac{T_{RH}}{10^{10}\,\mathrm{GeV}}\ . \tag{6.64}$$

Clearly, thermal production of gravitinos is more efficient for high reheating temperatures.

Now, if gravitinos are stable, they might either overclose the Universe, which leads to the constraint $T_{RH} \lesssim 2\times 10^{10}\,$GeV, or if they provide the dominant contribution to dark matter, their relic density might be greater than the inferred density $\Omega_{dm}h^2 = 0.1143 \pm 0.0034$ [40]. Assuming that gravitinos provide the sole contribution to dark matter, one has

$$\Omega_{dm}h^2 = \Omega_{3/2}h^2 \simeq 2.78 \times 10^{10}\, Y_{3/2}\, \frac{m_{3/2}}{100\,\mathrm{GeV}}. \tag{6.65}$$

This relation strongly constraints the reheating temperature, as can be seen in fig.(6.7), where we plot the relic density of gravitinos (assumed to correspond to the total dark matter abundance). In this plot, we further assume that gravitinos are only produced via thermal scatterings [124], which may not always be the case. Indeed, assuming that gravitinos are the lightest supersymmetric particles (LSP), decays of the next-to-LSP may give rise to a non-thermal production of gravitinos. However, we see that a stable gravitino implies $T_{RH} \lesssim 10^{10}\,\mathrm{GeV}$, which is slightly above the leptogenesis bound.

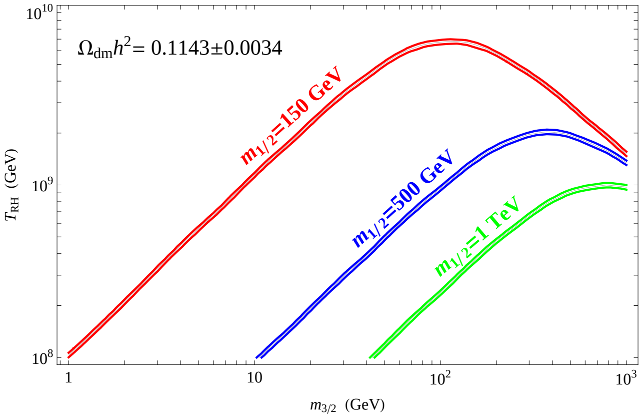

Figure (6.7): Constraint on the reheating temperature from gravitino abundance, assuming $\Omega_{dm} = \Omega_{3/2}$. The plot has been obtained assuming universal boundary conditions for the gaugino masses, with $m_{1/2} = 1$ TeV (green), $m_{1/2} = 500\,\mathrm{GeV}$ (blue) and $m_{1/2} = 150\,\mathrm{GeV}$ (red). For each case, upper and lower curves represent $\Omega_{3/2} = 0.11435 + 0.0034$ and $\Omega_{3/2} = 0.11435 - 0.0034$ respectively, while the central value is indicated by a grey line. Plot adapted from refs.[124].

As already stated, it is also possible to have unstable gravitinos. Nonetheless they can be long-lived particles and decay late. If these decays happen during or after BBN, $T \lesssim T_{BBN}$, the entropy released might jeopardise the successful predictions of BBN [122]. As the decay rate of gravitinos is roughly

$$\Gamma_{3/2} \simeq \frac{m_{3/2}^3}{M_{Pl}^2}\ , \tag{6.66}$$

gravitinos decay after BBN if $\Gamma_{3/2} \lesssim H(T_{BBN})$. Assuming this is the case, the gravitino abundance is required to be small enough to not affect BBN, implying an upper-bound on the reheating temperature. For $m_{3/2} \lesssim 1$ TeV, one requires $T_{RH} \lesssim 10^{5-6}\,\mathrm{GeV}$.This value is clearly incompatible with thermal leptogenesis. If one has $1\,\mathrm{TeV} \lesssim m_{3/2} \lesssim 50\,\mathrm{TeV}$, then the constraint roughly reads $T_{RH} \lesssim 10^9\,\mathrm{GeV}$.

Assuming even heavier gravitinos, one evades the BBN constraint, but then gravitino decays will result in a non-thermal production of the LSP, which is assumed to be stable and the dominant (if not the only) contribution to the observed dark matter abundance. Considering only this non-thermal production for the LSP, its number density is related to the gravitino one by

$$\Omega_{LSP} h^2 \simeq 2.78 \times 10^{10} \times Y_{3/2} \left(\frac{m_{\chi_1^0}}{100\,\mathrm{GeV}} \right) , \tag{6.67}$$

where χ_1^0 is the lightest neutralino (in this case the LSP). Under the constraint that $\Omega_{LSP} \lesssim \Omega_{dm}$, reheating temperatures below 3×10^{10} GeV are required.

To summarise this discussion, we can say that even if the gravitino abundance puts stringent constraints on the reheating temperature, leading in some models to a clear incompatibility with the scenario of thermal leptogenesis, there are however possibilities in which the upper-bound on the reheating temperature is sufficiently high to allow for a successful leptogenesis.
Therefore, even if aware of this caveat, in the following we study the thermal scenario of leptogenesis, assuming that $T_{RH} = 10^{11}$ GeV. This high reheating temperature will already allow us to distinguish the solutions which provide enough baryon asymmetry from those which do not. Then, in a later stage, we will investigate more realistic values for T_{RH}.

6.3.5 Boltzmann equations

As before, the evolution of the comoving number densities is obtained by solving the set of Boltzmann equations. For the RH (s)neutrino one has:

$$\begin{aligned} Y'_{N_i}(z) &= -2\,K_i\ (D_i(z) + S_i(z))\ \left(Y_{N_i}(z) - Y^{eq}_{N_i}(z)\right) , \\ Y'_{\tilde{N}_i}(z) &= -2\,K_i\ (D_i(z) + S_i(z))\ \left(Y_{\tilde{N}_i}(z) - Y^{eq}_{\tilde{N}_i}(z)\right) , \end{aligned} \tag{6.68}$$

where $z = M_1/T$. In this equation, Y_{N_i} is compared to the number density in thermal equilibrium[4] $Y^{eq}_{N_i}$, which is given by the following equation:

$$Y^{eq}_{N_i}(z) \simeq \frac{135\zeta(3)}{8\pi^4 g_*} R_i^2 z^2 K_2(R_i z) \overset{T \gg M_i}{\longrightarrow} \frac{135\zeta(3)}{4\pi^4 g_*} \simeq 1.8 \times 10^{-3} , \tag{6.69}$$

where we have introduced $R_i = M_i/M_1$.
In the MSSM, the number of degrees of freedom in the thermal bath is $g_* = 228.75$ (without RH

---

[4] Assuming a Maxwell-Boltzmann (MB) distribution for the equilibrium abundance gives $Y^{eq}_{N_i} = Y^{eq}_{\tilde{N}_i}$. Taking Fermi-Dirac (FD) or Bose-Einstein (BE) distributions, the abundances differ at high temperatures by a spin factor [66]

$$n_{FD}(T \gg M) = \frac{3}{4} n_{BE}(T \gg M) = \frac{3\zeta(3)}{4} n_{MB}(T \gg M) ,$$

and are equal at low temperatures. So even if we assume a MB statistic for the distribution functions, we nevertheless correct the abundances by the high temperature expansion, and therefore we take $Y^{eq}_{N_i} = \frac{3}{4} Y^{eq}_{\tilde{N}_i}$, with $Y^{eq}_{N_i}$ given by eq. (6.69).

neutrinos or triplets). The individual $B-L$ asymmetries $Y_{\Delta\alpha}$ are driven by:

$$\begin{aligned} Y'_{\Delta\alpha}(z) &= -2\sum_{i=1,2} \varepsilon_{i\alpha}\, K_i\, \left(D_i(z)+S_i(z)\right).\left(Y_{N_i}(z)-Y^{eq}_{N_i}(z)+\left(Y_{\tilde{N}_i}(z)-Y^{eq}_{\tilde{N}_i}(z)\right)\right) \\ &+ 2\sum_{i=1,2}\kappa_{i\alpha}\sum_{\beta} W_i(z)\, A_{\alpha\beta}\, Y_{\Delta\beta}(z)\ . \end{aligned} \tag{6.70}$$

The washout parameters $\kappa_{i\alpha}$ are as usual given by:

$$\kappa_{i\alpha} \equiv \frac{\Gamma(N_i \to \ell_\alpha H_d)}{H(M_i)} = \frac{\tilde{m}_{i\alpha}}{m_*}\ , \tag{6.71}$$

but with a slight modification of $\tilde{m}$ and m_*:

$$\begin{aligned} \tilde{m}_{i\alpha} &= \frac{\lambda_{i\alpha}\lambda^\dagger_{\alpha i} v_u^2}{M_i}\,, \\ m_* &= \frac{16\pi^{5/2}\sqrt{g^*}}{3\sqrt{5}}\,\frac{v_u^2}{M_{Pl}} \simeq 1.56\times 10^{-3}\mathrm{eV}\ . \end{aligned} \tag{6.72}$$

The total washout parameter K_i is obtained by summing over flavour indices:

$$K_i = \sum_\alpha K_{i\alpha} = \frac{\tilde{m}_i}{m_*} \simeq \frac{\tilde{m}_i}{1.56\times 10^{-3}\mathrm{eV}}\ . \tag{6.73}$$

The thermally averaged decay rate D_i are given by:

$$D_i(z) = z\, R_i^2\, \frac{\mathcal{K}_1(R_i z)}{\mathcal{K}_2(R_i z)}\ . \tag{6.74}$$

The $\Delta L = 1$ scatterings are Higgs-mediated processes involving top quarks and antiquarks, and receive contributions from the $s-$ and $t-$channels:

$$S_i(z) = 2\gamma^i_s(z) + 4\gamma^i_t(z)\,. \tag{6.75}$$

The washout term $W_i(z) = W_i^{id}(z) + W_i^s(z)$ results from the contribution from inverse decays

$$W_i^{id}(z) = \frac{1}{4}\, R_i^4\, z^3\, \mathcal{K}_1(R_i z)\ , \tag{6.76}$$

and $\Delta L = 1$ scatterings

$$W_i^s(z) = \frac{W_i^{id}(z)}{D_i(z)}\left(2\gamma^i_s(z)\left(\frac{Y_{N_i}(z)}{Y^{eq}_{N_i}(z)} + \frac{Y_{\tilde{N}_i}(z)}{Y^{eq}_{\tilde{N}_i}(z)}\right) + 8\gamma^i_t(z)\right)\ . \tag{6.77}$$

A careful study of the reheating problem should be done by considering the influence of the inflaton field on the expansion rate of the Universe, similarly to eqs.(6.63), as done in [58, 87, 125]. We do not carry such an analysis, but take the reheating into account in an effective way. We consider that the inflaton field decays instantaneously when the temperature drops below T_{RH}, and thus we consider that the temperature at which leptogenesis starts T_{in} coincides with T_{RH}. For masses $M_i \lesssim T_{RH}$, this is a rather good approximation. On the other hand, for heavier masses, thermalisation processes of N_i are Boltzmann suppressed and for $M_i \gtrsim (2-3) \times T_{RH}$ the number density of the created RHns is negligible.

Had we properly included the contribution of the inflaton field, such a suppression of the thermalisation processes would not have occurred; however, as for $T \gtrsim T_{RH}$ the Universe is dominated by the inflaton energy density, the large Hubble expansion rate $\propto \sqrt{\rho_\phi + \rho_R + \rho_N} \sim \sqrt{\rho_\phi}$ would have diluted processes involving RHns. The difference between the naïve reheating we consider, and the proper treatment similar to eq.(6.63) has been done, for example, in [124] for the gravitino abundance, where it has been found that the naïve prescription, albeit twice larger, is of the correct order of magnitude.

As already stated, in a first stage we will use $T_{in} = 10^{11}\,\text{GeV}$ to discriminate among solutions, and then we will lower this value to more acceptable values.

6.4 Results for the four typical solutions

Now that the framework of our model has been set up, we can examine the viability of thermal leptogenesis for the four characteristic solutions we will focus on:

- Solution $(+,+,+)$ for which the pure type II seesaw dominates at large v_R, and where RHn masses continuously grow.
- Solution $(+,-,+)$, an interesting type I+II mixed solution where, contrary to M_2 (which increases with v_R), M_1 reaches a plateau close to the type I bound.
- Solution $(+,+,-)$, which is also a mixed solution, with M_1 reaching a constant value, but with $M_1 \simeq 10^5\,\text{GeV}$, far below the type I bound.
- Solution $(-,-,-)$, which tends to the type I in the high v_R limit. As in the previous case, $M_1 \ll 10^9\,\text{GeV}$.

From the above spectra, we can infer that for $(+,+,+)$, the lightest RH neutrino will contribute dominantly to the lepton asymmetry production, while for $(+,-,+)$, N_2 might play a role since M_1 could be excessively light. On the other hand, for the remaining solutions $(\pm,\pm,-)$, it is obvious that N_2 is the (ultra) dominant contribution.

We first assume that $m_d = m_e$, with a high reheating temperature $T_{RH} = 10^{11}\,\text{GeV}$, and then relax these assumptions in order to study their influence. In the next section, we will study the dependence on low-energy parameters that are the light neutrino mass, the CP violating phase δ_{PMNS} and the mixing angle θ_{13}, but for the moment, we fix $m_1 = 10^{-3}\,\text{eV}$, $\theta_{13} = 0$, put δ_{PMNS} to zero as well as all the other phases, except for $\phi_2^u = \pi/4$.

6.4.1 Influence of flavours

We first investigate the influence of flavours on our four characteristic solutions by considering fig.(6.8), where we plot the baryon asymmetry as a function of the $B-L$ breaking scale, including

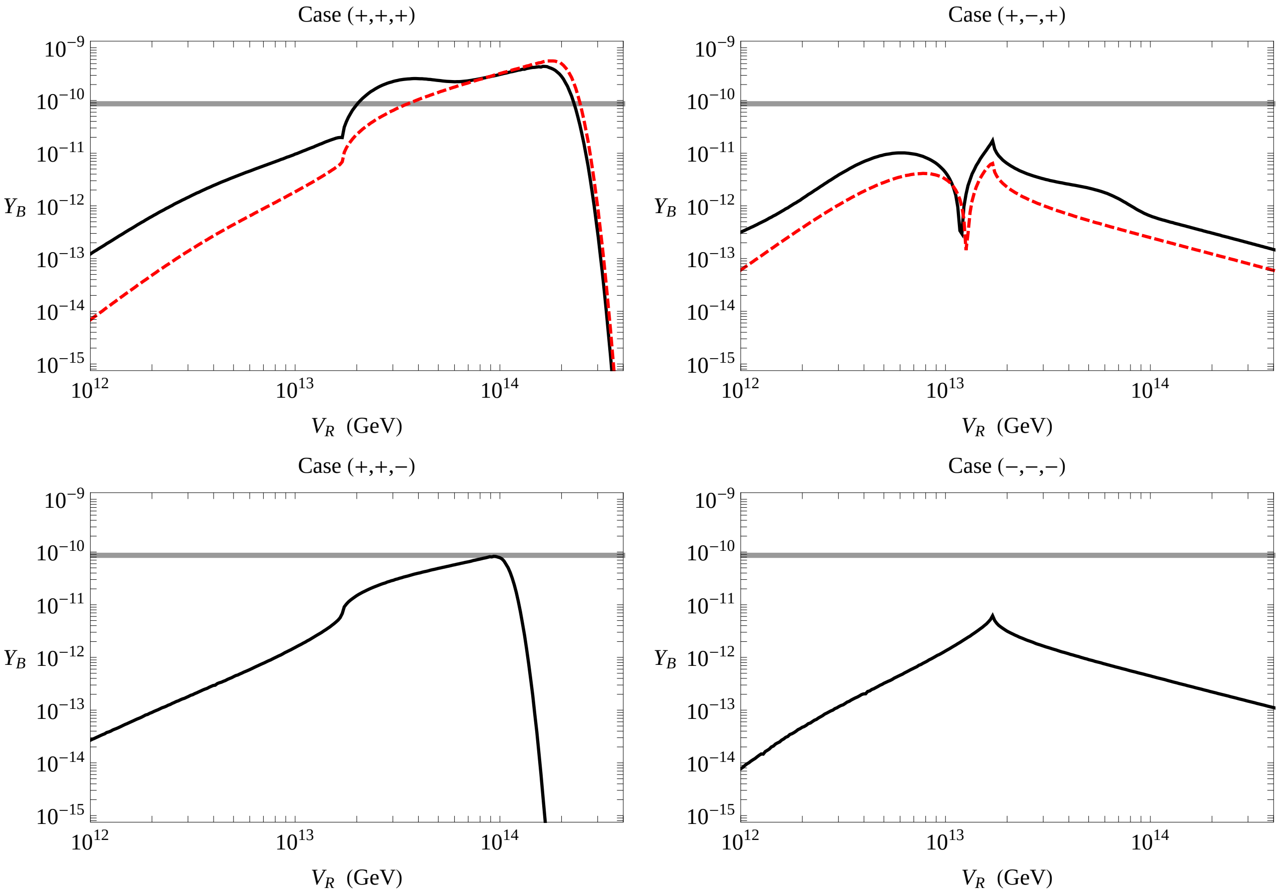

Figure (6.8): Evolution of the baryon asymmetry as a function of the $B - L$ breaking scale v_R, for the four characteristic solutions. In these plots we compared the flavoured case, depicted in solid-black lines, and the unflavoured case, in dashed-red lines.

lepton flavours (solid black line) or not (red dashed line).

The different behaviours are more easily understood by looking at fig.(6.9), where we plot the CP asymmetries and washout factors involving the dominant RHn for the various solutions (see the caption for the colour code).

We first notice that for the present choice of parameters, in the flavoured case (black lines) $(+,+,+)$ can easilly saturate the observed baryon asymmetry, while $(+,+,-)$ is only marginally compatible. This is easily understood in fig.(6.9). These two solutions have in common that the dominant RHn strongly couples to the τ flavour (in green). Hence an important CP asymmetry is created in this direction, even if somehow compensated by the strong washout. For $(+,+,+)$, we see that around $v_R \sim (2-3) \times 10^{13}\,\text{GeV}$, $\varepsilon_{1,\tau} \gtrsim 10^{-6}$ while at the same time the washout decreases, dropping from $\sim 10^2$ down to ~ 5. Hence the baryon asymmetry is enhanced, as can be seen from the bump in Y_B around $v_R \sim (2-3) \times 10^{13}\,\text{GeV}$.

Why is then $(+,+,-)$ comparatively so small?

It is because the τ flavour, even if copiously produced, is also strongly washed-out: for $v_R \gtrsim (2-3) \times 10^{13}\,\text{GeV}$, $\kappa_{2,\tau} \simeq 20$. Hence, a washout four times larger than for the $(+,+,+)$ case

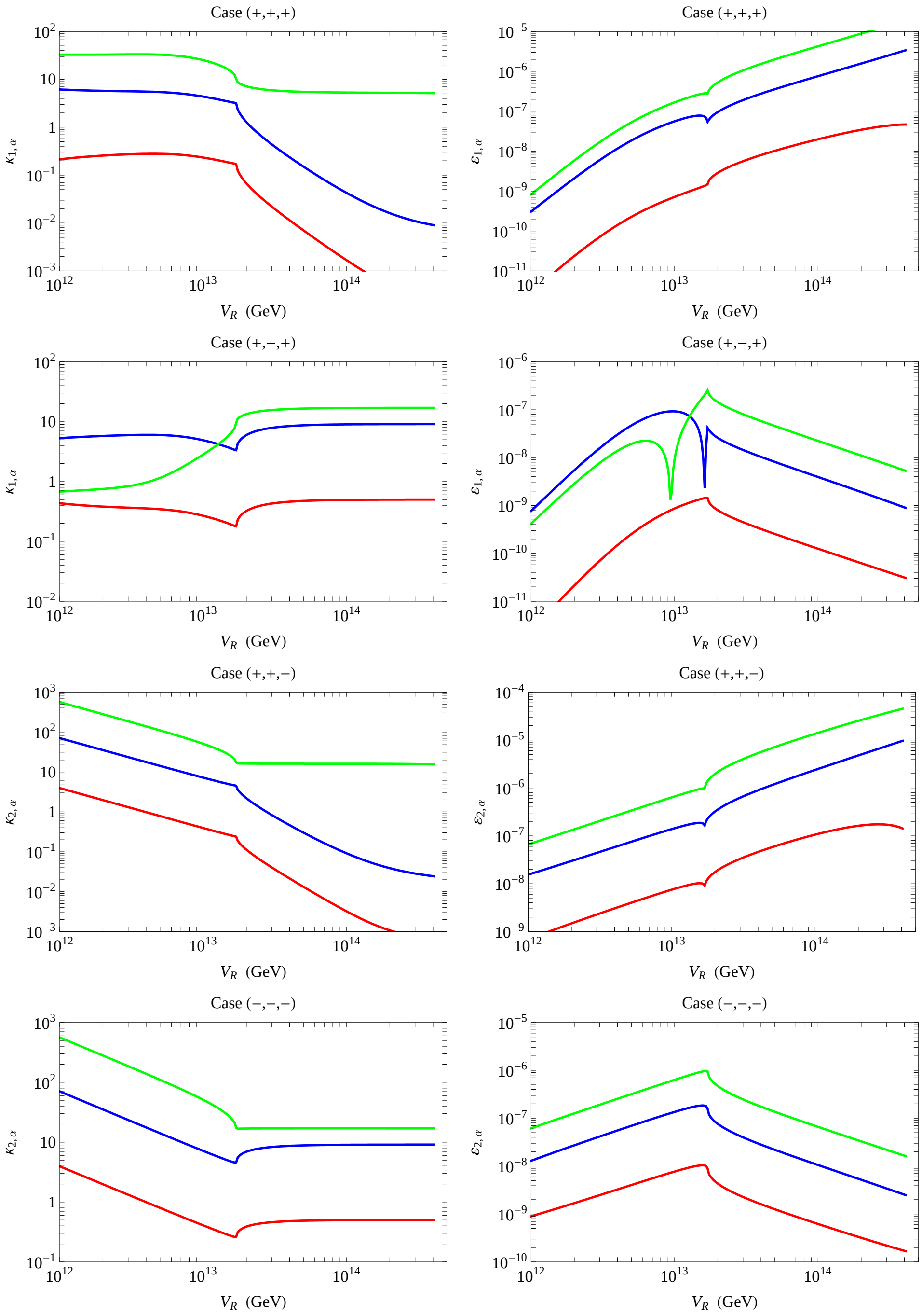

Figure (6.9): Evolution of individual CP asymmetries $\varepsilon_{i,\alpha}$ and washout factors $\kappa_{i\alpha}$ as a function of v_R for the four characteristic solutions. Working in a three flavour scheme, we depicted in green the tau flavour, in blue the muon flavour and in red the electron one. We only plot the $\varepsilon_{i,\alpha}$s and $\kappa_{i,\alpha}$s corresponding to the RHn N_i that provides the dominant contribution to leptogenesis.

requires a CP asymmetry four times greater, and such a value for the CP asymmetry can only be reached for higher v_R.

Finally, as v_R increases, M_1 or M_2 approach $T_{in} = 10^{11}\,\text{GeV}$, and so N_1 or N_2 are no longer efficiently produced by inverse decays, thus the dramatic fall of Y_B.

We observe a huge difference when we consider the unflavoured case (dashed red line): while for $(+,+,+)$ the unflavoured case is close to the flavoured one, particularly in the high v_R-ε_{CP} regime, the $(+,+,-)$ is highly suppressed[5]. In the next section, we will concentrate on this feature, which corresponds to the case discussed in [86, 126].

Let us examine the remaining $(\pm,-,\pm)$ solutions. For the parameters chosen, the observed value Y_B^{obs} is not reached. Still, the qualitative description carried for the previous case holds, up to the different behaviours of the CP asymmetries. Notice also the strong suppression of the unflavoured Y_B in the $(-,-,-)$ case, which also nicely illustrates the survival of the asymmetry produced by N_2 due to flavour effects [86] that we now discuss in greater detail.

Survival of N_2 leptogenesis due to lepton flavour effects

As we just saw, for solutions $(+,+,-)$ and $(-,-,-)$ a huge difference exists between the flavoured and the unflavoured picture.

Assuming that all high energy phases and angles are set to zero, except for $\Phi_2^u = \pi/4$[6], we have for example the following CP asymmetries and washout parameters at $v_R \simeq 10^{14}\,\text{GeV}$:

$(-,-,-)$	N_1, e	N_1, μ	N_1, τ	N_2, e	N_2, μ	N_2, τ
$\varepsilon_{i\alpha}$	1.1×10^{-16}	9.6×10^{-15}	5.8×10^{-14}	-1.2×10^{-7}	-6.4×10^{-8}	-3.4×10^{-7}
$\kappa_{i\alpha}$	0.04	17.2	16.2	2.3	0.7	2.7

$(+,+,-)$	N_1, e	N_1, μ	N_1, τ	N_2, e	N_2, μ	N_2, τ
$\varepsilon_{i\alpha}$	1.2×10^{-16}	9.7×10^{-15}	5.7×10^{-14}	7.0×10^{-7}	2.0×10^{-7}	2.6×10^{-6}
$\kappa_{i\alpha}$	0.04	17.2	16.2	0.5	0.2	3.5

We see that in both solutions the washout parameters and the CP asymmetries exhibit similar patterns. In both cases, the CP asymmetry from N_1 decays is very small, and one can neglect the lepton asymmetry produced by N_1. Moreover, in both cases N_1 interactions present important differences regarding the washout of lepton flavours: while the electron flavour is very weakly washed out ($\kappa_{1e} \simeq 4 \times 10^{-2}$), the $\mu - \tau$ flavours are strongly washed out ($\kappa_{1\mu,\tau} \simeq 15$).

On the other hand, e, μ and τ couplings to N_2 are of the same order.

Hence, once N_2 has completely decayed, the three asymmetries (L_e, L_μ, L_τ) are comparable, until $z \sim 1$, when L_μ and L_τ are strongly suppressed by N_1 washouts. However, since the electron flavour is not affected by these washouts, the baryon asymmetry generated by N_2 processes is not erased by N_1 leptogenesis, opposed to what occurs in the single flavour approximation. The effects of (L_e, N_1) orthogonality can be seen without ambiguity in figs.(6.10). Notice also the dramatic effect of flavour conversion on the muon and tau flavours, albeit this effect is only sub-leading for the baryon asymmetry.

---

[5] Actually, in this case, as in the $(-,-,-)$ one, the unflavoured picture gives $Y_B \simeq 10^{-18}$; but due to the numerical precision required to generate these plots, some instabilities arise, so we preferred to impose a cut around $Y_B \sim 10^{-15}$. See the next section for a plot with an increased precision to avoid the instabilities in $(\pm,\pm,-)$ solutions.

[6] The case considered here corresponds to a non-trivial U_m. For convenience, we rather choose the set 1 of U_m, defined in section 6.2.1. This choice only affects the quantitative result, and not the discussion. For example, while we obtain $Y_B \simeq 1.25 \times 10^{-10}$, had we taken $U_m = 1$ we would have obtained $Y_B \simeq 7.8 \times 10^{-11}$, slightly below the observed value.

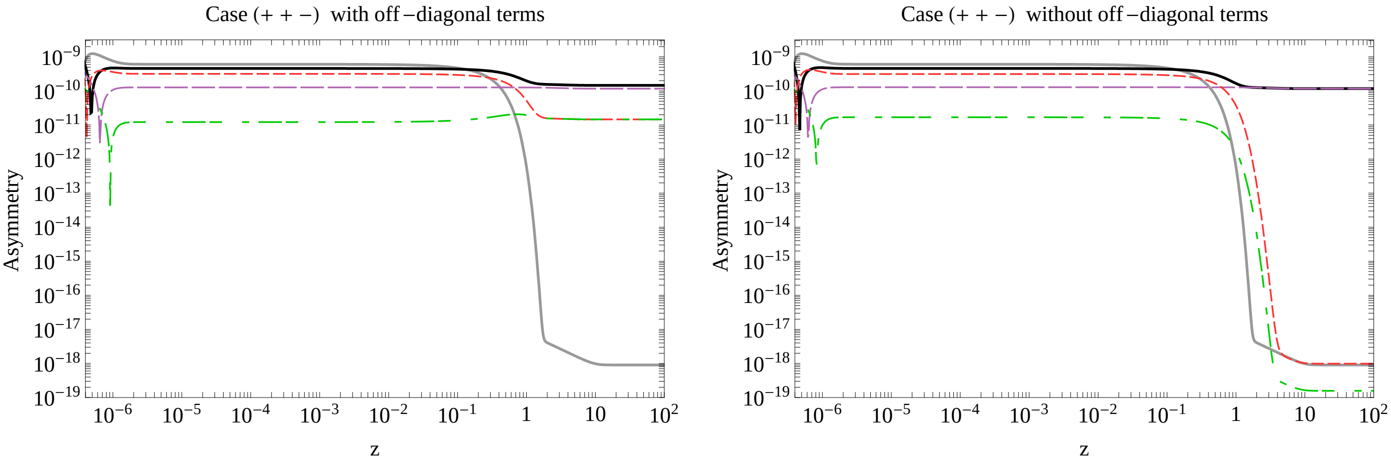
Case (+ + −) with off−diagonal terms

Case (+ + −) without off−diagonal terms

Figure (6.10): Evolution of the asymmetries in the (+ + -) case, as a function of $z = M_1/T$. The thick black and grey lines represent the baryon asymmetry computed with and without flavour effect, respectively, highlighting the very effect of lepton flavours in leptogenesis. The thin lines represent the contribution to the baryon asymmetry of the different flavours: electron (purple), muon (red) and tau (green). On the left panel we include off-diagonal terms when solving the BE, whereas in comparison those terms are not included in the right panel. This clearly illustrates the muon and tau survival due to their non-diagonal couplings to the electron flavour.

Following [86], we evaluate those effects in the illustrative $(+ + -)$ solution. Given that right-handed neutrino masses are very hierarchical, we can address N_2 and N_1 leptogenesis independently. Neglecting off-diagonal terms of the matrix A, after N_2 leptogenesis the asymmetries are given by:

$$\begin{aligned} Y_{\Delta e_{|N_2}} &\simeq -4 \times 10^{-10} \ , \quad & Y_{\Delta \mu_{|N_2}} &\simeq -4 \times 10^{-11} \ , \\ Y_{\Delta \tau_{|N_2}} &\simeq -1 \times 10^{-9} \ , \quad & Y_{L_{|N_2}} &\simeq 6 \times 10^{-10} \ . \end{aligned}$$

As the Universe cools down, the comoving number densities remain constant until $z \sim 1$, where N_1 washout processes come into equilibrium, damping the asymmetries according to:

$$Y'_{\Delta\alpha}(z) = 2\kappa_{1\alpha} A_{\alpha\alpha} W_1(z) Y_{\Delta\alpha}(z) + 2\kappa_{1\alpha} \sum_{\beta\neq\alpha} A_{\alpha\beta} W_1(z) Y_{\Delta\beta}(z) \ , \qquad (6.78)$$

and yielding the formal solution

$$\begin{aligned} Y_{\Delta\alpha_{|N_1}}(z) &\simeq Y_{\Delta\alpha_{|N_2}} \times e^{2\, A^{\alpha\alpha} \kappa_{1\alpha} \int_{zin}^{z} dx \ W_1(x)} \\ &+ \ 2\, \kappa_{1\alpha} \sum_{\beta} A_{\alpha\beta} \int_{z_{in}}^{z} dx\, W_1(x) Y_{\Delta\beta}(x)\, e^{2\, A^{\alpha\alpha} \kappa_{1\alpha} \int_{x}^{z} dy \ W_1(y)} \ . \qquad (6.79) \end{aligned}$$

The first term corresponds to the depletion of the $Y_{\Delta\alpha}$ from N_1 washouts, whereas the second term represents the effect of non-diagonal couplings between flavours. The contribution of the former to the final asymmetry turns out to be:

$$Y^{d}_{\Delta\alpha} \simeq Y_{\Delta\alpha_{|N_2}} \times e^{\frac{3\pi}{4}\, A^{\alpha\alpha}\kappa_{1\alpha}} \ , \tag{6.80}$$

and the second term, evaluated in [90], gives a contribution which is:

$$Y^{od}_{\Delta\alpha} \simeq \sum_{\beta\neq\alpha} Y^{d}_{\Delta\beta} \times A_{\alpha\beta} \frac{\kappa_{1\alpha}}{1+0.8(-A_{\alpha\alpha}\kappa_{1\alpha})^{1.17}} \ . \tag{6.81}$$

The above formulae show that only the electron flavour survives N_1 washouts, while muon and tau flavours are suppressed by a factor $\simeq 10^{-6}$, illustrated on the right panel of fig.(6.10). The baryon asymmetry, produced from the electron flavour, is:

$$Y_B \simeq \frac{10}{31}\sum_{\alpha} Y_{\Delta\alpha} \simeq \frac{10}{31}\, 1.19\, Y_{\Delta e_{|N_2}} \simeq -1.25\times 10^{-10} \ , \tag{6.82}$$

which is slightly above the observed value (notice the excellent agreement with the numerical result $Y_B \simeq -1.45\times 10^{-10}$).

In the one flavour approximation, N_1 washouts exponentially suppress the total lepton asymmetry, as seen in fig.(6.10):

$$Y_L \simeq Y_{L_{|N_2}} \times e^{-\frac{3\pi}{4}\kappa_1}. \tag{6.83}$$

We further notice the effect of the off-diagonal couplings which prevent the total depletion of the μ, τ asymmetries:

$$Y^{od}_{\Delta\mu(\tau)} \simeq 0.12\, Y_{\Delta e} \simeq 0.12 Y_{\Delta e_{|N_2}}\, e^{\frac{3\pi}{4}A_{ee}\kappa_{1e}} \simeq -4.4\times 10^{-11} \ . \tag{6.84}$$

This effect is spectacular for the individual lepton asymmetries, but only marginal for the baryon asymmetry.

This example clearly illustrates how the orthogonality of the leptonic directions and the decay of N_1 and N_2 in flavour space allow N_2 leptogenesis to survive the washout of N_1.

In the following, we do not pursue the discussion of the unflavoured picture.

6.4.2 Influence of mass corrections

Let us now examine the influence of the correction to the relation $m_e = m_d$. This correction entails a redefinition of the down-quark Yukawa coupling $\lambda_d \to U_m^*\, \lambda_d\, U_m^\dagger$ through the matrix U_m which diagonalises the charged lepton masses. Going to the basis where down-quark masses are diagonal, the neutrino Yukawa couplings are affected by U_m, as is the right-handed neutrino spectrum, as well as the CP asymmetries and washout factors. Using the four sets of U_m defined in section 6.2.1, we plot in fig.(6.11) the baryon asymmetry as a function of v_R. We do not

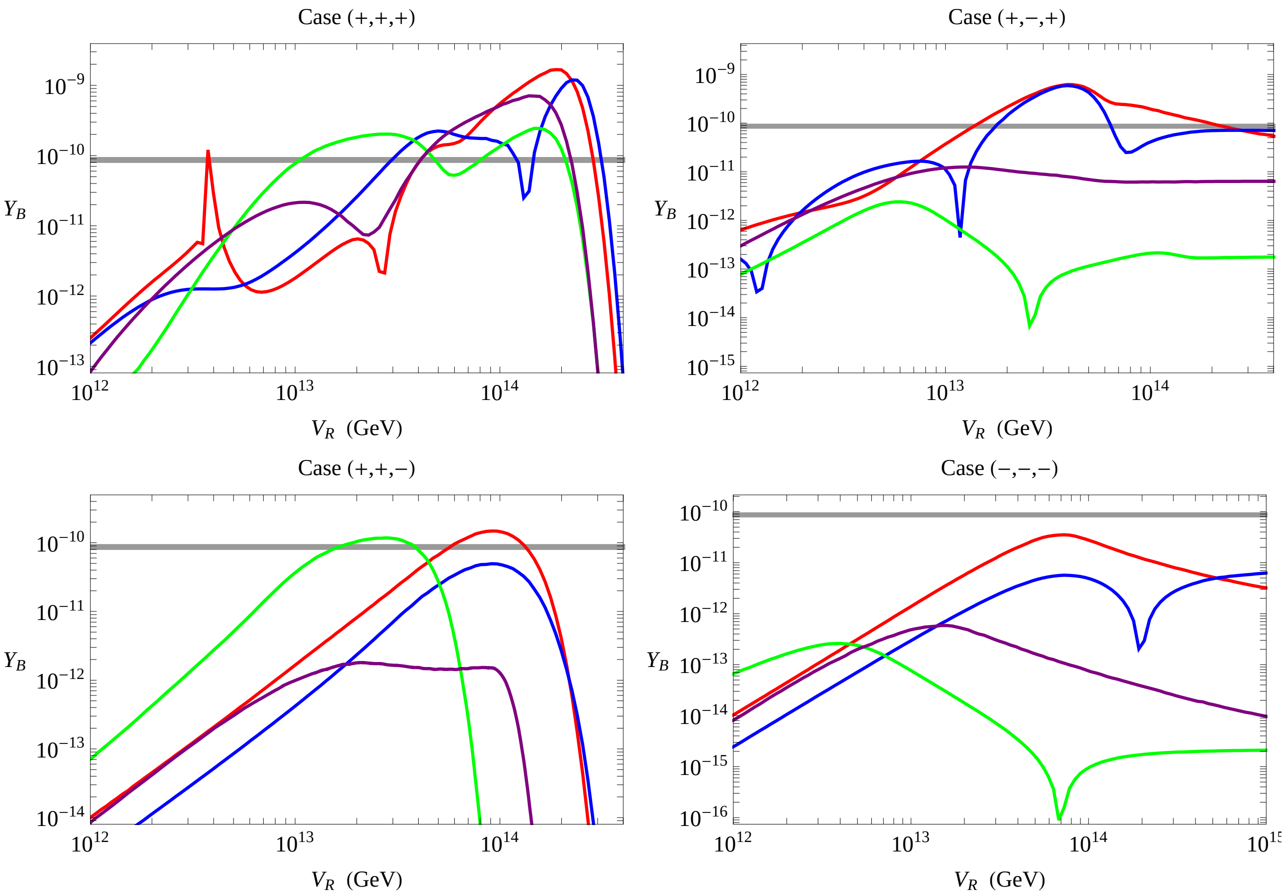

Figure (6.11): Evolution of the baryon asymmetry as a function of the $B-L$ breaking scale v_R, for the four characteristic solutions, and for the four sets of matrix U_m defined in section 6.2.1. The different colours represent the different sets, with sets 1,2,3 and 4 depicted in red, blue, green and purple respectively.

analyse the different U_m separately, but just remark their main features.

The first thing to notice is that for solutions $(+,+,\pm)$, the qualitative picture remains unchanged: Y_B increases with v_R, until the right-handed neutrino becomes too heavy and thus its production is suppressed, accounting for the fall of Y_B at high v_R. If we look more carefully, we see that these two solutions are enhanced, especially for the set 1 (in red), for which both two solutions reach the observed value.

Interestingly, for the $(+,+,+)$ case, N_1 and N_2 become partially degenerate around $v_R \simeq 4 \times 10^{12}$ GeV, leading to a resonance of the baryon asymmetry, as can be seen from the peak in Y_B for this solution. This resonance is shown in fig.(6.12), where we plot the baryon asymmetry as a function of v_R and the corresponding right-handed neutrino masses.

Nevertheless, this degeneracy is accidental and is not a generic feature of this model. Moreover, relying on resonances to obtain a sufficiently large baryon asymmetry, while $M_i \simeq 10^9$ GeV may appear as extremely fine-tuned, and so we no longer consider this possibility.

A more robust and welcome consequence of having included the mass correction stems from the success of the $(+,-,+)$ solution, for which the observed baryon asymmetry is reached for

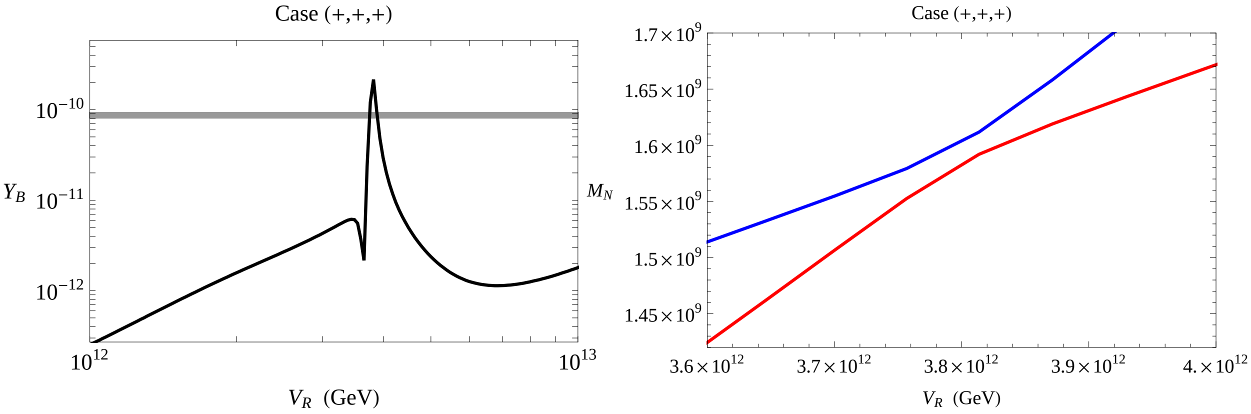

Figure (6.12): Zoom on the quasi-degenerate region of the $(+,+,+)$ solution depicted in red in fig.(6.11). On the right-hand side, the plot shows the evolution of M_1 and M_2, which become quasi-degenerate around $v_R \simeq 3.8 \times 10^{12}$ GeV. This quasi-degeneracy implies a resonance of the baryon asymmetry, as shown on the left-hand side.

10^{13} GeV $\lesssim v_R \lesssim 10^{14}$ GeV.

Consider for example the solution corresponding to the first set of U_m (in red) of fig.(6.11), which has the same high-energy phases $\phi_u^2 = \pi/4$ of that in fig.(6.8). For $v_R \simeq 10^{13-14}$ GeV, we see that the baryon asymmetry is enhanced by two orders of magnitude when the mass correction is included.

This comes from the very different behaviours of the CP asymmetries and washout factors, as can be seen by comparing figs.(6.9) and (6.13). In the former case the maximum CP asymmetry is reached for $v_R \simeq 2\times10^{13}$ GeV, and is $\varepsilon_{1\tau} \simeq 10^{-7}$ with a washout $\kappa_{1\tau} \simeq 20$. In the latter, when the mass correction is included, the CP asymmetry is comparatively enhanced by one order of magnitude, while the washout factor is reduced by one order of magnitude.

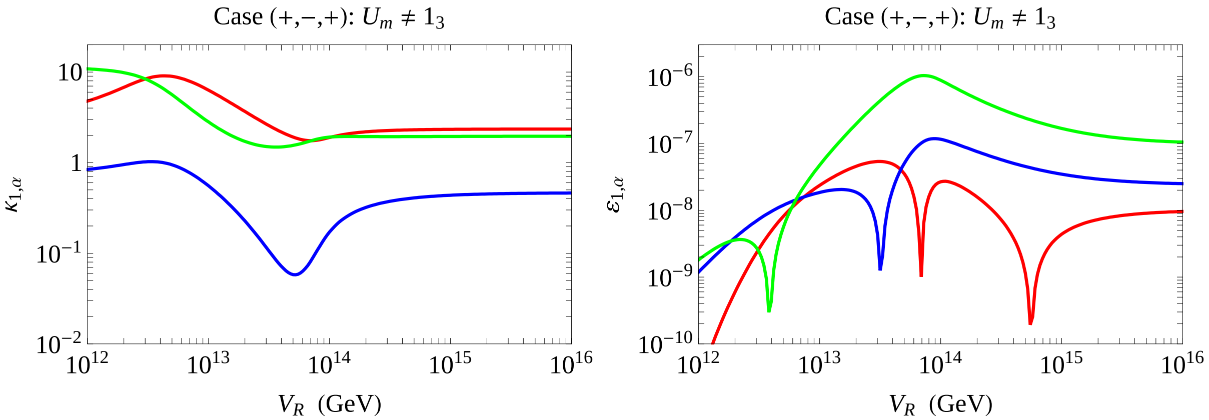

Figure (6.13): CP asymmetries and washout factors for the $(+,-,+)$ solution depicted in red fig.(6.11). Colour code as in fig.(6.9).

The enhancement of the baryon asymmetry coming from the inclusion of the mass correction can be analytically explained from the influence of θ_{12}^m of the matrix U_m. Indeed, we roughly have that

$$\begin{aligned} M_1 &\propto v_R \left(f_1 \, |\cos(\theta_{13}^m)\cos(\theta_{12}^m)|^2 + f_2 \, |\cos(\theta_{13}^m)\sin(\theta_{12}^m)|^2 + ... \right) , \\ M_2 &\propto v_R \left(f_1 \, |\cos(\theta_{23}^m)\sin(\theta_{12}^m)|^2 + f_2 \, |\cos(\theta_{23}^m)\cos(\theta_{12}^m)|^2 + ... \right) , \end{aligned} \tag{6.85}$$

where the dot stands for terms of the same order for M_1 and M_2. Hence, all other parameters being fixed, varying θ_{12}^m modifies the relative $(f_1 - f_2)$ weights, and so potentially increases M_1, which was previously slightly below the type I bound (cf. fig.(6.2)).

In the following, we will only consider the favourable case which is depicted in red in fig.(6.11).

6.4.3 Dependence on the reheating temperature

Let us now discuss the important question in thermal leptogenesis of the lower bound on M_i, or equivalently, the lowest possible reheating temperature. In the type I seesaw, a bound is derived on M_1, namely $M_1 \gtrsim 2 \times 10^9\,\text{GeV}$, which follows from the constraint of having a large enough CP asymmetry. This bound implies a lower bound on T_{RH}, which must be $\gtrsim 2 \times 10^9\,\text{GeV}$. In the type II seesaw, assuming strong hierarchy among right-handed neutrinos, the individual CP asymmetries are bounded by [113]:

$$\varepsilon_{1,\alpha} \lesssim \frac{3}{8\pi} \frac{M_1 \, m_\nu^{\max}}{v_u^2} \, . \tag{6.86}$$

According to the mass pattern for the RHn we have encountered, this relation is not likely to apply, since either the neutrino that dominantly contributes to the asymmetry production is N_2, with $M_1 \ll M_2 \ll M_3$, or else the main contribution comes from N_1, but with a mild hierarchy between N_1 and N_2.

Nevertheless, we partially answer this question with fig.(6.14), where, for the four solutions represented in the $T_{RH} - v_R$ parameter-space, we display the limits above which the computed baryon asymmetry at least equals the observed one (except for the $(-,-,-)$ case, cf. figure caption). In order to derive this plot, we fix all other parameters, with $m_1 = 10^{-3}\,\text{eV}$, and choose the first set for U_m, with $\Phi_2^u = \pi/4$, the other phases as well as θ_{13} being set to zero.

The first thing to notice is the failure of $(-,-,-)$ to produce enough baryon asymmetry.

Solution $(+,+,-)$ works for $T_{RH} \gtrsim 5 \times 10^{10}\,\text{GeV}$; for lower temperatures, N_2 becomes heavier than T_{RH} and its production is Boltzmann suppressed.

Particularly interesting are the solutions $(+,\pm,+)$, for which the reheating temperature can be brought down to more reasonable values: the lower bound derived in these cases is $T_{RH} \gtrsim 5 \times 10^9\,\text{GeV}$.

However, we again want to stress that we do not scan over the entire parameter space, but restrict ourselves to the case where only one high energy CP violating phase is non-zero. As a consequence, the lower bound on T_{RH} should be seen only as a rough approximation of the true lower bound.

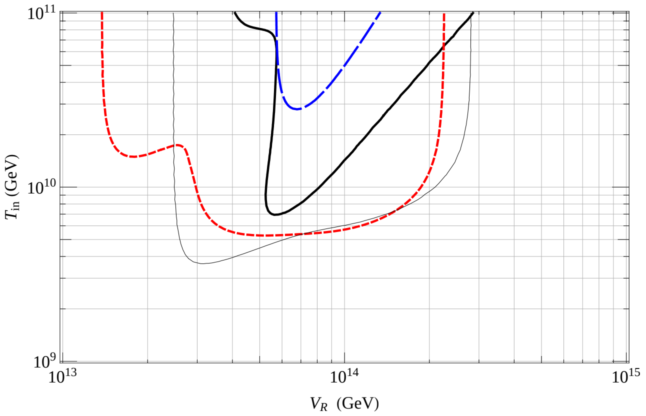

Figure (6.14): Contour lines of the ratio of the computed baryon asymmetry over the observed one as function of v_R and T_{in}, for the different characteristic solutions: solution $(+++)$ is depicted in thick black line, solution $(++-)$ is in thick long-dashed blue, whereas solution $(+-+)$ is in thick dashed red. For these three solutions, the contours represent a unit ratio, and inside the contour we have $Y_B^{num}/Y_B^{obs} \gtrsim 1$. We have depicted in a thin black line the solution $(---)$ for which the observed bound is not reached, and so for this solution we plotted the ratio $Y_B^{num}/Y_B^{obs} = 0.1$.

6.5 Dependence on the low energy parameters

As stated many times before, the conclusion of this study crucially depends on the different input parameters. The high energy parameter-space, which is 10 dimensional, exceeds our computation ability, and furthermore is not implied in low-energy experiments. On the other side, m_ν, θ_{13} and δ) are very important low-energy parameters which are involved, for example, in a possible violation of CP in neutrino oscillations. In this section we numerically investigate their influence.

6.5.1 Dependence on the light-neutrino mass

We first examine the influence of the light neutrino mass scale, assuming a normal mass ordering. As can be seen from fig.(6.1), where we plot the f_is for $m_1 = 0.1\,\text{eV}$ and $10^{-5}\,\text{eV}$, increasing m_1 raises the right-handed neutrino masses corresponding to a " $+$ " solution, while conversely decreasing its value lowers masses which correspond to a " $-$ " solution. This behaviour can be seen in the contour plot of fig.(6.15), where we show for our characteristic solutions the region in the $(m_{\nu_1} = m_1, v_R)$ plane where enough baryon asymmetry is created. We choose $T_{RH} = 10^{11}\,\text{GeV}$, and the second set for $U_m - \Phi_2^u$.
We notice the strong influence of m_1 on the different solutions.
Furthermore, even if solution $(-,-,-)$ fails to produce enough baryon asymmetry, its behaviour is similar to the one of $(+,+,-)$, as expected. These two solutions rely on the decays of N_2, but also strongly on the washouts from inverse decays producing N_1, as we saw in the previous section. The fact is that when m_1 increases, $\kappa_{1,\alpha}$s also increase, hence the asymmetry produced by N_2 leptogenesis will be erased by subsequent N_1 processes. For these solutions, we have an

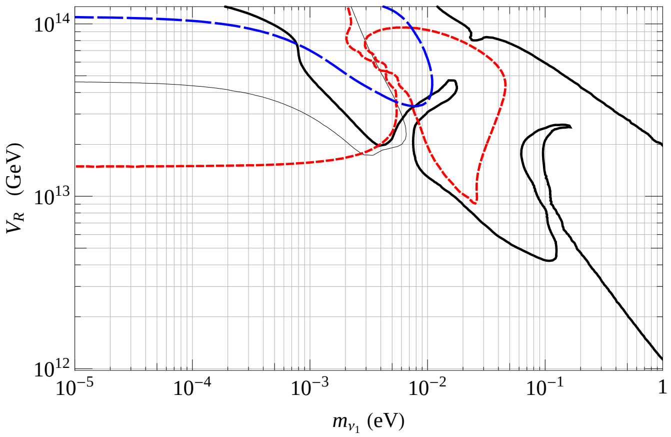

Figure (6.15): Contour lines of the ratio of the computed baryon asymmetry over the observed one, as functions of v_R and light neutrino mass scale m_1. The ratio $Y_B^{num}/Y_B^{obs} = 1$ is fulfilled for the three solutions: $(+++)$ depicted in thick black line, $(++-)$ in thick long-dashed blue, and $(+-+)$ in thick dashed red. Inside the contours we have $Y_B^{num}/Y_B^{obs} \gtrsim 1$. In the case of solution $(---)$, for which the observed bound cannot be reached, we have depicted in thin black line the ratio $Y_B^{num}/Y_B^{obs} = 0.1$.

upper-bound on m_1, namely $m_1 \lesssim 2 \times 10^{-2}$ eV.

In the $(+,-,+)$ case, when m_1 increases, M_1, which corresponds to the "$-$" solution decreases, dropping below 10^9 GeV. This could be somewhat compensated with the increase of M_2, but since $M_2 \gtrsim 10^{11}$, its contribution is suppressed. For this solution, a similar bound on m_1 is derived, namely $m_1 \lesssim 5 \times 10^{-2}$ eV, with $v_R \gtrsim 10^{13}$ GeV.

In the $(+,+,+)$ case, increasing m_1 increases M_1, and consequently the efficiency of leptogenesis, until $M_1 \gtrsim (2-3) \times T_{RH}$ and Y_B drops. To avoid this decrease in Y_B, lower values of M_1 are required, and so lower values of v_R.

6.5.2 Dependence on low-energy mixing angles and phases.

Let us now discuss the influence of the low-energy CP violating phase δ and mixing angle θ_{13}. These two quantities are crucial for low energy neutrino physics, since $\theta_{13} = 0°$ and $\delta = 0, \pi$ would imply that CP is conserved in neutrino oscillations [127].

In order to derive constraints, we choose $T_{RH} = 7 \times 10^9$ GeV for $(+,\pm,+)$, and $T_{RH} = 5 \times 10^{10}$ GeV for the remaining solutions, according to fig.(6.14). We further take $m_1 = 10^{-3}$ eV, since this value suits all solutions.

We first consider in fig.(6.16) the influence of θ_{13} on Y_B, when v_R varies, with a fixed CP phase $\delta = 0$.

We see that the influence of θ_{13} on Y_B strongly depends on the type of solutions.

For all the solutions, we notice that for $\delta = 0$, $\theta_{13} = 0$ gives the best results. For the $(\pm,\pm,-)$ solutions, we observe a huge dependence on θ_{13}: Y_B^{max} decreases by two orders of magnitude when θ_{13} goes from 0° to its upper-bound, 13°. We can consequently say that $\delta = 0$ favours

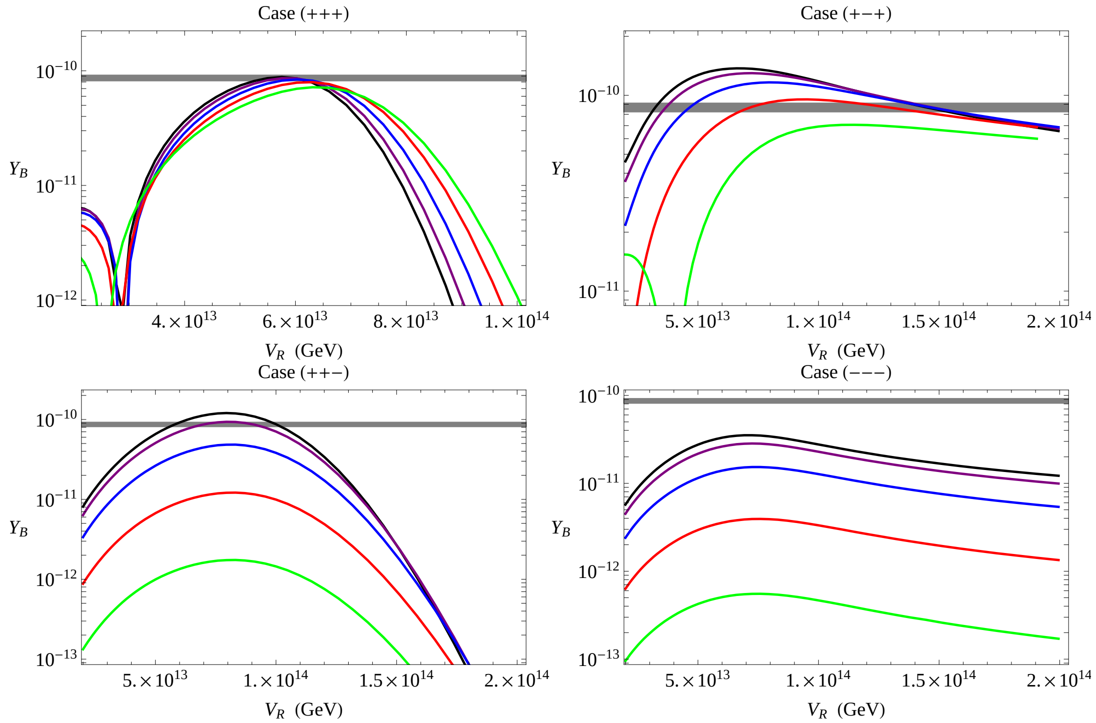

Figure (6.16): Baryon asymmetry as a function of v_R, for the four typical solutions. In these plots are displayed Y_B for different values of θ_{13}, taking $\delta = 0$. We represent in black, purple, blue, red and green the values $\theta_{13} = 0°, 2°, 5°, 9°, 13°$, respectively. For the top panel, we choose $T_{RH} = 7 \times 10^9$ GeV, while for the bottom panel $T_{RH} = 5 \times 10^{10}$ GeV.

$\theta_{13} = 0°$. What about non-vanishing values of δ?

To study the influence of δ, we fix $v_R = 6 \times 10^{13}$ GeV for $(+, \pm, +)$ and $v_R = 5 \times 10^{13}$ GeV for $(\pm, \pm, -)$, keeping the values of T_{RH} quoted above; we then plot in fig.(6.17) Y_B in the $\theta_{13} - \delta$ plane.

We see that changing these parameters does not improve the situation for $(-, -, -)$, which still fails to produce enough baryon asymmetry. However, we notice that its behaviour is very similar to the $(+, +, -)$ case, for which the observed bound can be reached: in both cases, the baryon asymmetry is larger for small values of θ_{13}, with a factor ~ 100 between $\theta_{13} = 0°$ and $\theta_{13} = 13°$. Moreover, we clearly see a preference of these solutions for $\delta \simeq \pi$, for which higher values of θ_{13} are possible. Actually $\delta = \pi$ is the most favourable case for $(+, +, -)$, while $(-, -, -)$ seems to favour $\delta \simeq \pi - \pi/8$.

This preference for $\delta \simeq \pi$ is also observed for the $(+, \pm, +)$ solutions, but in these cases non-zero values of θ_{13} maximise Y_B.

We can conclude that, for the choice of parameters made, our model points towards non-zero values of δ, in fact values close to π. Hence it implies small CP violation in oscillation experiments [127].

However, we stress once again that this conclusion is not general, being based on a partial scan

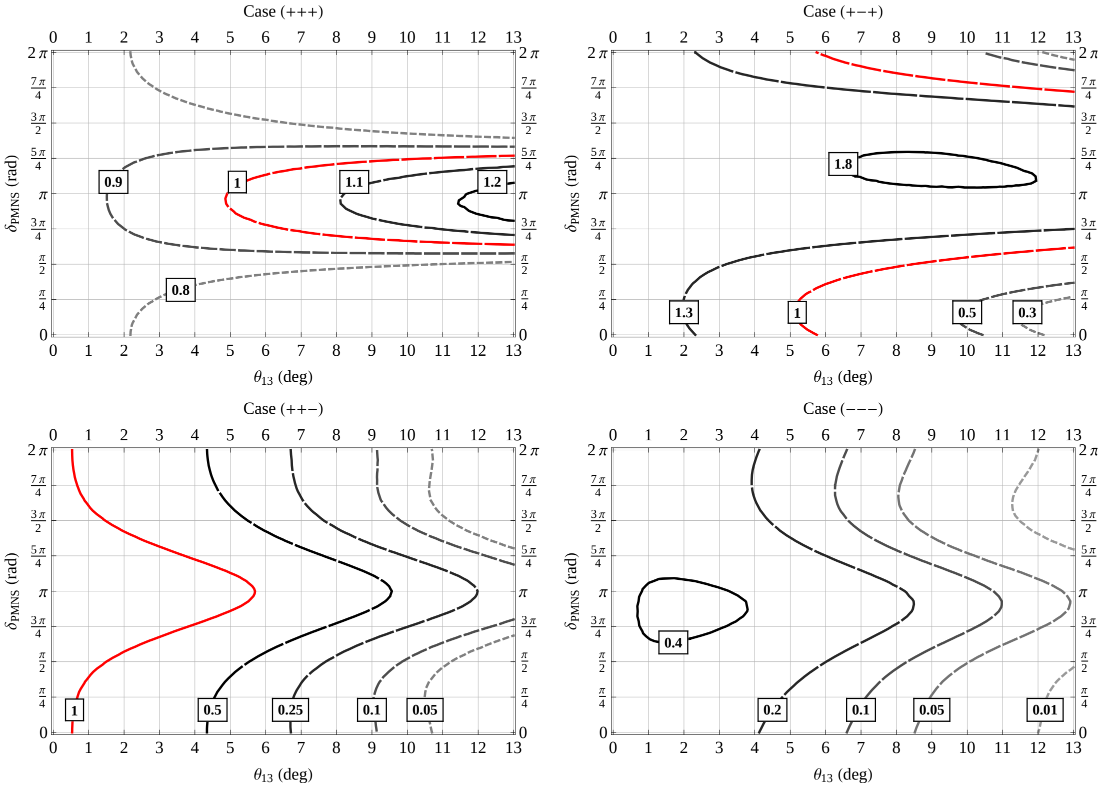

Figure (6.17): Contour lines of the ratio of the computed baryon asymmetry over observed one, as a function of the low-energy parameters δ and θ_{13}. We depicted in red lines the unit ratio, if reached.

of the 17-dimensionnal parameter space.

6.6 Summary

In this chapter we have studied leptogenesis in the type II seesaw. This model has the interesting feature of containing two sources of lepton number violation, originating from the couplings with the scalar $SU(2)_L$ triplet and with the right-handed neutrinos.

Moreover, our model is embedded in a SUSY-GUT framework: it has the advantage of constraining the neutrino Yukawa couplings, the ignorance of which is one of the weakness of the model we studied in the previous chapter. Furthermore, the fact that we assume a Left-Right symmetry enables us to invert the seesaw relation, and so to characterise right-handed neutrinos in terms of light neutrino and up-type quark properties. For the RHn spectrum, 8 solutions are found, which can be grouped in four pairs according to their different properties. We focus on one solution per pair, which exhibits either the dominance of one (pure) type of seesaw, for $(+,+,+)$ and $(-,-,-)$, or else an interesting mixing between type I and pure type II, for $(+,-,+)$ and $(+,+,-)$. We thus discriminate among this eightfold degeneracy with the requirement that leptogenesis is viable.

The leptogenesis criterion has already been used by the authors of [99], but as they already stressed, the study was far from being definitive, mainly for two reasons. Firstly, the treatment of leptogenesis was not correct, since it was based on the single flavour picture. Secondly, the fact that only a pair of **10** Higgs representations had been included to give mass to light particles, imposed the relation $m_e = m_d$ at the GUT scale, which clearly does not hold. Therefore in this chapter, which is based on [98], we improved the study regarding these two points.

Thus, we have included the effects of lepton flavours, inclusion which is not only required [75], but instrumental [71]. This is especially true in the case we considered here, where usually the total washout K_1 is strong but the individual ones are not. We further included heavy neutrino flavours, at least partially, since the heaviest RHn is usually much heavier than the other two RHns. This inclusion follows the fact that in the $(\pm, \pm, -)$ cases, while N_1 is too light to be of use for leptogenesis, N_2 is of the good order of magnitude.

We found that indeed, adding both light and heavy flavours, improves the situation. The most spectacular example is the $(+, +, -)$ solution, where the asymmetry is produced due to N_2 decays, and the inclusion of lepton flavours prevents this asymmetry from being completely washed-out by N_1 processes, as it would be the case in the unflavoured picture.

Moreover, by adding in an effective manner a non-renormalisable term involving a **45** Higgs representation, which is thought to be present in typical $SO(10)$-based GUT, the correction of the GUT relation $m_e = m_d$ constitutes a clear improvement of the model towards realistic fermion masses. This correction implies a redefinition of the lepton right handed neutrino Yukawa couplings λ, which turns out to modify the right-handed spectra, individual washouts and CP asymmetries, the relevant quantities for leptogenesis. Owing to some freedom in this redefinition, we found that correcting fermion masses greatly improves the results. A typical example is the success of the $(+, -, +)$ case.

Requiring that leptogenesis successfully predicts the observed amount of baryon asymmetry, we thus found that 3 of our 4 characteristic solutions do work. However, these results might be pointless, since these might be a conflict with the reheating temperature. Examining this problem, we found that the solutions $(+, +, +)$ and $(+, +, -)$ work in a large part of the parameter space with $T_{RH} \lesssim 10^{10}\,\text{GeV}$, whereas $(+, +, -)$ would require $T_{RH} \gtrsim 5 \times 10^{10}\,\text{GeV}$. Under the constraint that $T_{RH} \lesssim 2 \times 10^{10}\,\text{GeV}$ we thus found that two of our four characteristic solutions satisfy the leptogenesis criterion. Hence, we can say that four of the eight solutions are compatible with leptogenesis. Nevertheless, our model suffers from its lack of predictivity, since the 10 dimensional high-energy parameter-space remains unconstrained. Therefore, it would be interesting to link the constraints coming from leptogenesis to other constraints coming, for example, from lepton-flavour violation. It could be also interesting to build a complete $SO(10)$ GUT model which provides the LR symmetric seesaw, together with the required proton stability, doublet-triplet splitting and realistic fermion masses and mixings.

Conclusions

We have seen that under the assumption that neutrinos get their masses through the seesaw mechanism, leptogenesis qualitatively occurs; in chapter 3, we discussed the requirements under which the single flavour picture can quantitatively work. These conditions are:

- The matrix R must be complex, and furthermore CP violation has to be large enough in order to have $\varepsilon_{CP} \gtrsim 5 \times 10^{-7}$.
- The right-handed neutrino masses are bounded: $2 \times 10^9\,\mathrm{GeV} \lesssim M_1 \lesssim 10^{12}\,\mathrm{GeV}$. The lower bound comes from the requirement that ε_{CP} is large enough, while the upper-bound represents the temperature below which electroweak sphalerons come in-equilibrium.
- Assuming hierarchical heavy neutrinos, the light neutrino masses are upper-consrained: $m_i \lesssim 0.15\,\mathrm{eV}$.

This is for the single flavour picture.
However, we showed [75] that lepton flavours have to be included in leptogenesis, since for $M_1 \lesssim 10^{12}\,\mathrm{GeV}$, the interactions involving the charged lepton Yukawa couplings are in-equilibrium. Since the different lepton flavours have different Yukawa couplings, the lepton doublet interacting with the RHns has to be decomposed into the different flavours. Consequently, one has to consider lepton flavour asymmetries.
In chapter 4, we show how to include the evolution of flavoured asymmetries in the Boltzmann equations, and what are the constraints under which the flavours are relevant. We showed in this chapter that, for instance, when the tau Yukawas are in-equilibrium, then the quantum correlations between the tau flavour and the other flavours are exponentially damped, which is not the case for the correlations between the muon and the electron flavours. Regardless of whether leptogenesis is efficient or not, we identified different temperature regimes:

- If $10^9\,\mathrm{GeV} \lesssim M_1 \lesssim 10^{12}$, only the interactions involving the tau Yukawa couplings are in-equilibrium, and therefore 2 flavours are distinguishable: the tau flavour and the coherent sum of $e + \mu$ flavours.
- If $M_1 \lesssim 10^9$, then the muon-Yukawa interactions are also in-equilibrium, and the lepton asymmetry is projected onto a three-flavour space, (τ, μ, e).

The electron-Yukawa interactions are in-equilibrium for $M_1 \lesssim 10^6\,\text{GeV}$, that is for masses far below what is required by leptogenesis.

We subsequently applied these flavoured recipes to the type I seesaw in the SM model, and to the type II seesaw in a GUT model, respectively in chapter 5 and 6.

The chapter 5 is based on [75, 71, 90], and provides the main results obtained during my thesis, which can be compared with the constraints of the single-flavour picture above.

- In the flavoured context, the R-matrix can be real, with non-zero lepton flavoured CP asymmetries, since the latter now depend on the CP phases of the lepton mixing matrix U_{PMNS}. However, the lower bound on the CP asymmetries is still $\varepsilon \gtrsim 5 \times 10^{-7}$. A noticeable modification, which may provide one of the most important effects of lepton flavours, is the modification of the upper-bound on the CP asymmetry in the regime of degenerate light neutrinos. Indeed, while in the single flavour picture $\varepsilon_{CP} \propto m^{-1}$ and is thus suppressed, when flavours are included the upper-bound rather reads $\varepsilon_\alpha \simeq m$ and is even enhanced in this limit.

- Regarding the lower bound on right-handed neutrinos, lepton flavours do not significantly modify the picture, with $M_1 \gtrsim 2.5 \times 10^9\,\text{GeV}$.

- On the contrary, since individual CP asymmetries are no-longer suppressed in the regime of degenerate light neutrinos, the allowed parameter-space is enlarged, and light neutrino masses are no longer upper-constrained by leptogenesis when right-handed neutrinos are hierarchical.

The main effect of lepton flavours lies in the degenerate regime, which corresponds to a regime of strong washout. This is simply because the couplings of different flavours with the right-handed neutrino are not equal, and so the flavours interact at different rates.

Another aspect of leptogenesis, which perhaps constitutes one of its weakness, is the lack of predictivity regarding the different CP violating phases and especially for the high-energy sector. In the single flavour picture and in the flavoured one as well, only optimal regions in the parameter-space can be inferred.

In order to remedy to this problem, we studied in chapter 6 supersymmetric leptogenesis in a Left-Right symmetric type II seesaw model. In this model, the GUT embedding yields the interesting result that the Dirac type mass of light neutrinos is no longer free, but related to the masses of the other fermions. This is a clear gain compared to a non-GUT scenario.

In this scenario, the high-energy sector was reconstructed from an inversion of the seesaw formula, but nevertheless suffers from an "eightfold" ambiguity in the solutions. We therefore investigated if leptogenesis enabled us to discriminate among these solutions. Furthermore, given the spectra we encountered, for half of the solutions it was clear that only the second lightest right-handed neutrino was relevant for leptogenesis. We therefore studied leptogenesis, including both light and heavy flavour effects. In this case, we found that 2 of our 8 solutions survived, namely the solution which correspond to a pure type II seesaw in the high $B - L$ breaking scale limit.

We further refined our model, correcting the GUT relation among charged lepton and down type quark masses, through the inclusion of non-renormalisable operators. We found that this step towards more realistic fermion masses strongly affects leptogenesis, increasing to 6 the number of allowed solutions. We further found a nice illustration of the importance of both light and heavy flavours for the case where the lepton asymmetry is generated by the decays of N_2, and the inclusion of lepton flavours prevents this asymmetry from being washed-out by N_1 processes. However, since we were working in a supersymmetric extension, we had to have in mind reheating temperature constraints. When investigating whether or not leptogenesis could work with $T_{RH} \lesssim 10^{10}\,\mathrm{GeV}$, we found that 4 solutions were compatible, in a large part of the parameter space. We then consider whether the requirement of successful leptogenesis enabled us to make some predictions for the seesaw parameters. Unfortunatly, the "cure seems worse than the disease", since our GUT model contains more free parameters than the non-GUT one.

This lack of predictivity is a common plague to high-energy seesaw models, and thus to the thermal scenario of leptogenesis. One then one asks: is there a remedy? There are at least several ways out: the first one would be to link the different observables which involve seesaw couplings, another could be to study leptogenesis in a complete and consistent GUT scenario, where the number of free parameters is dramatically reduced or even over-determined. Finally, lowering the seesaw scale could provide additionnal observable effects at the LHC or other future experiments and is therefore an interesting solution. Nevertheless, lowering the seesaw scale enters in conflict with the scenario of thermal leptogenesis that we discussed in this thesis. Hence the need to low-energy leptogenesis models.

Appendix A

A few words on particle physics

A.1 The Standard Model

The Standard Model of particles relies on the local invariance under $SU(3)_c \times SU(2)_L \times U(1)_Y$ symmetry, the matter sector being composed of 3 generations of 15 fundamental fermion fields which are given in the following table:

field	G_{32}	Q_{T^3}	Q_Y	B	L
u_L	$(\mathbf{3},\mathbf{2})$	$1/2$	$1/3$	$1/3$	0
d_L	$(\mathbf{3},\mathbf{2})$	$-1/2$	$1/3$	$1/3$	0
u_R	$(\mathbf{3},\mathbf{1})$	0	$4/3$	$1/3$	0
d_R	$(\mathbf{3},\mathbf{1})$	0	$-2/3$	$1/3$	0
ν_L	$(\mathbf{1},\mathbf{2})$	$1/2$	-1	0	1
e_L	$(\mathbf{1},\mathbf{2})$	$-1/2$	-1	0	1
e_R	$(\mathbf{1},\mathbf{1})$	0	-2	0	1

(A-1)

The SM successfully describes the strong and electroweak interactions thanks to the exchange of vector bosons, which are in the adjoint representation of the different groups: the 8 gluons for $SU(3)$, the 3 W bosons of $SU(2)$ and the vector B_μ of $U(1)_Y$.
Fermion mass terms emerge from the coupling of fermion bilinears with the scalar sector, which consists, in the SM, in a scalar field, doublet under $SU(2)$

$$\phi = \begin{pmatrix} \phi^+ \\ \phi^0 \end{pmatrix} . \tag{A-2}$$

The neutral component of ϕ is singlet under $SU(3)_c \times U(1)_{em}$, and so it can take a vev $\langle \phi^0 \rangle = v/\sqrt{2} \simeq 246\,\mathrm{GeV}$, leaving the low-energy group invariant and in the meanwhile fermions aquire masses, thanks to the Yukawa couplings:

$$\mathcal{L}_m = \lambda_e \frac{v}{\sqrt{2}} \overline{e_L}\, e_R + \lambda_d \frac{v}{\sqrt{2}} \overline{d_L}\, d_R + \lambda_d \frac{v}{\sqrt{2}} \overline{u_L}\, u_R + h.c. \tag{A-3}$$

The SM does not contain a right-handed neutrino, hence $m_\nu = 0$. Furthermore, all interaction terms are renormalisable. This renormabilisity, together with the field content given above, imply that besides the invariance under the local symmetry G_{321}, 4 global $U(1)$s are conserved: the baryon number B, and the lepton flavour number $L_{e,\mu,\tau}$, and consequently the total lepton number L. As a consequence of this, the neutrino remains massless to all orders of perturbation.

A.2 Sphalerons

Baryon and Lepton numbers are accidental symmetries of the Standard Model. This means that they do not reflect a higher symmetry but are satisfied given the particle content and the renormalisable couplings of the model. B and L are conserved at tree level and to all order in perturbation theory.

However, 'T Hooft showed [13] that non-perturbative effects, called instantons, can lead to the violation of $B+L$, while conserving the orthogonal $B-L$. This property is associated with the topological structure of any $SU(N)$ gauge group. The ground state of the theory is not unique, but degenerate vacua exist which are topologically inequivalent. Going from one vacuum to another vacuum can be done by tunnelling through field configurations called instantons, but typically the probability will be highly suppressed. Another possibility arise from the existence of static but unstable field configurations that help the transition to occur: these are the sphalerons. In concrete terms, the baryonic and leptonic number currents,

$$\begin{aligned} J^L_\mu &= \sum_i \bar{\ell_L}_i \gamma_\mu \ell_{L\,i} - \bar{e_L}_i^{\,c} \gamma e^c_{L\,i} \ , \\ J^B_\mu &= \frac{1}{3} \sum_i \bar{Q_L}_i \gamma_\mu Q_{L\,i} - \bar{u_L}_i^{\,c} \gamma u^c_{L\,i} - \bar{d_L}_i^{\,c} \gamma d^c_{L\,i} \ , \end{aligned} \tag{A-4}$$

have a non-zero divergence from the ABJ triangle anomaly[128]:

$$\partial^\mu J^B_\mu = \partial^\mu J^L_\mu = \frac{N_g}{32\pi^2} \left(g^2 W^{\mu\nu} \tilde{W_{\mu\nu}} - g'^2 B^{\mu\nu} \tilde{B_{\mu\nu}} \right) \ , \tag{A-5}$$

where $W_{\mu\nu}$ and $B_{\mu\nu}$ are $SU(2)$ and $U(1)$ field-strengths respectively, and N_g the number of fermions generations. Therefore, we see that $B-L$ is conserved, as $\partial\mu(J^L_\mu - J^B_\mu) = 0$. The orthogonal combinaison, $B+L$ is violated:

$$\partial\mu(J^L_\mu + J^B_\mu) = 2N_g \partial_\mu K^\mu \ . \tag{A-6}$$

The interesting point is that K_μ is related to the topological structure of the vacuum, by:

$$N_{CS}(t_i) - N_{CS}(t_0) = \int_{t_0}^{t_i} dt \int d^3x \partial_\mu K^\mu \equiv n \ , \tag{A-7}$$

where n is an integer, and N_{CS} are Chern-Simons number. Therefore we see that if during a time Δt a transition between two vacua with distinct topological charges occurs, this will induce a baryon+lepton number violation, as

$$\Delta(B+L) = N_g \Delta N_{CS} \ . \tag{A-8}$$

At zero temperature however, the transition rate between two vacua is exponentially suppressed, with

$$\Gamma \simeq e^{-8\pi^2/g^2} \simeq e^{-173}\,, \tag{A-9}$$

and effectively no transition occurs. The picture changes however at high temperature, $T \gtrsim T_{EW}$, as showed by Kuzmin, Rubakov and Schapovnikov[14]: instead of tunnelling through the barrier, the available thermal energy allows to step over it, thanks to the Higgs and gauge boson field configurations that lie on the top of the energy barrier separating two topologically inequivalent vacua. The situation is schematically depicted in fig.A-1.

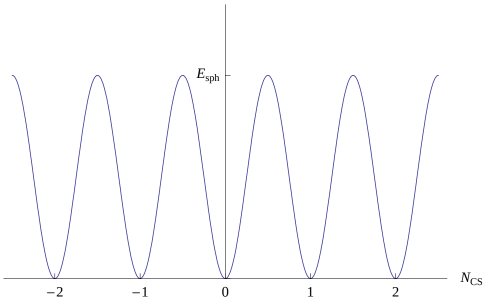

Figure A-1: Energy of gauge field configuration versus Chern-Simons number

The sphaleron transition amplitude is roughly $\mathcal{A} \simeq e^{-E_{sph}/T}$, with E_{sph} the height of the energy barrier

$$E_{sph} \simeq \frac{8\pi\, v}{g}\,. \tag{A-10}$$

Hence, for $T \gg E_{sph}$, the transition amplitude gets unsuppressed and rapidly occurs.
In the Standard Model, we have the strong sphalerons, which are related to the $SU(3)$ gauge structure, and whose density rate is given by[129]:

$$\Gamma_{QCD}/V \simeq 250\,\alpha_s^5\,T^4\,. \tag{A-11}$$

As $V \sim T^3$, the QCD-sphalerons enter in-equilibrium when $\Gamma_{QCD}(T) \lesssim H(T)$, which happens at $T \lesssim 10^{13}$ GeV, and then induce an effective interaction

$$\mathcal{O}_{QCD} = \Pi_{i=1,2,3}(q_{L\,i} q_{L\,i}\, u^c_{R\,i}\, d^c_{R\,i})\ , \tag{A-12}$$

which relate left and right-handed quarks.
The SM also contains electroweak instantons, which are related to the $SU(2)$ gauge structure, with a density rate[130]:

$$\Gamma_{EW}/V \simeq 25\,\alpha_W^5\,T^4\,. \tag{A-13}$$

If in-equilibrium, these sphalerons induce an effective interaction

$$\mathcal{O}_{EW} = \Pi_{i=1,2,3}(q_{L\,i} q_{L\,i} q_{L\,i} \ell_{L\,i})\ , \tag{A-14}$$

which consist in a $B \leftrightarrow L$ exchange. The $SU(2)$ sphalerons are faster than the Hubble expansion rate for $T \lesssim 10^{12}$ GeV. Hence, for $T_{EW} \lesssim T \lesssim 10^{12}$ GeV, any $B+L$ number will be driven to zero by the fast $B+L$ violating sphalerons. On the other hand, $B-L$ asymmetries are not affected by sphalerons transition. The early GUT baryogenesis model were based on $SU(5)$, which conserves $B-L$, hence the possible B number creation was wiped out as soon as electroweak sphalerons enter in-equilibrium and this models cannot work. On the contrary of leptogenesis models, were the asymmetry is produced in the L direction, which is then reprocessed into the $-B$ direction.

Appendix B

Thermodynamics

The evolution of the Universe is described by the Einstein equation which relate the geometry of the Universe to its content:

$$\mathcal{R}_{\mu\nu} - \frac{1}{2}g_{\mu\nu}\mathcal{R} = 8\pi G_N T_{\mu\nu} + \Lambda g_{\mu\nu} \, . \tag{B-1}$$

In this equation $\mathcal{R}$ is the Ricci scalar, $\mathcal{R}_{\mu\nu}$ the Ricci tensor, $T_{\mu\nu}$ the stress-energy tensor, $g_{\mu\nu}$ the space-time metric and Λ is the cosmological constant. G_N is the Newton constant,

$$G_N = \frac{1}{Mpl^2} \, , \tag{B-2}$$

$$Mpl \simeq 1.221 \times 10^{19}\,\mathrm{GeV} \, . \tag{B-3}$$

Assuming that the Universe content is a perfect fluid, we can write the stress-energy tensor as:

$$T_{\mu\nu} = -p g_{\mu\nu} + (p+\rho) u_\mu u_\nu \, , \tag{B-4}$$

where p is the pressure and ρ the energy density of the perfect fluid. The velocity vector of the fluid, u_μ is given in the rest frame of the plasma by $u = (1, 0, 0, 0)$.
Assuming further homogeneity and isotropy of the Universe, it can be described through a Robertson-Walker metric,

$$ds^2 = dt^2 - a(t)^2 d\bar{r}^2 \, , \tag{B-5}$$

so that the (0-0) component of the Einstein equation can be written:

$$\left(\frac{\dot{a}}{a}\right)^2 + \frac{k}{a^2} = \frac{8\pi G_N}{3}\rho + \frac{\Lambda}{3} \, , \tag{B-6}$$

where $k = 0, +1, -1$ is the curvature of the Universe (resp. flat, open and closed geometry), and $a(t)$ is the scale factor of the expanding Universe. The Hubbler expansion rate H is defined as:

$$H \equiv \left(\frac{\dot{a}}{a}\right)^2 \, , \tag{B-7}$$

and tells us how fast the Universe is expanding.
The species which compose the Universe are liable to interaction. In an expanding Universe, if this rate is faster than the Hubble expansion rate, then theses particles will be maintained causally connected with the thermal bath: the species are in-equilibrium and in that case they all have the same temperature. However, Uinverse is cooling. Then it is likely that at some temperature T_f, interactions will not be able to keep species in equilibrium as they freeze-out: $\Gamma(T) \lesssim H(T)$ for $T \lesssim T_f$.
When out-of-equilibrium, the species decouple from the thermal bath and evolves independently of it. The criterion $\Gamma(T_f) \simeq H(T_f)$ gives a rough picture of the decoupling, but a more accurate description require to study microscopic evolution of the particle number densities, by solving the Boltzmann equations. This appendix briefly introduce equilibrium and out-of-equilibrium thermodynamics, which is needed when studying leptogenesis. We refer the reader to refs.[1],[66] for more detailled presentations of section 1 and 3.

B.1 Equilibrium thermodynamics

Species in-equilibrium can be described by ideal Fermi-Dirac (FD) or Bose-Einstein (BE) fluid, whose distribution function is:

$$f_i^{eq}(\mathbf{p}, \mu_i, T) = \frac{g_i}{\exp((E_i - \mu_i)/T) \pm 1} \ , \tag{B-8}$$

where g_i denotes the number of degree of freedom of the species i, $E_i = \sqrt{\mathbf{p}^2 + m_i^2}$ and μ_i is the chemical potential of the species. The $+$ $(-)$ sign refers to FD (BE) statistic. The classical approximation of Maxwell-Boltzmann (MB) statistic, which will extensively use in the network of Boltzmann equations, is:

$$f_i^{eq} = g_i \ \exp((E_i - \mu_i)/T) \ . \tag{B-9}$$

Given these distribution functions, one defines the equilibrium number density n_i and the equilibrium energy density ρ_i are given by:

$$\begin{aligned} n_i^{eq}(T) &= \int \frac{d^3\mathbf{p}}{(2\pi)^3} f_i^{eq}(\mathbf{p}, \mu_i, T) = \frac{g_i}{2\pi^2} \int_{m_i}^{\infty} dE \frac{\sqrt{E^2 - m_i^2} E}{\exp((E_i - \mu_i)/T) \pm 1} & \text{(B-10)} \\ \rho_i^{eq}(T) &= \int \frac{d^3\mathbf{p}}{(2\pi)^3} f_i^{eq}(\mathbf{p}, \mu_i, T) E(\mathbf{p}) = \frac{g_i}{2\pi^2} \int_{m_i}^{\infty} dE \frac{\sqrt{E^2 - m_i^2} E^2}{\exp((E_i - \mu_i)/T) \pm 1} & \text{(B-11)} \end{aligned}$$

Defining $z_i = m_i/T$, the number density for a massive particle is given by:

$$n_i^{eq}(\mu, T)^{MB} = \frac{g_i T^3}{2\pi^2} e^{-\frac{\mu_i}{T}} \, z_i^2 \, K_2(z_i) \, , \tag{B-12}$$

for Maxwell-Boltzmann statistic, and:

$$n_i^{eq}(\mu, T)^{BE}_{FD} = \frac{g_i T^3}{2\pi^2} \sum_{k=0}^{\infty} \frac{(\pm e^{\mu_i/T})^k}{k+1} \, z_i^2 K_2\left((k+1) z_i\right) \ , \tag{B-13}$$

for fermions and bosons. Here $K_n(x)$ is the modified Bessel function of the second kind. The asymptotic expansion of Bessel functions is well known and one can therefore deduce asymptotic behaviour of the number densities.

- For high temperatures $T \gg m_i$, neglecting chemical potential:

$$\begin{aligned} n_i^{eq}(T)^{MB} &\simeq \frac{g_i T^3}{\pi^2}\left(1 - \frac{1}{4}z_i^2 + \dots\right) \ , & \text{(B-14)} \\ n_i^{eq}(T)^{BE} &\simeq \frac{g_i T^3}{\pi^2}\left(\zeta(3) + \frac{1}{4}z_i^2 \log(z_i) + \dots\right) \ , & \text{(B-15)} \\ n_i^{eq}(T)^{FD} &\simeq \frac{g_i T^3}{\pi^2}\left(\frac{3}{4}\zeta(3) + z_i^2 \frac{\log(2)}{2} + \dots\right) \ , & \text{(B-16)} \end{aligned}$$

  where $\zeta(3) \simeq 1.202$.

- The low-temperature expansion reads:

$$n_i^{eq}(T)^{MB} \simeq n_i^{eq}(T)^{BE} \simeq n_i^{eq}(T)^{FD} \simeq g_i \left(\frac{m_i T}{2\pi}\right)^{3/2} e^{-m_i/T} \ . \tag{B-17}$$

The usual assumption is to disregard quantum statistic and handle fermions and bosons in terms of MB particle, with either

$$n_X^{eq} = \frac{g_X T^3}{2\pi^2}\, z_X^2\, K_2(z_X)\,, \tag{B-18}$$

for a massive particle, or

$$n_X^{eq} = \frac{g_X\, T^3}{\pi^2} \tag{B-19}$$

for a massless one. Similarly, one obtains the asymptotic behaviour of the energy density:

- for the high temperature expansion $T \gg m_i$ one has:

$$\begin{aligned} \rho_i^{eq}(T)^{BE} &\simeq \frac{\pi^2}{30} g_i T^4 \ , & \text{(B-20)} \\ \rho_i^{eq}(T)^{FD} &\simeq \frac{7}{8}\frac{\pi^2}{30} g_i T^4 \ . & \text{(B-21)} \end{aligned}$$

- For the low temperature expansion $T \ll m_i$,

$$\rho_i^{eq}(T) = m_i\, n_i^{eq}(T) \propto e^{-m_i/T} \ . \tag{B-22}$$

  .

Therefore, at a given temperature T, the energy density of non-relativistic species will be exponentially suppressed, thus being safely neglected in the total energy density of the Universe

$$\rho_{tot} = \frac{\pi^2}{30} g_* T^4 \ , \tag{B-23}$$

where g_* counts the effective number of degrees of freedom:

$$g_* = \sum_{i=BE} g_i \left(\frac{T_i}{T}\right)^4 + \frac{7}{8} \sum_{i=FD} g_i \left(\frac{T_i}{T}\right)^4 \; . \tag{B-24}$$

Here, T_i is the temperature of the species i: $T_i \propto T$ with equality when the species i are in-equilibrium. For the typical temperatures we consider, $T \gg 100\,\mathrm{GeV}$, $g_* = 106.75$ in the Standard Model, while $g_* = 228.75$ in the MSSM.

Therefore, according to eq.(B-6), assuming flatness and negligible cosmological constant, that is valid in the very early Universe, one deduces

$$H(T) = \sqrt{\frac{8\pi\rho_{tot}}{3M_{pl}^2}} \simeq 1.66 g_*^{1/2} \frac{T^2}{M_{pl}} \; . \tag{B-25}$$

In the radiation dominated epoch $a \sim t^{1/2}$ and therefore one relates time and temperature by:

$$\frac{t(T)}{1\,\mathrm{s}} \simeq 2.42\, g_*^{1/2} \left(\frac{T}{1\,\mathrm{MeV}}\right)^{-2} \; . \tag{B-26}$$

Neglecting the chemical potential we have for the entropy density:

$$s = \frac{\rho + P}{T} = \frac{2\pi^2}{45}\, q_*\, T^3 \; , \tag{B-27}$$

where

$$q_* = \sum_{i=BE} g_i \left(\frac{T_i}{T}\right)^3 + \frac{7}{8} \sum_{i=FD} g_i \left(\frac{T_i}{T}\right)^3 \; . \tag{B-28}$$

If all relativistic species are in-equilibrium, then $T_i = T$ and $q_* = g_*$. Furthermore, since $T \propto a^{-1}$ and $s \propto a^{-3}$, as long as the number of particles remains constant, the comobile number density $Y_i = n_i/s$ is constant. On the other hand, when degrees of freedom freeze and become non-relativistic, the conservation of entropy implies that $q_*^< \, T_<^3 = q_*^> \, T_>^3$ and thus:

$$T_> = T_< \left(\frac{q_*^<}{q_*^>}\right)^{1/3} \; . \tag{B-29}$$

That is, when dof decouple from the thermal bath, their entropy is transfered to species that are in thermal equilibrium, and their temperature therefore increase: entropy creation (re)heats the Universe.

Given the above definitions, we further have that

$$s = \frac{q_*\, \pi^4}{45\, \zeta(3)}\, n_\gamma \simeq 1.8\, q_*\, n_\gamma \, , \tag{B-30}$$

so that the actual entropy and photon number density are related according to

$$s_0 \simeq 1.8\, q_{*0}\, n_{\gamma 0} \, \simeq 7.04\, n_{\gamma 0} \, . \tag{B-31}$$

B.2 Relating B and L numbers

Let us see how to relate the baryon number of the Universe to the lepton number that is produced during leptogenesis [83]. Since that particles and antiparticles have an opposite chemical potential $\mu_x = -\mu_{\overline{x}}$, the net number density of a particle x can be written, for small μ_X/T

$$n_x - n_{\overline{x}} = \frac{g_x T^3}{6} \times \begin{cases} \mu_X/T & \text{for a fermion} \\ 2\,\mu_X/T & \text{for a boson} \end{cases} . \tag{B-32}$$

Therefore, since B is stored both in $SU(2)_L$ doublet and singlet components, the baryon number is

$$B = \frac{g_x T^2}{6} \sum_i \left(\mu_{u^i_L} + \mu_{d^i_L} + \mu_{u^i_R} + \mu_{d^i_R}\right) , \tag{B-33}$$

where the sum is made over the different asymmetries that are populated.
Similarly, the lepton number is

$$L = \sum_i L_i = \frac{g_x T^2}{6} \sum_i \left(\mu_{\nu^i_L} + \mu_{e^i_L} + \mu_{e^i_R}\right) . \tag{B-34}$$

The different species undergo reactions, which if in-equilibrium enforce algebraic relations among the chemical potentials involved, since for a $i + j \leftrightarrow k + l$ interaction, the equilibrium condition implies

$$\mu_i + \mu_j = \mu_k + \mu_l . \tag{B-35}$$

Then, according to the different chemical equilibriums that hold at a given temperature, B and L_i can be related. Actually in the SM, B and L are only related through the effective interaction induced by the electroweak sphalerons. Since this interaction is in-equilibrium for $T \lesssim 10^{12}$ GeV, no baryon asymmetry can be generated via leptogenesis for $T \gtrsim 10^{12}$ GeV. Furthermore, since these interactions conserve $B - L$ but violate $B + L$, which they set to zero, one could naïvely think that

$$B = \frac{B+L}{2} + \frac{B-L}{2} \rightarrow \frac{B-L}{2} , \tag{B-36}$$

when electroweak sphalerons are in-equilibrium. Actually, since the latter only involve left-handed fields, while the lepton and baryon number are stored both in $SU(2)$ doublets and singlets, the situation is more involved, and relating B to the L_i require to determine which interactions are in-equilibrium when the lepton asymmetry is created. Since leptogenesis occurs at $T \sim M_1$, the different temperature regime then correspond to range of M_1.
We can list the different interactions and the temperature at which they become in-equilibrium[83],[76].

- Gauge interactions are always in-equilibrium. Consequently, gluons and B^0 have a null chemical potential, and furthermore the different quark colours have a same μ. Interactions with the $W^{\pm}$ enforce

$$\begin{aligned}\mu_W &= \mu_{\phi^-} + \mu_{\phi^0}\,,\\ \mu_W &= -\mu_{u_L} + \mu_{d_L}\,,\\ \mu_W &= -\mu_{\nu_L} + \mu_{e_L}\,,\end{aligned} \qquad \text{(B-37)}$$

where $\mu_W = \mu_{W^-} = -\mu_{W^+}$, and ϕ denotes the Higgs doublet.

Moreover, since $SU(2)$ is gauged, the sum of third weak-isospin component should be zero:

$$\frac{3}{2}\sum_i \left(\mu_{u^i_L} - \mu_{d^i_L}\right) + \frac{1}{2}\sum_i \left(\mu_{\nu^i_L} - \mu_{e^i_L}\right) - \frac{2\,m}{2}\left(\mu_{\phi^0} + \mu_{\phi^-}\right) - 4\,\mu_W = 0\,, \qquad \text{(B-38)}$$

where m is the number of Higgs doublet. This relation implies that $\mu_W = 0$ and so all $SU(2)$ doublet components have an equal chemical potential $\mu_{u_L} = \mu_{d_L} = \mu_{q_L}$ and $\mu_{\nu_L} = \mu_{e_L} = \mu_{\ell_L}$.

- The requirement that the total hypercharge is null enforces:

$$\sum_i \left(\mu_{q^i_L} + 2\,\mu_{u^i_R} - \mu_{d^i_R}\right) - \sum_i \left(\mu_{e^i_R} + \mu_{\ell^i_L}\right) + 2\,\mu_\phi = 0\,. \qquad \text{(B-39)}$$

- For $T \lesssim 10^{13}\,$GeV, QCD sphalerons are in-equilibrium:

$$\sum_i \left(\mu_{q^i_L} - \mu_{u^i_R} - \mu_{d^i_R}\right) = 0\ . \qquad \text{(B-40)}$$

For $T \lesssim 10^{12}\,$GeV, the electroweak sphalerons are in-equilibrium and so B and L doublets are related according to:

$$\sum_i \left(3\,\mu_{q^i_L} + \mu_{\ell^i_L}\right) = 0\ . \qquad \text{(B-41)}$$

Finally, the interactions involving charged fermion Yukawas, when in-equilibrium, yield the following relations:

$$\begin{aligned}\mu_{u^i_R} &= \mu_{q^i_L} + \mu_{\phi^0}\,,\\ \mu_{d^i_R} &= \mu_{q^i_L} - \mu_{\phi^0}\,,\\ \mu_{e^i_R} &= \mu_{\ell^i_L} - \mu_{\phi^0}\,,\end{aligned} \qquad \text{(B-42)}$$

for up-type quarks, down-type quarks and charged leptons, respectively.

We are interested in relating the $\Delta_\alpha \equiv B/3 - L_\alpha$ asymmetries to the leptonic doublet ones $\ell_{L\,\alpha}$, and this relation depends on the temperature regime.

- If $M_1 \gtrsim 10^{12}\,$GeV, none of the charged lepton Yukawas are in-equilibrium. Therefore, the $SU(2)_L$ singlets do not store any asymmetry, since only the left-handed part interact with the gauge bosons. Consequently the lepton number and the leptonic doublet number are equal. Since no baryon number is generated, as electroweak sphalerons are out-of-equilibrium, we have $Y_{\Delta\alpha} = Y_\Delta = -Y_L$.

- If $10^9 \lesssim M_1 \lesssim 10^{12}\,\mathrm{GeV}$, then the tau-Yukawas are in-equilibrium, as well as electroweak sphalerons. A non-zero asymmetry can thus be stored in τ_R. Since t, b and c quarks are in-equilibrium, the conversion matrix reads:

$$\begin{pmatrix} Y_{\Delta e} \\ Y_{\Delta\mu} \\ Y_{\Delta\tau} \end{pmatrix} = \frac{T^3}{6\,s} \begin{pmatrix} -\frac{4}{9}-2 & -\frac{4}{9} & -\frac{4}{9} \\ -\frac{4}{9} & -\frac{4}{9}-2 & -\frac{4}{9} \\ -\frac{2}{9} & -\frac{2}{9} & -\frac{4}{9}-3+\frac{16}{45} \end{pmatrix} \cdot \begin{pmatrix} \mu_{e_L}/T \\ \mu_{\mu_L}/T \\ \mu_{\tau_L}/T \end{pmatrix} . \tag{B-43}$$

However, the e and μ flavours are indistinguishable, therefore one should rather consider the asymmetry produced in $e+\mu$ direction, that is, one should sum the chemical potentials $\mu_{e_L} + \mu_{\mu_L}$, so that

$$\begin{pmatrix} Y_{\Delta e+\mu} \\ Y_{\Delta\tau} \end{pmatrix} = \frac{T^3}{6\,s} \begin{pmatrix} -\frac{26}{9} & -\frac{8}{9} \\ -\frac{2}{9} & -\frac{139}{45} \end{pmatrix} \cdot \begin{pmatrix} \mu_{e_L}/T + \mu_{\mu_L}/T \\ \mu_{\tau_L}/T \end{pmatrix} . \tag{B-44}$$

Since $Y_{\ell_{L,\alpha}} = \frac{T^3}{6\,s}\left(2\,\mu_{\ell_{L,\alpha}}/T\right)$, we obtain

$$Y_{\ell_\alpha} = \begin{pmatrix} -\frac{417}{589} & \frac{120}{589} \\ \frac{30}{589} & -\frac{390}{589} \end{pmatrix} . Y_{\Delta\alpha} . \tag{B-45}$$

- If $M_1 \lesssim 10^9\,\mathrm{GeV}$, the muon Yukawas are in-equilibrium, as well as the s-ones. Thus, the three lepton flavours are distinguishable, and one has

$$\begin{pmatrix} Y_{\Delta e} \\ Y_{\Delta\mu} \\ Y_{\Delta\tau} \end{pmatrix} = \frac{T^3}{6\,s} \begin{pmatrix} -\frac{4}{9}-2 & -\frac{4}{9} & -\frac{4}{9} \\ -\frac{4}{9}-\frac{1}{6} & -\frac{4}{9}-2-\frac{11}{15} & -\frac{4}{9}-\frac{4}{15} \\ -\frac{4}{9}-\frac{1}{6} & -\frac{4}{9}-\frac{4}{15} & -\frac{4}{9}-2-\frac{11}{15} \end{pmatrix} \cdot \begin{pmatrix} \mu_{e_L}/T \\ \mu_{\mu_L}/T \\ \mu_{\tau_L}/T \end{pmatrix} , \tag{B-46}$$

that is,

$$Y_{\ell_\alpha} = \frac{1}{179} \begin{pmatrix} -151 & 20 & 20 \\ \frac{25}{2} & -\frac{344}{3} & \frac{14}{3} \\ \frac{25}{2} & \frac{14}{3} & -\frac{344}{3} \end{pmatrix} . Y_{\Delta\alpha} . \tag{B-47}$$

Finally, the baryon asymmetry is related to the $B/3 - L_\alpha$ ones by the relation[83]:

$$Y_B = \frac{32+4m}{98+13m} \sum_\alpha Y_{\Delta\alpha} , \tag{B-48}$$

which gives $Y_B = 12/37 \sum_\alpha Y_{\Delta\alpha}$ in the SM with $(m = 1)$ one Higgs doublet.

B.3 Out-of-equilibrium thermodynamics: Boltzmann equations

Let us see how to characterise species which undergo non-elastic collisions. The evolution of the distribution function is given by the Boltzmann equations (BE)

$$L[f] = C[f],$$

where C is the collision term and L is the Liouville operator,

$$L[f] = p^\alpha \frac{\partial}{\partial x^\alpha} - \Gamma^\alpha_{\beta\delta}\, p^\beta p^\delta \frac{\partial}{\partial x^\alpha},$$

which is conveniently express in a homogeneous and isotopric space-time as :

$$L[f] = E\frac{\partial f}{\partial t} - H(t)\, p\, \frac{\partial f}{\partial E}\ . \tag{B-49}$$

Integrating over momentum, one recover the usual BE:

$$\dot{n}_i + 3H(t)n_i = C_i\ . \tag{B-50}$$

All the work will then to evaluate the collision term. For a generic 2-to-2 scattering $i+j \leftrightarrow k+l$, it can be written as:

$$\begin{aligned} C_i &= (2\pi)^4 \int \delta(p_i + p_j - p_k - p_l)\frac{g_i d^3\mathbf{p}_i}{2(2\pi)^3 E_i}\cdots\frac{g_l d^3\mathbf{p}_l}{2(2\pi)^3 E_l} \\ &\times\ |\mathcal{M}|^2 \times ((1\pm f_i)(1\pm f_j)f_k f_l - f_i f_j(1\pm f_k)(1\pm f_l))\ , \end{aligned} \tag{B-51}$$

where + (-) stands for FD (BE) statistics, and $\mathcal{M}$ is the invariant amplitude. We can simplify this expression by using MB statistics and neglecting Pauli blocking and stimulating emission factors (*i.e.*, quantum statistic), so that the collision term reads:

$$\begin{aligned} C_i &= (2\pi)^4 \int \delta(p_i + p_j - p_k - p_l)\frac{g_i d^3\mathbf{p}_i}{2(2\pi)^3 E_i}\cdots\frac{g_l d^3\mathbf{p}_l}{2(2\pi)^3 E_l} \\ &\times\ |\mathcal{M}|^2 \times (f_k f_l - f_i f_j)\ . \end{aligned} \tag{B-52}$$

Since that for what concern us, the elastic scatterings, which conserve particle densities but not their distribution, are much faster than inelastic scatterings, we can approximate $f_X = f_X^{eq}\, n_X/n_X^{eq}$, so that the collision term can be further simplified:

$$C_i = \frac{n_k}{n_k^{eq}}\frac{n_l}{n_l^{eq}}\gamma^{kl}_{ij} - \frac{n_i}{n_i^{eq}}\frac{n_j}{n_j^{eq}}\gamma^{ij}_{kl}\ , \tag{B-53}$$

where we define the reaction density γ^{ij}_{kl}:

$$\gamma^{ij}_{kl} = (2\pi)^4 \int \delta(p_i + p_j - p_k - p_l)\frac{g_i d^3\mathbf{p}_i}{2(2\pi)^3 E_i}\cdots\frac{g_l d^3\mathbf{p}_l}{2(2\pi)^3 E_l} \quad\times\quad |\mathcal{M}|^2 \times f_i^{eq} f_j^{eq}\ . \tag{B-54}$$

Given this, the BE reads:

$$\dot{n}_i + 3\,H(t)\,n_i = \sum_{k,l,j}\left(\frac{n_k}{n_k^{eq}}\frac{n_l}{n_l^{eq}}\gamma^{kl}_{ij} - \frac{n_i}{n_i^{eq}}\frac{n_j}{n_j^{eq}}\gamma^{ij}_{kl}\right)\ . \tag{B-55}$$

B.4 Boltzmann equations in leptogenesis

It is customary in leptogenesis to parametrise number density evolution in function of the variable

$$z \equiv M_i/T \ , \tag{B-56}$$

instead of the time t, where M. The relation between those two is

$$\frac{dz}{dt} = -\frac{M_{N_1}}{T^2}\frac{dT}{dt} = z\,H(z) \ . \tag{B-57}$$

It is also customary to use the comoving number density Y_X that are defined by

$$Y_X \equiv \frac{n_X}{s} \ , \tag{B-58}$$

where s is the entropy density. Such transformation is done because both n_x and s scale as T^3, and therefore Y is constant during the cooling of the Universe, up to non-elastic processes.
With these two redefinitions, the BE eq.(B-50) translates to

$$\frac{dY_i}{dz} = -\frac{1}{szH(z)}C_i(z) \ , \tag{B-59}$$

$$C_i(z) = \sum_{X,j}\left(\frac{Y_k}{Y_k^{eq}}\frac{Y_l}{Y_l^{eq}}\gamma_{ij}^{kl} - \frac{Y_i}{Y_i^{eq}}\frac{Y_j}{Y_j^{eq}}\gamma_{kl}^{ij}\right) \ . \tag{B-60}$$

This is the general form of the Boltzmann equations for comoving number densities. It is written here for a two-to-two scattering, but the collision term should obviously include all relevant processes of the model under consideration. In this manuscript, we only focus on decays $X \to ij$ and on 2-to-2 scatterings. The density rate for a two body decay is given by:

$$\gamma_{ij}^{X}(z_x) = n_x^{eq}(z_x) \times \frac{K_1(z_x)}{K_2(z_x)}\,\Gamma(X \to ij) \ , \tag{B-61}$$

where $K_{1,2}$ are the modified Bessel function of the second kind, and $\Gamma(X \to ij)$ is the decay rate evaluated in the rest-frame of the decaying particle. For a two body scattering, one has:

$$\gamma_{kl}^{XY}(z) = \frac{1}{64\pi^4}\frac{s_{min}^2}{z_m}\int_1^\infty dx\,\sqrt{x}\,K_1(\sqrt{x}\,z_m)\hat{\sigma}(x) \ , \tag{B-62}$$

where $s_{min} = \max\left((m_X+m_Y)^2,(m_k+m_l)^2\right)$, $z_m = \sqrt{s_{min}}/T$ and $\widehat{\sigma}(x)$ is the reduced cross-section, the cross section summed over initial phase space:

$$\widehat{\sigma}(s) = \frac{2\lambda(s,m_X^2,m_Y^2)}{s}\sigma(s) = \frac{2\left(s-(m_X+m_Y)^2\right)\left(s-(m_X-m_Y)^2\right)}{s}\sigma(s) \ . \tag{B-63}$$

Decays/inverse decays and top-scatterings

Let us discuss the different terms that we consider in this thesis.
At first order, we included decays and inverse, that are given by:

$$\begin{aligned}\kappa_1\,D(z) &\equiv \frac{z}{s\,H(M_1)}\frac{\gamma_{\ell\phi}^{N}}{Y_N^{eq}(z)} = \kappa_1\,z\,\frac{K_1(z)}{K_2(z)} \ , \\ \kappa_1\,W_{id}(z) &= \frac{\kappa_1}{2}\frac{Y_N^{eq}(z)}{Y_\ell^{eq}(z)}D(z) = \frac{\kappa_1}{4}\,z^3\,K_1(z) \, .\end{aligned} \tag{B-64}$$

where κ_1 (denoted K_1 in the thesis), is the wash-out parameter,

$$\kappa_1 = \frac{\Gamma(N \to \ell)}{H(M_1)} \,. \tag{B-65}$$

Given the high temperature expansion

$$K_2(z \ll 1) \;\simeq\; \frac{2}{z}\, K_1(z \ll 1) \simeq \frac{2}{z^2}\,, \tag{B-66}$$

we have that $D(z \ll 1) \simeq 2\,W_{id}(z \ll 1) z^2/2 \ll 1$: decays and inverse decays are highly suppressed. In the opposite low-temperature regime, since

$$\begin{aligned} K_1(z \gg 1) &\simeq \frac{e^{-z}}{\sqrt{z}}\sqrt{\frac{\pi}{2}}\left(1+\frac{3}{8\,z}\right)\,, \\ K_2(z \gg 1) &\simeq \frac{e^{-z}}{\sqrt{z}}\sqrt{\frac{\pi}{2}}\left(1+\frac{15}{8\,z}\right) \end{aligned} \tag{B-67}$$

we obtains

$$\begin{aligned} D(z \gg 1) &\simeq z - \frac{3}{2}\,, \\ W_{id}(z) &\simeq \frac{e^{-z}}{4}\sqrt{\frac{\pi}{2}}\, z^{5/2}\left(1+\frac{3}{8\,z}\right)\,. \end{aligned} \tag{B-68}$$

Hence, while decays increase with z, the inverse decays get Boltzmann suppressed at low temperature. The latter reach their maximum for $z \simeq 2.4$, at $W_{id}(z) \simeq 0.29$.

We also include $\Delta L = 1$ neutrino-top scatterings, which are mediated by a Higgs field in the $s-$ and $t-$ channels, as seen in chapter 3.

The reduced cross-section for these scatterings, involving a right-handed neutrino N_i, is given by [57]:

$$\widehat{\sigma}_s(x) = \frac{3\alpha_t}{2}\,\kappa_i\,\frac{x^2 - a_i^2}{x^2}\,, \tag{B-69}$$

where $x = s/M_1^2$ is the rescaled energy in the centre-of-mass frame, $a_i = M_i^2/M_1^2$ and $\alpha_t = h_t^2/4\pi$.

The $t-$channel contribution reads [57]:

$$\widehat{\sigma}_s(x) = 3\,\alpha_t\,\kappa_i\,\frac{x - a_i}{x}\left(\frac{x - 2\,a_i + 2\,a_h}{x - a_i + a_h} + \frac{a_i - 2\,a_h}{x - a_h}\ln\left(\frac{x - a_i + a_h}{a_h}\right)\right)\,, \tag{B-70}$$

where a_h correspond to the rescaled Higgs mass, which is used to regularise an infrared divergence, $a_h = (\mu/M_1)^2 \simeq 10^{-16}$.

At high temperatures, the reaction density scales as T^4, and one has [59]:

$$\frac{z}{s\,H(M_1)}\frac{\gamma_{s,t}}{Y_N^{eq}} \overset{z \ll 1}{\simeq} \frac{9}{4\pi^2}\frac{m_t^2}{2\,v^2} \simeq 0.1\ , \tag{B-71}$$

and $D(z) + S(z) \simeq S(z) \simeq 0.1$, $z \ll 1$.

In the opposite regime of low temperatures, $D(z) + S(z) \simeq D(z) \simeq z$.

Bibliography

[1] E. W. Kolb and M. S. Turner, “The Early universe,” Front. Phys. **69** (1990) 1.

[2] K. A. Olive, D. N. Schramm, G. Steigman, M. S. Turner and J. M. Yang, “Big Bang Nucleosynthesis As A Probe Of Cosmology And Particle Physics,” Astrophys. J. **246** (1981) 557.
S. Burles, K. M. Nollett and M. S. Turner, “Big-Bang Nucleosynthesis Predictions for Precision Cosmology,” Astrophys. J. **552** (2001) L1 [arXiv:astro-ph/0010171].
J. P. Kneller and G. Steigman, “BBN For Pedestrians,” New J. Phys. **6** (2004) 117 [arXiv:astro-ph/0406320].

[3] A. Strumia, “Baryogenesis via leptogenesis,” arXiv:hep-ph/0608347.

[4] G. Steigman, “Primordial nucleosynthesis: Successes and challenges,” Int. J. Mod. Phys. E **15** (2006) 1 [arXiv:astro-ph/0511534].

[5] V. Simha and G. Steigman, “Constraining The Early-Universe Baryon Density And Expansion Rate,” arXiv:0803.3465 [astro-ph].

[6] B. Fields and S. Sarkar, “Big-bang nucleosynthesis (PDG mini-review),” arXiv:astro-ph/0601514.

[7] http://map.gsfc.nasa.gov/

[8] W. Hu, “Lecture Notes on CMB Theory: From Nucleosynthesis to Recombination,” arXiv:0802.3688 [astro-ph].
M. Giovannini, “Why CMB physics?,” Int. J. Mod. Phys. A **22** (2007) 2697 [arXiv:astro-ph/0703730].

[9] J. Dunkley *et al.* [WMAP Collaboration], “Five-Year Wilkinson Microwave Anisotropy Probe (WMAP) Observations: Likelihoods and Parameters from the WMAP data,” arXiv:0803.0586 [astro-ph].

[10] See, *e.g.* A. R. Liddle, “An introduction to cosmological inflation,” arXiv:astro-ph/9901124.

[11] A. D. Sakharov, “Violation of CP Invariance, c Asymmetry, and Baryon Asymmetry of the Universe,” Pisma Zh. Eksp. Teor. Fiz. **5**, 32 (1967) [JETP Lett. **5**, 24 (1967 SOPUA,34,392-393.1991 UFNAA,161,61-64.1991)].

[12] M. Yoshimura, “Unified Gauge Theories And The Baryon Number Of The Universe,” Phys. Rev. Lett. **41** (1978) 281 [Erratum-ibid. **42** (1979) 746].
S. Dimopoulos and L. Susskind, “On The Baryon Number Of The Universe,” Phys. Rev. D **18** (1978) 4500.
S. Weinberg, “Cosmological Production Of Baryons,” Phys. Rev. Lett. **42** (1979) 850.
D. V. Nanopoulos and S. Weinberg, “Mechanisms For Cosmological Baryon Production,” Phys. Rev. D **20** (1979) 2484.
S. M. Barr, G. Segre and H. A. Weldon, “The Magnitude Of The Cosmological Baryon Asymmetry,” Phys. Rev. D **20**, 2494 (1979).

[13] G. ’t Hooft, “Symmetry breaking through Bell-Jackiw anomalies,” Phys. Rev. Lett. **37** (1976) 8.
G. ’t Hooft, “Computation of the quantum effects due to a four-dimensional pseudoparticle,” Phys. Rev. D **14** (1976) 3432 [Erratum-ibid. D **18** (1978) 2199].
A. A. Belavin, A. M. Polyakov, A. S. Shvarts and Yu. S. Tyupkin, “Pseudoparticle solutions of the Yang-Mills equations,” Phys. Lett. B **59** (1975) 85.

[14] V. A. Kuzmin, V. A. Rubakov and M. E. Shaposhnikov, “On The Anomalous Electroweak Baryon Number Nonconservation In The Early Universe,” Phys. Lett. B **155** (1985) 36.

[15] N. S. Manton, “Topology In The Weinberg-Salam Theory,” Phys. Rev. D **28** (1983) 2019.
F. R. Klinkhamer and N. S. Manton, “A Saddle Point Solution In The Weinberg-Salam Theory,” Phys. Rev. D **30** (1984) 2212.
V. A. Rubakov and M. E. Shaposhnikov, “Electroweak baryon number non-conservation in the early universe and in high-energy collisions,” Usp. Fiz. Nauk **166** (1996) 493 [Phys. Usp. **39** (1996) 461] [arXiv:hep-ph/9603208], and references therein.

[16] A. G. Cohen, D. B. Kaplan and A. E. Nelson, “Progress in electroweak baryogenesis,” Ann. Rev. Nucl. Part. Sci. **43** (1993) 27 [arXiv:hep-ph/9302210].
M. Trodden, “Electroweak baryogenesis,”

Rev. Mod. Phys. **71** (1999) 1463 [arXiv:hep-ph/9803479].
A. Riotto, "Theories of baryogenesis," arXiv:hep-ph/9807454.
J. M. Cline, "Baryogenesis," arXiv:hep-ph/0609145.

[17] M. B. Gavela, P. Hernandez, J. Orloff and O. Pene, "Standard model CP violation and baryon asymmetry," Mod. Phys. Lett. A **9** (1994) 795 [arXiv:hep-ph/9312215].
P. Huet and E. Sather, "Electroweak baryogenesis and standard model CP violation," Phys. Rev. D **51** (1995) 379 [arXiv:hep-ph/9404302].
M. B. Gavela, P. Hernandez, J. Orloff, O. Pene and C. Quimbay, "Standard model CP violation and baryon asymmetry. Part 2: Finite temperature," Nucl. Phys. B **430** (1994) 382 [arXiv:hep-ph/9406289].

[18] R. Barate *et al.* [LEP Working Group for Higgs boson searches], "Search for the standard model Higgs boson at LEP," Phys. Lett. B **565** (2003) 61 [arXiv:hep-ex/0306033].

[19] G. F. Giudice, "The Electroweak phase transition in supersymmetry," Phys. Rev. D **45** (1992) 3177.
G. R. Farrar and M. Losada, "SUSY and the electroweak phase transition," Phys. Lett. B **406** (1997) 60 [arXiv:hep-ph/9612346].
M. S. Carena, M. Quiros, M. Seco and C. E. M. Wagner, "Improved results in supersymmetric electroweak baryogenesis," Nucl. Phys. B **650** (2003) 24 [arXiv:hep-ph/0208043].

[20] M. S. Carena, M. Quiros and C. E. M. Wagner, "Opening the Window for Electroweak Baryogenesis," Phys. Lett. B **380** (1996) 81 [arXiv:hep-ph/9603420].
B. de Carlos and J. R. Espinosa, "The baryogenesis window in the MSSM," Nucl. Phys. B **503** (1997) 24 [arXiv:hep-ph/9703212].

[21] S. J. Huber, T. Konstandin, T. Prokopec and M. G. Schmidt, "Electroweak phase transition and baryogenesis in the nMSSM," Nucl. Phys. B **757** (2006) 172 [arXiv:hep-ph/0606298].

[22] I. Affleck and M. Dine, "A New Mechanism For Baryogenesis," Nucl. Phys. B **249** (1985) 361.
M. Dine, L. Randall, S. D. Thomas, "Baryogenesis from flat directions of the supersymmetric standard model," Nucl. Phys. B **458** (1996) 291. [arXiv:hep-ph/9507453]

[23] M. Fukugita and T. Yanagida, "Baryogenesis Without Grand Unification," Phys. Lett. B **174** (1986) 45.

[24] M. A. Luty, "Baryogenesis Via Leptogenesis," Phys. Rev. D **45** (1992) 455.

[25] S. Davidson, E. Nardi and Y. Nir, "Leptogenesis," arXiv:0802.2962 [hep-ph].

[26] W. Pauli, "Dear radioactive ladies and gentlemen," Phys. Today **31N9** (1978) 27.

[27] G. Danby, J. M. Gaillard, K. Goulianos, L. M. Lederman, N. B. Mistry, M. Schwartz and J. Steinberger, "Observation of high-energy neutrino reactions and the existence of two kinds of neutrinos," Phys. Rev. Lett. **9** (1962) 36.

[28] K. Kodama *et al.* [DONUT Collaboration], "Observation of tau-neutrino interactions," Phys. Lett. B **504** (2001) 218 [arXiv:hep-ex/0012035].

[29] R. J. Davis, D. S. Harmer and K. C. Hoffman, "Search for neutrinos from the sun," Phys. Rev. Lett. **20** (1968) 1205.
B. T. Cleveland *et al.*, "Measurement of the solar electron neutrino flux with the Homestake chlorine detector," Astrophys. J. **496**, 505 (1998).
J. N. Abdurashitov *et al.* [SAGE Collaboration], "Measurement of the solar neutrino capture rate with gallium metal," Phys. Rev. C **60** (1999) 055801 [arXiv:astro-ph/9907113].
M. Altmann *et al.* [GNO Collaboration], "GNO solar neutrino observations: Results for GNO I," Phys. Lett. B **490** (2000) 16 [arXiv:hep-ex/0006034].
Q. R. Ahmad *et al.* [SNO Collaboration], "Direct evidence for neutrino flavor transformation from neutral-current interactions in the Sudbury Neutrino Observatory," Phys. Rev. Lett. **89** (2002) 011301 [arXiv:nucl-ex/0204008].
S. Fukuda *et al.* [Super-Kamiokande Collaboration], "Determination of solar neutrino oscillation parameters using 1496 days of Super-Kamiokande-I data," Phys. Lett. B **539** (2002) 179 [arXiv:hep-ex/0205075].
T. Araki *et al.* [KamLAND Collaboration], "Measurement of neutrino oscillation with KamLAND: Evidence of spectral distortion," Phys. Rev. Lett. **94** (2005) 081801 [arXiv:hep-ex/0406035].

[30] K. S. Hirata *et al.* [Kamiokande-II Collaboration], "Observation of a small atmospheric ν_μ/ν_e ratio in Kamiokande," Phys. Lett. B **280** (1992) 146.

R. Becker-Szendy *et al.*, "The Electron-neutrino and muon-neutrino content of the atmospheric flux," Phys. Rev. D **46** (1992) 3720.

[31] www.pi.infn.it/ astrumia/review.html

[32] S. M. Bilenky and B. Pontecorvo, "Lepton Mixing And Neutrino Oscillations," Phys. Rept. **41** (1978) 225.

[33] Y. Fukuda *et al.* [Super-Kamiokande Collaboration], "Evidence for oscillation of atmospheric neutrinos," Phys. Rev. Lett. **81** (1998) 1562 [arXiv:hep-ex/9807003].

[34] B. Pontecorvo, "Mesonium and antimesonium," Sov. Phys. JETP **6** (1957) 429 [Zh. Eksp. Teor. Fiz. **33** (1957) 549].
Z. Maki, M. Nakagawa and S. Sakata, "Remarks on the unified model of elementary particles," Prog. Theor. Phys. **28** (1962) 870.

[35] Y. Declais *et al.* [Bugey Collaboration], "Search for neutrino oscillations at 15-meters, 40-meters, and 95-meters from a nuclear power reactor at Bugey," Nucl. Phys. B **434** (1995) 503.
M. Apollonio *et al.* [CHOOZ Collaboration], "Limits on neutrino oscillations from the CHOOZ experiment," Phys. Lett. B **466** (1999) 415 [arXiv:hep-ex/9907037]. M. Apollonio *et al.* [CHOOZ Collaboration], "Search for neutrino oscillations on a long base-line at the CHOOZ nuclear power station," Eur. Phys. J. C **27** (2003) 331 [arXiv:hep-ex/0301017].

[36] D. G. Michael *et al.* [MINOS Collaboration], "Observation of muon neutrino disappearance with the MINOS detectors and the NuMI neutrino beam," Phys. Rev. Lett. **97** (2006) 191801 [arXiv:hep-ex/0607088].

[37] T. Schwetz, "Neutrino oscillations: present status and outlook," AIP Conf. Proc. **981** (2008) 8 [arXiv:0710.5027 [hep-ph]].

[38] C. Jarlskog, "A Basis Independent Formulation Of The Connection Between Quark Mass Matrices, CP Violation And Experiment," Z. Phys. C **29** (1985) 491.

[39] A. D. Dolgov, "Neutrinos in cosmology," Phys. Rept. **370** (2002) 333 [arXiv:hep-ph/0202122].
J. Lesgourgues and S. Pastor, "Massive neutrinos and cosmology," Phys. Rept. **429** (2006) 307 [arXiv:astro-ph/0603494].

[40] E. Komatsu *et al.* [WMAP Collaboration], "Five-Year Wilkinson Microwave Anisotropy Probe Observations:Cosmological Interpretation," arXiv:0803.0547 [astro-ph].

[41] C. Kraus *et al.*, "Final results from phase II of the Mainz neutrino mass search in tritium beta decay," Eur. Phys. J. C **40** (2005) 447 [arXiv:hep-ex/0412056].

[42] A. I. Belesev *et al.*, "Results of the Troitsk experiment on the search for the electron anti-neutrino rest mass in tritium beta decay," Phys. Lett. B **350** (1995) 263.

[43] R. G. H. Robertson [KATRIN Collaboration], "KATRIN: an experiment to measure the neutrino mass," arXiv:0712.3893 [nucl-ex].

[44] H. V. Klapdor-Kleingrothaus *et al.* [Heidelberg-Moscow Collaboration], "Latest results from the Heidelberg-Moscow double-beta-decay experiment," Eur. Phys. J. A **12** (2001) 147 [arXiv:hep-ph/0103062].
R. Arnold *et al.* [NEMO Collaboration], "First results of the search of neutrinoless double beta decay with the NEMO 3 detector," Phys. Rev. Lett. **95** (2005) 182302 [arXiv:hep-ex/0507083].
S. Pascoli and S. T. Petcov, "Majorana Neutrinos, Neutrino Mass Spectrum and the $|\langle m\rangle| \sim 0.001$ eV Frontier in Neutrinoless Double Beta Decay," arXiv:0711.4993 [hep-ph].

[45] H. V. Klapdor-Kleingrothaus, A. Dietz, H. L. Harney and I. V. Krivosheina, "Evidence for neutrinoless double beta decay," Mod. Phys. Lett. A **16** (2001) 2409 [arXiv:hep-ph/0201231].

[46] S. Weinberg, "Baryon And Lepton Nonconserving Processes," Phys. Rev. Lett. **43** (1979) 1566.

[47] M. Shaposhnikov, "The nuMSM, leptonic asymmetries, and properties of singlet fermions," arXiv:0804.4542 [hep-ph].

[48] A. Zee, "A Theory Of Lepton Number Violation, Neutrino Majorana Mass, And Oscillation," Phys. Lett. B **93** (1980) 389 [Erratum-ibid. B **95** (1980) 461].

[49] K. S. Babu, "Model of 'Calculable' Majorana Neutrino Masses," Phys. Lett. B **203** (1988) 132.

[50] P. Minkowski, "Mu → E Gamma At A Rate Of One Out Of 1-Billion Muon Decays?," Phys. Lett. B **67** (1977) 421.

M. Gell-Mann, P. Ramond and R. Slansky, “Complex Spinors And Unified Theories,” in *Supergravity*, edited by P. van Nieuwenhuizen and D. Freedman, (North-Holland, 1979), p. 315;
T. Yanagida, in *Proceedings of the Workshop on the Unified Theory and the Baryon Number in the Universe*, edited by O. Sawada and A. Sugamoto (KEK Report No. 79-18, Tsukuba, 1979), p. 95;
R. N. Mohapatra and G. Senjanovic, “Neutrino mass and spontaneous parity nonconservation,” Phys. Rev. Lett. **44** (1980) 912.

[51] J. A. Casas and A. Ibarra, “Oscillating neutrinos and mu –> e, gamma,” Nucl. Phys. B **618** (2001) 171 [arXiv:hep-ph/0103065].

[52] M. Raidal and A. Strumia, “Predictions of the most minimal see-saw model,” Phys. Lett. B **553** (2003) 72 [arXiv:hep-ph/0210021].
A. Ibarra and G. G. Ross, “Neutrino phenomenology: The case of two right handed neutrinos,” Phys. Lett. B **591** (2004) 285 [arXiv:hep-ph/0312138].

[53] M. Magg and C. Wetterich, “Neutrino Mass Problem And Gauge Hierarchy,” Phys. Lett. B **94**, 61 (1980).
G. Lazarides, Q. Shafi and C. Wetterich, “Proton Lifetime And Fermion Masses In An SO(10) Model,” Nucl. Phys. B **181** (1981) 287.
R. N. Mohapatra and G. Senjanovic, “Neutrino Masses And Mixings In Gauge Models With Spontaneous Parity Violation,” Phys. Rev. D **23** (1981) 165.
C. Wetterich, “Neutrino Masses And The Scale Of B-L Violation,” Nucl. Phys. B **187** (1981) 343.

[54] R. Foot, H. Lew, X. G. He and G. C. Joshi, “Seesaw neutrino masses induced by a triplet of leptons,” Z. Phys. C **44** (1989) 441.
E. Ma, “Pathways to naturally small neutrino masses,” Phys. Rev. Lett. **81** (1998) 1171 [arXiv:hep-ph/9805219].

[55] S. Lavignac, I. Masina and C. A. Savoy, “tau –> mu gamma and mu –> e gamma as probes of neutrino mass models,” Phys. Lett. B **520** (2001) 269 [arXiv:hep-ph/0106245].
E. K. Akhmedov, M. Frigerio and A. Y. Smirnov, “Probing the seesaw mechanism with neutrino data and leptogenesis,” JHEP **0309** (2003) 021 [arXiv:hep-ph/0305322].
B. Bajc, M. Nemevsek and G. Senjanovic, “Probing seesaw at LHC,” Phys. Rev. D **76** (2007) 055011 [arXiv:hep-ph/0703080].
A. Abada, C. Biggio, F. Bonnet, M. B. Gavela and T. Hambye, “Low energy effects of neutrino masses,” JHEP **0712** (2007) 061 [arXiv:0707.4058 [hep-ph]].
W. Rodejohann, “The see-saw mechanism: neutrino mixing, leptogenesis and lepton flavor violation,” arXiv:0804.3925 [hep-ph].

[56] T. Hambye, Y. Lin, A. Notari, M. Papucci and A. Strumia, “Constraints on neutrino masses from leptogenesis models,” Nucl. Phys. B **695** (2004) 169 [arXiv:hep-ph/0312203].
C. H. Albright and S. M. Barr, “Leptogenesis in the type III seesaw mechanism,” Phys. Rev. D **69** (2004) 073010 [arXiv:hep-ph/0312224].

[57] M. Plumacher, “Baryogenesis and lepton number violation,” Z. Phys. C **74** (1997) 549 [arXiv:hep-ph/9604229].
W. Buchmuller and M. Plumacher, “Baryon asymmetry and neutrino mixing,” Phys. Lett. B **389** (1996) 73 [arXiv:hep-ph/9608308].
M. Plumacher, Ph.D. thesis, “Baryon asymmetry, neutrino mixing and supersymmetric SO(10) unification,” arXiv:hep-ph/9807557.

[58] G. F. Giudice, A. Notari, M. Raidal, A. Riotto and A. Strumia, “Towards a complete theory of thermal leptogenesis in the SM and MSSM,” Nucl. Phys. B **685** (2004) 89 [arXiv:hep-ph/0310123].

[59] W. Buchmuller, P. Di Bari and M. Plumacher, “Leptogenesis for pedestrians,” Annals Phys. **315** (2005) 305 [arXiv:hep-ph/0401240].

[60] J. Liu and G. Segre, “Reexamination of generation of baryon and lepton number asymmetries by heavy particle decay,” Phys. Rev. D **48** (1993) 4609 [arXiv:hep-ph/9304241].

[61] L. Covi, E. Roulet and F. Vissani, “CP violating decays in leptogenesis scenarios,” Phys. Lett. B **384** (1996) 169 [arXiv:hep-ph/9605319].

[62] A. Pilaftsis, “CP violation and baryogenesis due to heavy Majorana neutrinos,” Phys. Rev. D **56** (1997) 5431 [arXiv:hep-ph/9707235].
W. Buchmuller and M. Plumacher, “CP asymmetry in Majorana neutrino decays,” Phys. Lett. B **431** (1998) 354 [arXiv:hep-ph/9710460].

[63] A. Anisimov, A. Broncano and M. Plumacher, “The CP-asymmetry in resonant leptogenesis,”

Nucl. Phys. B **737** (2006) 176 [arXiv:hep-ph/0511248].

[64] S. Davidson and A. Ibarra, "A lower bound on the right-handed neutrino mass from leptogenesis," Phys. Lett. B **535** (2002) 25 [arXiv:hep-ph/0202239].

[65] T. Hambye, Y. Lin, A. Notari, M. Papucci and A. Strumia, "Constraints on neutrino masses from leptogenesis models," Nucl. Phys. B **695** (2004) 169 [arXiv:hep-ph/0312203].

[66] E. W. Kolb and S. Wolfram, "Baryon Number Generation In The Early Universe," Nucl. Phys. B **172** (1980) 224 [Erratum-ibid. B **195** (1982) 542].

[67] http://mathworld.wolfram.com/LambertW-Function.html

[68] S. Y. Khlebnikov and M. E. Shaposhnikov, "The Statistical Theory of Anomalous Fermion Number Nonconservation," Nucl. Phys. B **308** (1988) 885.

[69] S. Blanchet and P. Di Bari, "Flavor effects on leptogenesis predictions," JCAP **0703** (2007) 018 [arXiv:hep-ph/0607330].

[70] W. Buchmuller, P. Di Bari and M. Plumacher, "Cosmic microwave background, matter-antimatter asymmetry and neutrino masses," Nucl. Phys. B **643** (2002) 367 [Erratum-ibid. B **793** (2008) 362] [arXiv:hep-ph/0205349].

[71] A. Abada, S. Davidson, A. Ibarra, F. X. Josse-Michaux, M. Losada and A. Riotto, "Flavour matters in leptogenesis," JHEP **0609**, 010 (2006) [arXiv:hep-ph/0605281].

[72] E. Nardi, J. Racker and E. Roulet, "CP violation in scatterings, three body processes and the Boltzmann equations for leptogenesis," JHEP **0709**, 090 (2007) [arXiv:0707.0378 [hep-ph]].

[73] A. Pilaftsis and T. E. J. Underwood, "Resonant leptogenesis," Nucl. Phys. B **692**, 303 (2004) [arXiv:hep-ph/0309342].

[74] W. Buchmuller, P. Di Bari and M. Plumacher, "A bound on neutrino masses from baryogenesis," Phys. Lett. B **547** (2002) 128 [arXiv:hep-ph/0209301].
W. Buchmuller, P. Di Bari and M. Plumacher, "The neutrino mass window for baryogenesis," Nucl. Phys. B **665** (2003) 445 [arXiv:hep-ph/0302092].

[75] A. Abada, S. Davidson, F. X. Josse-Michaux, M. Losada and A. Riotto, "Flavour issues in leptogenesis," JCAP **0604** (2006) 004 [arXiv:hep-ph/0601083].

[76] E. Nardi, Y. Nir, E. Roulet and J. Racker, "The importance of flavor in leptogenesis," JHEP **0601** (2006) 164 [arXiv:hep-ph/0601084].

[77] G. Sigl and G. Raffelt, "General kinetic description of relativistic mixed neutrinos," Nucl. Phys. B **406** (1993) 423.

[78] R. Barbieri, P. Creminelli, A. Strumia and N. Tetradis, "Baryogenesis through leptogenesis," Nucl. Phys. B **575**, 61 (2000) [arXiv:hep-ph/9911315].

[79] E. Nardi, Y. Nir, J. Racker and E. Roulet, "On Higgs and sphaleron effects during the leptogenesis era," JHEP **0601** (2006) 068 [arXiv:hep-ph/0512052].

[80] B. A. Campbell, S. Davidson, J. R. Ellis and K. A. Olive, "On the baryon, lepton flavor and right-handed electron asymmetries of the universe," Phys. Lett. B **297** (1992) 118 [arXiv:hep-ph/9302221].
J. M. Cline, K. Kainulainen and K. A. Olive, "Protecting the primordial baryon asymmetry from erasure by sphalerons," Phys. Rev. D **49** (1994) 6394 [arXiv:hep-ph/9401208].

[81] S. Blanchet, P. Di Bari and G. G. Raffelt, "Quantum Zeno effect and the impact of flavor in leptogenesis," JCAP **0703** (2007) 012 [arXiv:hep-ph/0611337].

[82] A. De Simone and A. Riotto, "On the impact of flavour oscillations in leptogenesis," JCAP **0702**, 005 (2007) [arXiv:hep-ph/0611357].

[83] J. A. Harvey and M. S. Turner, "Cosmological baryon and lepton number in the presence of electroweak fermion number violation," Phys. Rev. D **42** (1990) 3344.

[84] H. K. Dreiner and G. G. Ross, "Sphaleron Erasure Of Primordial Baryogenesis," Nucl. Phys. B **410** (1993) 188 [arXiv:hep-ph/9207221].

[85] cf. first reference of [57]

[86] O. Vives, "Flavoured leptogenesis: A successful thermal leptogenesis with N(1) mass below 10**8-GeV," Phys. Rev. D **73** (2006) 073006 [arXiv:hep-ph/0512160].

[87] S. Antusch and A. M. Teixeira, "Towards constraints on the SUSY seesaw from flavour-

dependent leptogenesis," JCAP **0702** (2007) 024 [arXiv:hep-ph/0611232].

[88] S. Pascoli, S. T. Petcov and A. Riotto, "Connecting low energy leptonic CP-violation to leptogenesis," Phys. Rev. D **75** (2007) 083511 [arXiv:hep-ph/0609125].
S. Pascoli, S. T. Petcov and A. Riotto, "Leptogenesis and low energy CP violation in neutrino physics," Nucl. Phys. B **774** (2007) 1 [arXiv:hep-ph/0611338].

[89] E. Molinaro and S. T. Petcov, "The Interplay Between the 'Low' and 'High' Energy CP-Violation in Leptogenesis," arXiv:0803.4120 [hep-ph].

[90] F. X. Josse-Michaux and A. Abada, "Study of flavour dependencies in leptogenesis," JCAP **0710**, 009 (2007) [arXiv:hep-ph/0703084].

[91] G. C. Branco, T. Morozumi, B. M. Nobre and M. N. Rebelo, "A bridge between CP violation at low energies and leptogenesis," Nucl. Phys. B **617** (2001) 475 [arXiv:hep-ph/0107164].
G. C. Branco, R. Gonzalez Felipe, F. R. Joaquim and M. N. Rebelo, "Leptogenesis, CP violation and neutrino data: What can we learn?," Nucl. Phys. B **640** (2002) 202 [arXiv:hep-ph/0202030].
S. Davidson and A. Ibarra, "Leptogenesis and low-energy phases," Nucl. Phys. B **648** (2003) 345 [arXiv:hep-ph/0206304].

[92] G. C. Branco, R. Gonzalez Felipe and F. R. Joaquim, "A new bridge between leptonic CP violation and leptogenesis," Phys. Lett. B **645** (2007) 432 [arXiv:hep-ph/0609297].

[93] S. T. Petcov, W. Rodejohann, T. Shindou and Y. Takanishi, "The see-saw mechanism, neutrino Yukawa couplings, LFV decays l(i) –> l(j) + gamma and leptogenesis," Nucl. Phys. B **739** (2006) 208 [arXiv:hep-ph/0510404].
G. C. Branco, A. J. Buras, S. Jager, S. Uhlig and A. Weiler, "Another look at minimal lepton flavour violation, l(i) –> l(j) gamma, leptogenesis, and the ratio M(nu)/Lambda(LFV)," JHEP **0709** (2007) 004 [arXiv:hep-ph/0609067].

[94] S. Davidson, J. Garayoa, F. Palorini and N. Rius, "Insensitivity of flavoured leptogenesis to low energy CP violation," Phys. Rev. Lett. **99** (2007) 161801 [arXiv:0705.1503 [hep-ph]].

[95] E. Nezri and J. Orloff, "Neutrino oscillations vs. leptogenesis in SO(10) models," JHEP **0304** (2003) 020 [arXiv:hep-ph/0004227].

[96] J. C. Pati and A. Salam, "Lepton Number As The Fourth Color," Phys. Rev. D **10** (1974) 275 [Erratum-ibid. D **11** (1975) 703].

[97] R. N. Mohapatra and J. C. Pati, "Left-Right Gauge Symmetry And An Isoconjugate Model Of CP Violation," Phys. Rev. D **11** (1975) 566.
R. N. Mohapatra and J. C. Pati, "A Natural Left-Right Symmetry," Phys. Rev. D **11** (1975) 2558.
G. Senjanovic and R. N. Mohapatra, "Exact Left-Right Symmetry And Spontaneous Violation Of Parity," Phys. Rev. D **12** (1975) 1502.
D. Chang, R. N. Mohapatra and M. K. Parida, "A New Approach To Left-Right Symmetry Breaking In Unified Gauge Theories," Phys. Rev. D **30** (1984) 1052.
H. Fritzsch and P. Minkowski, "Unified Interactions Of Leptons And Hadrons," Annals Phys. **93** (1975) 193.

[98] A. Abada, P. Hosteins, F. X. Josse-Michaux and S. Lavignac, "Successful Leptogenesis in SO(10) Unification with a Left-Right Symmetric Seesaw Mechanism," arXiv:0808.2058 [hep-ph].

[99] P. Hosteins, S. Lavignac and C. A. Savoy, "Quark-lepton unification and eight-fold ambiguity in the left-right symmetric seesaw mechanism," Nucl. Phys. B **755** (2006) 137 [arXiv:hep-ph/0606078].

[100] H. Georgi and C. Jarlskog, "A New Lepton - Quark Mass Relation In A Unified Theory," Phys. Lett. B **86** (1979) 297.

[101] T. Fukuyama, A. Ilakovac, T. Kikuchi, S. Meljanac and N. Okada, "SO(10) group theory for the unified model building," J. Math. Phys. **46** (2005) 033505 [arXiv:hep-ph/0405300].

[102] E. K. Akhmedov and M. Frigerio, "Seesaw duality," Phys. Rev. Lett. **96** (2006) 061802 [arXiv:hep-ph/0509299].

[103] N. Cabibbo, "Unitary Symmetry and Leptonic Decays," Phys. Rev. Lett. **10** (1963) 531.
M. Kobayashi and T. Maskawa, "CP Violation In The Renormalizable Theory Of Weak Interaction," Prog. Theor. Phys. **49** (1973) 652.

[104] M. Jamin, "Quark masses", talk given at the University of Granada, March 2006 http://personal.ifae.es/jamin/my/talks/mq_granada06.pdf.

[105] W. M. Yao *et al.* [Particle Data Group], "Review of particle physics," J. Phys. G **33** (2006) 1 (and 2007 partial update for edition 2008).

[106] S. Antusch, J. Kersten, M. Lindner, M. Ratz and M. A. Schmidt, "Running neutrino mass parameters in see-saw scenarios," JHEP **0503** (2005) 024 [arXiv:hep-ph/0501272]; http://users.physik.tu-muenchen.de/rge/REAP/index.html.

[107] G. L. Fogli, E. Lisi, A. Marrone and A. Palazzo, "Global analysis of three-flavor neutrino masses and mixings," Prog. Part. Nucl. Phys. **57** (2006) 742 [arXiv:hep-ph/0506083].

[108] M. S. Carena, M. Olechowski, S. Pokorski and C. E. M. Wagner, "Electroweak symmetry breaking and bottom - top Yukawa unification," Nucl. Phys. B **426** (1994) 269 [arXiv:hep-ph/9402253].
T. Blazek, S. Raby and S. Pokorski, "Finite supersymmetric threshold corrections to CKM matrix elements in the large tan Beta regime," Phys. Rev. D **52** (1995) 4151 [arXiv:hep-ph/9504364].

[109] E. Ma, S. Sarkar and U. Sarkar, "Scale of SU(2)R symmetry breaking and leptogenesis", Phys. Lett. B **458** (1999) 73 [arXiv:hep-ph/9812276].

[110] T. Hambye, E. Ma and U. Sarkar, "Supersymmetric triplet Higgs model of neutrino masses and leptogenesis," Nucl. Phys. B **602** (2001) 23 [arXiv:hep-ph/0011192].

[111] T. Hambye and G. Senjanovic, "Consequences of triplet seesaw for leptogenesis", Phys. Lett. B **582** (2004) 73 [arXiv:hep-ph/0307237].

[112] N. Cosme, "Leptogenesis, neutrino masses and gauge unification," JHEP **0408** (2004) 027 [arXiv:hep-ph/0403209].

[113] S. Antusch and S. F. King, "Type II leptogenesis and the neutrino mass scale", Phys. Lett. B **597** (2004) 199 [arXiv:hep-ph/0405093].

[114] G. D'Ambrosio, T. Hambye, A. Hektor, M. Raidal and A. Rossi, "Leptogenesis in the minimal supersymmetric triplet seesaw model," Phys. Lett. B **604** (2004) 199 [arXiv:hep-ph/0407312].

[115] E. K. Akhmedov and M. Frigerio, "Interplay of type I and type II seesaw contributions to neutrino mass", Phys. Rev. Lett. **96** (2006) 061802 [arXiv:hep-ph/0609046].
E. K. Akhmedov, M. Blennow, T. Hallgren, T. Konstandin and T. Ohlsson, "Stability and leptogenesis in the left-right symmetric seesaw mechanism", JHEP 0704:022,2007, [arXiv:hep-ph/0612194].

[116] S. Carlier, J. M. Frere and F. S. Ling, "Gauge dilution and leptogenesis", Phys. Rev. D **60** (1999) 096003 [arXiv:hep-ph/9903300].

[117] S. Antusch, "Flavour-dependent type II leptogenesis", Phys. Rev. D **76** (2007) 023512 [arXiv:0704.1591 [hep-ph]].

[118] M. Plumacher, "Baryon asymmetry, neutrino mixing and supersymmetric SO(10) unification," Nucl. Phys. B **530** (1998) 207 [arXiv:hep-ph/9704231].

[119] P. Van Nieuwenhuizen, "Supergravity," Phys. Rept. **68** (1981) 189.

[120] M. Y. Khlopov and A. D. Linde, "Is It Easy To Save The Gravitino?," Phys. Lett. B **138** (1984) 265.

[121] F. D. Steffen, "Gravitino dark matter and cosmological constraints," JCAP **0609** (2006) 001 [arXiv:hep-ph/0605306].

[122] K. Kohri, T. Moroi and A. Yotsuyanagi, "Big-bang nucleosynthesis with unstable gravitino and upper bound on the reheating temperature," Phys. Rev. D **73** (2006) 123511 [arXiv:hep-ph/0507245].
M. Kawasaki, K. Kohri, T. Moroi and A. Yotsuyanagi, "Big-Bang Nucleosynthesis and Gravitino," arXiv:0804.3745 [hep-ph].

[123] M. Bolz, A. Brandenburg and W. Buchmüller, "Thermal productions of gravitinos", Nucl. Phys. B **606** (2001) 518 [arXiv:hep-ph/0012052].
J. Pradler and F. D. Steffen, "Thermal gravitino production and collider tests of leptogenesis," Phys. Rev. D **75** (2007) 023509 [arXiv:hep-ph/0608344].

[124] V. S. Rychkov and A. Strumia, "Thermal production of gravitinos," Phys. Rev. D **75** (2007) 075011 [arXiv:hep-ph/0701104].

[125] F. Hahn-Woernle and M. Plumacher, "Effects of reheating on leptogenesis," arXiv:0801.3972 [hep-ph].

[126] G. Engelhard, Y. Grossman, E. Nardi and Y. Nir, "The importance of N2 leptogenesis," Phys. Rev. Lett. **99** (2007) 081802 [arXiv:hep-ph/0612187].

[127] T. Schwetz, "What is the probability that theta(13) and CP violation will be discovered in future neutrino oscillation experiments?," Phys. Lett. B **648** (2007) 54 [arXiv:hep-ph/0612223].

[128] S. L. Adler, "Axial vector vertex in spinor electrodynamics," Phys. Rev. **177** (1969) 2426.
J. S. Bell and R. Jackiw, "A PCAC puzzle: pi0 → gamma gamma in the sigma model," Nuovo Cim. A **60** (1969) 47.

[129] G. D. Moore, "Computing the strong sphaleron rate," Phys. Lett. B **412** (1997) 359 [arXiv:hep-ph/9705248].

[130] P. Arnold, D. Son and L. G. Yaffe, "The hot baryon violation rate is O(alpha(w)**5 T**4)," Phys. Rev. D **55** (1997) 6264 [arXiv:hep-ph/9609481].
D. Bodeker, G. D. Moore and K. Rummukainen, "Chern-Simons number diffusion and hard thermal loops on the lattice," Phys. Rev. D **61** (2000) 056003 [arXiv:hep-ph/9907545].